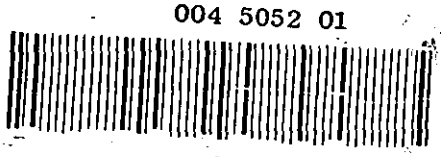

THE USE OF MATHEMATICAL MODELS IN STUDIES ON SCALE-UP AND IMPELLER GEOMETRIES IN A CONTINUOUS FLOW REACTOR.

H.I.BERRESFORD

Submitted for the degree of

Doctor of Philosophy of

Loughborough University of Technology.

October 1969

Acknowledgements

The author wishes to thank Professor D.C. Freshwater for his interest and encouragement; Mr. H.W. Kropholler for his stimulating supervision; Dr. B.A. Buffham, Dr. L.G. Gibilaro, Dr. D.J. Spikins for their invaluable comments and the Science Research Council for their financial support in this research.

1. ABSTRACT

Abstract

A modified version of the single loop recirculation model is proposed for the simulation of the dynamics of turbine and propeller agitated continuous systems. The model predictions characterise experimentally determined responses for a variety of operating conditions and a wide range of impeller speeds. The model is verified, using thin fluids, for various diameter impellers placed in vessels of different diameter.

Analytical expressions are obtained for batch mixing time using a matrix technique, having formulated batch conditions by a reduction of the continuous flow model. Experimentally determined batch mixing times appear to match the analytical solutions more favourably than the predictions of various empirical correlations.

A new approach, based on the intensity function, is suggested for the assessment of continuous mixing time.

The continuous flow model parameter (q/Q), the ratio of impeller pumping capacity to system throughput, is proposed as the first dynamic scale-up rule. If held constant this criterion ensures identical residence time distributions in the laboratory and pilot plant vessels.

A variance analysis assesses the merits of different feed inlet positions, for the continuous case, and shows that inlet feed directed away from the outlet stream and impeller region produces the most effective mixing.

Scale-up using constant impeller tip speed is shown to provide an economic optimum for the scale-up of continuous systems.

2. INTRODUCTION

Introduction

This research into the dynamics of continuous flow reactors was conducted in the Department of Chemical Engineering of Loughborough University of Technology. The aim was to establish a mathematical model which could accommodate changes in impeller geometries, tank diameters and fluid properties, and subsequently to use this background to investigate the use of mathematical models in studies on scale-up.

A single-loop recirculation model has been developed, for turbine and propeller agitated vessels, from consideration of the fluid flow pattern. The model configuration attempts to represent an analogy with the actual physical flow pattern induced in the fluid by the impellers. The model has been verified experimentally for thin fluids, by impulse response tests, for various diameter turbines and propellers in vessels of different size.

The model parameter (q/Q), the ratio of impeller pumping capacity to system throughput, has been proposed as a scale-up rule for continuous blenders. If held constant this criterion ensures identical residence time distributions in the unscaled and scaled systems. The model has been used to compare the residence time distributions obtained on the laboratory scale with those computed for the plant-scale, after having scaled the impeller speed by some of the well known batch criteria.

Streak-photography experiments, for the turbine positioned at one third of the liquid height from the base of the vessel, have shown that the flow pattern could be equally described by a double-loop or single-loop configuration. Hence, the recently proposed multi-loop model of Gibilaro was compared with the experimental response curves for each turbine agitated system.

The model fitting method was by direct comparison of experimental residence time distributions with model predictions. As the correspondence between experimental results and model solutions was excellent over a wide range of operating conditions, no further criteria for curve fitting or manipulation of the model parameter was considered.

Various allied topics emerged from this background and have subsequently been developed. Analytical expressions for batch mixing time have been derived from both models using a matrix technique. They have been compared with experimentally determined results and the predictions of the known empirical correlations. A new approach for the assessment of continuous mixing time has also been suggested.

From a series of technical and economic design criteria, an optimisation of the continuous stirred vessel has been carried out and an economic scale-up rule derived.

The merits of the single loop and double loop models for the simulation of turbine stirred tanks have been assessed by comparison of; experimental residence time distributions, predicted steady state conversions for a first order reaction, a variance analysis, and an intensity function comparison.

Parts of Chapter 8 have been presented in a paper to be published in the Transactions of the Institution of Chemical Engineers.

3. LITERATURE SURVEY

3.1. Principles of Scale-up

There are certain general concepts for the scale-up of batch liquid systems, which have their roots in the principle of similarity. The following types of similarity are associated with fluid mixing systems:-

(a) Geometric Similarity.

Geometric similarity exists when the linear dimensions of the unscaled and scaled up vessels bear a constant ratio to each other.

(b) Kinetic Similarity.

If the two systems are geometrically similar, then kinetic similarity exists when the ratio of velocities between corresponding points in each system is equal.

(c) Dynamic Similarity.

After having obtained geometric and kinetic similarity between two systems, dynamic similarity exists if the ratio of forces between corresponding points in each system is the same.

Further criteria of similarity exist such as Thermal and Chemical Similarity, but as these similarities are difficult to maintain practically their use is limited.

The principle of similarity can be expressed as:-

$$A = f\ (B, C, D, \ldots\ldots\ldots\ )\qquad (3.1)$$

where A is a dimensionless group which is a function of other dimensionless groups, B, C, D, (37).

The groups A, B, C, D can be derived for any particular system either from the basic equations, in this case of fluid mixing, the Navier-Stokes equation, or by dimensional analysis. Each method gives an expression for the behaviour of the system

using the minimum number of independent variables. From the above expression, the interconnection between the principle of similarity and dimensionless groups becomes apparent. As nearly all data for batch liquid mixing systems has been correlated using the method of dimensionless groups, this correspondence is essential.

Any dimensionless group in an expression similar to equation 3.1 can be used as a scale-up criterion. If however, there is interaction between the dimensionless groups reliable scale-up cannot be achieved. One of the groups must dominate the remainder in the expression. This is the regime concept. If a pure regime exists, one dimensionless group being dominant, scale-up is comparatively easy. In the case of a mixed regime, no group dominating, scale-up is virtually impossible. If it is usual in this case to conduct experiments in which one of the effects is eliminated and subsequently to derive a new expression with only one dominant group.

To illustrate the regime concept, consider the expression derived from dimensional analysis for stirred liquid systems (62). The Weber group is ignored as it only applied when separate physical phases are present in the system.

$$\frac{Pg_c}{\rho N^3 D^5} = K \cdot \frac{\rho N D^2}{\mu} \cdot \frac{N^2 D^2}{g_c} \cdot \frac{T}{D} \cdot \frac{Z}{D} \cdot \frac{C}{D} \cdot \frac{P}{D} \cdot \frac{W}{D} \cdot \frac{L}{D} \cdot \frac{N_1'}{N_1'} \qquad (3.2)$$

The last seven terms of the above relationship describe the system geometry; $\frac{N_1'}{N_2'}$ accounts for any change in the number of blades. If complete geometric similarity is assumed, the expression reduces to:-

$$\frac{Pg_c}{\rho N^3 D^5} = K \cdot \frac{\rho N D^2}{\mu} \cdot \frac{N^2 D^2}{g_c} \qquad (3.3)$$

As Reynolds Number is proportional to (ND^2) and Froude Number proportional to (N^2D^2), it can be seen that if either the Reynolds Number group or the Froude Number group is used as a basis for scale-up, the value of the other group is changed, if the physical properties of the fluid remain the same. This is a mixed regime. If the fluid properties in the original and scaled up case are different, then scale-up with both Reynolds Number and Froude Number constant is possible.

A relatively pure regime, with Reynolds Number dominant, can be obtained by suppressing the vortex effect. This is achieved experimentally by the introduction of baffles to reduce the swirling motion of the fluid. A correlation can then be found relating the unknown variable with Reynolds Number.

Equation 3.3 leads to two general rules of scale-up. They are scale-up by constant Reynolds Number and constant Froude Number. Scale-up using the latter criterion is rarely met, but when employed it attempts to ensure similarity between the gravitational effects in the two vessels. Scale-up at constant Reynolds Number is used as an attempt to obtain hydrodynamic similarity between the two vessels and also because of the ease of its measurement. Rushton (63) found that this scale-up criterion gave the same overall flow pattern in laboratory and pilot plant vessels, but not equality of instantaneous velocities. These differed considerably between the original and the scaled-up vessel. This fact has caused other relationships to be developed.

Scale-up at constant tip speed was the first alternative to be proposed. Bowers (6,7,8), using a hot-wire anemometer, found that the tangential and vertical flows produced in a cylindrical vessel by paddle and turbine impellers, were proportional to the

agitator speed. He concluded that the fluid velocity at any particular point in the fluid could be expressed as a constant fraction of the agitator tip speed. Experiments showed that this fraction remained approximately the same for geometrically similar points in geometrically similar systems. Cutter (18) performed similar experiments; his results supporting those of Bowers.

Another facet of Bower's work was an investigation into the turbulence produced by impellers. The intensity of turbulence, defined as the root mean square of the fluctuations in velocity at a given point, was found to be proportional to the agitator speed. However, the relationships between intensity of turbulence and tip speed were found to be characteristic of a particular system. The intensity contours of the laboratory vessel were not reproduced in the scaled vessel, after scaling up using constant tip speed. Identical turbulence contours could be obtained by adopting a different impeller design for the scaled vessel.

This turbulence and velocity phenomena lends itself to the mixed regime concept, i.e. for geometrically similar systems identical velocity contours are obtained but the intensity of turbulence relationships are not reproducible; with a different impeller design, (loss of geometric similarity), the intensity of turbulence can be maintained in both systems but the velocity contours are changed. Although this knowledge tends to detract from the use of constant tip speed as a scale-up criterion, it must be noted that this criterion is the first to be associated with actual flows present in the vessels and thus superior to the dimensionless group approach.

The use of a constant dimensionless group as a rule of scale-up leaves much to be desired, as it gives no indication of the final process result of the scaled up system. It would be of great advantage to have a relationship of power, impeller size and speed to point velocities and turbulence. Then more reliable scale-up could take place.

In an attempt to bring about a closer relationship between the final products obtained in the laboratory and scaled up mixing vessel, the rule of scale-up using constant power per unit volume was introduced. Although this rule has been much maligned due to its excessive power requirements in the scaled vessel, it has been found to give good results over a wide range of applications where reasonable rates of flow and shear were required. (32, 33).

The derivation of criteria to assess impeller ability has always been dictated by the techniques and the equipment available at that particular period of time. In recent years many new parameters have emerged in fluid mixing. These are introduced in the following sections and their application to scale-up discussed.

3.2 Mixing in Stirred Vessels

A search of the literature will reveal three distinct eras in the history of fluid mixing. They may be classified as follows:-

i) The empirical approach.

ii) The impeller characteristic approach.

iii) The process dynamic approach, model building.

3.2.1. The empirical approach

White (74) and later Hixson (31) were the stalwarts of the empirical approach to mixing. During this initial period, research was directed towards the publication of dimensionless plots of Power Number against Reynolds Number for a variety of impeller and tank configurations. Rushton, Costich, and Everitt (62) were responsible for a comprehensive paper of many such plots. Various criteria were also proposed which gave some help in the selection of the impeller-type for a particular system, but their range of application was limited.

The development of scale-up rules arising from this era has been discussed in the preceeding section.

3.2.2. Impeller characteristic approach

Impeller characteristics were first proposed by Rushton and Miller (58). They produced four criteria by which the prowess of any agitator could be assessed, and these have since found general use in the chemical and allied industries.

i) Power Requirement.

ii) Impeller Discharge Capacity.

iii) Velocity of Discharge.

iv) Shearing Characteristics.

With the advent of these rules research progressed on new lines. Dimensionless plots were still forthcoming, but now greater attention was focused on the development of expressions relating impeller characteristics to the mixing taking place in the vessel.

3.2.3. Flow patterns

The investigation of fluid flow patterns was an obvious extension of the research. Such investigation showed that the choice of impeller was governed by the flow pattern required. An illustration of this phenomena is a suspended solid system; the need for an upward velocity from the impeller is apparent in order to prevent the solids settling. Thus an impeller producing a large axial component of flow is necessary.

Excellent work in this field was performed by Nagata et al (47, 48, 49) using photographic methods; they investigated the patterns set-up by turbine impellers. Porcelli and Marr (55) did similar work for propellers. The following diagrams show the basic induced flow patterns for turbine and propeller agitators which evolved from their work.

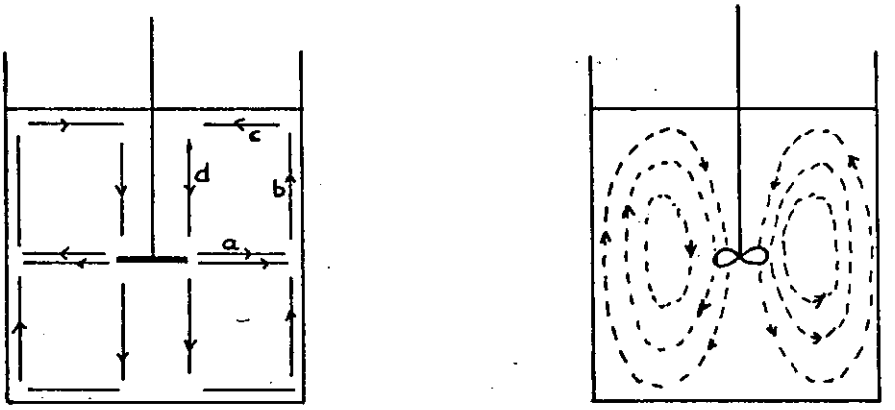

Fig. 3.1.

(a) turbine (b) propeller

The recirculatory flow pattern of a turbine stirred tank may be described as:

a) Horizontal discharge jet running from the blade to the wall.

b) Separation of the flow into a two vertical components at the wall.

c) Horizontal component returning the fluid to the stirrer shaft.

d) Two vertical flow components back to the impeller region.

The radial component of flow produced by the turbine impeller is not found in the propeller agitated system; with the propeller an axial component dominates the induced flow pattern. The streamlines produced by each impeller have a centre which is known as the circulation eye. The position of this "eye" is dictated by the impeller position in the fluid (47, 34).

The introduction of baffles into a tank converts the angular momentum component into a vertical component of flow; the vessel is subdivided into distinct sections, Fig. 3.2. The overall flow pattern, however, remains unchanged.

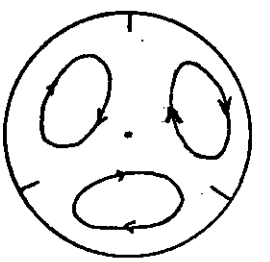

Fig. 3.2

The induced flow has been found to be a function of tank geometry; the ratio of induced flow to impeller discharge flow being dependent on the tank/impeller diameter ratio. Investigation has shown that some mixing operations require relatively large mass flows for effective mixing, whereas others require a large amount of turbulence. The ratio of mass flow to turbulence, for the same power input, depends on the size and rotational speed of the impeller; hence different flow regimes can be achieved by proper sizing of the impeller.

3.2.4. Pumping capacity

After the realisation that an impeller rotating in a fluid was acting as submerged pump, many attempts were made involving a variety of ingenious methods to equate the volumetric flow of liquid discharged to impeller dimensions and speed.

Ruston (59) developed a "double-tank experiment" where the volume of liquid pumped from the inner to the outer tank was equal to the impeller pumping capacity. Rushton et al (61) also developed a streak-photography technique. Illuminated particles were photographed using an exposure time which resulted in the particles appearing as streaks on the developed print; measurement of a large number of these streaks enabled the magnitude and direction of point velocities to be obtained throughout the system. Other published techniques involve the use of velocity measuring probes of the pitot-tube type. A velocity traverse of the impeller with such a device, enables the total flow to be found by an integration procedure.

A simple technique, applicable for all impeller types was developed by Marr and Johnson (44) using a zero buoyancy float; the average time taken by the float to complete a cycle of the tank, i.e. from impeller into the body of the vessel and back to the impeller, was an indication of the pumping capacity of the impeller. This technique, along with the photographic method, has the added advantage of not interferring with the basic flow pattern.

Numerous theoretical treatments have been published (15), (68), without experimental verification. These along with experimentally derived expressions have usually led to the pumping capacity being expressed as a function of impeller speed, width/diameter ratios, blade number, etc. It is normal to find an

expression which relates the pumping capacity (q) directly to the product of impeller speed (N) and the third power of the impeller diameter (D).

$$q = KND^3 \qquad (3.4)$$

The proportionality constant (K) is a characteristic of impeller type. The possible direct use of constant pumping capacity as a scale-up rule has been suggested (15),but as will be shown later there is no justification in doing so.

Extension of the rules proposed by Rushton and Miller (58) resulted in many more new terms hitherto unassociated with the choice of impellers and with mixing in general. These terms have proved to be of great value in establishing a better understanding of impeller proficiencies and applicability in design and scale-up. A discussion of some such terms follows.

3.2.5 Batch mixing time

If a pulse of tracer solution is added to a stirred vessel the initial concentration between the pulse and vessel contents will decay with time, until all parts of the vessel fluid have a uniform concentration. The time taken to obtain this uniformity is described as the "mixing time", and is characteristic of the impeller/tank configuration, the fluid flow patterns and the fluid velocity and properties.

Batch mixing time is a criterion which has been used extensively to compare the merits of different impellers. van de Vusse (67) Fox and Gex (23), Metzner and Norwood (50), Kramers et al (38) and Oldshue (53) derived by dimensional analysis, empirical relationships for a "mixing time group" as a function of other dimensionless groups. They then proceeded by experiment to study

the effect of each of these groups in turn on the mixing time group. The following are the most widely used correlations.

Metzner and Norwood (50):- Correlation for turbine impellers. Fig. 3.3.

$$N\theta\left(\frac{D}{T}\right)^2 \cdot \frac{g^{1/6}}{(N^2 D)^{1/6}} \cdot \frac{T^{1/2}}{Z^{1/2}} = f(N_{Re}) \qquad (3.5)$$

for $N_{Re} > 10^5$

$$\theta = K_2 \cdot \frac{T^2 (N^2 D)^{1/6} Z^{1/2}}{N D^2 g^{1/6} T^{1/2}} \qquad \text{where } K_2 = 5 \qquad (3.6)$$

Experiments were conducted for a range of geometrically similar disk and vane-type turbines, diameter 2" - 6", W/D = 1/5, and for tank diameters of 5" - 15.5". The tanks were also baffled with 0.1D baffles. All experiments were performed with the turbine centrally positioned at a height of 35% of the liquid depth from the base of the tank. Mixing times were measured as the time required to neutralise a known amount of acid, dispersed in the fluid, by an equivalent amount base. The base was added at a point near the turbine, and the indicator used was methyl red. They noted that the mixing time group versus Reynolds Number plot was analogous to the Power Number versus Reynolds Number plots of earlier researchers. The Metzner and Norwood correlation can be adapted for scale-up of the impeller variable at constant mixing time. The mixing time group yields the following expression for the stirrer speed in terms of the scale ratio (L), for geometrically similar systems.

$$N_2 = L^{1/8} N_1 \quad , \quad \left(N_{Re} > 10^5\right) \qquad (3.7)$$

Metzner-Norwood: Correlation for turbine batch mixing time

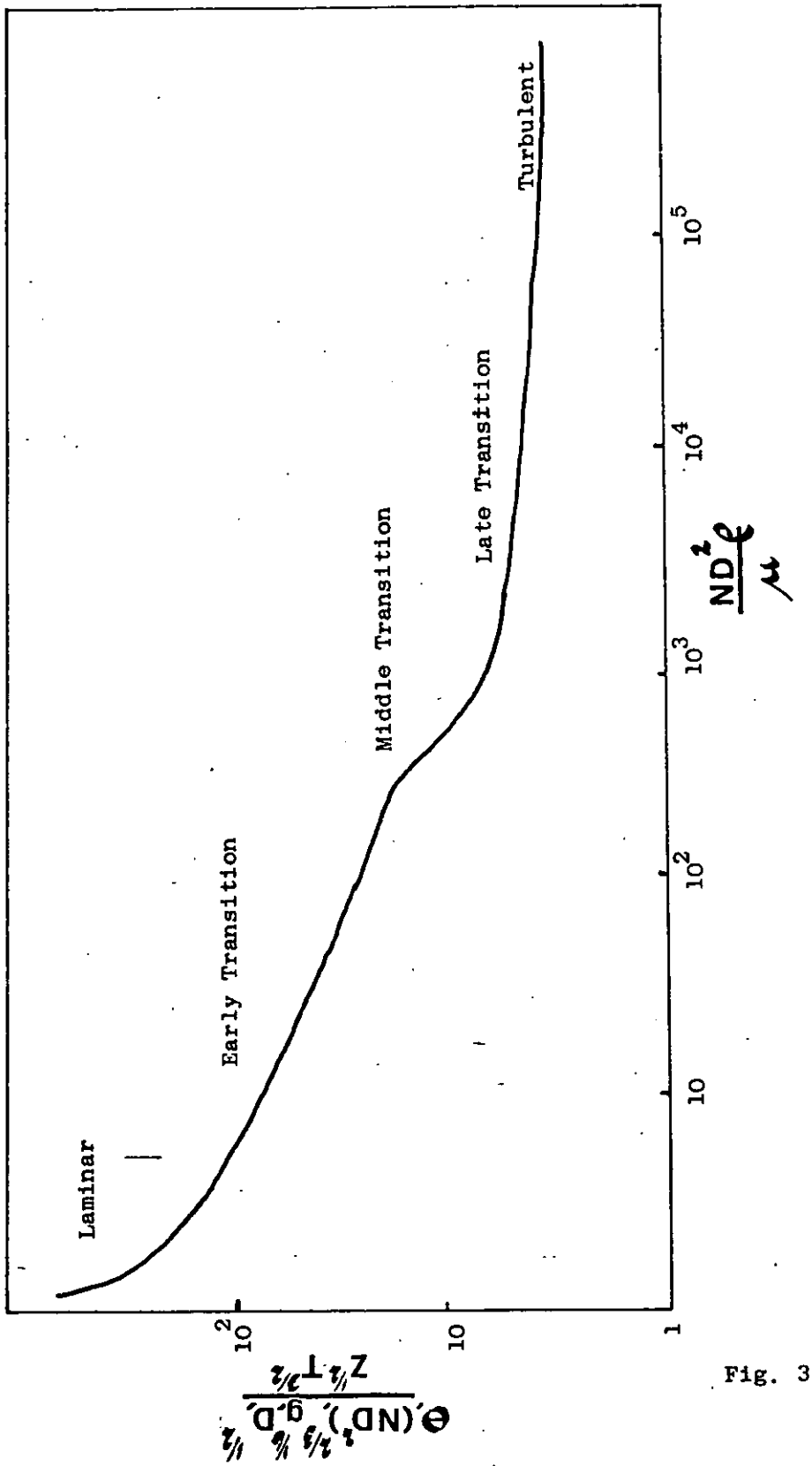

Fig. 3.3

Fox and Gex (23):- Correlation for propellers; a similar correlation exists for jet mixing.

$$N\Theta\left(\frac{D}{T}\right)^{3/2}\cdot\frac{g^{1/6}}{(N^2D)^{1/6}}\cdot\left(\frac{T}{Z}\right)^{1/2} = f\left(N_{Re}\right) \qquad (3.8)$$

They produced, by dimensional analysis, correlations for jet and propeller agitated vessels; the indicator technique was used to verify their derivations. The propellers were of a square-pitch design with diameters ranging from 1" - 22". The tank diameters ranged from 6" to 14'. The propeller position was not stated but it was specified that no general swirl or rotation was present. The effects of rotational speed, liquid depth and viscosity on mixing time were investigated.

Using Reynolds Number as abscissae, their correlation produced a plot of dimensionless mixing time group against impeller Reynolds Number. From this plot it was apparent that a change in slope occured at the transition point between the laminar and turbulent region. The similarity between this plot and the Fanning friction chart initiated their term of "mixing time factor".

Again a simple expression is derived for scale-up of constant mixing time using the Fox and Gex correlation. For geometrically similar systems it reduces to:-

$$N_2 = N_1 L^{1/4}, \quad \left(N_{Re} > 10^5\right) \qquad (3.9)$$

van de Vusse's Correlation (67)

$$\frac{Qq}{V} = f_1\cdot\frac{ND^2\rho}{\mu}\cdot f_2\cdot\frac{\rho N^2D^2}{\Delta\rho g Z}\cdot f_3\cdot\frac{D^3}{T^{2.5}Z^{0.5}} \qquad (3.10)$$

which reduces for geometrically similar systems, to

$$\frac{\theta q}{V} \propto \left(\frac{N^2 D^2}{\Delta \rho g Z}\right)^{-a} , \quad N_{Re} > 10^5 \qquad (3.11)$$

a = 0.25 for propellers.

a = 0.30 for flat paddle impellers.

a = 0.35 for pitch blade paddle impellers.

van de Vusse adopted a different experimental procedure for determining batch mixing time. He developed a Schlieren technique to determine the time when refractive index differences in the fluid disappeared. This he took as the mixing time. Initially, two liquids of approximately equal density were added sequentially to form two layers with a definite interface in the vessel. Differences in refractive index in points in the fluid resulted in shadows which were related to the patterns inside the vessel. After the contents had become completely mixed, the light beam was unaffected and the shadows disappeared. The experimental work was conducted in unbaffled vessels for a variety of impeller shapes and sizes.

This correlation was the first to make definite reference to the impeller pumping capacity (q); the term appears in one of the dimensionless groups.

The simple scale-up rule derived from the correlation of van de Vusse, for a geometrically similar system is:-

$$N_2 = N_1 L^{-\frac{1}{6}} , \quad N_{Re} > 10^5 \qquad (3.12)$$

As the respective "mixing time groups" of the three previous correlations are functions of Reynolds Number for ($N_{Re} < 10^5$), their use for scale-up at constant mixing time

is limited. However, in all cases the "mixing time group" is constant for ($N_{Re} > 10^5$), thus scale-up expressions can be derived for this range.

These empirical correlations are best suited to the prediction of mixing time after having scaled the stirrer variable by one of the other known scale-up criteria. It must be stressed that the correlations of Fox and Gex, and Metzner and Norwood are of a one-off nature. They are not general correlations encompassing all turbines and propellers. Any variation in impeller characteristics such as width/diameter ratios, pitch, number of blades, etc. is not catered for by these expressions. van de Vusse attempts to rectify this by incorporating impeller pumping capacity into his "mixing time group", thus making his correlation more general.

Another technique employed in the experimental determination of mixing time is the use of conductivity cells. Biggs (5), operating with a conductivity cell placed at the outlet of a continuous stirred vessel, determined mixing time from the chart recording made by the response of this cell to a pulse of tracer injected into the inlet stream. He conducted experiments for a whole range of impellers and derived a correlation from the results. His results for the disk-vane turbine compared favourably with those of Metzner and Norwood. This is not altogether conclusive as there was a difference in (W/D) ratio and therefore the pumping capacity used by the two experimenters. (Biggs, W/D = 1.8, M and N, W/D = 1.5).

Kramers et al (38) using the conductivity cell technique in a batch vessel, with probes situated at distances of 1/8 of the liquid height from the liquid surface and from the bottom of the vessel, produced a correlation involving the power requirement of the impeller. The impulse of tracer was injected at the liquid

surface. They further investigated the effect of eccentricity of the propeller on mixing time and showed that mixing time was increased as the distance of the impeller from the central axis was increased. Variation of the angle of inclination of the stirrer was noted to have little effect on the mixing time. This correlation along with the correlation of Oldshue (53) has been shown to give the same scale-up rule as that derived by Corrsin(17) for isotropic turbulence. Assuming geometric similarity in all cases the expression is:-

$$P_2 = P_1 L^5$$

Prochaka and Landau (56) using a 6 blade disk-type turbine, a pitch blade turbine and a marine impeller, placed in vessels of equal liquid height to tank diameter, produced a relationship for each of the three cases for Reynolds Number greater than 10^4. Agreement was found between these results and those of Kramer et al (38).

Holmes et al (34) produced a simple expression for the calculation of batch mixing times, which incorporated the pumping capacity of the impeller and the circulation time of the fluid. They defined circulation time as the residence time in a loop averaged over all the streamlines. In their experiments conductivity cells were located at the vessel wall at a height equal to one half of the liquid depth. On injection of an impulse of tracer, a constant reading was obtained after five successive peaks had been recorded. The peaks were found to be of constant freequency, for a particular impeller speed, and therefore said to be a measure of the circulation time. The mixing time was taken to be 5 times the interval between the peaks, which results in equation 3.13.

$$5\,\Theta_c = \Theta_m \qquad (3.13)$$

Equation 3.13 results in the simple rule for scale-up using either constant circulation time or constant mixing time, for geometrically similar systems of scale ratio L.

$$N_1 = N_2 \qquad (3.14)$$

Voncken et al (72) extended this work to the continuous system but although the frequency of the response was reproducible the amplitude of the peaks was not.

Marr and Johnson (45) simulated batch mixing by equating the throughput in the real time expression for continuous mixing, derived from a continuous flow model to zero. Consequently they obtained an expression which described the concentration fluctuation, after an injection of an impulse of tracer into a batch system. From this expression they found that the time required to reach a given level of homogenity, the batch mixing time, was inversely proportional to the impeller speed. They complemented these results with the following direct mathematical treatment of the batch system.

Fluid elements follow different streamlines and require a range of times to describe their passage through the circulation loop and back to the impeller. The concentration at the stirrer, after an impulse of tracer, may therefore be simulated by the summation of a series of terms.

$$C_B(s) = \Delta C_B \left[G(s) + G^2(s) + \ldots\ldots G^n(s) \right] \qquad (3.15)$$

By approximation of the series expansion and using two stages in series to simulate the mixing in the circulation loop (G(s)), equation 3.14 can be inverted to give:-

$$C_B(t) = \frac{\Delta C_B}{V} q \left[1 - \exp\left(\frac{-4\theta}{V} q \right) \right] \qquad (3.16)$$

thus,

$$\frac{C_B(\infty)-C_B(t)}{C_B(\infty)} = \exp\left(\frac{-4\theta q}{V}\right) \qquad (3.17)$$

The batch mixing time θ is the time required for the left hand side of the equation 3.17 to reach an arbitrary small value. Therefore equation 3.17 reduces to:-

$$\theta \propto \frac{V}{q} \propto \frac{1}{N} \qquad (3.18)$$

As (V/q) is the ratio of vessel volume to impeller pumping capacity, i.e. the circulation time, the results of Marr and Johnson are found to be in agreement with the expressions of van de Vusse (67) and Holmes et al (34). The expressions derived by these workers, Equation 3.13 and Equation 3.18 show mixing time to be directly proportional to circulation time. Thus scale-up of geometrically similar systems, using equation 3.18, would again be described by Equation 3.14.

3.2.6. Mixing mechanisms

The primary purpose of mixing fluids is to distribute components of a non uniform system rapidly in a random manner to produce a uniform one (40). Following the introduction of the mixing time concept, the mechanisms by which homogenity is achieved, were discussed. In order to distinguish between the modes of mixing the terms macromixing and micromixing were introduced.

Micromixing is the type of mixing which takes place when individual molecules are free to move about the liquid, to collide and intermix with all other molecules of the fluid. The turbulence which comes from the velocity fluctuations near the

discharge stream in the body of the fluid, gives rise to this effect.

Macromixing is the term used to describe mixing which takes place on any level other than a molecular one. The molecules are held together and move about the fluid in an aggregative manner without any mixing taking place within the group. It is produced by the conversion of mechanical energy from the impeller into the discharge flow stream which has been displaced by the impeller. This flow stream is responsible for the flow pattern established throughout the vessel.

Further terms which are now commonplace in mixing are degree of segregation, scale of turbulence, etc. but as these are not used here their discussion will be limited.

3.3. The Dynamic Approach - Model Building

The continuous flow process in industry was initiated to bring about greater effectiveness and profitability from existing batch processes. With the advent of this new era, the need arose for better plant control and assessment of system parameters. In order to accomodate this, a new range of mathematical techniques were developed, in an attempt to characterise dynamic systems.

Research was subsequently directed towards the production of mathematical models for mixing systems, from both a theoretical standpoint and by means of various new techniques, such as dynamic testing.

If the outlet response of a steady state system which has been subjected to a disturbance, is measured with respect to time, the response obtained is characteristic of the dynamic behaviour within the vessel. The disturbance used can be in the form of an impulse, a pulse, a step, or a continuous sinusoidal function. Each type of disturbance gives the same

information for linear systems; the results are interchangeable and the choice of forcing function a practical one. The one most frequently adopted is the impulse disturbance, as for practical purposes it may be assumed to be a true Dirac delta function, because its duration is negligible compared with that of the system response. Mathematically the Dirac delta function is also easily manipulated.

Danckwerts (19) in 1953 presented the now standard procedure for the interpretation of the response of continuous flow systems to impulse and step disturbances. The probabilistic content of these responses was shown to be closely related to the internal and external age distribution functions respectively. Following this publication a considerable amount of research was directed towards the study of non-ideal mixing in continuous flow systems.

3.3.1. Residence time distribution models

The manner in which mixing takes place in a mechanically - agitated vessel depends upon the impeller characteristics and the flow pattern induced within the fluid. The residence time distribution depends on the nature of the mixing and of the process. This concept has found great application in model building. (40) In a perfect mixer, one in which all elements have an equal chance of leaving, the residence time distribution is an exponential decay. This can only be approximated in reality.

The first attempt to obtain a theoretical model to describe the real behaviour of a stirred tank produced a series of models which were not based on the flow pattern within the vessel. Cholette and Cloutier (12) offered the following reasons for the deviation of measured residence time distributions from the exponential decay of an ideal system; stagnant regions in the

vessel; by-passing of a fraction of the feed directly to the outlet, and regions of the vessel through which material flows but in which no mixing takes place.

A further addition to the list of empirical models was that of the time delay model; this consisted ofawell mixed stage in series with a plug flow region. This simple model received wide use in early model building. (32) Other models then came to light which described the behaviour of continuous flow systems that deviated significantly from the ideals of perfect mixing and plug flow. Such models as the tanks in series and the dispersion model were a definite advancement in the extension of model building. However, it was apparent that characterisation of systems with mathematical expressions derived from an analogy with the physical reality, would be more advantageous. Such models would explain why the residence time of elements in the system were so distributed. In the case of the stirred tank reactor this has led to the development of the recirculation model.

3.3.2 Single loop recirculation model

The fluid flow patterns induced in mechanically agitated systems are predominantly of a recirculatory nature:- fluid pumped by the impeller flows through the body of the fluid before returning to the impeller region. The single loop recirculation model incorporates this phenomena. This basic model has been proposed for a number of simulations; variety having been introduced by the manner in which mixing in the recirculation loop and the impeller region has been characterised.

Weber (73) suggested using a simple recirculation model, with plug flow recirculation, as a design criteria for fluid blenders.

Norwood and Metzner (50) also assumed plug flow recirculation as the mechanism whereby the contents of a turbine agitated vessel were conveyed to the immediate vicinity of the impeller, where mixing was sufficiently intense on a molecular level to promote an instantaneous neutralisation reaction. Marr and Johnson (45) in a study of propeller mixers assumed perfect mixing close to the impeller and that the flow in the recirculation loop could be characterised by the tanks in series model. Holmes et al (34) proposed a similar version of the same model for turbine agitators but chose to characterise mixing in the loop by a dispersion term.

Engh (22) showed that the effectiveness of large stirred buffer storage vessels could be increased by adding an external recirculation loop. The model chosen consisted of regions of plug flow and perfect mixing in series with recycle; this same model had previously been suggested by Gibilaro (25), the recycle being produced internally by the pumping action of the impeller.

The plug flow with recycle model has been advocated in other less obvious applications. Gillespie and Carberry (29) used it as a purely descriptive model, in preference to the tanks-in-series and dispersion models, to account for non-idealities in mixing; this was shown to considerably simplify reactor calculations for systems where plug flow rate equations are available. In another paper (30) the same authors applied the model to a kinetic scheme in which the optimum mixing level lay between perfect mixing and plug flow. van de Vusse (70) also used recycle models to obtain the optimum recycle for various reaction schemes where selectivity and reactor volume are affected. Rippin (57) showed that the plug-flow-with-recycle reactor is always a "maximum mixedness" reactor in that the

mixing occurs as early as is compatible with the residence time distribution. Clegg and Coates (13) used a single loop model consisting of two parallel regions, each characterised by stages-in-series, for describing the behaviour of a filled cylindrical vessel agitated solely by the non-axial entering and leaving streams. The addition of a recycle loop has been suggested as a means of increasing the flexibility of the stages-in-series model for general descriptive purposes (16).

3.3.3. The generalised single loop recirculation model

The general single loop recycle model is shown in Figure 3.4; the loop is divided by the inlet and outlet streams and the two regions are characterised by the transfer functions $F_1(s)$ and $F_2(s)$ as shown; the throughput flow is Q, the recycle rate q, the inlet and outlet concentrations Ci and Co respectively. The table lists the characterisation of $F_1(s)$,$F_2(s)$ used by the authors.

3.3.4. Multiloop recirculation models

The development of multiloop models followed the investigation of flow patterns by Nagata et al (47), Figure 3.1a. van de Vusse (71) made the first published attempt to represent the multi-circulation-loop flow pattern of turbine stirred vessels, with an analogous three-loop model. However the simplification he adopted for the inversion of the model Laplace transform reduced the multiloop interpretation to that of a single loop model. Later, Gibilaro et al (27) were able to overcome this by using a numerical integration procedure. They also proposed a generalised multiloop model which could be adapted for various operating conditions. The development of this model receives a detailed analysis in Chapter 4.

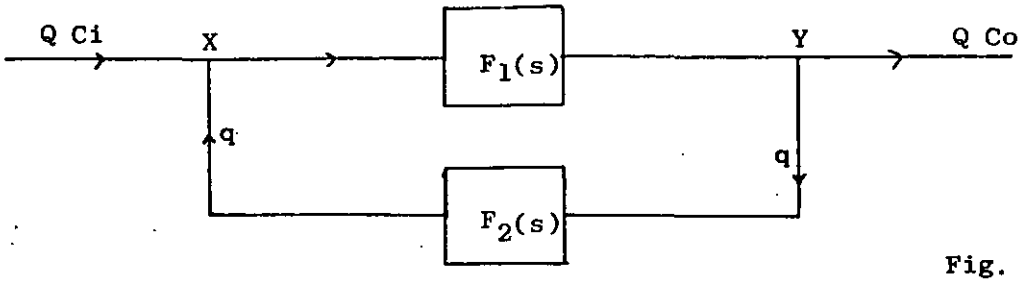

Fig. 3.4

Mass Balance at X and Y

$$QCi + qCo.F_2(s) = (q + Q)Cx$$

$$(q + Q)Co = (q + Q)Cx.F_1(s)$$

hence

$$G(s) = \frac{Co}{Ci} = \frac{Q}{(Q + q)/F_1(s) - qF_2(s)} \qquad (3.19)$$

Table of Authors $F_1(s)$, $F_2(s)$

Reference		$F_1(s)$	$F_2(s)$	Application
Clegg & Coates	13	C.S.T.R. in series	C.S.T.R. in series	Characterisation of unstirred vessel.
Engh	22	C.S.T.R. in series with P.F.R.	——	Efficiency of buffer storage tanks.
Gibilaro	27	——	C.S.T.R. in series	Characterisation of turbine stirred tank.
Gillespie & Carberry	29	P.F.R.	——	Reactor Design
Marr & Johnson	44	——	C.S.T.R. in series	Propeller batch mixing time.
Norwood & Metzner	50	C.S.T.R.	P.F.R.	Turbine batch mixing time.
Rippin	57	P.F.R.	——	Model comparison
van de Vusse	67	——	C.S.T.R. in series	Characterisation of turbine stirred tank.
Voncken et al	72	——	Diffusion term	Characterisation of stirred tank.
Weber	73	——	P.F.R.	Design criteria
Wood	76	C.S.T.R.	P.F.R.	Characterisation of stirred vessel.

C.S.T.R. - ideal mixing stage
P.F.R. - plug flow reactor

3.3.5. The gamma function model

The gamma function model is an extension of the tanks in series approach to process simulation. It is an empirical model with a single easily manipulated parameter (9).

Consider (n) ideal stages in series of volume (v), total system volume V, and system meantime τ ; the transfer function for one small stage is:-

$$G(s) = \frac{1}{\left(\frac{\tau s}{n} + 1\right)}$$

For n stages,

$$G_n(s) = \frac{1}{\left(\frac{\tau s}{n} + 1\right)^n} \qquad (3.20)$$

Inverted equation (3.20) becomes,

$$G(t) = \frac{e^{-nt/\tau}\, t^{n-1}}{\Gamma n} \left(\frac{n}{\tau}\right)^n \qquad (3.21)$$

The tanks in series model has proved inadequate for low values of (n), so much so that Corrigan (16) added a recycle stream to the normal configuration to give the model greater flexibility. This addition in no way changes the basic shape of the residence time distribution of the model. However, the gamma function model has the property of producing different residence time distributions for various values of (n). For (n) less than unity the response is a distorted exponential decay with a maximum at infinity for time zero. For (n) greater than unity the model reaches a maximum after a definite time interval. The gamma function approach has a wide range of application because of this inherent difference in residence time distribution for

various values of (n). It supersedes the tanks in series simulation.

3.3.6. Continuous mixing time

The residence time distribution of the single loop model proposed by Marr and Johnson (45) led them to suggest a criterion for assessing continuous mixing time. The basic configuration of this model is shown in Figure 3.6. The impeller "blender" region is assumed to be of zero volume; with the flow streams being instantaneously mixed there. The distributor region was assumed to be equivalent to two stages in series, i.e. the mixing in the steamlines was characterised by this representation. Figure 3.6 can be further simplified to Figure 3.7.

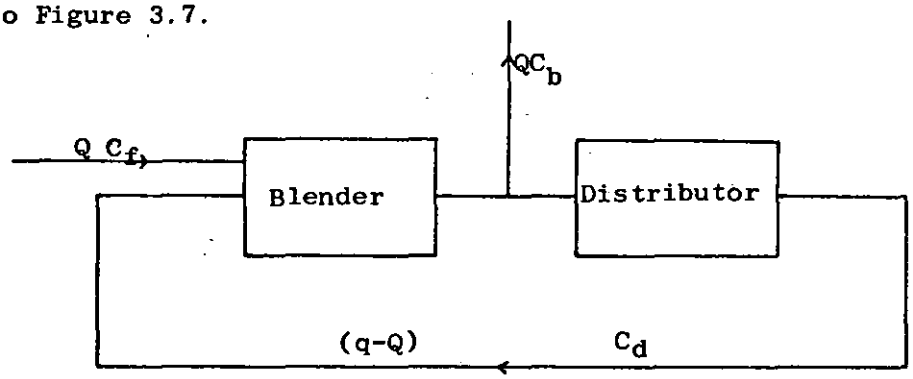

Fig. 3.6

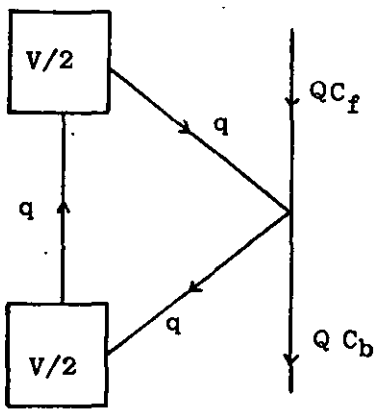

Fig. 3.7

A typical normalised response of this model is illustrated in Figure 3.8, a fraction of the pulse being directed immediately to the outlet giving an impulse at time zero.

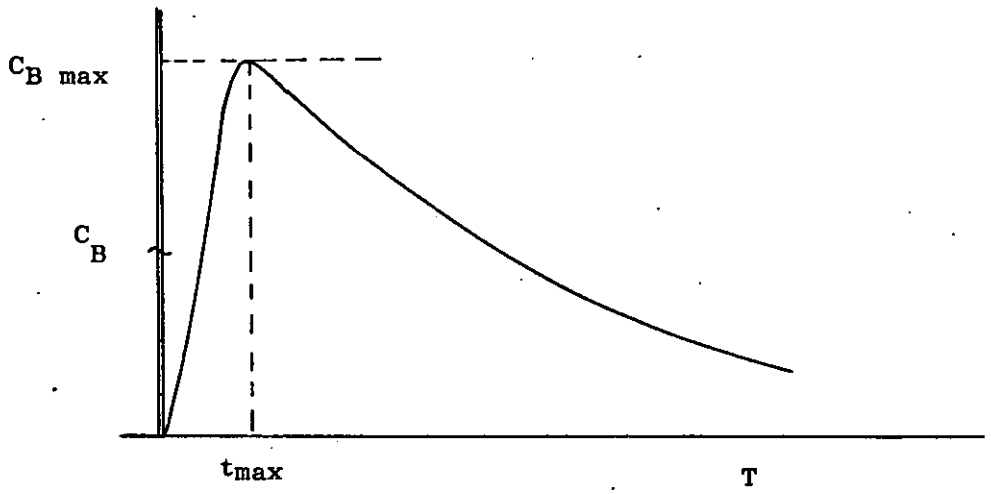

Fig. 3.8

Continuous mixing time was assumed to be the finite time (t_{max}) taken for the response to reach a maximum ($C_{B\ max}$), this interval should correspond to the time for a pulse of tracer to be mixed uniformly throughout the vessel. The location of this maximum can be obtained mathematically by setting the derivative of the real time expression, with respect to time, to zero. They also used the comparison of the slopes of concentration versus time (impluse response data) plotted on a log-linear scale, as a further indication of continuous mixing time. They found a time of twice (t max) gave a straight line plot, for all values of the model parameter.

As previous workers have shown, and as will be further amplified in this work, feed directed to the impeller results in a by-passing phenomena in the residence time distribution; such responses do not have a definite peak at a finite time. The maximum occurs at (t = 0) and is infinite, the responses being asymptotic to the concentration axis. As Marr's model was

proposed for feed to the impeller, it leaves much to be desired that his model has a maximum after a finite time. In a later section a comparison of Marr's model with experimental responses takes place and the discrepancies of this model are further illustrated.

Conover (14) developed an expression for assessing continuous mixing time using the same initial assumption and mathematical interpretation as Marr. In this case the mixing was characterised by a series of first order operations with the same time constant. This approach incorporates the first use of the gamma function in process simulation. By setting the real time expression of the gamma function model equal to zero he obtained the following expression for tmax.

$$t\,max = \left(\frac{n-1}{n}\right)\tau \qquad (3.22)$$

The model parameter (n) and the time constant (T) were computed by a least squares method. Although the approach is a novel one it has a limited application. This work will show that $n > 1$ characterises residence time distributions of stirred vessels which have inlet feed lines directed into the upper loop region of the fluid; for feed directed into the impeller the responses are characterised by ($n < 1$). As equation 3.20 only has any real meaning for $n > 1$, it would appear that this technique has little application for other than feed to the loop.

The use of the maximum of the real time response as the basis for assessing continuous mixing time is reasonable, but as the analytical expressions are solely dependant on the type of model proposed, the subsequent difference in results leads to confusion. The assumption that a pulse of tracer is well mixed,

giving complete homogenity in the system at the time the response starts to decay is debatable. As continuous mixing time is assessed from an expression which characterises the outlet response it is unlikely that it is truly indicative of the actual conditions (degree of homogenity) inside the vessel. An expression relating intensity and scale of turbulence with concentration fluctuations, and impeller pumping capacity/ throughput ratios would be of greater advantage. A comparison conducted in Chapter 5 further illustrates the variation in continuous mixing time arising from these and other techniques of assessment.

3.4. Economic Scale-up:- Batch System

An interesting approach to the scale-up of batch liquid systems has recently been suggested by Standart (64). Using the following basic relationships he was able to express the cost of a batch mixing system as a function of the vessel diameter.

$$N\bar{T}' = k_1$$

$$P = k \rho N^3 D^5$$

$$D^3 = k_3 V\bar{T}'$$

$$£ = k_4 P + k_5 D^2$$

The cost of the operation was expressed as the sum of a power and a depreciation cost, calculated using the 2/3 power law. Thus for a given production rate he was able to find the optimum diameter for a minimum operating cost.

$$D^6 opt = 2 \rho k_2 k_4 (k_1 k_3)^3 V^3 / k_5$$

On eliminating the production rate, he found a relationship between the optimum vessel diameter and optimum impeller speed; the only combination of system variables which was independent of the production rate.

$$N_{opt}\, D_{opt} = \left(\frac{k_5}{2\rho k_2 k_4}\right)^{1/3} \qquad (3.23)$$

Equation 3.23 is identical with scale-up at constant impeller tip speed, the advantages of which have already been discussed.

This approach to scale-up of stirred vessels is most worthwhile. It is the resultant requirement of a series of technical and economic factors, which further illustrate the limitations of empirical scale-up rules.

4. DERIVATION OF THE MODELS

4.1. Derivation of the Models

The main use of mathematical models is to facilitate design, for predictive purposes and to enable the optimisation of operating conditions to be performed. Thus any model developed from basic concepts and bearing an analogy with the physical process will be of greater use than one of a purely empirical nature. The dominating factors which govern the operation of a stirred vessel are flow patterns and impeller pumping capacity. Thus in order to derive a worthwhile model, it is essential to incorporate these factors. In this chapter two models are presented which do this.

The effect of impeller position on induced flow pattern, for turbine and propeller agitated systems was examined using a streak photography technique. The photographs obtained for the turbine system, P.1. - P.8, clearly illustrate the effect of impeller position on the overall flow pattern. P.1, (turbine positioned just above the base of the vessel), shows a single-loop pattern. A vortex, between the wall and the base of the vessel is clearly defined, and the flow pattern in the upper regions of the fluid is shown to be of random nature. P.2, P.3 illustrate the same phenomena. In P.4, the flow pattern in the upper region is more distinct. For this turbine position (0.35Z), Z is the liquid height, a single or double loop representation of the flow pattern would be equally correct as there is no indication as to which pattern is predominant. In P.5 - P.6, turbine positioned at 0.45Z and 0.6Z respectively, the double loop flow pattern is clearly seen; upper and lower vortex regions being distinctly defined. With the turbine positioned higher in the fluid P.7 - P.8, the upper vortex dominates the flow pattern with the lower vortex becoming less distinct. Consequently the flow pattern in the lower

P.1 Turbine Position 0.025Z

Single Loop

P.2 Turbine Position 0.15Z

Single Loop

P.3 Turbine Position 0.25Z

Single Loop

P.4 Turbine Position 0.35Z

Single Loop - Double Loop

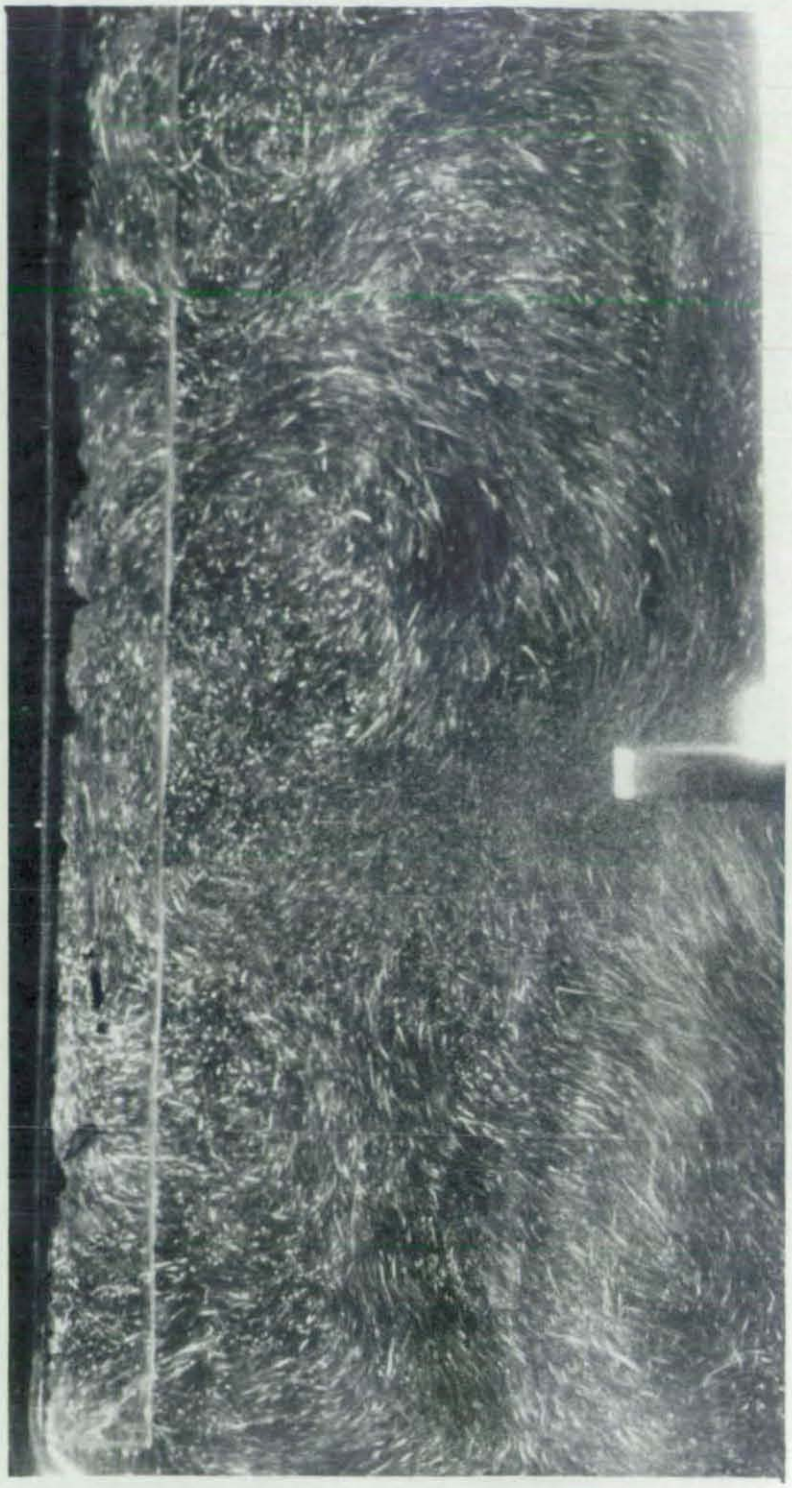

P.5 Turbine Position 0.45Z

Double Loop

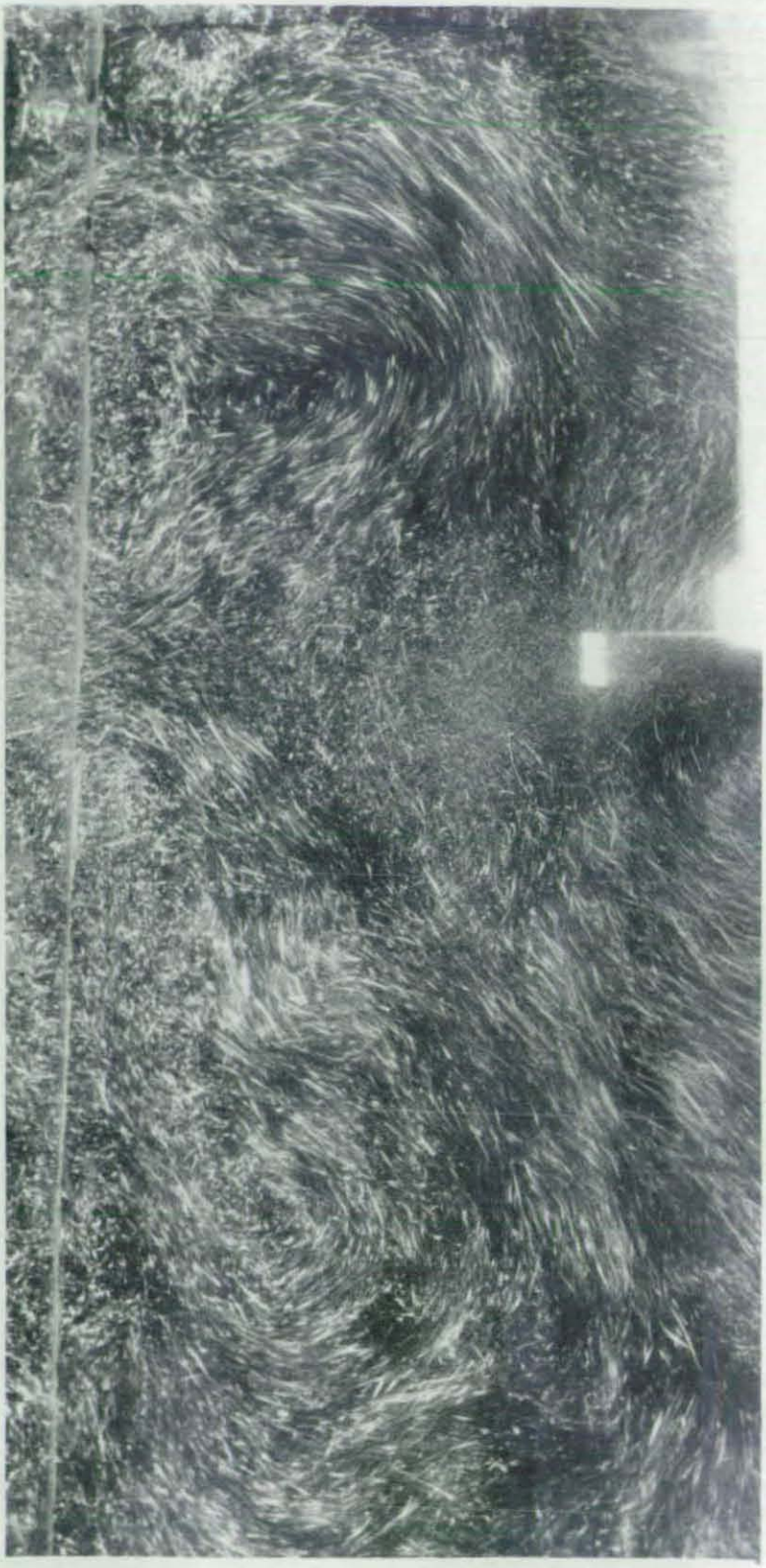

P.6 Turbine Position 0.60Z

Double Loop

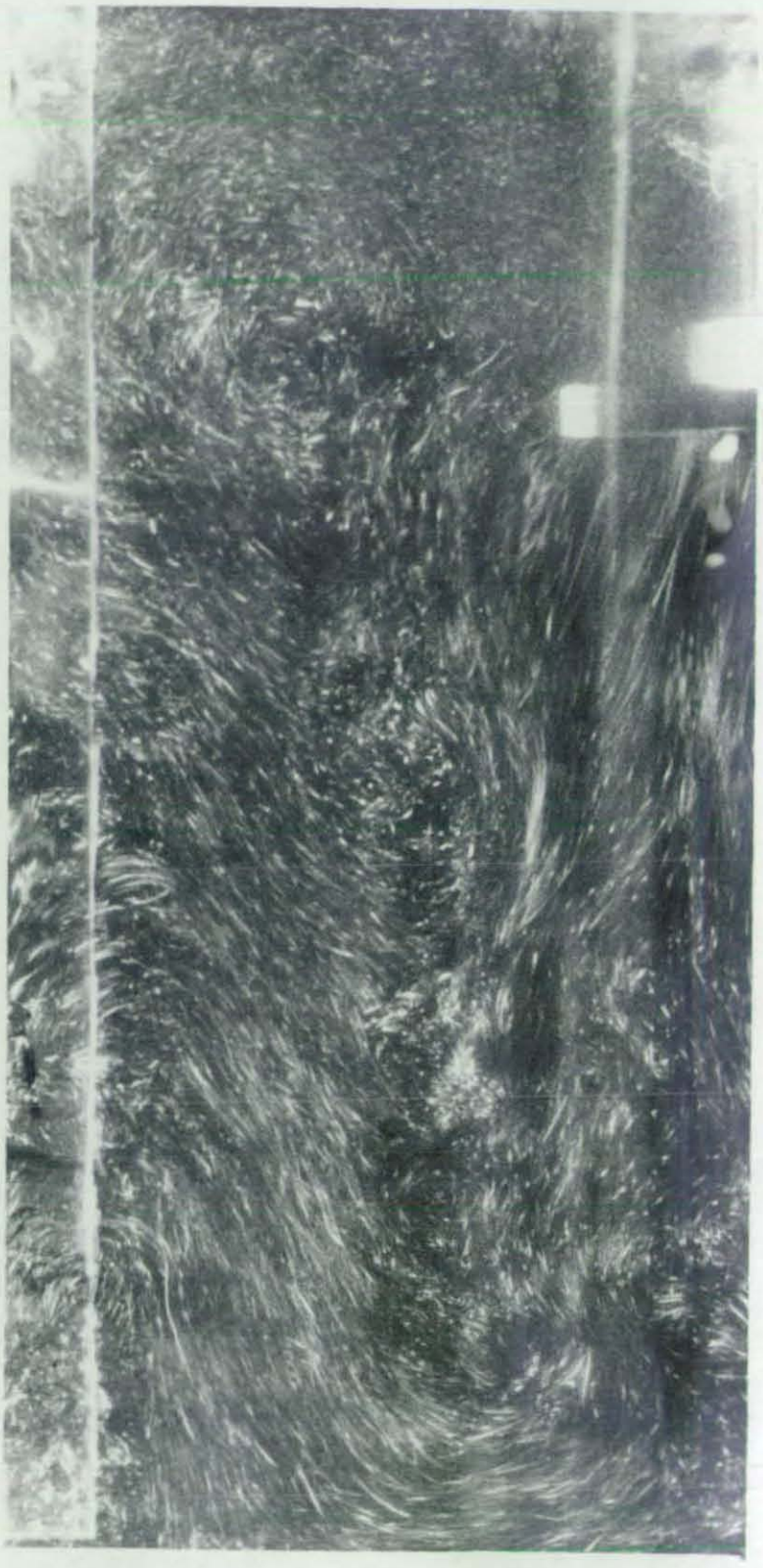

P.7 Turbine Position 0.75Z

Single Loop

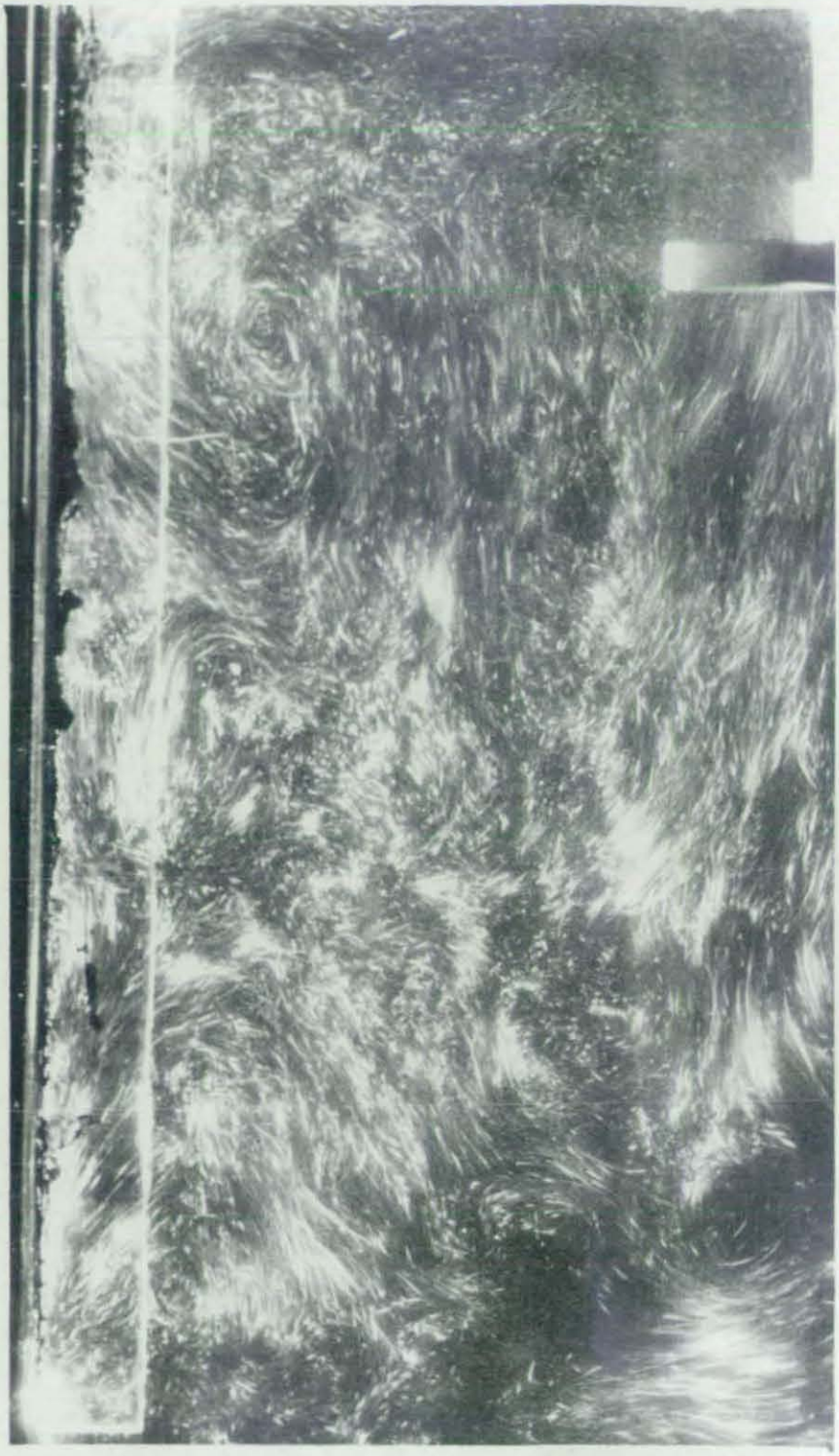

P.8 Turbine Position 0.85Z

Single Loop

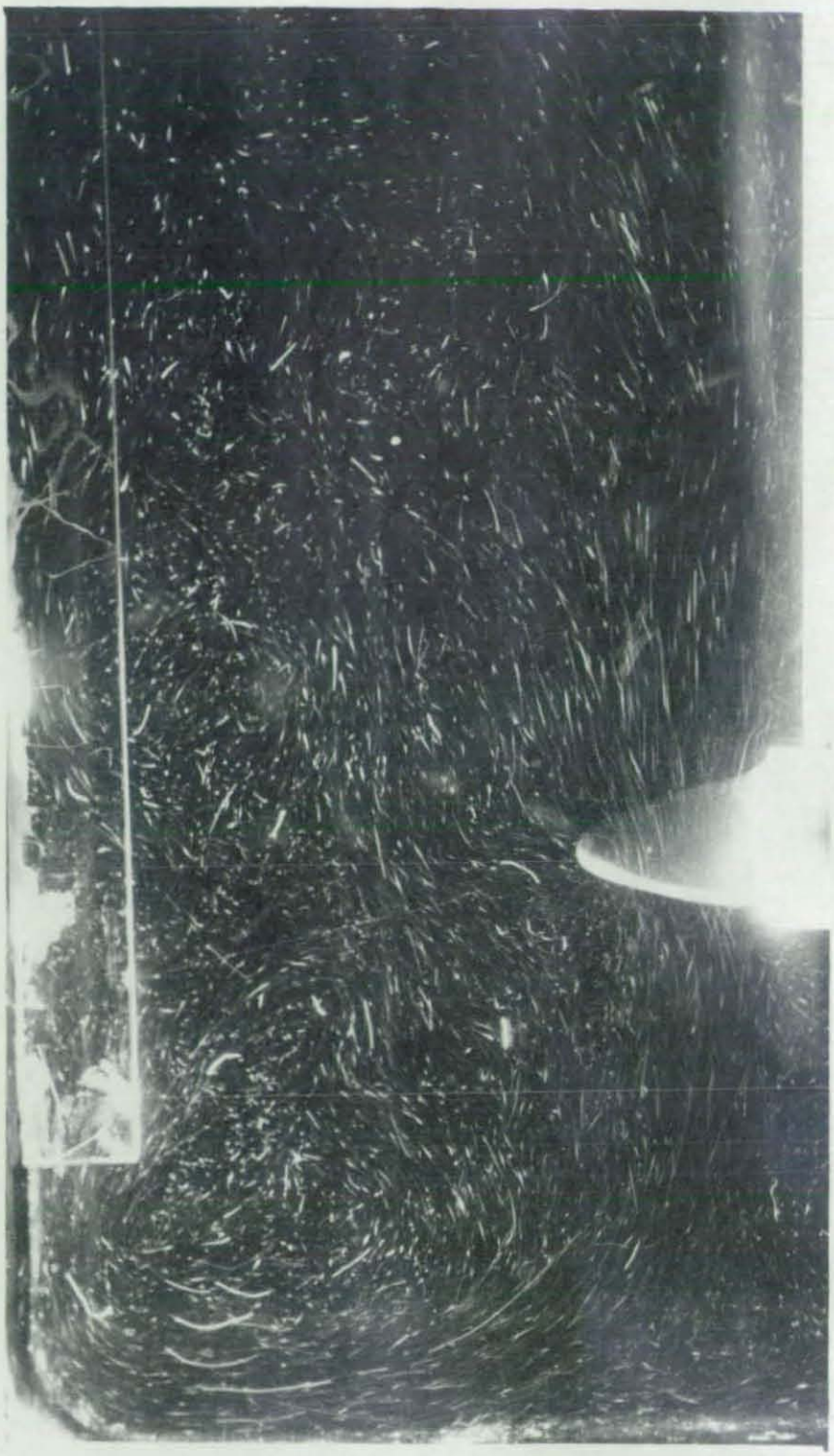

P.9 Propeller Position 0.45Z
Single Loop

region acquires a random form.

From this study two ill-defined turbine positions emerge at which the induced flow could be interpreted by either a single or double loop circulation pattern. The turbine positions being approximately one third and two thirds of the liquid height from the bottom of the vessel. If situated above or below these limits the turbine induces a single loop circulation into the system. If, however, the turbine is positioned between these limits a double loop flow pattern is produced. The position of these boundaries will undoubtedly vary for different (Z/D) ratios.

It is apparent from these photographs that the radial component of flow, associated with a turbine device, on reaching the vessel wall splits into an upward and downward component of flow. In the case of the turbine positioned (Z/3) or below, the formation of the lower circulation loop is inhibited due to the proximity of the base of the vessel. Thus only one circulation loop results. The random nature of the fluid flow pattern in the upper region exists because the impeller discharge rate is insufficient to envelop all the fluid; the momentum induced by the turbine being dissipated in the bulk of the fluid, before reaching the upper regions of the fluid.

Variations of impeller position has little effect on the overall flow pattern in propeller agitated systems. Photograph P.9 is typical of the type of flow pattern observed. As the position of the propeller is raised the centre of the vortex rises accordingly. The axial component of flow associated with such devices dictates that a single loop circulation pattern should predominate all propeller positions.

4.2. Turbine/Propeller Single-loop Recirculation Model

As the overall flow patterns of the propeller and turbine agitated systems, impeller position (Z/3), have been shown to be

almost identical, the following derivation will hold for both impellers. For a vessel with three baffles the single loop flow pattern can be represented by the configuration shown in Figure 4.1. Two ideal mixing stages in series of equal volume, are used to characterise the mixing in the circulation loop.

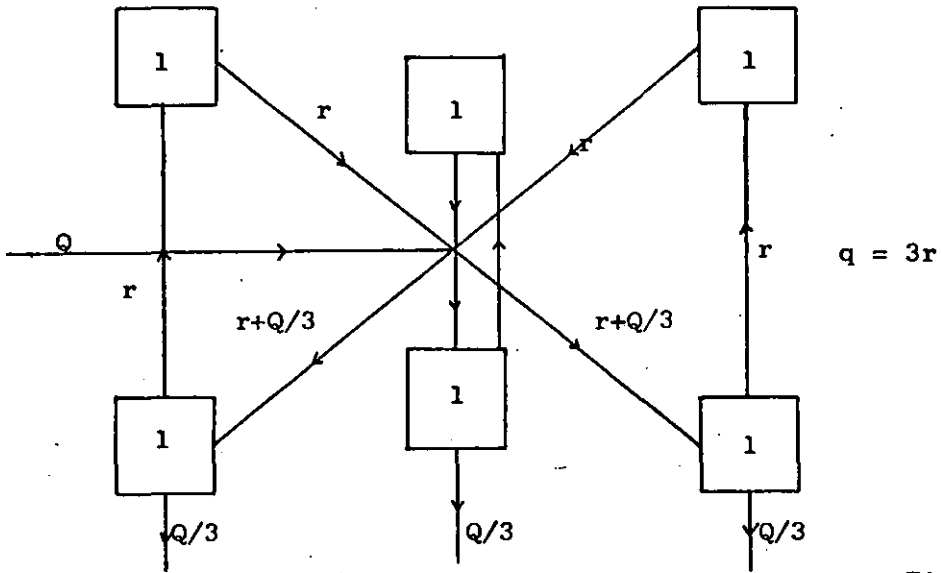

Fig. 4.1

Figure 4.1. can be further simplified, (by symmetry) to the following single loop recirculation models.

Feed to the impeller, unbaffled/baffled.

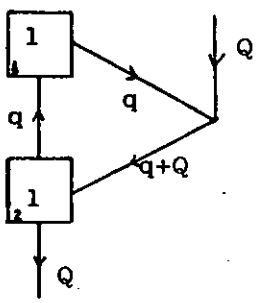

Fig. 4.2

The three symmetrical loops of Figure 4.1. can be lumped together to form the single loop model of Figure 4.2., the presence of baffles in a vessel, in which the induced flow pattern is of a single loop nature, should have little effect on the mixing, as the motion of the fluid is in an axial direction.

Feed to loop, unbaffled/baffled

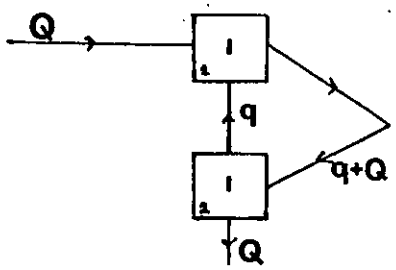

Fig. 4.3

If the feed is directed into the rotational flow of the fluid, the three loops of Figure 4.1 can be considered symmetrical. Thus forming the single loop model of Figure 4.3.

The Laplace transforms and their inversions are shown below for the two models.

Feed to propeller, baffled/unbaffled. Figure 4.2

$$G(s) = \frac{F_2}{\left(1 + q/Q\right) - q/Q \cdot F_1 . F_2 .} \qquad (4.1)$$

where $F_1 = \dfrac{1}{\frac{V_T}{2q}.s+1}$, $F_2 = \dfrac{1}{\frac{V_T}{2(q+Q)}.s+1}$

$$G(t) = Ae^{-xt} + Be^{-yt} \qquad (4.2)$$

where $A = \dfrac{Q}{V_T}\left(1 - \dfrac{Q}{\sqrt{4q^2+Q^2}}\right)$, $B = \dfrac{Q}{V_T}\left(1 + \dfrac{Q}{\sqrt{4q^2+Q^2}}\right.$

$$x = \frac{2q+Q}{V_T} - \frac{\sqrt{4q^2+Q^2}}{V_T} , \quad y = \frac{2q+Q}{V_T} + \frac{\sqrt{4q^2+Q^2}}{V_T}$$

Feed to loop, baffled/unbaffled. Figure 4.3

$$G(s) = \frac{F_1 F_2}{(1+q/Q) - q/Q \cdot F_1 F_2} \qquad (4.3)$$

where $F_1 = F_2 = \dfrac{1}{\frac{V_T}{2(Q+q)}.s + 1}$

$$G(t) = \frac{V_T}{2(Q+q)}\sqrt{\frac{q+Q}{q}}.e^{\frac{-2(q+Q).t}{V_T}} \sinh \sqrt{\frac{q}{Q+q}} . \frac{2(q+Q)t}{V_T} \qquad (4.4)$$

4.3 Double-loop Turbine Recirculation Model

From a combination of Figure 3.1 (a), Figure 3.2, and P.5, P.6, it follows that using the multiloop concept, a realistic flow model for a baffled turbine agitated vessel, should incorporate 6 loops as shown in Figure 4.4.

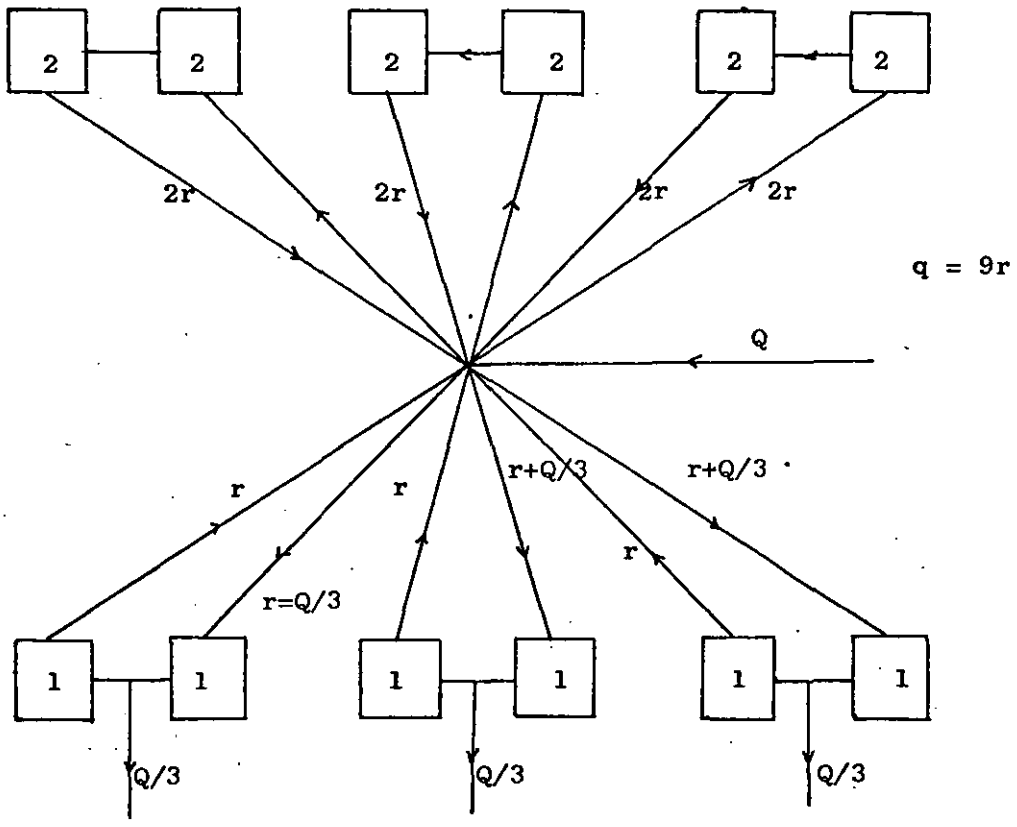

Fig. 4.4

Figure 4.4 shows the ccnfiguration adopted for feed to the impeller region, with the impeller positioned (Z/3) from the tank bottom. It is assumed that the volumetric discharge from the impeller is distributed between the upper and lower loops in the ratio of the volume above the impeller to the volume below it, so as to give equal circulation times in both loops.

The volume allotted to each ideal mixing stage is determined by the position of the impeller in the liquid. If the impeller is situated at one third of the liquid depth from the base of the vessel, the stages in the upper loop have twice the

volume of those in the lower one, by the fact that there is twice the actual volume of the fluid above the impeller as below it. If the impeller was positioned midway in the fluid, the ideal mixing stages of the upper and lower loops would have equal volumes.

The analogy between the circulation loop and the ideal mixing stages needs further amplification. The streamlines forming the circulation loop have a wide range of velocities, hence shear forces are set up, and with diffusion also present, mixing takes place. Inspection of Figure 4.4. shows that two stages in series have been chosen to characterise this mixing.

For a turbine positioned at (Z/3) and with q = 3r, Figure 4.4. can be further simplified for the following cases.

Feed to the impeller, baffled/unbaffled.

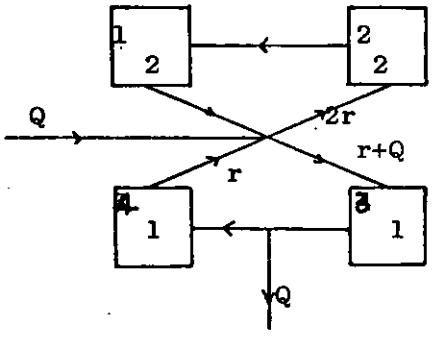

q = 3r

Fig. 4.5

With baffles present the upper and lower loops are symmetrical and can be joined together forming a simple double loop model, Figure 4.5. The model for the unbaffled case is similarly deduced.

Feed to loop, unbaffled.

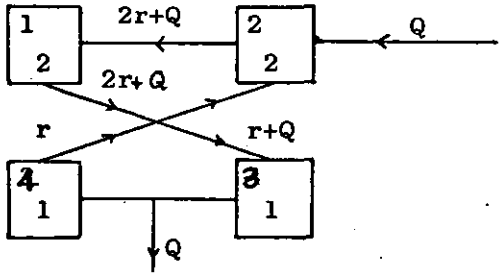

q =3r

Fig. 4.6

For flow into the upper regions of the fluid, Figure 4.4. reduces to the representation shown in Figure 4.6.

Feed to loop, baffled.

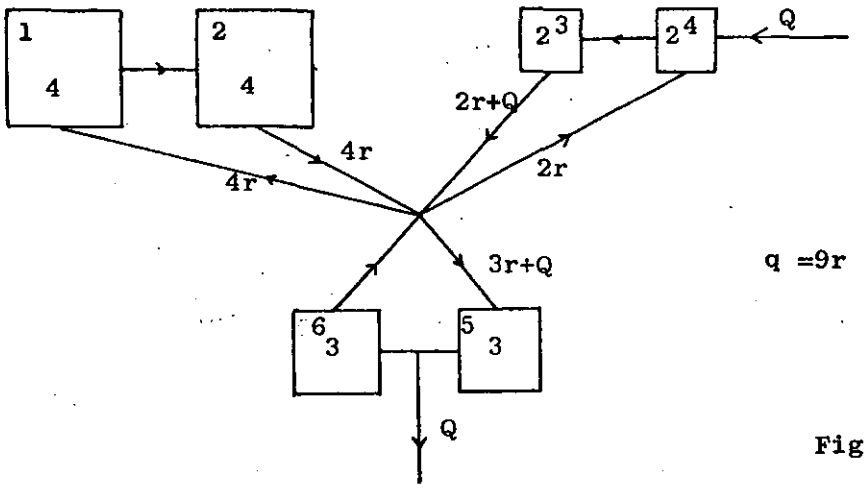

Fig. 4.7

For the baffled case of feed directed into the upper region of the vessel, Figure 4.4 reduces to Figure 4.7. Two of the upper loops remain unaffected and can be joined together. The symmetrical lower loops can be similarly treated.

The following are the transfer functions of the three preceeding models. They have been derived by dynamic mass balances on each stage. The subscripted numbers correspond to those presented in the Figures.

(i) Feed to turbine, baffled/unbaffled. Figure 4.5.

$$G(s) = \frac{Q F_3}{(3r+Q) - 2r F_1 . F_2 . - r . F_4 . F_3 .} \quad , \tag{4.5}$$

where $q = 3r$, $F_1 = F_2 = \dfrac{1}{\frac{V_1}{2r} . s + 1}$,

$$F_3 = \frac{1}{\frac{V}{r+Q} . s + 1} \quad , \quad F_4 = \frac{1}{\frac{V_4}{r} . s + 1}$$

(ii) Feed to loop, unbaffled. Figure 4.6.

$$G(s) = \frac{Q F_1 . F_2 . F_3 .}{(3r+Q) - 2r F_1 F_2 - r F_4 F_3} \tag{4.6}$$

where $q = 3r$, $F_1 = F_2 = \dfrac{1}{\frac{V_1}{2r+Q} . s + 1}$,

$$F_3 = \frac{1}{\frac{V_3}{r+Q} . s + 1} \quad , \quad F_4 = \frac{1}{\frac{V_4}{r} . s + 1}$$

(iii) Feed to loop, unbaffled. Figure 4.7.

$$G(s) = \frac{(2r+Q)\,Q.F_3.F_4.F_5.}{(9r+Q) - 3r.F_5.F_6. - 4rF_1.F_2. - (2r+Q)F_3.F_4.2r} \qquad (4.7)$$

where $q = 9r$,

$$F_1 = F_2 = \frac{1}{\frac{V_1}{4r}s+1},$$

$$F_3 = F_4 = \frac{1}{\frac{V}{2r+Q}s+1},$$

$$F_5 = \frac{1}{\frac{V_5}{3r+Q}s+1},$$

$$F_6 = \frac{1}{\frac{V_6}{3r}s+1}.$$

The models discussed and developed in this section will be compared with experimentally determined normalised responses, for a wide range of operating conditions. They are also used in an analysis of batch and continuous mixing times.

5. DERIVATION OF MIXING TIME EXPRESSIONS

5.1. Derivation of Mixing Time Expressions

Hitherto batch mixing time expressions have been of a predominately empirical nature. The following mathematical treatment is an attempt to find a more realistic analytical expression to describe batch mixing time in terms of system parameters.

5.1.1. Derivation from real time solution of the single loop model

As the real time expressions for continuous mixing of the single loop flow model have been derived, it is possible by equating the throughput flow to zero, to derive an expression for the batch mixing time.

Equation 4.2, feed to the impeller case, reduces to:-

$$C_B(t) = \frac{V_T}{4q}\left(1 + e^{-4qt/V_T}\right) \qquad (5.1)$$

Equation 4.4, feed to the loop case, reduces to:-

$$C_B(t) = \frac{V_T}{4q}\left(1 - e^{-4qt/V_T}\right) \qquad (5.2)$$

The above equations simplify to:-

$$\frac{C_B(\infty) - C_B(t)}{C_B(\infty)} = \exp\left(\frac{-4q\Theta}{V_T}\right) \qquad (5.3)$$

The batch mixing time Θ is the time required for the left hand side of equation 5.3 to reach an arbitrary small value (δ). Hence:-

$$\Theta = \frac{V_T}{q} \cdot \ln\left(\frac{1}{\delta}\right). \qquad (5.4)$$

$$\Theta \propto \frac{V_T}{q} \propto \frac{1}{N}$$

5.1.2. Derivation from a matrix formulation of the batch system

If the throughput flow of the double loop continuous flow model shown in Figure 5.1, is removed, the network will assume the form of the batch case. Batch mixing time can then be determined by deriving an explicit relationship for the concentration, with respect to time, of each individual stage in the network. The time taken for each stage to reach the same concentration level, after an impulse of tracer, is the batch mixing time.

Impeller Position Z/3

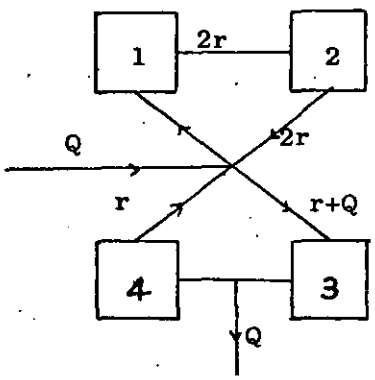

continuous Fig. 5.1.

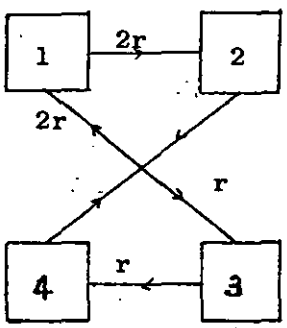

batch Fig. 5.2

The solution of this problem can be obtained in the following way. The general equation which describes the concentration fluctuation in any network of stirred tanks may be written in matrix notation as:-

$$V\dot{C} = A\bar{C} \qquad (5.5)$$

hence

$$\dot{C} = V^{-1}A\bar{C} \qquad (5.6)$$

V is a diagonal matrix representing the volume of the stages in the network. A is a flow matrix which is formed by conducting dynamic mass balances over each stage.

For the double loop representation of Figure 5.2

$$\mathbf{A} = \begin{vmatrix} -2r & 4r/3 & 0 & 2r/3 \\ 2r & -2r & 0 & 0 \\ 0 & 2r/3 & -r & r/3 \\ 0 & 0 & r & -r \end{vmatrix}$$

and $$\mathbf{V} = \begin{vmatrix} V_1 & 0 & 0 & 0 \\ 0 & V_2 & 0 & 0 \\ 0 & 0 & V_3 & 0 \\ 0 & 0 & 0 & V_4 \end{vmatrix}$$

Equation5.6 becomes

$$\dot{\bar{C}} = \bar{V}^{-1}\bar{A}\bar{C} = \begin{vmatrix} -1/T & 2/3T & 0 & 1/3T \\ 1/T & -1/T & 0 & 0 \\ 0 & 2/3T & -1/T & 1/3T \\ 0 & 0 & 1/T & -1/T \end{vmatrix} \begin{bmatrix} C_1 \\ C_2 \\ C_3 \\ C_4 \end{bmatrix} \qquad (5.7)$$

The formulation of the linear differential equations in this manner allows for immediate solution for the variation of concentration with respect to time, of each individual stage, $C_1(t)$, $C_2(t)$, etc., using Cramers technique.

i.e.

$$Ci(t) = \frac{\left|Is\ -Y\right|\ i}{\left|Is\ -Y\right|} \quad , \qquad (5.8)$$

where the ith column of the determinant $\left|Is\ -Y\right|$ i has been replaced by the forcing function.

For the injection of an impulse of unit quantity of tracer into the loop region, i.e. into stage (1), the forcing function vector representation in terms of concentration is $\begin{bmatrix} 3/V_T \\ 0 \\ 0 \\ 0 \end{bmatrix}$.

As the discharge rate of the impeller is divided in a ratio of the volume above the impeller, to the volume below, an injection of an impulse of unit quantity of tracer into the impeller region, will be split in the following manner; 2/3 into stage (1) and 1/3 into stage (3). The vector representation of this in terms of concentration is therefore:-

$$\begin{bmatrix} 2/V_T \\ 0 \\ 2/V_T \\ 0 \end{bmatrix}$$

For the condition of impulse to the loop, a combination of equations 5.7 and 5.8 gives;

$$C_1(s) = \frac{\begin{vmatrix} 3/V_T & -2/3T & 0 & 1/3T \\ 0 & (s+1/T) & 0 & 0 \\ 0 & -2/3T & (s+1/T) & -1/3T \\ 0 & 0 & -1/T & (s+1/T) \end{vmatrix}}{\begin{vmatrix} (s+1/T) & -2/3T & 0 & 1/3T \\ -1/T & (s+1/T) & 0 & 0 \\ 0 & -2/3T & (s+1/T) & -1/3T \\ 0 & 0 & -1/T & (s+1/T) \end{vmatrix}} C \qquad (5.9)$$

$$C_1(s) = \frac{3/V_T\,(s+1/T)\,(s^2 + 2s/T + 2/3T^2)}{s(s + 1/T)^2\,(s + 2/T)}\,C \qquad (5.10)$$

Inversion of equation 5.10 by partial fractions gives the real time solution for the outlet concentration of stage (1) in the network. $C_2(t)$, $C_3(t)$, $C_4(t)$ are found using the same procedure.

$$C_1(t) = \frac{1}{V_T}\left(1 + e^{-2qt/V_T} + e^{-4qt/V_T}\right) \quad (5.11)$$

$$C_2(t) = \frac{1}{V_T}\left(1 + \frac{t}{T}e^{-2qt/V_T} - e^{-4qt/V_T}\right) \quad (5.12)$$

$$C_3(t) = \frac{1}{V_T}\left(1 - 2e^{-2qt/V_T} + e^{-4qt/V_T}\right) \quad (5.13)$$

$$C_4(t) = \frac{1}{V_T}\left(1 - \frac{2t}{T}^{-2qt/V_T} - e^{-4qt/V_T}\right) \quad (5.14)$$

The following expressions are derived for the impulse into the impeller case:-

$$C_1(t) = \frac{1}{V_T}\left(1 + e^{-4qt/V_T}\right) \quad (5.15)$$

$$C_2(t) = \frac{1}{V_T}\left(1 - e^{-4qt/V_T}\right) \quad (5.16)$$

$$C_3(t) = \frac{1}{V_T}\left(1 + e^{-4qt/V_T}\right) \quad (5.17)$$

$$C_4(t) = \frac{1}{V_T}\left(1 - e^{-4qt/V_T}\right) \quad (5.18)$$

Similarly, the real time response of each stage in the single loop network can be derived, for the injection of an impulse of unit quantity of tracer. Figure 5.3 illustrates the continuous flow model and Figure 5.4 the corresponding batch configuration.

Impeller Position Z/3

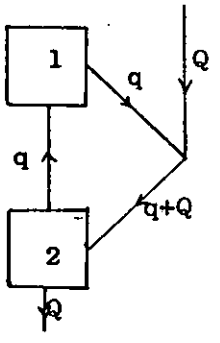

Continuous Fig. 5.3.

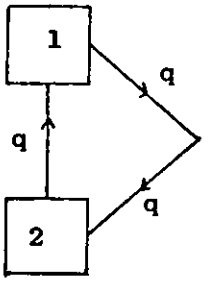

batch Fig. 5.4.

For impulse into the loop region (stage (1)),

$$C_1(t) = \frac{1}{V_T}\left(1 + e^{-4qt/V_T}\right) \tag{5.19}$$

$$C_2(t) = \frac{1}{V_T}\left(1 - e^{-4qt/V_T}\right) \tag{5.20}$$

For impulse into the impeller region (stage (2)),

$$C_1(t) = \frac{1}{V_T}\left(1 - e^{-4qt/V_T}\right) \tag{5.21}$$

$$C_2(t) = \frac{1}{V_T}\left(1 + e^{-4qt/V_T}\right) \tag{5.22}$$

The equations derived (5.15 - 5.22) for each individual stage in the network are identical to equations 5.1 and 5.2 hence in conjunction with equation 5.3 they show batch mixing time to be inversely proportional to impeller speed.

For the case of an injection of tracer into the impeller region, the batch network illustrated in Figure 5.1 has symmetrical loops and can be further simplified to the configuration illustrated in Figure 5.4, i.e. the single loop model. However for an injection of tracer into the loop region, the double loop model retains its individuality; the dissymetry of the network arrangement preventing any further simplification.

These points are illustrated by the similarity of equations 5.15 - 5.18 and 5.21 - 5.22, and the dissimilarity of equations 5.11 - 5.14 and 5.19 - 5.20.

5.2. Continuous Mixing Time

The techniques previously adopted for the determination of batch mixing time cannot be successfully applied for the derivation of an analytical expression for the continuous case. As the mixing in a continuous blender takes place in time and space

it is very difficult to represent mathematically.

In section 3.3.6 previously published techniques for assessing continuous mixing time have been discussed and have been shown to be related to the residence time distribution of the system. The residence time distribution gives the probability of an element leaving a system in the next time interval (dt) and it is independent of the past history of that element. The use of residence time distribution is therefore inferior to an intensity function approach.

5.2.1. Assessment of continuous mixing time:- the intensity function approach

The intensity function is defined as:-

$$I(t) = \frac{f(t)}{1-F(t)} \qquad (5.23)$$

where f(t) is the impulse response and F(t) the step response.

The intensity function gives the probability that an element, after having stayed in the system during a period (t), will leave the system in the next time interval (dt). This definition lends itself immediately to the assessment of continuous mixing time. If I(t) is constant after a time (t), the probability of elements leaving the system will be the same throughout the remainder of the mixing. Therefore the time taken to reach this constant value is a good measure of the continuous mixing time. In an ideal system the intensity function is always unity, the continuous mixing time is zero as all the contents are instantaneously and uniformly mixed in such a system.

Figures 5.5 - 5.7, feed to the impeller, and Figures 5.8 - 5.10, feed to loop, illustrate typical intensity function curves for the single and double loop models. They were computed by

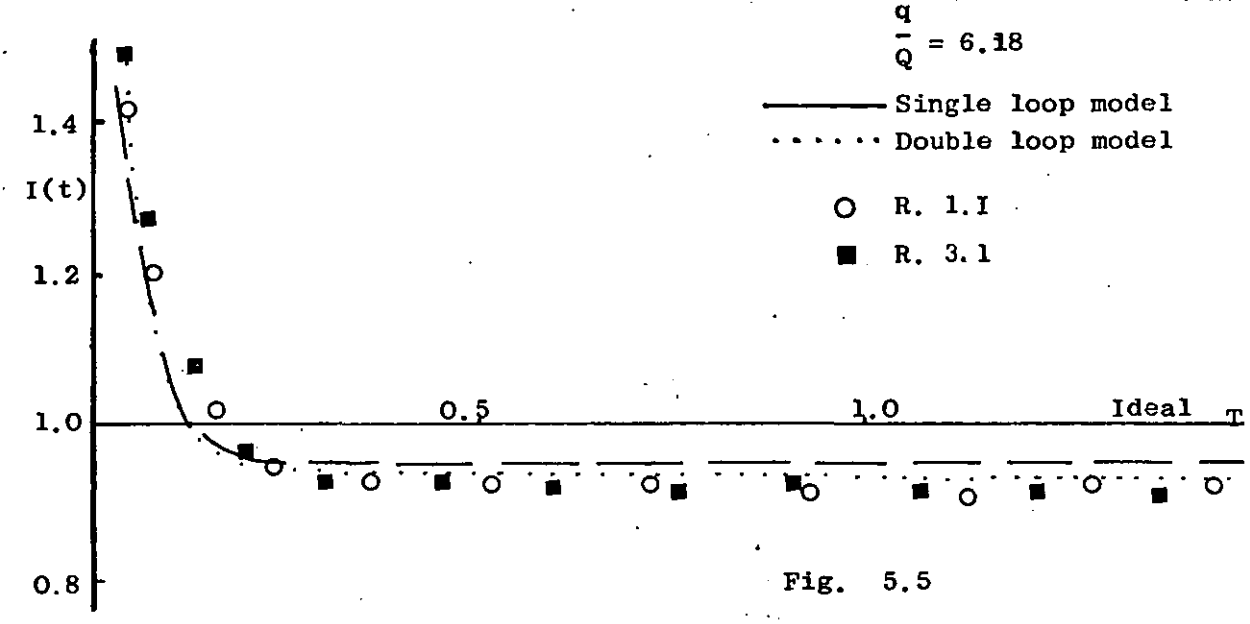

Fig. 5.5

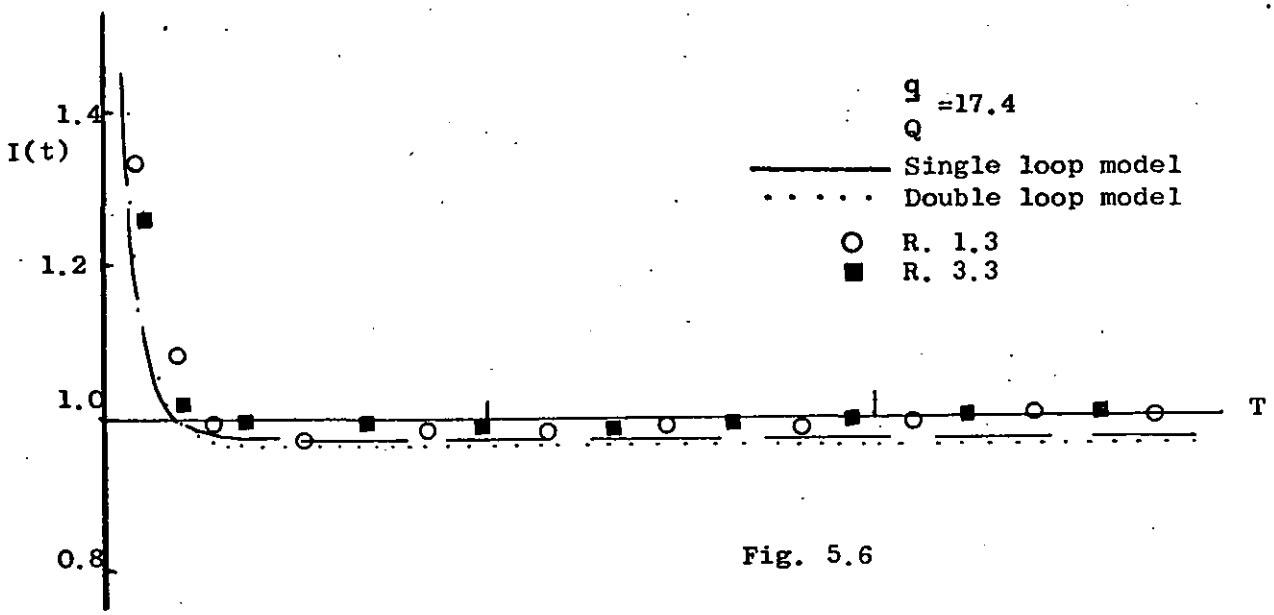

Fig. 5.6

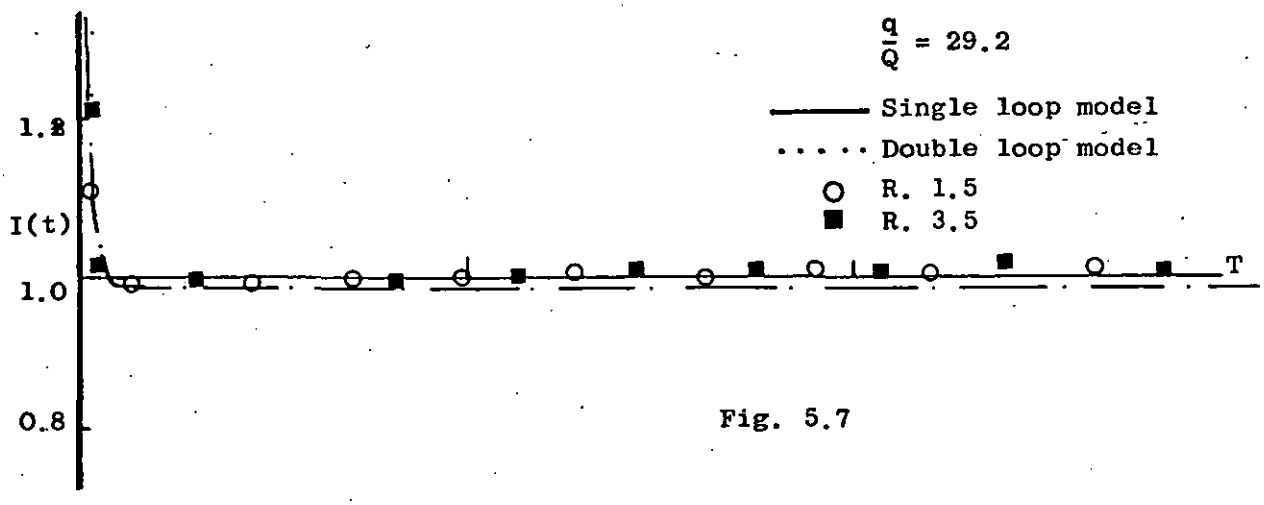

Fig. 5.7

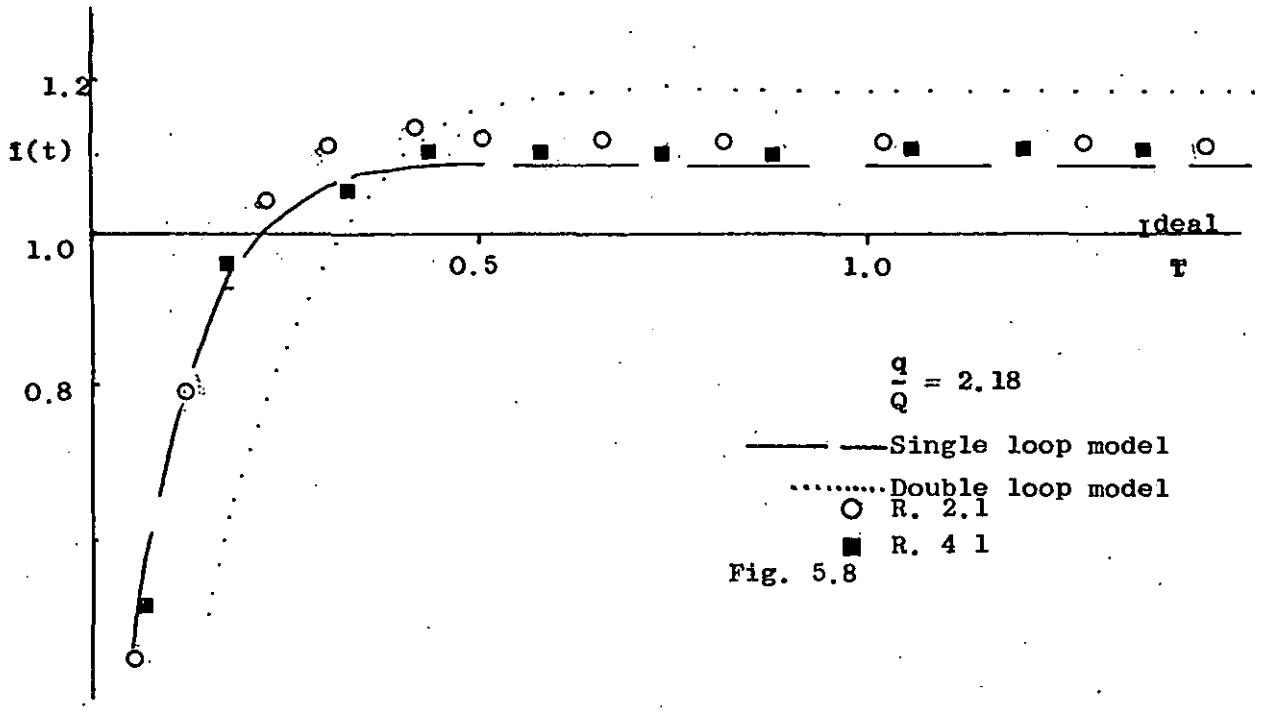

Fig. 5.8

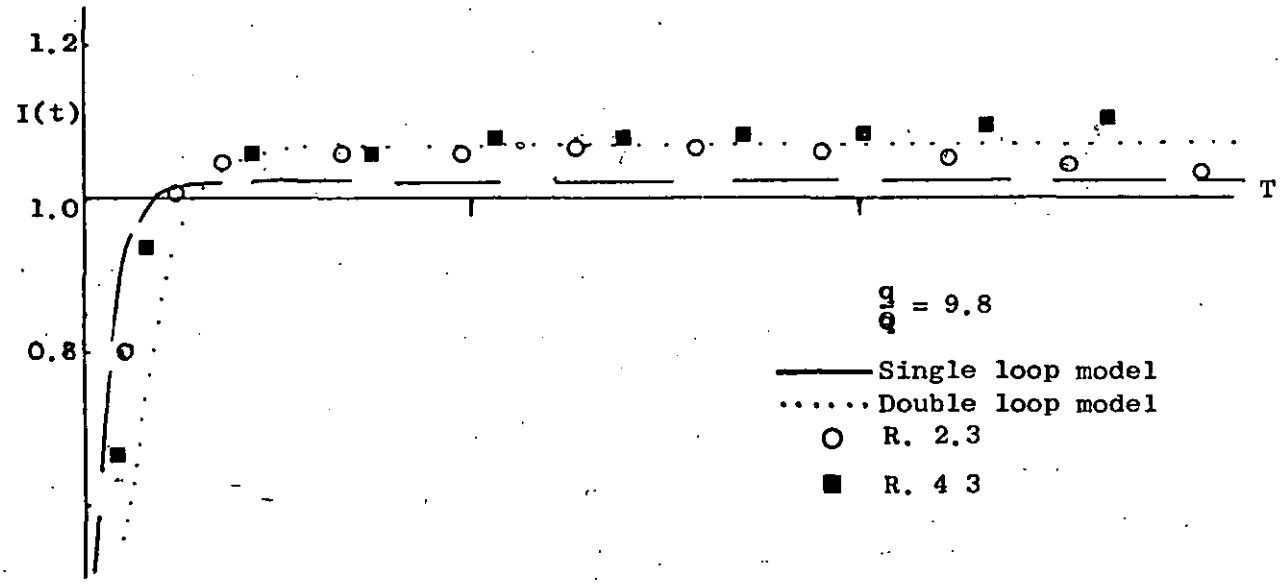

Fig. 5.9

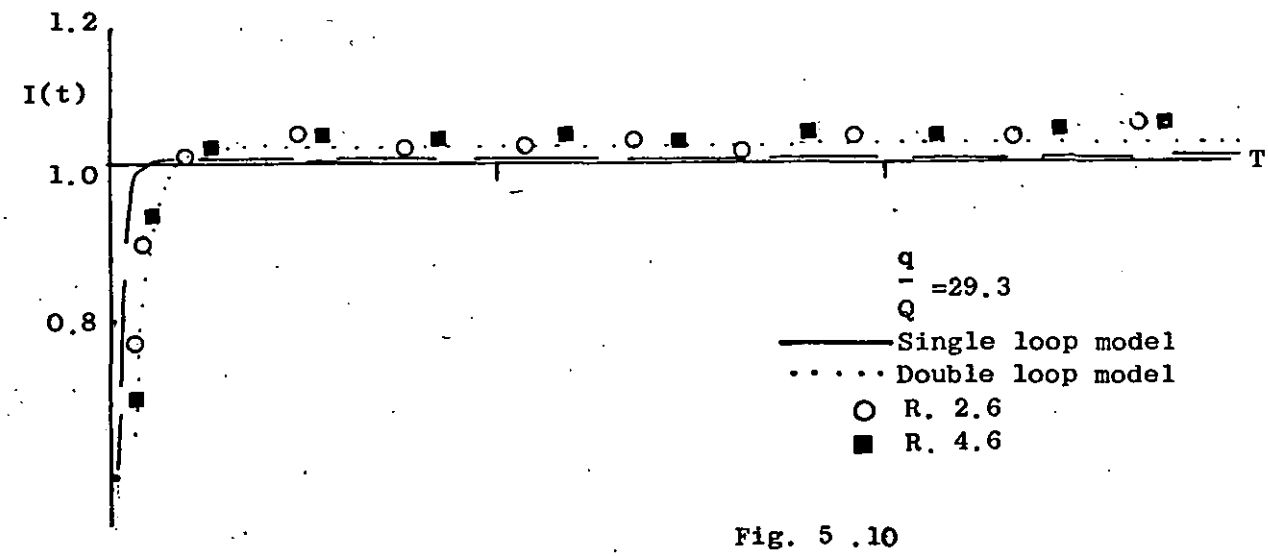

Fig. 5 .10

a modification of the programme described in Appendix 3. The curves tend towards a constant value, throughout the range of model parameter considered and for both inlet feed positions. Also shown in these figures are intensity function curves computed from experimental response data; the step response being calculated by numerically integrating the impulse response. The experimental I(t) results deviate slightly from the theoretical curves; the deviation being greatest after a time longer than the meantime of the system. This is caused by the numerator and the denominator of equation 5.23 having small absolute values at the tail of the response. Consequently any small error in the impulse response will produce an error in the step response which will be magnified in the intensity function curve.

Values for continuous mixing time were obtained from these figures and other similar plots and compared with the results derived from other criteria. Figures 5.11, 5.12 illustrate typical plots of impulse response data on a log—linear scale for both the single and double loop models. The time required for the curve to acquire a constant gradient was obtained from these and other similar plots for a wide range of model parameter.

Using a modification of the programme described in Appendix 3 the time taken for the response to reach its maximum (tmax) was computed, for various values of the model parameter. This analysis was restricted to the feed to the loop case.

The results obtained from these three methods of assessment of continuous mixing time are shown in Figures 5.13 - 5.15. The salient feature of these plots is the wide deviation between the predicted results of each criterion. The semi-log approach gives completely different results to the (t max) solutions which in

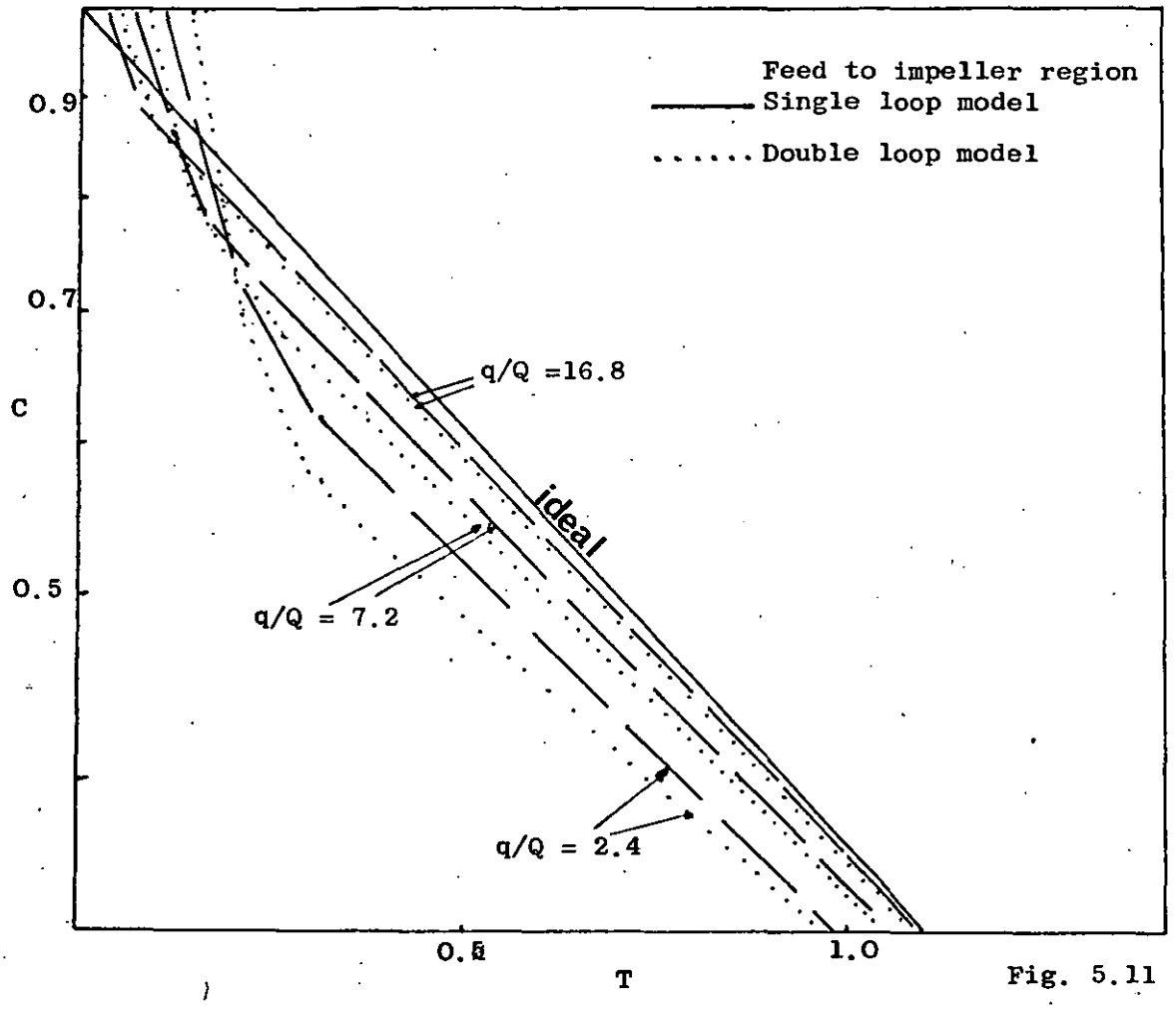

Fig. 5.11

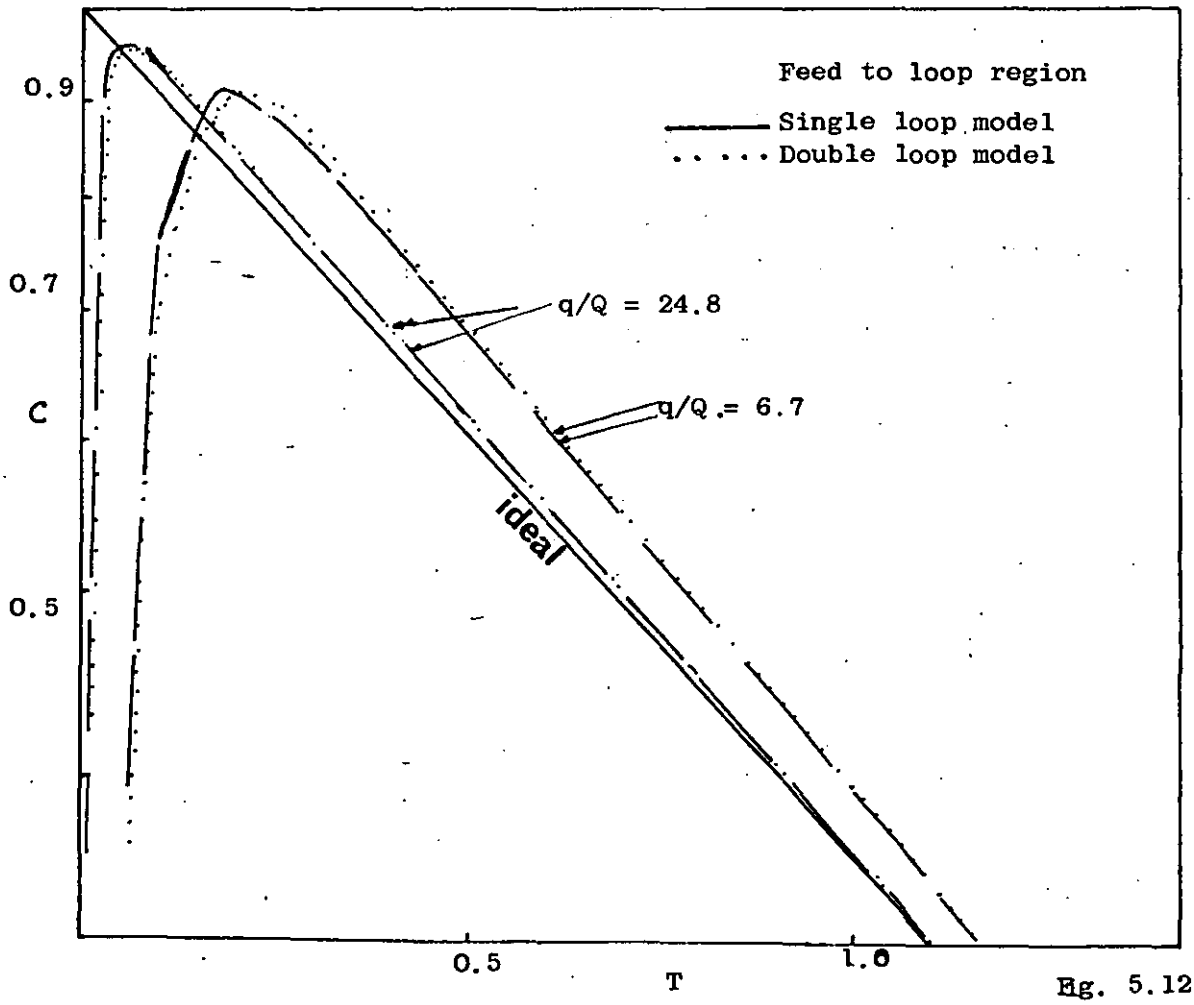

Fig. 5.12

turn differ considerably from the intensity function predictions.

Comparison of Figures 5.13 and 5.14, feed to the loop condition, shows the semi-log predictions for the two models to be almost identical. However, the predicted results of the intensity function and tmax techniques for the single loop model are completely different from those of the double loop model. For the condition of feed to the impeller, Figure 5.15, the predictions of the intensity function approach compare well for both models as do the results of the semi-log method. The variation between the predictions of the criteria is still apparent.

As all three criteria are dependent on the model used for simulation, differences in predicted solutions between the single and double loop models can be expected. A conservative estimate of continuous mixing time is provided by taking the average of the semi-log and intensity function values. As the results of these two criteria are obtained from plots, the value taken is subjective, thus an average would tend to remove this.

The tmax approach produces the only definite value of continuous mixing time, although its application is limited to the feed to loop case. Inspection of Figures 5.13 - 5.14 shows that the value obtained using this technique is approximately a direct ratio of the values obtained from the other methods of assessment. Multiplication of the tmax values by a factor of 2 produces the values derived from taking the average of the results of the I(t) and semi-log methods.

Continuous mixing time:- Predictions of Single loop model

Feed to loop region

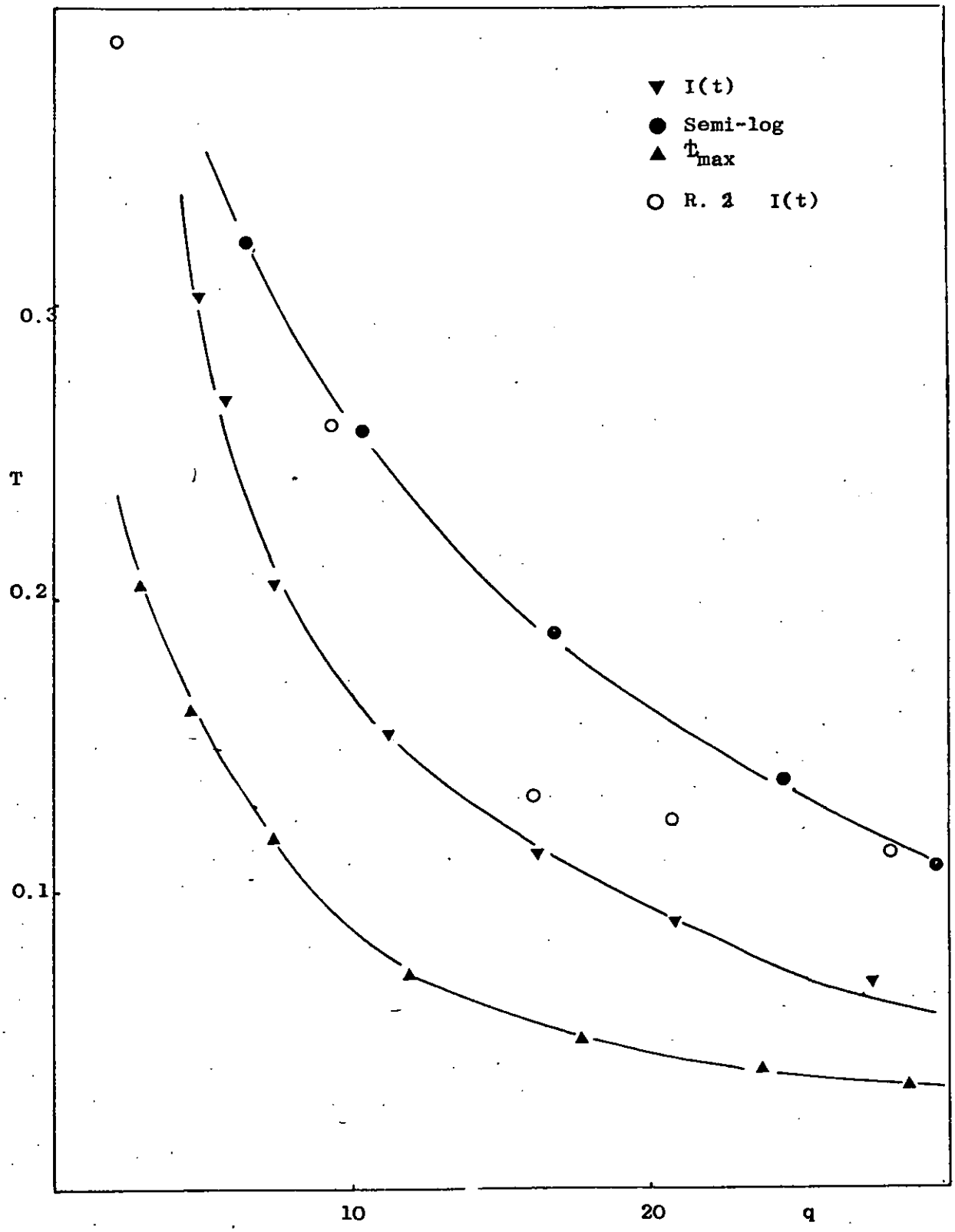

Fig. 5.13

Continuous mixing time:- Predictions of Double loop model

Feed to loop region

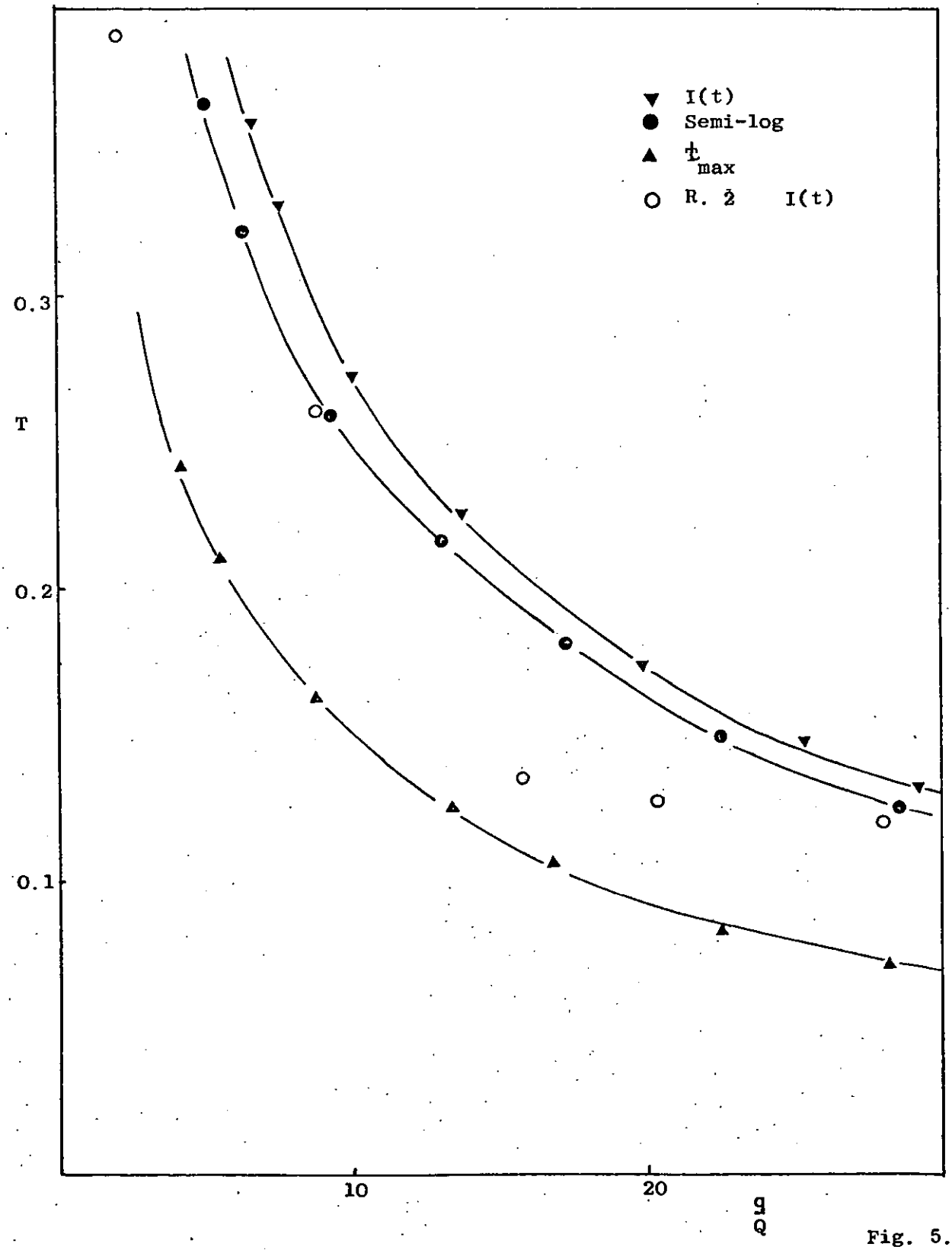

Fig. 5.14

Continuous mixing time:- Predictions of both models

Feed to impeller region

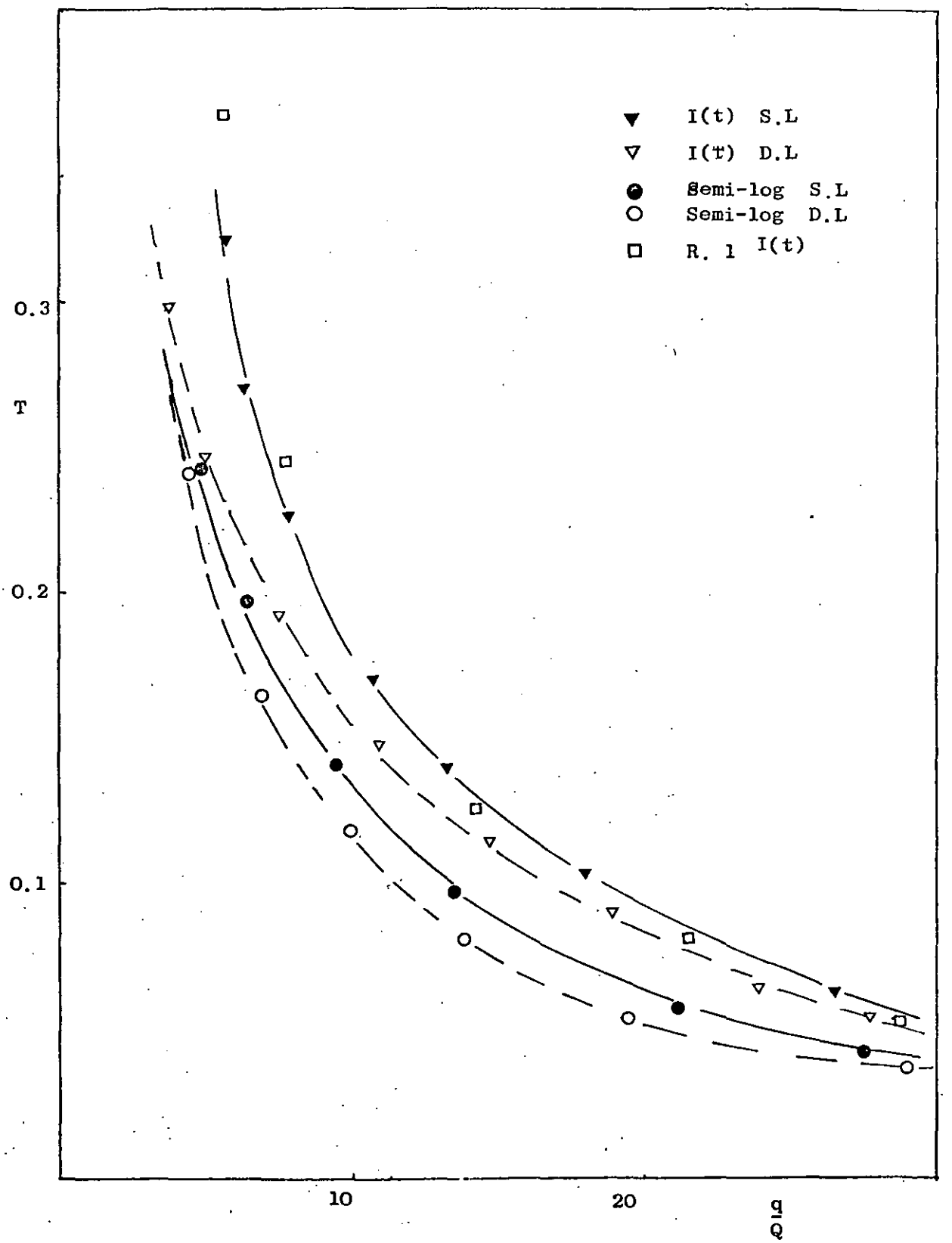

Fig. 5.15

6. DESCRIPTION OF APPARATUS AND EXPERIMENTAL PROCEDURE

OVERALL SYSTEM ARRANGEMENT

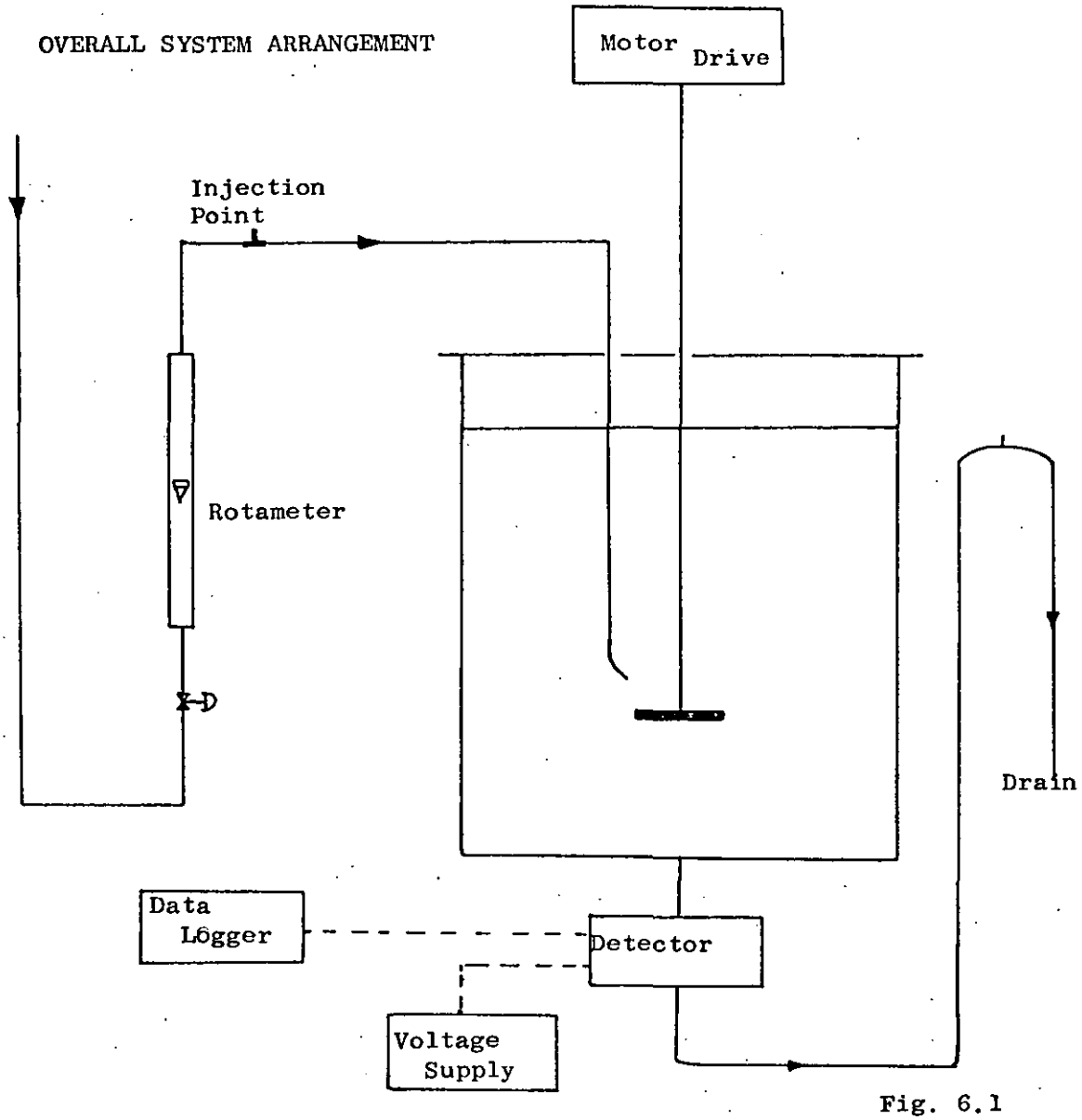

Fig. 6.1

THE IMPELLERS

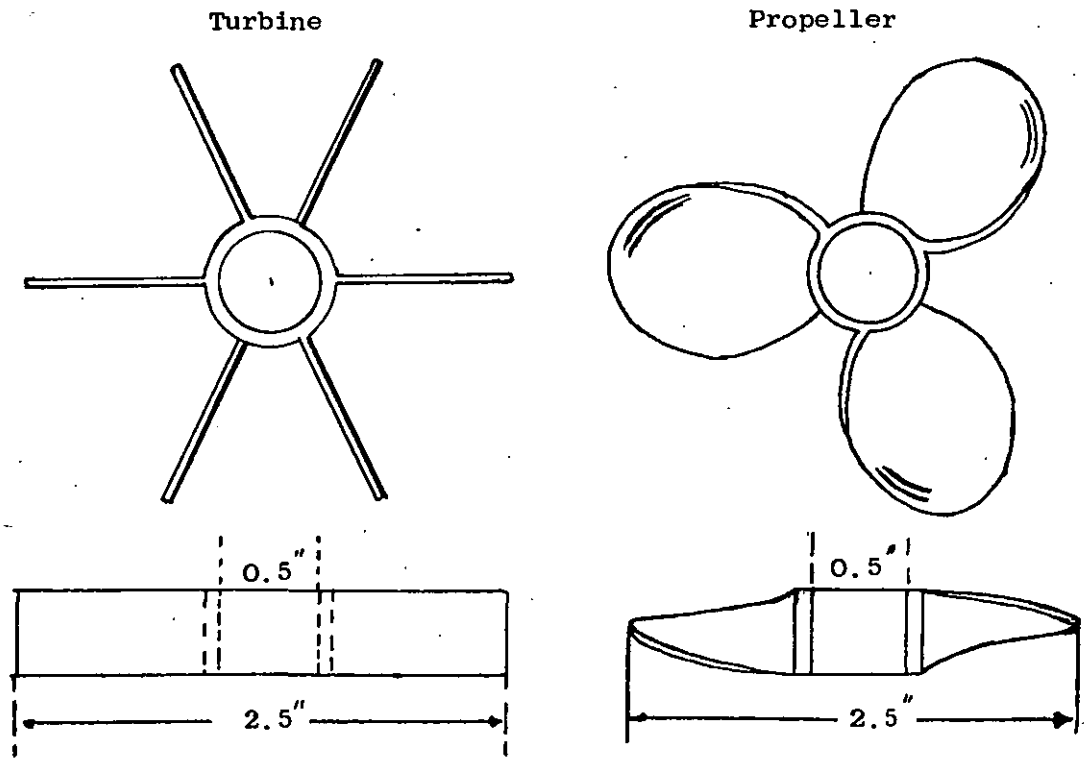

Fig. 6.2

6.1. Description of Apparatus and Experimental Procedure

Impulse response experiments were conducted in three cylindrical vessels of 9", 19" and 42" diameter for both turbine and propeller impellers. The effect of impeller speed, fluid inlet position and degree of baffling was studied for each system. The effect of fluid viscosity was also investigated for a turbine impeller in the 9" diameter vessel. In all experiments the ratio of liquid height to vessel diameter was unity and the impellers were positioned at one-third of the liquid height from the base of the vessel.

6.2. The Mixing Vessels

6.2.1. The 9" diameter cylindrical vessel

The vessel was constructed from a length of 9" diameter Keebush pipe. It was flat bottomed with a centrally positioned outlet which was adapted to connect directly to a 1" diameter glass line. The initial section of this line was the photocell detector. A perspex lid, held in place by two locating pins, supported a 0.4" diameter glass inlet line; the impeller shaft passing through a hole in its centre. Slots at the edge of this lid enabled three equispaced steel baffles, (0.12D), to be positioned against the vessel wall when required, perspex blocks cemented around these slots ensured a rigid fit. The overall arrangement is illustrated in Figure 6.1.

In this vessel 2.5" diameter impellers were used. The six straight bladed turbine, (W/D = 1/8), is illustrated in Figure 6.2(a) and the marine propeller (pitch 30°), shown in Figure 6.2 (b). The shaft on which the impellers were mounted was driven by a 0.25 H.P. motor, through a variable speed transmission unit, mounted directly

above the vessel. This enabled the impeller speed to be varied between 0 and 500 rpm.

Water from a header tank, flowed through a needlevalve, a metric 7 rotameter, a tee-piece (a leg of which was fitted with a subseal cap) and the glass inlet line into the vessel. Fluid leaving the vessel passed through the glass line carrying the photocell detector, a length of flexible hose and a syphon breaker, then to waste. The vessel holdup could be varied by adjusting the height of the syphon breaker.

The same apparatus was used for the glycerol/water solutions. These solutions were made up with pure glycerol and deionised water. In this case the fluid leaving the vessel was collected and recycled, by means of a pump, to a header tank. The detecting device, in these experiments, was a conductivity cell which could be connected directly to the glass section at the base of the vessel and the glass outlet line.

6.2.2. The 19" diameter cylindrical vessel

The arrangement of equipment for this vessel was as shown in Figure 6.1. The vessel and lid were made of polythene. The inlet rotameter was an M.F.G. type, and the inlet feed line 1" diameter; a number of experiments were conducted with a 0.4" diameter inlet line. Impellers of 4" diameter, geometrically similar to those illustrated in Figure 6.2 were used in this vessel. The shaft and motor unit were the same as for the smaller vessel. Baffles, (3 x 0.12D), supported by a circular framework, were introduced from the top of the tank when required.

6.2.3. The 42" diameter cyclindrical vessel

The arrangement of apparatus for this system was identical to that shown in Figure 6.1. The vessel was constructed from alkathene. The inlet rotameter and feed lines were the same as for the 19" diameter vessel. An 8" diameter turbine, geometrically similar to Figure 6.2(a), was the agitating device. The shaft and motor unit were again the same as previously described.

6.3 Tracer Injection Technique

The tracer was injected into the system, via the sub-seal cap on the tee-piece section of the inlet line, by means of a hypodermic syringe. Two tracers were used;nigrosine dye solution for the runs with pure water and concentrated KCl for the glycerol-water mixtures. Inthe 42" diameter vessel upto 10 ccs of nigrosine dye were injected; the injection time being about 5 seconds. For the experiments on the two smaller vessels 3 or 4 ccs of tracer were used with an injection time of less than 2 seconds. As the injection time was very much less than the mean residence time of each system, the input was assumed to be a true impulse.

6.4 Detecting Devices

6.4.1 The photocell

Construction

The concentration of the nigrosine dye was measured by a photocell detector built around an 11" section of the glass outlet line. The detector was a Mullard 90 A.V. photo emissive cell with a resistor connected in series, Figure 6.3. The cell was located directly opposite a 12 watt filament bulb, between which was the outlet line. This arrangement was secured

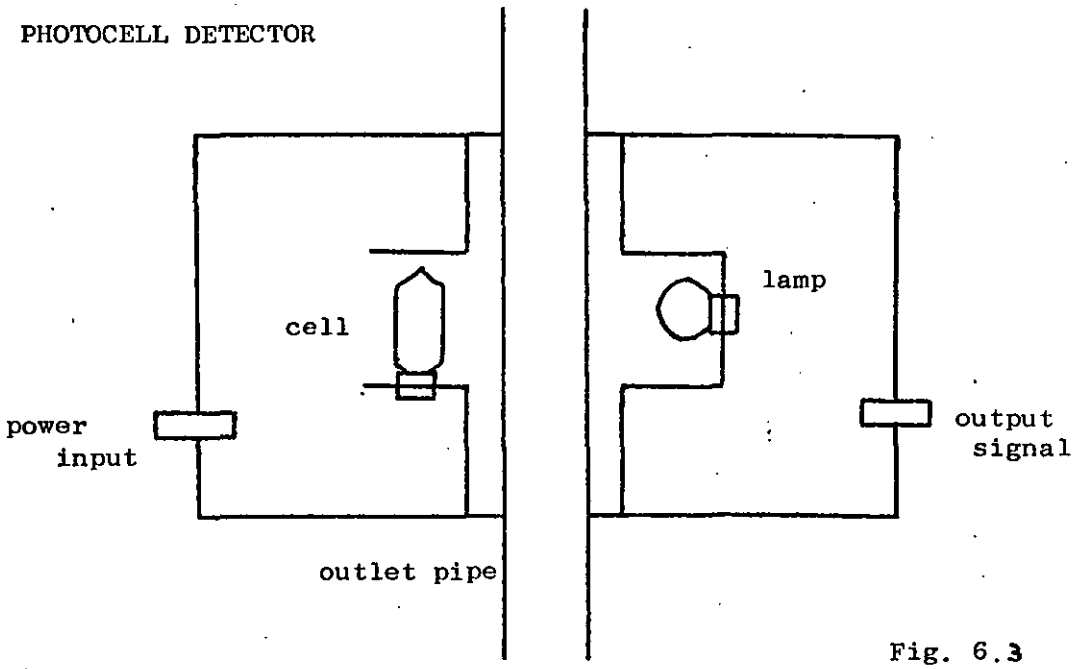

Fig. 6.3

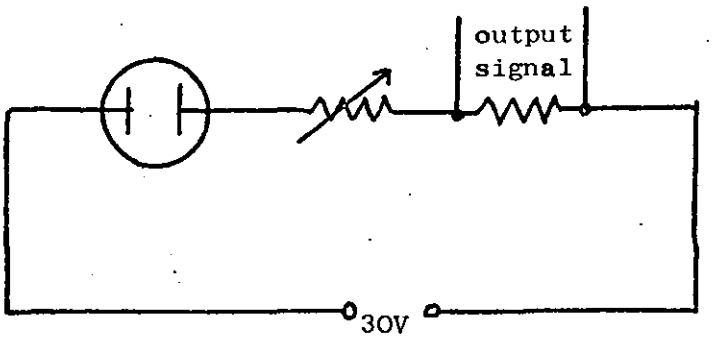

Fig.6.3b.

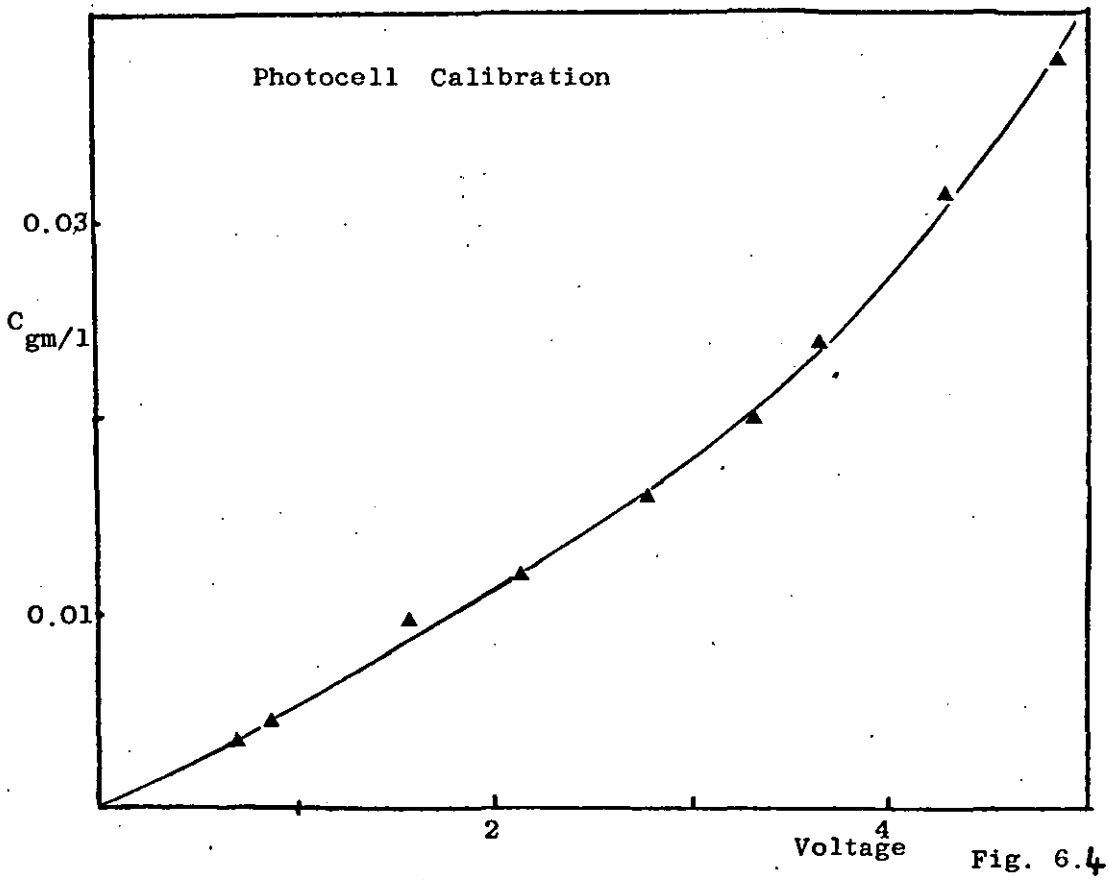

Fig. 6.4

by clamps to the detector shell. The cell was shielded so that nearly all the light falling on the sensitive cathode surfaces had first passed through the outlet line. Power to the valve and bulb was supplied by two transistorised power packs which provided constant voltage outputs to the cell and bulb of 30 volts and 11.6 volts respectively. To prevent temperature effects, a ventilation hole was drilled above the light source.

Different concentrations of tracer passing through the outlet line give rise to changes in output voltage from the photocell. Thus the photocell is an ideal device for impulse response experiments, after having determined the requisite concentration/voltage calibration.

Calibration

The photocell was calibrated before each set of runs. This was accomplished by disconnecting the cell from beneath the vessel. Standard solutions of nigrosine dye were then poured independently into the glass pipe section of the photocell. The output voltage was recorded for each concentration. Fig. 6.4 shows a typical concentration/voltage calibration curve. It was found that the voltage varied linearly with concentration in the dilute range, but for higher concentrations this linearity disappeared.

6.4.2. The conductivity cell

A conductivity cell type CEA - 10, constant 1.0, manufactured by Electronic Switchgear Ltd. was used in the tracer response experiments for the glycerol-water solutions; to facilitate the use of the same fluid for repeated experiments. The cell is a simple device comprising of a pair of precisely dimensioned electrodes critically spaced within a chamber of insulated material that electrically isolates an exactly determined volume of solution. Figure 6.5 illustrates this design.

The cell contains three annular ring electrodes equally spaced within a ½" diameter base in an epoxy resin moulding. The tubular base is threaded at each end to enable the cell to be mounted vertically as an integral part of the outlet line. Conduction through the solution within the cell takes place between the central electrode and the two outer rings, which are connected to the earthed terminal of the A/c autobalancing bridge. Electrical conduction is therefore confined entirely within the cell where it is not influenced by the presence of adjoining metal parts in the outlet line. The cell constant is 1.0, i.e. the conductivity as measured at the external terminals, is the conductivity of the solution inside, expressed in electrical units per centimetre cubed. These constants do not vary over years of continuous use.

Figure 6.6 illustrates the overall arrangement for the measurement of the output signal of the conductivity cell. The A/c autobalancing bridge gives a direct measurement of the conductivity and produces a voltage output. This signal is amplified by a Redcor Amplifier and logged via the data-logger on punched paper tape.

Calibration

The conductivity cell was disconnected from the outlet line and clamped vertically. Known concentrations of solution, made up with deionised water, were emptied individually into the cell. The amplified output voltage was recorded for each concentration. Figure 6.7 shows a typical calibration curve for the conductivity cell. The displacement of the bridge, i.e. the output voltage was found to be linear throughout the whole range of concentrations used. This property of the bridge allowed the fluid to be recycled without the need for repeated calibration of the detecting device.

CONDUCTIVITY CELL DETECTOR

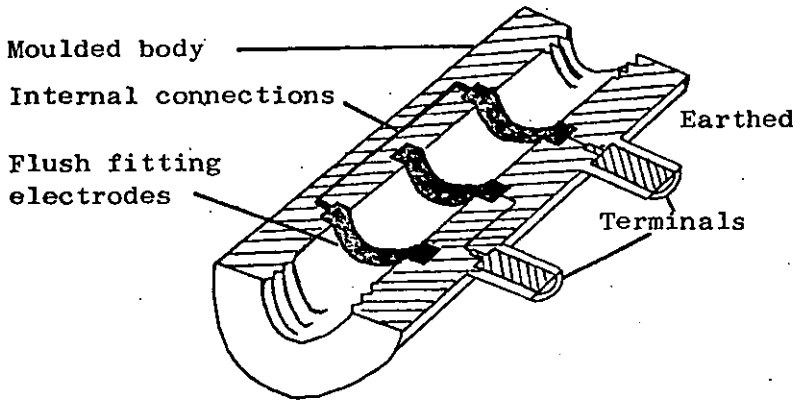

Fig. 6.5

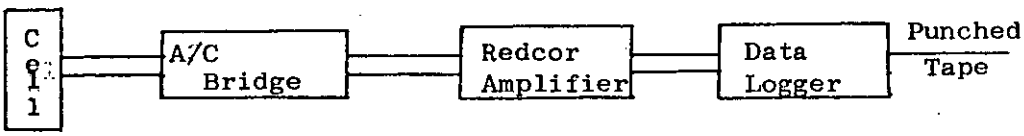

Fig. 6.6

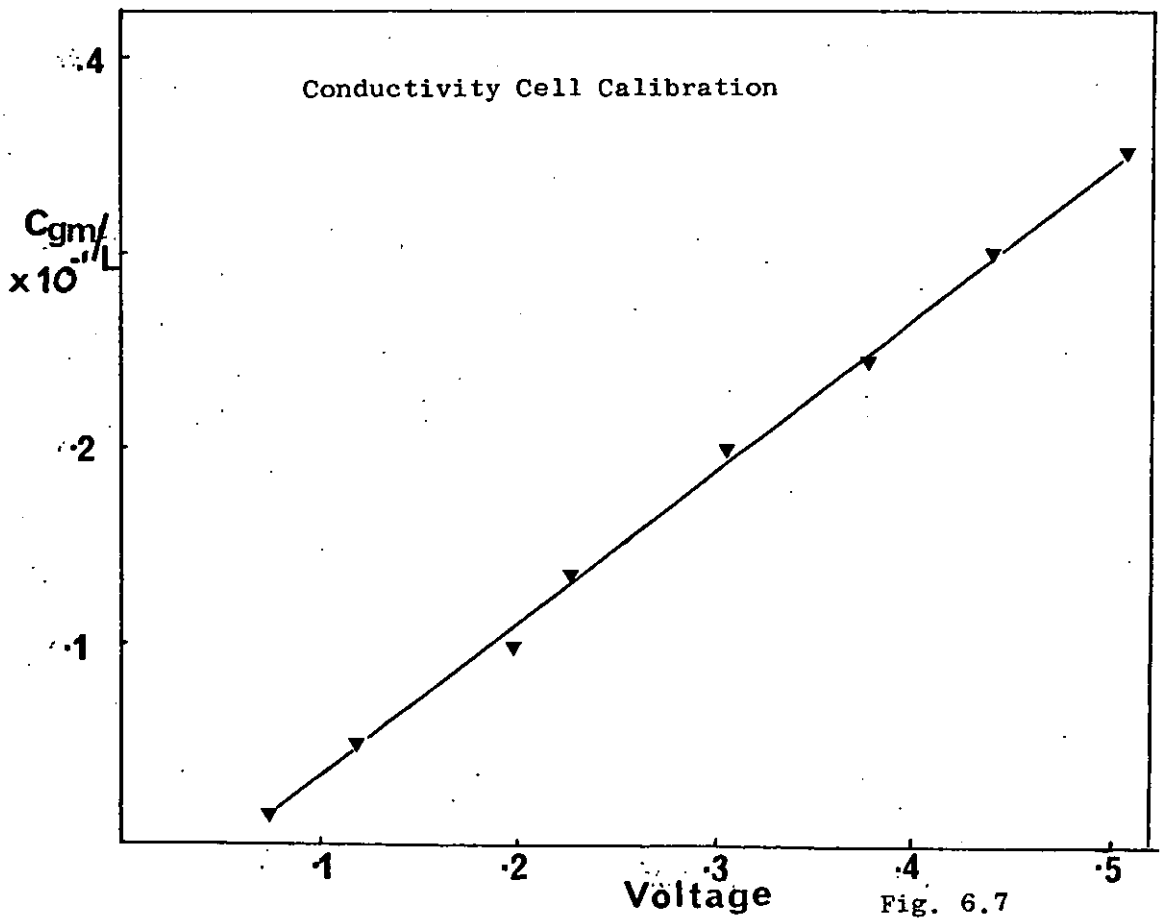

Fig. 6.7

6.5. Impluse Response Experiments in the 9" Diameter Vessel

The photocell was allowed to reach equilibrium, (a time of four hours), and then calibrated. It was then installed in the outlet line immediately below the vessel. The vessel was then filled to the measured mark. The flow rotameter was set and the flow calculated by collecting and weighing the liquid which has been discharged from the system in a given time. The rotameter was held at this value for the series of runs. The impeller speed was set by adjustment of the micrometer control on the variable speed transmission unit. The system was then allowed to reach steady state conditions.

The photocell output was connected to the data logger by means of a coaxial cable and the logger set to log this output on punched paper tape once per second. 4 ccs of concentrated nigrosine dye solution were then injected, through the sub seal cap, into the fluid inlet line, with a hypodermic syringe. At the same time the logger was started from an external switch mounted near the vessel.

After a time greater than twice the mean holdup time of the vessel the logging was stopped. The vessel was drained and flushed out. A different impeller speed was then chosen and the procedure repeated when steady state conditions had again been reached.

The logged voltage output tapes were then processed with the programme described in Appendix 2; to provide the normalised response curves for each run.

The same experimental technique was adopted for the glycerol-water experiments and with water in the 19" diameter, 42" diameter vessels.

6.6. Viscosity Determination

The viscosities of the glycerol-water solutions were determined by using an Ostwald viscometer. A comparison was drawn between the experimental solutions and pure water in order to calculate the absolute viscosity of the mixture.

6.7. Batch Mixing Time Experiments

Using a visual observation technique, experiments were carried out to determine the batch mixing time for different turbine and propeller agitated systems. Various ratios of impeller diameter to vessel diameter were used and the effect of baffles and different impeller positions were also investigated. The ratio of liquid height to vessel diameter was unity. The motor drive unit and impellers employed were as previously described in section 6.2.1.

6.7.1 Batch mixing vessels

The vessels used in these experiments were cylindrical flat bottomed vessels of 10",13", 19" diameter. The 10",13" diameter vessels were made of glass and the 19" diameter vessel from white polythene. A white paper background surrounded the two smaller tanks, but with the larger vessel this was unnecessary as the observations were made looking vertically downwards onto the fluid.

6.7.2 Experimental procedure

The same experimental procedure was used for the three tanks and for both turbine and propeller impellers.

5 ccs of 2N NaOH were added along with two drops of phenolphthalein solution to a vessel filled with water to the required level. The stirrer was set in motion to give the vessel contents a homogeneous pink colour. 5ccs of 2N HCl were then added to the vessel at the liquid surface and the time recorded for the last trace of pink to disappear. This was repeated five times for each impeller speed and the batch mixing time taken to be the average of these readings.

6.8. Streak Photography Experiments

6.8.1. Apparatus

A cylindrical glass tank, 10" diameter with 0.12D baffles, was placed inside a 12" cubic tank manufactured from 3/16" perspex. Two sides of the straight sided tank were completely covered with black paint. The third side was painted except for a vertical 1/8" band down the middle, and half of the fourth side was also painted. The vessels were surrounded by an iron framework which supported the impeller drive unit. The space between the cylindrical vessel and the outer tank was filled with water to eliminate the distortion in viewing the tank from the side.

The illumination was provided by a photoflood bulb mounted in a box. The light passed through two slits in the box forming a parallel beam which was directed into the body of the fluid through the 1/8" clear band on the side of the outer tank.

The camera used was an Exakta with a Tessar 2.8/50 lens. The films used were Kodak Tri-X and HP4 panchromatic; both are high speed films which produce high contrast photographs.

The tracer used was aluminium powder; these particles reflected sufficient light to photograph well.

The impellers used were of the type described in section 6.2.1.

6.8.2. Experimental procedure

The cylindrical tank was filled up to a height of 10", (Z/D = 1). The space between the two tanks was filled above this level. The impeller was positioned centrally in the inner vessel and the motor drive switched on. A small quantity of aluminium powder was then dropped on the fluid and given time to disperse through the tank.

Photographs were taken with the camera positioned in front of the half clear side, so that the plane passing through the centre of the tank and impeller was recorded. This was repeated for various impeller positions for both turbine and propeller. The impeller speed and camera position were the same for each photograph.

The negatives were developed by the normal method of immersion in developer, fixer and water.

7. COMPARISON OF EXPERIMENTAL RESULTS AND THEORETICAL PREDICTIONS

7.1. Impeller Pumping Capacities

The turbine pumping capacity relationship of $q = 0.94ND^3$ was employed. This expression was determined by Gibilaro (26) using a flow follower technique for turbines identical to those used in this work.

An expression was determined for the propeller pumping capacity from the theoretical treatment of Cooper and Wolf (15). The expression derived is $q = 0.95ND^3$. Experimental verification of this relationship for identically similar propellers has been provided by Gaskell and Whitehead (24).

7.2. Comparison of Turbine Impulse Response Results with Single and Double Loop Models

The normalised response results for all the turbine experiments are presented in Appendix 1.1.

In this section experimental normalised residence time distributions for the turbine impeller are compared with the theoretical predictions of the single and double loop models developed in Chapter 4. Tables are presented to indicate the vessel configuration, operating conditions and the variables investigated for each series of runs. The experiments were conducted for a wide range of impeller speed. The baffles were 0.12D.

The model parameter (q) was calculated for each individual impeller speed using the relationships discussed in section 7.1. The values obtained from the pumping capacity expression resulted in such excellent agreement between the experimental and theoretical response curves, that any further adjustment of the model parameter was considered unnecessary.

The computer programme described in Appendix 2 was used to calculate all the normalised experimental responses. The Markov programme, Appendix 3, was used to obtain the model solutions.

7.2.1. The 2½"/9"/9" cylindrical system:- water

	Series R.1	Series R.2	Series R.3	Series R.4
Liquid Holdup (litres)	9.37	9.37	9.37	9.37
Flow Rate (litres/min)	1.1	1.1	1.1	1.1
Maantime (mins)	8.5	8.5	8.5	8.5
Inlet Position	Into Impeller	Into Loop	Into Impeller	Into Loop
Baffles	Unbaffled	Unbaffled	Baffled	Baffled

Figures 7.1 -7.8 show the excellent comparison of experimental results and theoretical predictions for the 2½" dia. turbine in the 9"diameter cylindrical vessel.

For the case of feed to the impeller the fit is good, for both models, throughout the experimental range of q/Q studied, Figures 7.1 - 7.4. A small deviation appears between the experimental results and the model predictions, for $q/Q < 8$, in the feed to loop case, Fig. 7.5. The fit, for higher values of q/Q, is again reasonable for both models, Figures 7.7 -7.8.

The models predict that baffles will not affect the impulse response of the system. These figures verify this; experimental unbaffled and baffled responses being almost identical.

The discontinuous bold line describes the single loop model solutions and the "dots" the double loop model predictions.

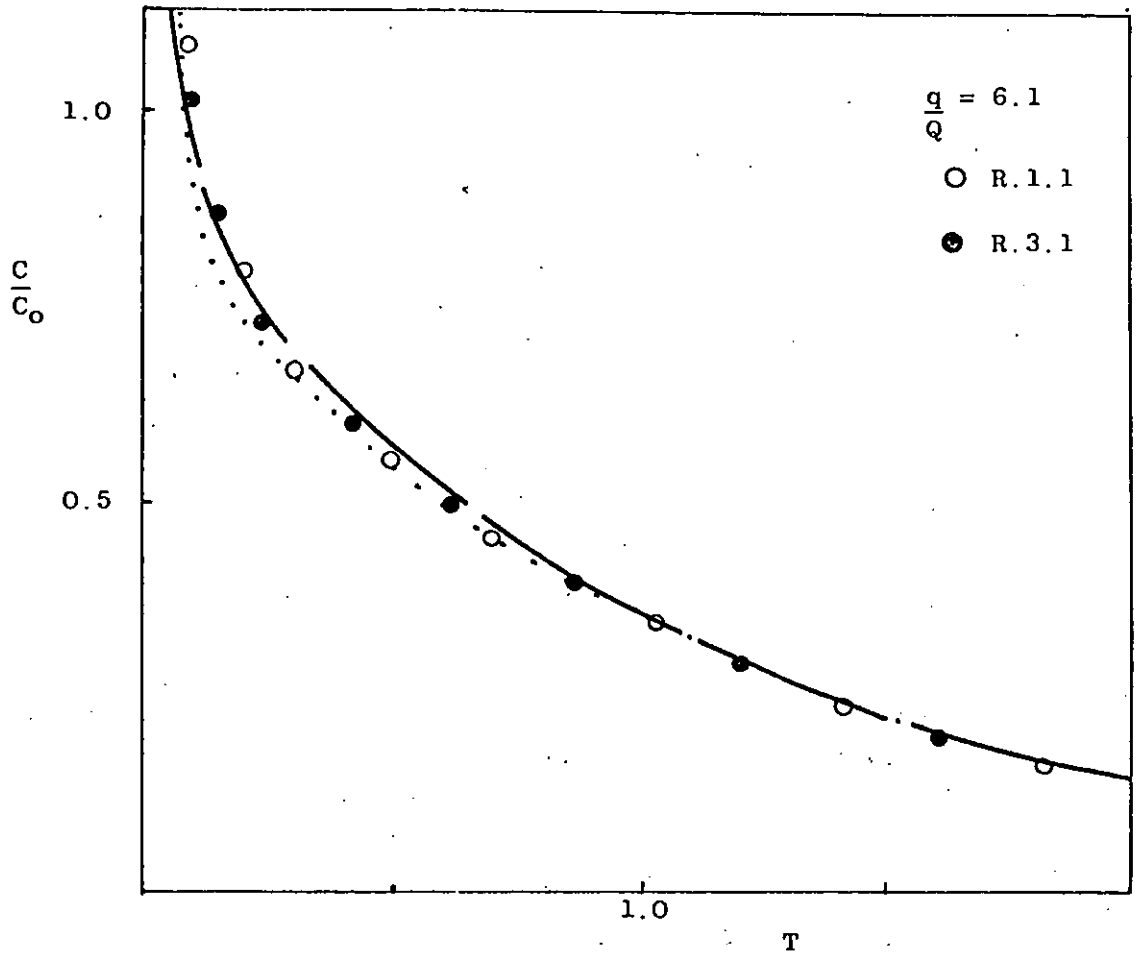

Fig. 7.1

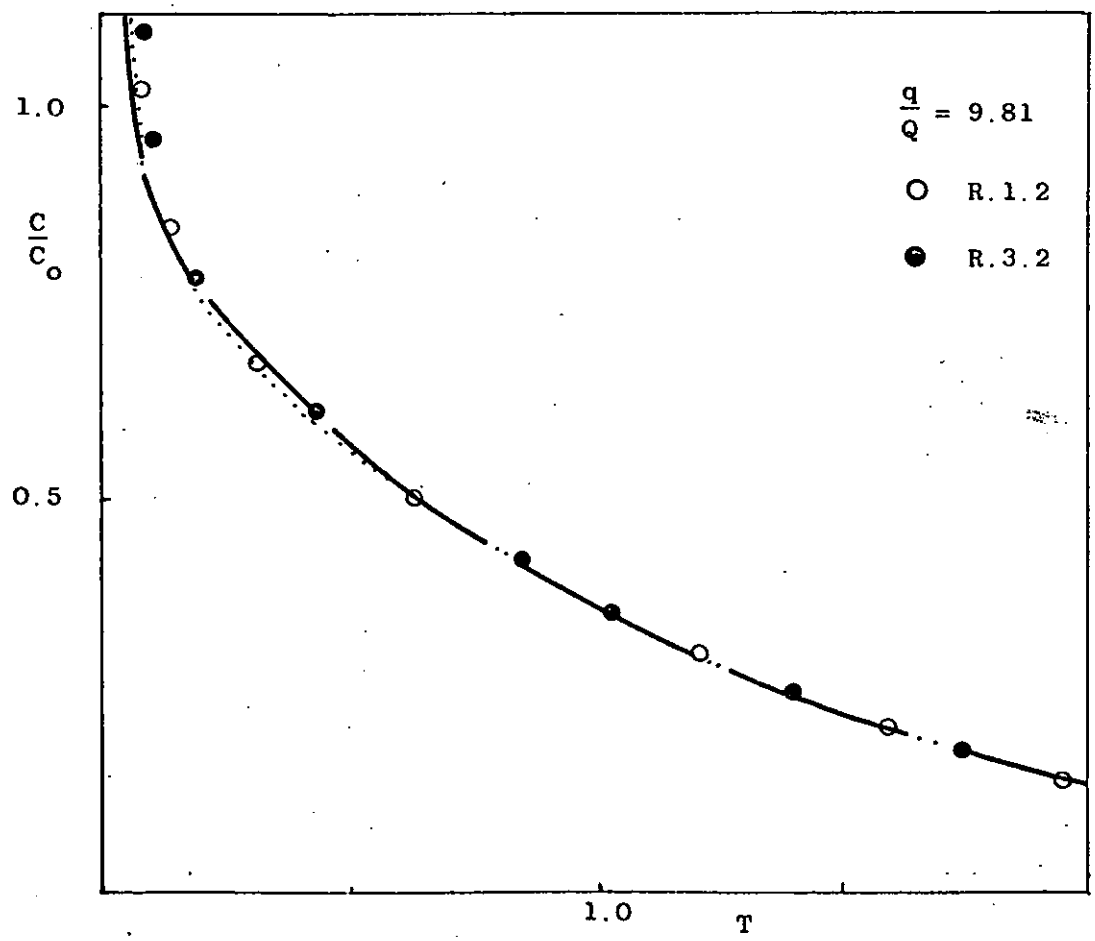

Fig. 7.2

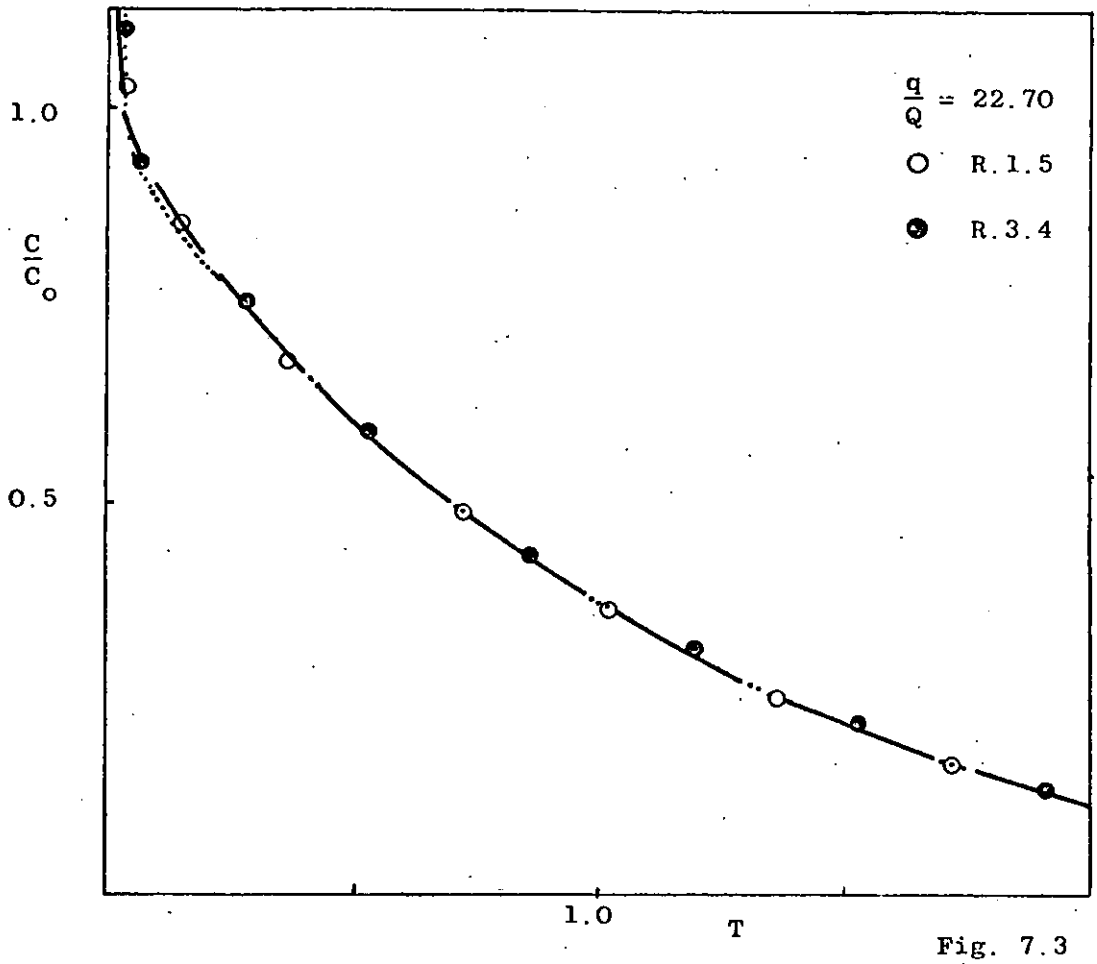

Fig. 7.3

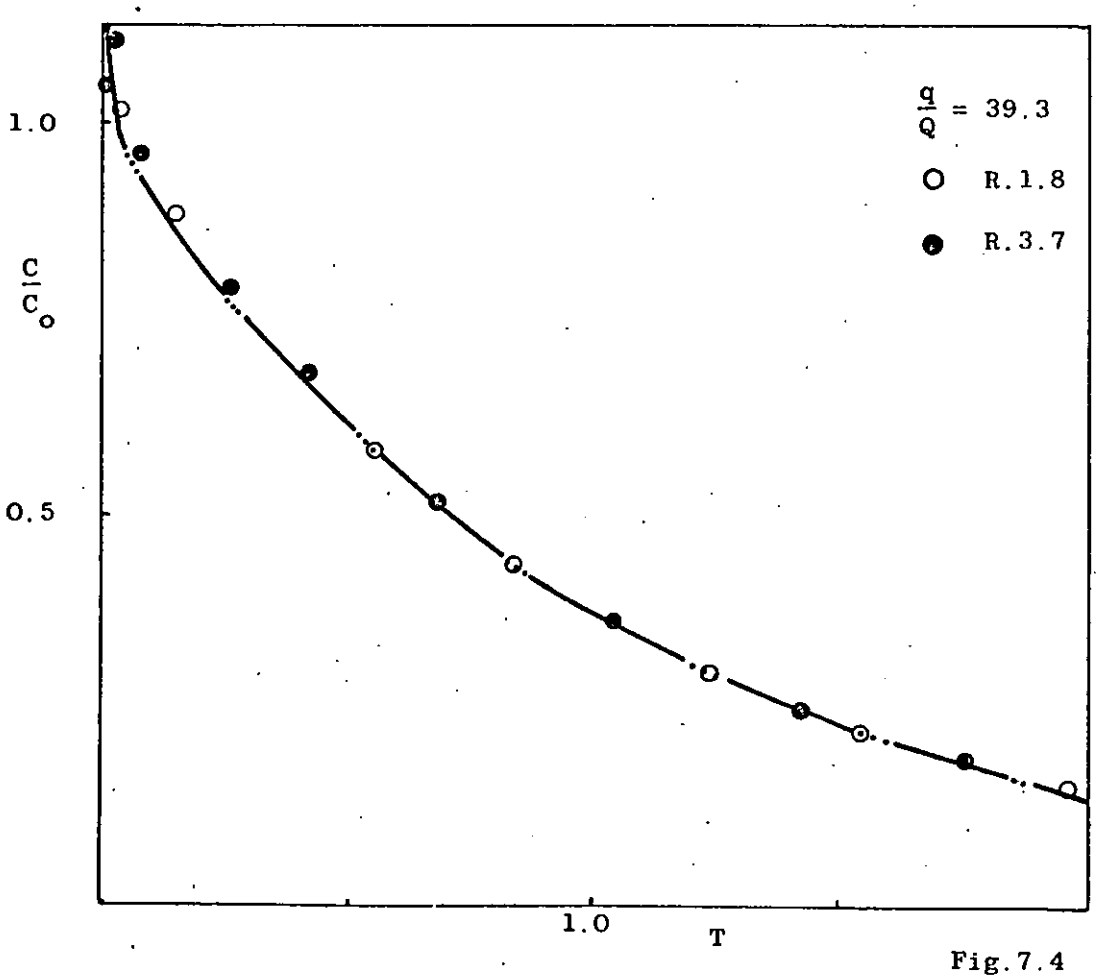

Fig. 7.4

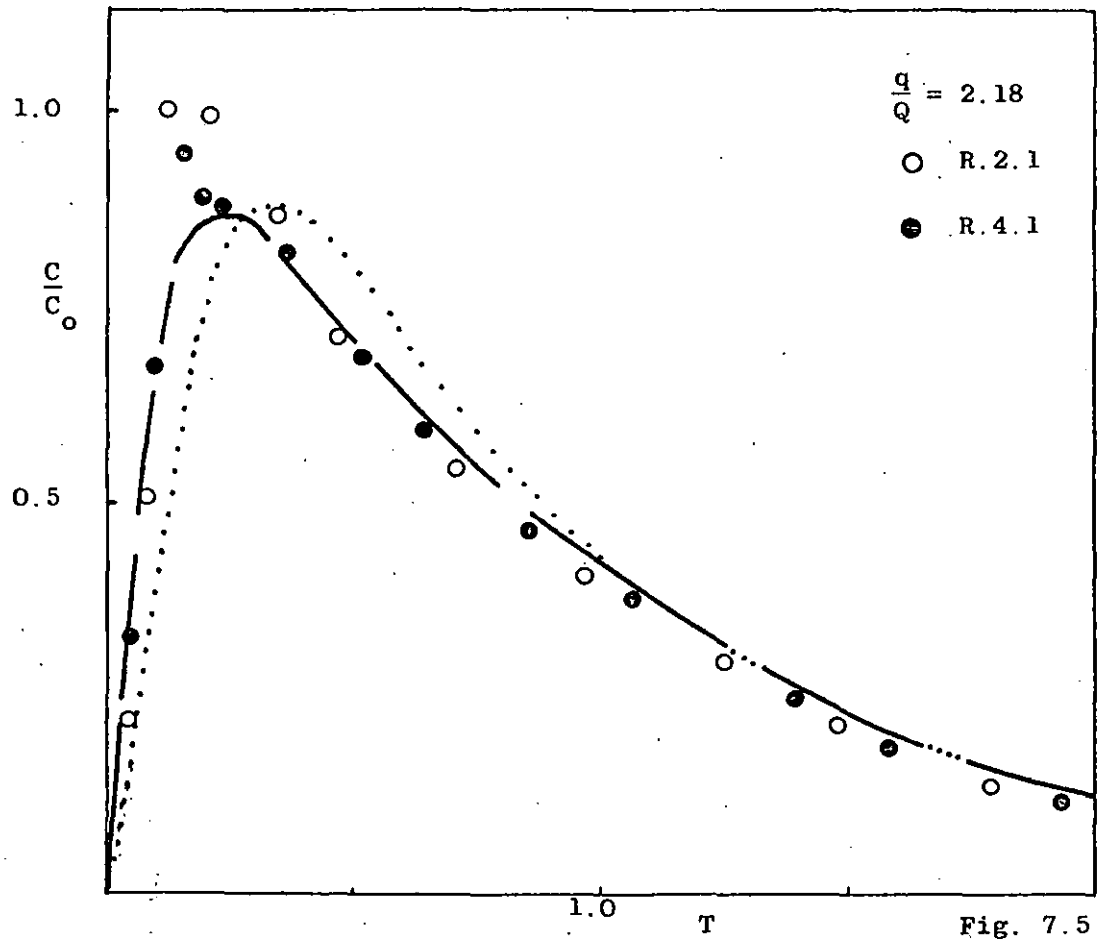

Fig. 7.5

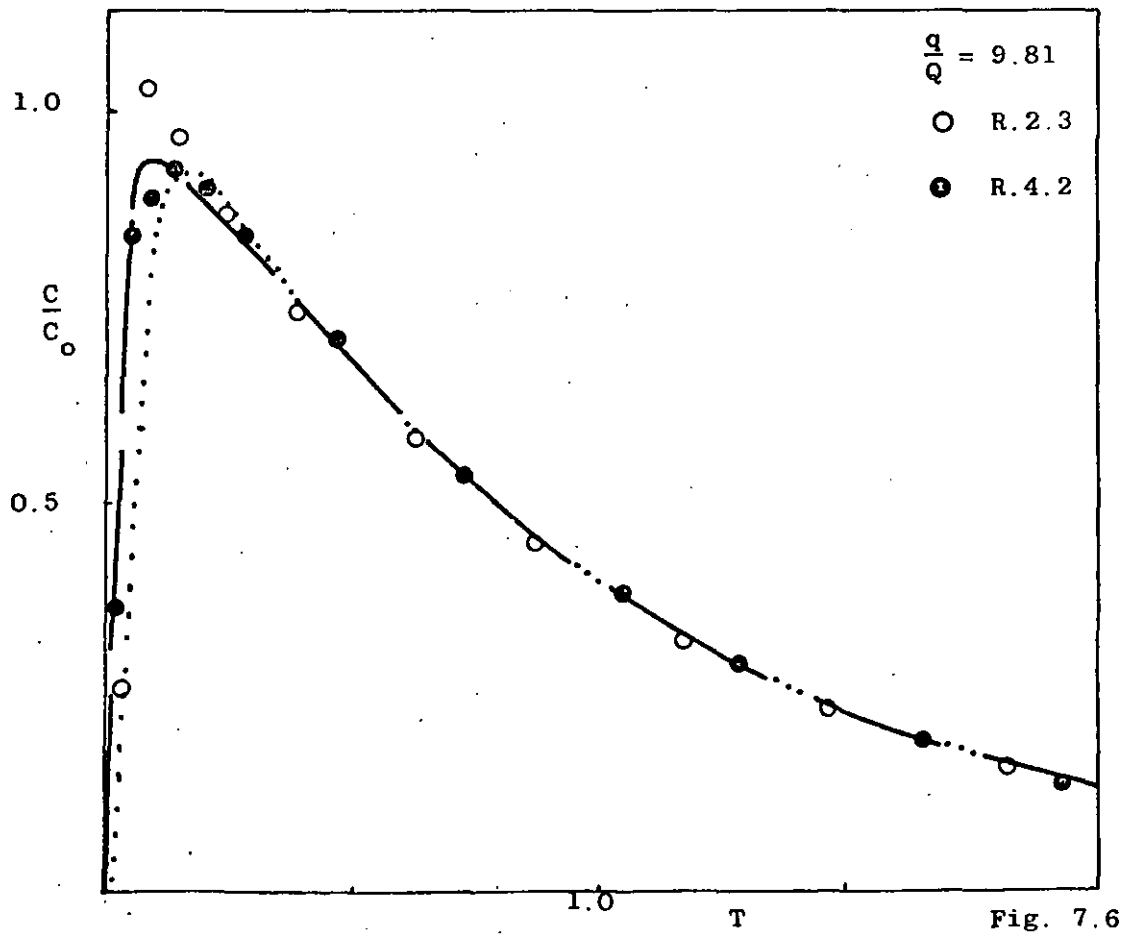

Fig. 7.6

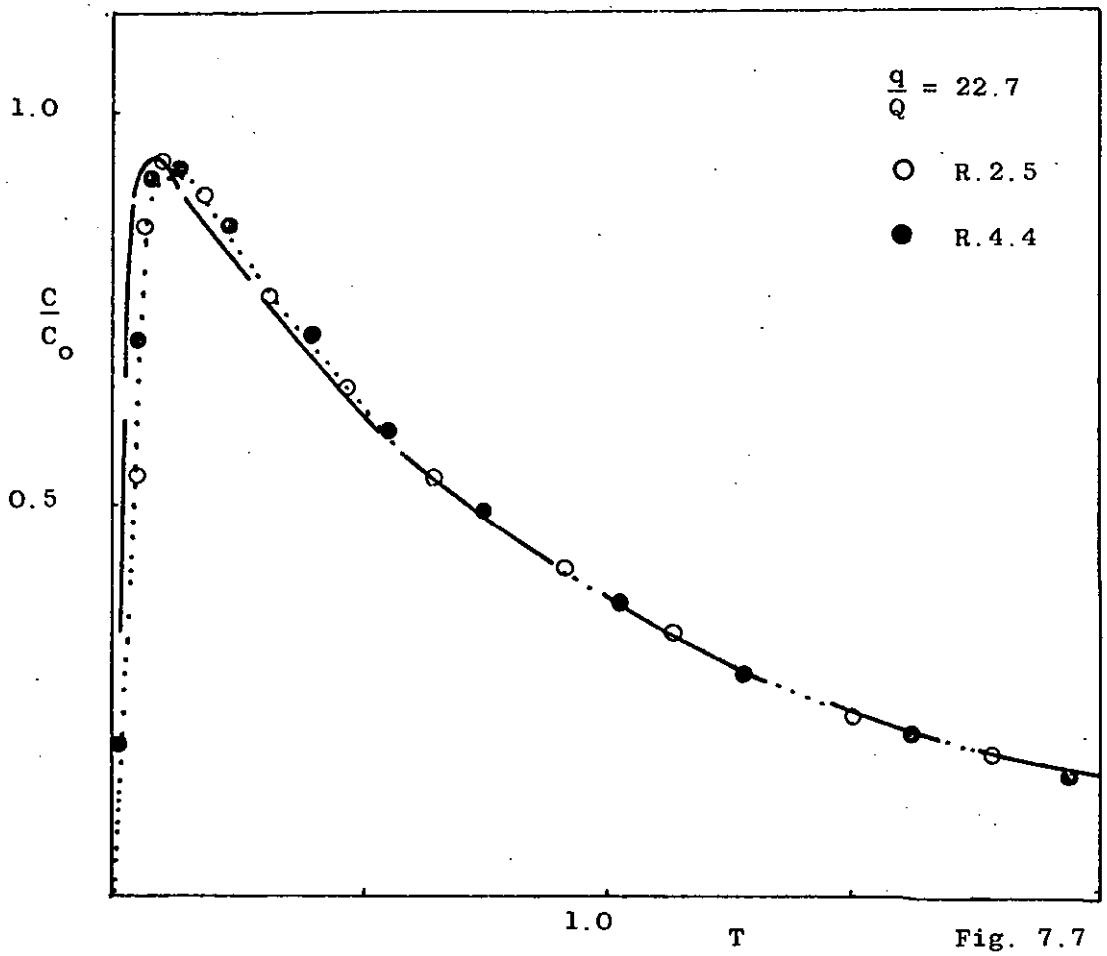

Fig. 7.7

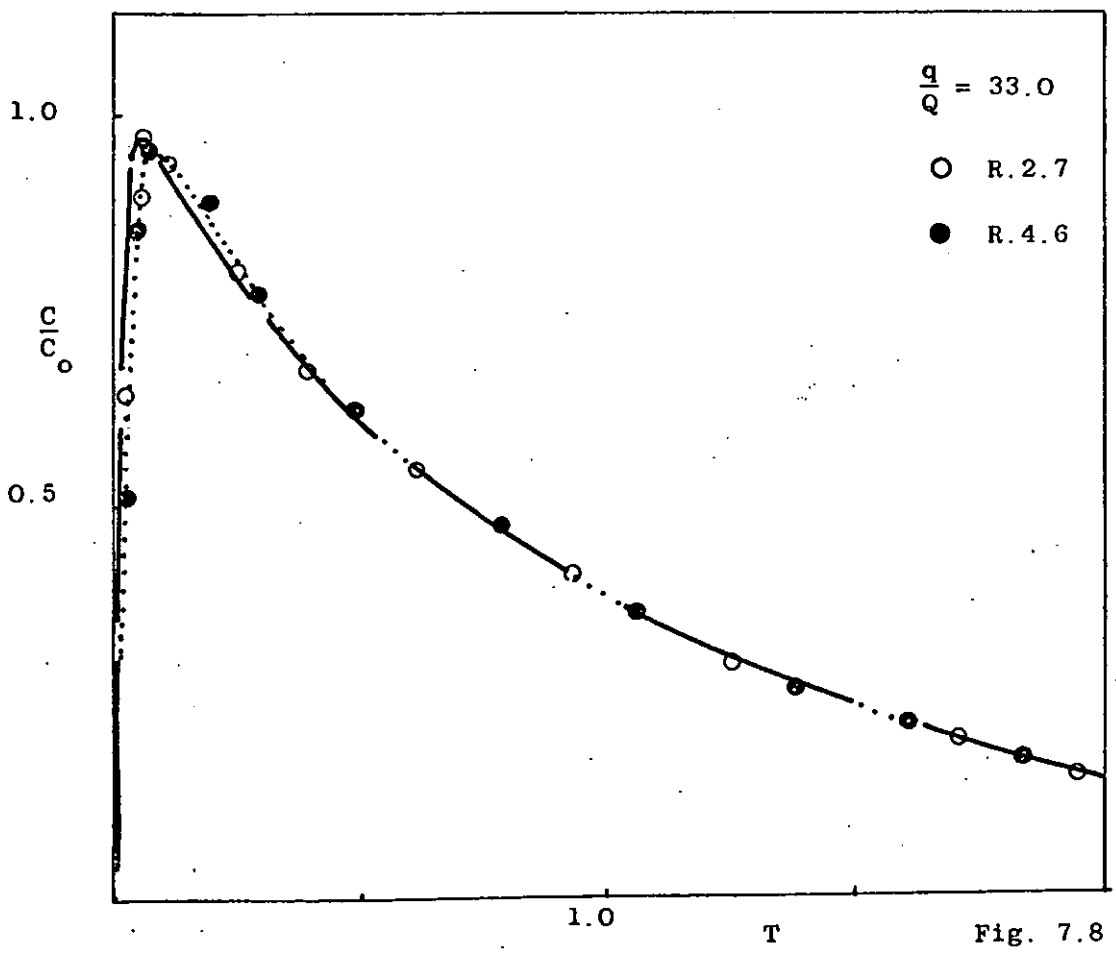

Fig. 7.8

7.2.2. The $2\frac{1}{2}$"/9"/9" cylindrical system:- glycerol/water solution (1.35 cp).

	Series R.5	Series R.6	Series R.7	Series R.8
Liquid Holdup (litres)	9.37	9.37	9.37	9.37
Flow Rate (litres/min)	1.0	1.0	1.0	1.0
Meantime (mins)	9.37	9.37	9.37	9.37
Inlet Position	Into Impeller	Into Loop	Into Impeller	Into Loop
Baffles	Unbaffled	Unbaffled	Baffled	Baffled

Figures 7.9 - 7.16 illustrate the excellent comparison of experimentally determined responses for the baffled and unbaffled ($2\frac{1}{2}$"/9") glycerol/water,1.35cp system and theoretical predictions. The difference between these responses and those of pure water is minimal and thus the comments about the correspondence between experimental and theoretical curves, for pure water, apply for solutions of 1.35cp. An additional factor that appeared was the increase in bypassing, in the case of feed to loop, for low values of q/Q. . Figure 7.13.

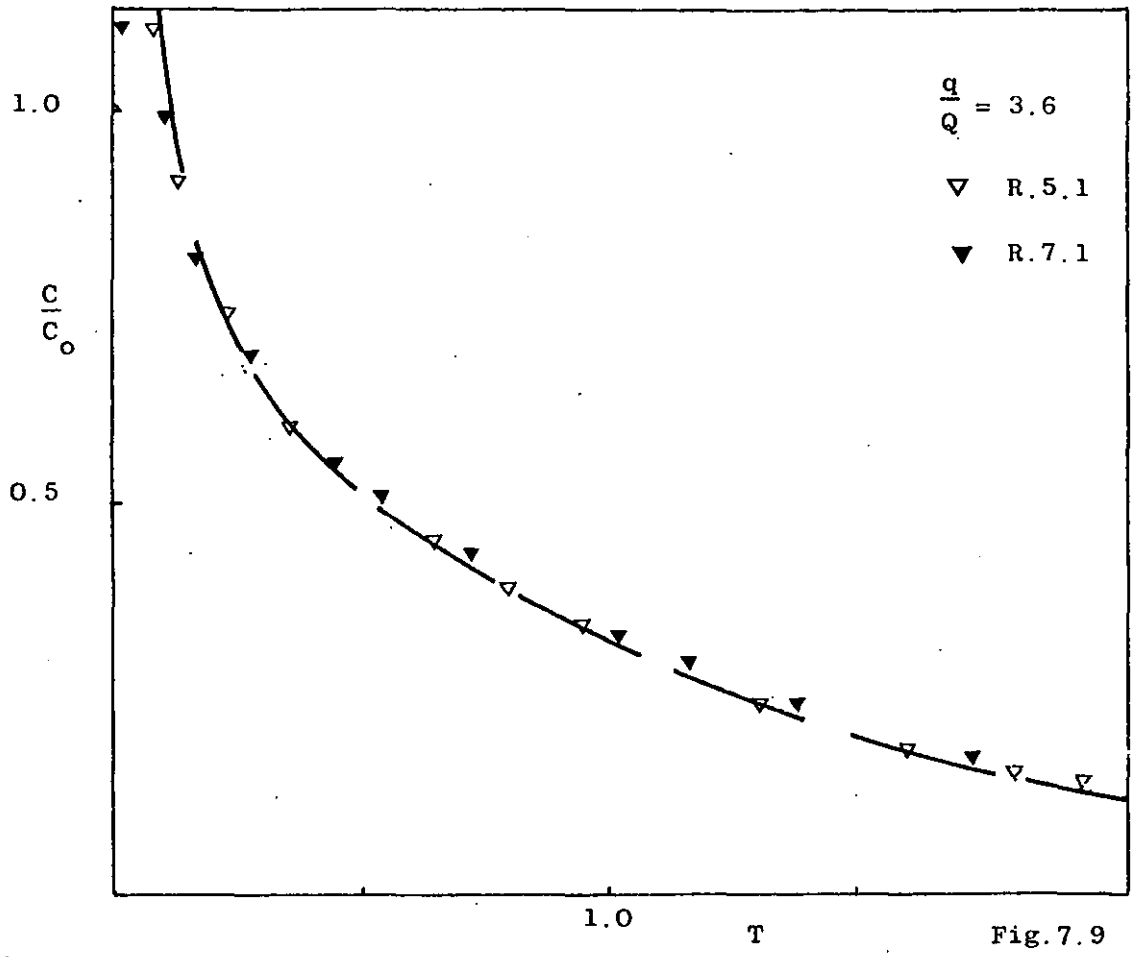

Fig.7.9

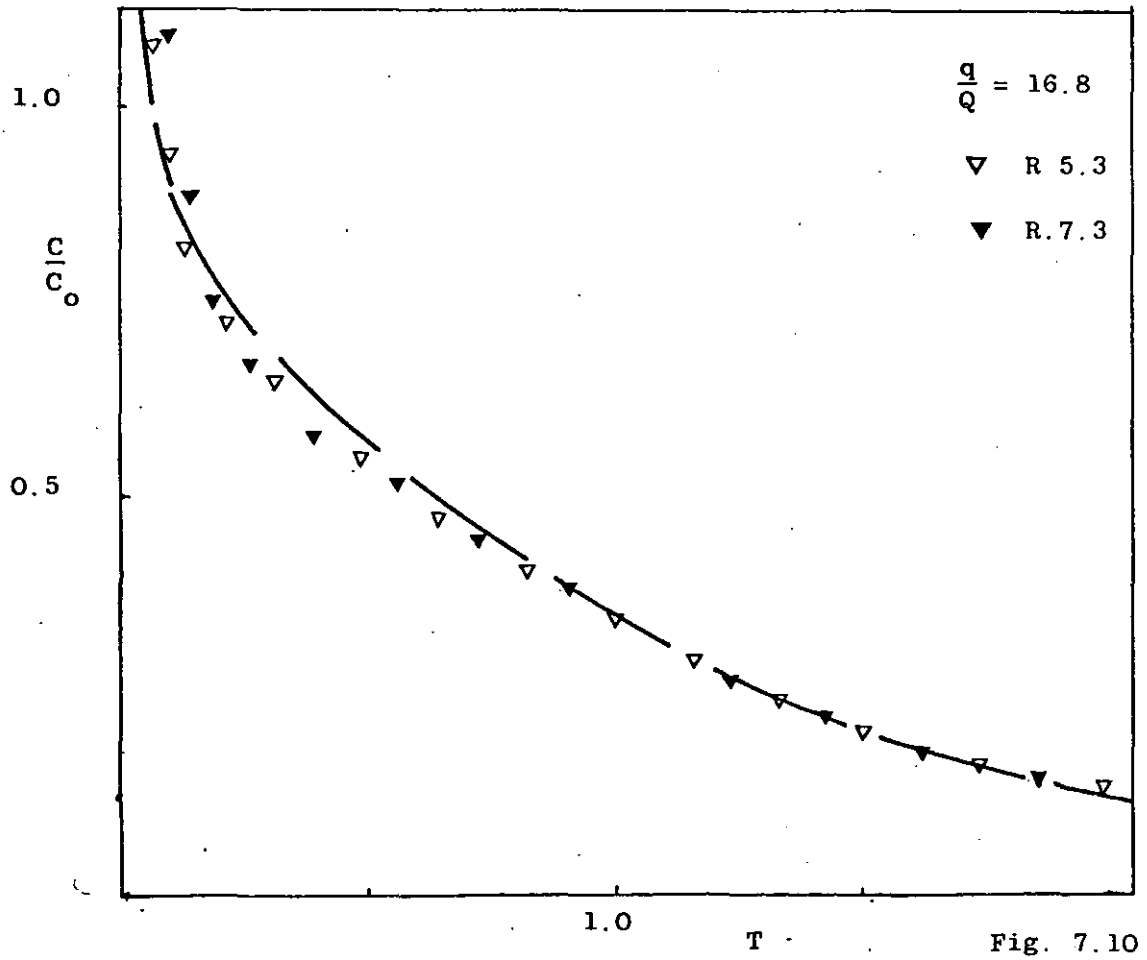

Fig. 7.10

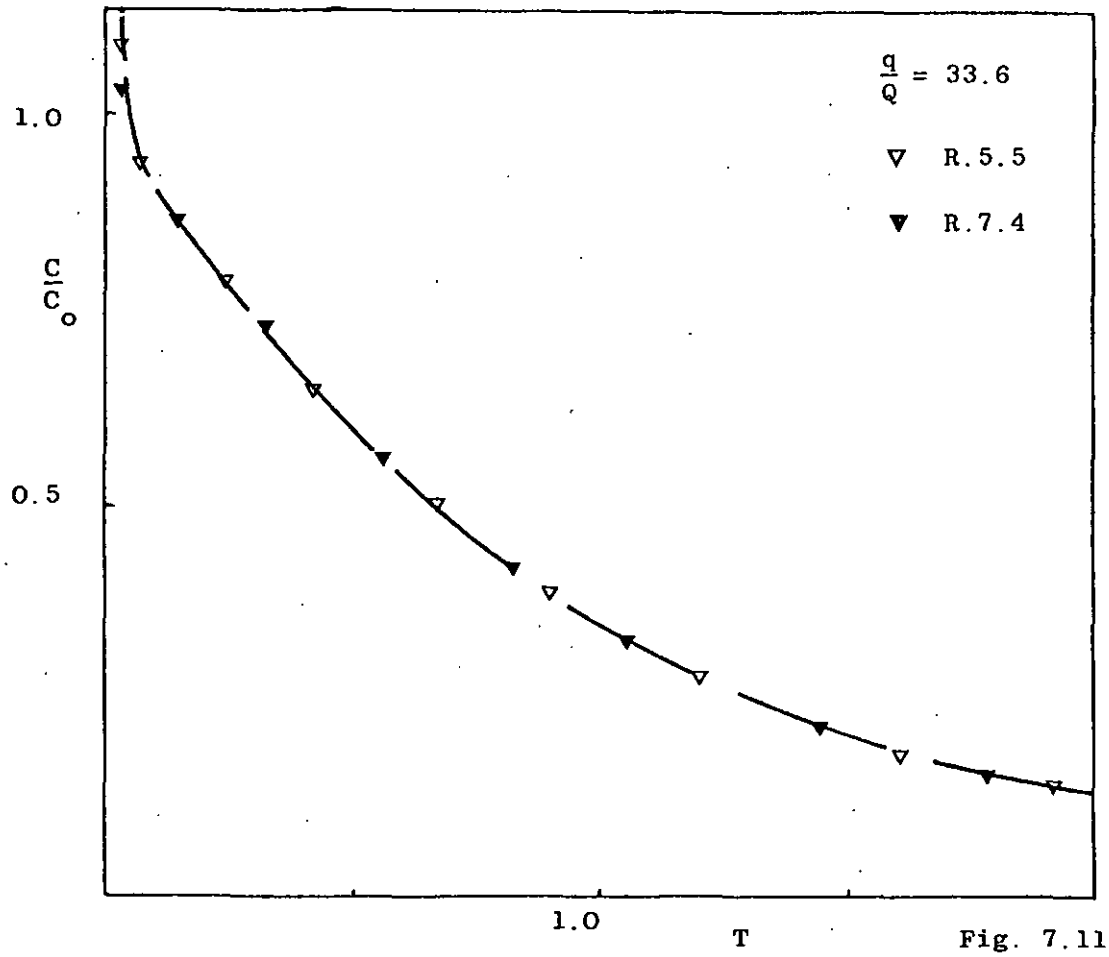

Fig. 7.11

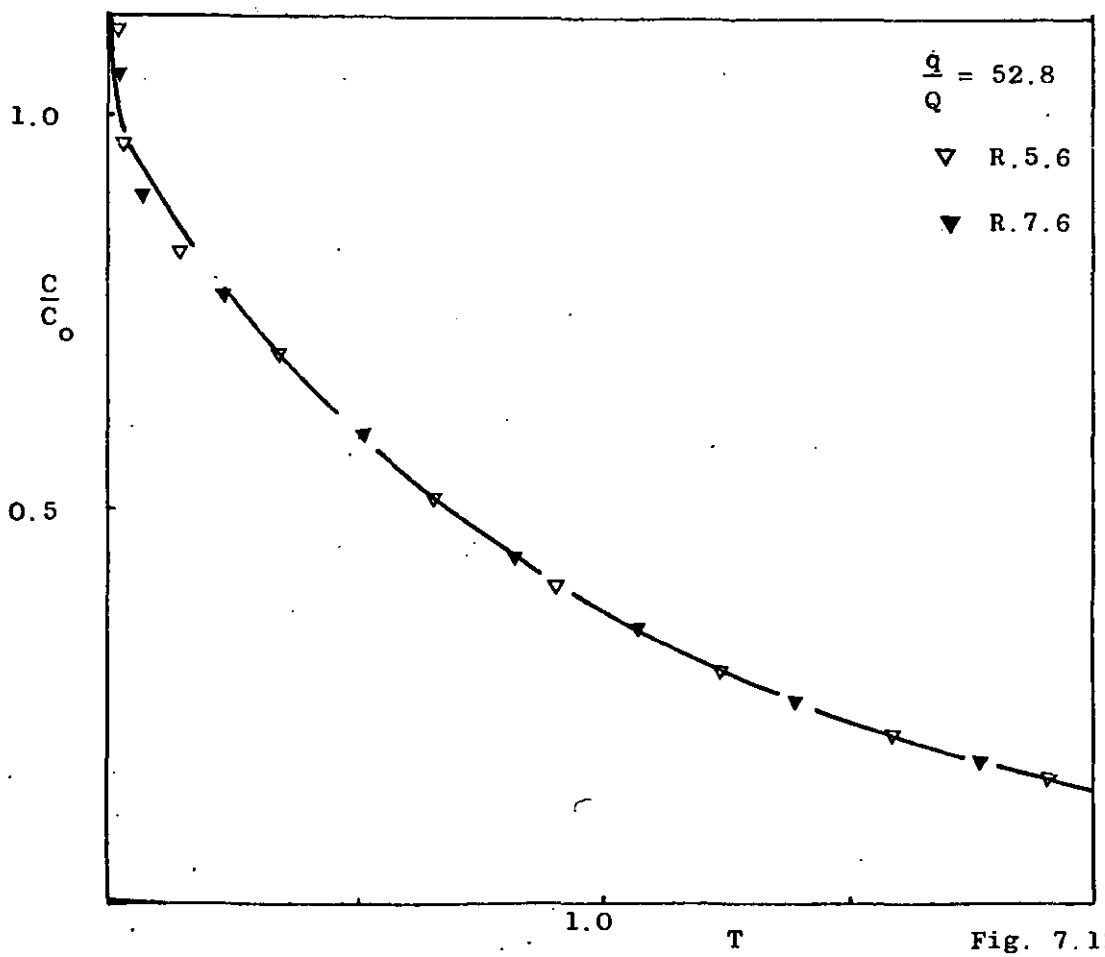

Fig. 7.12

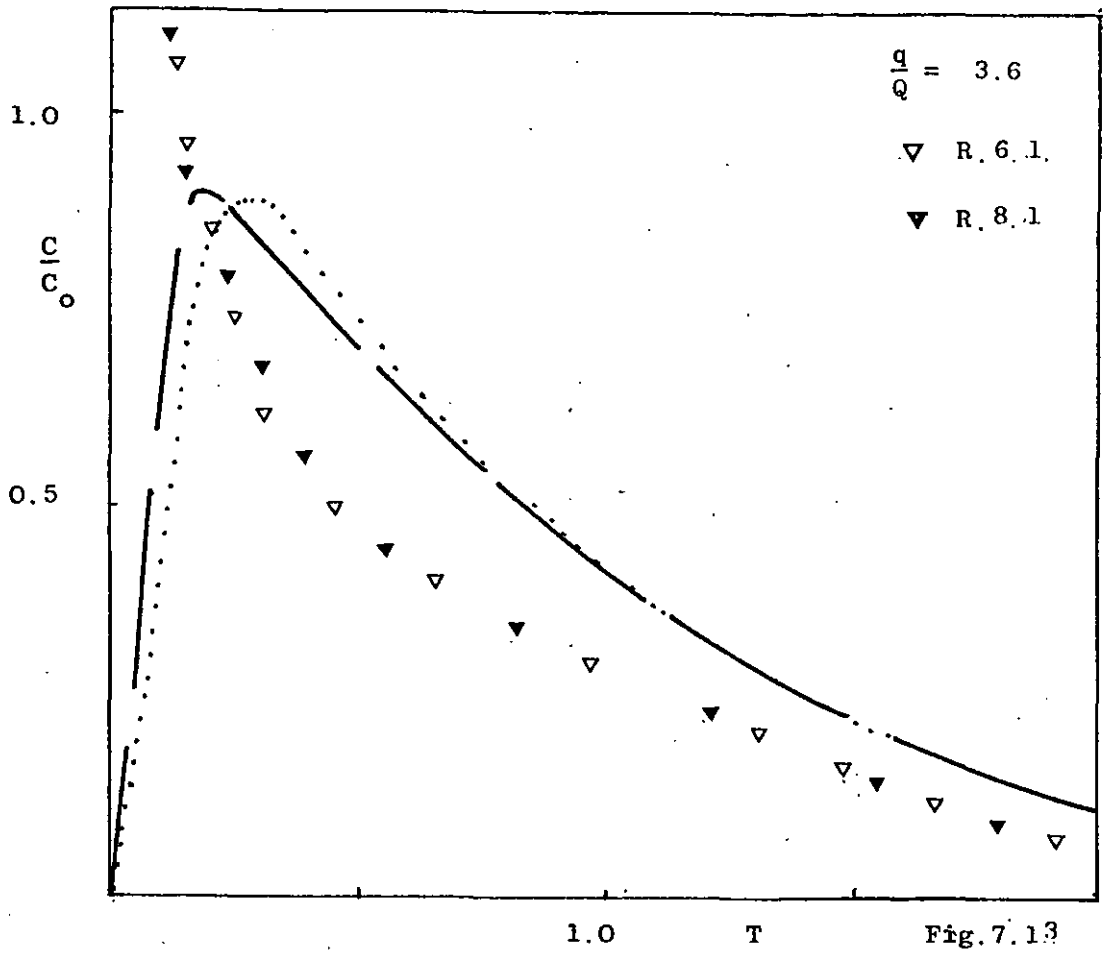

Fig. 7.13

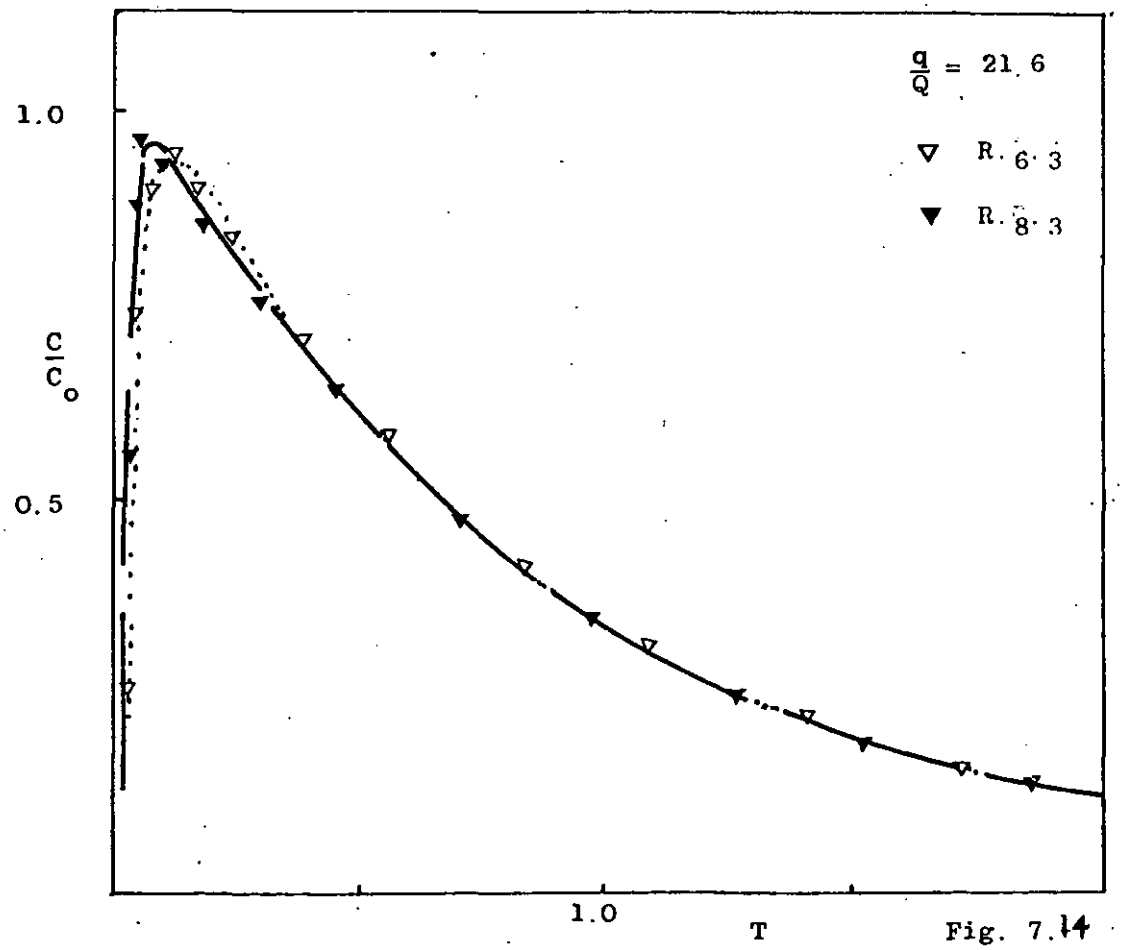

Fig. 7.14

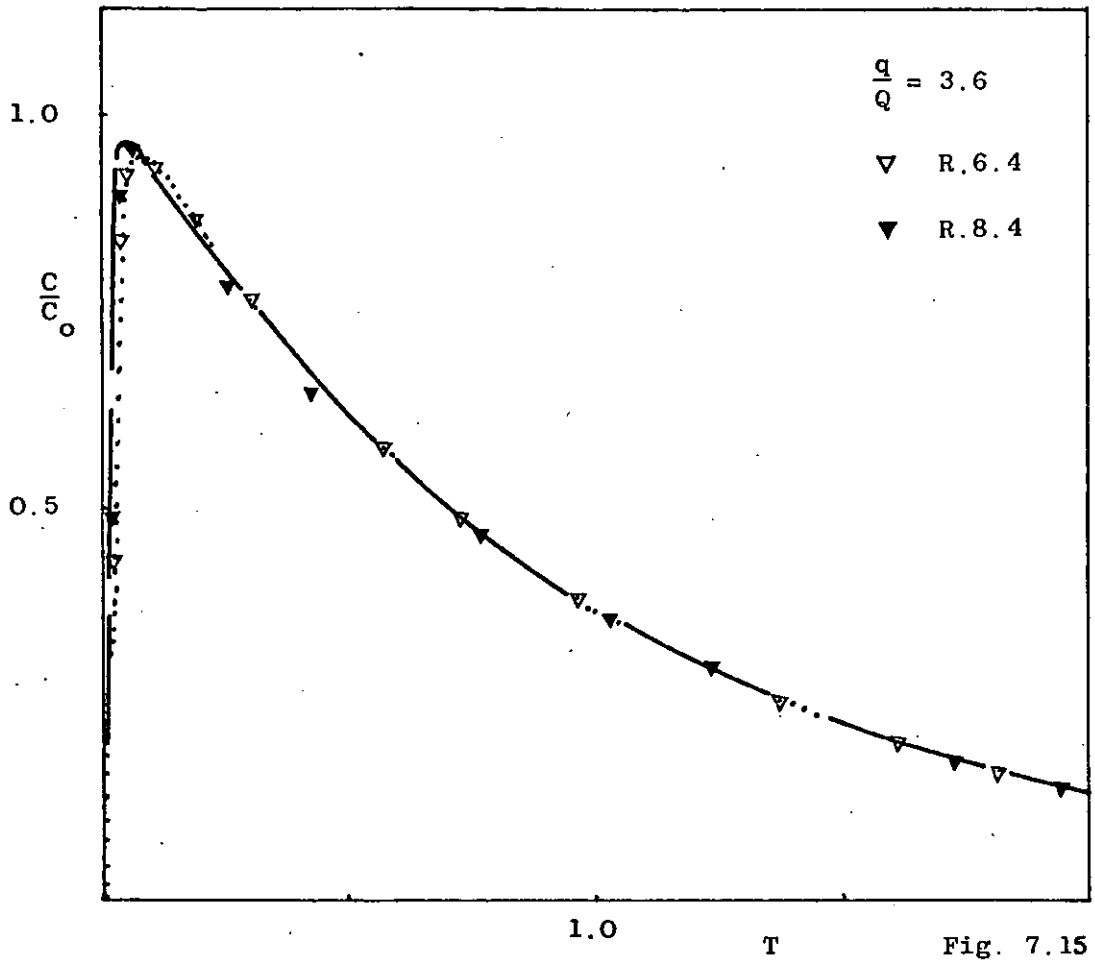

Fig. 7.15

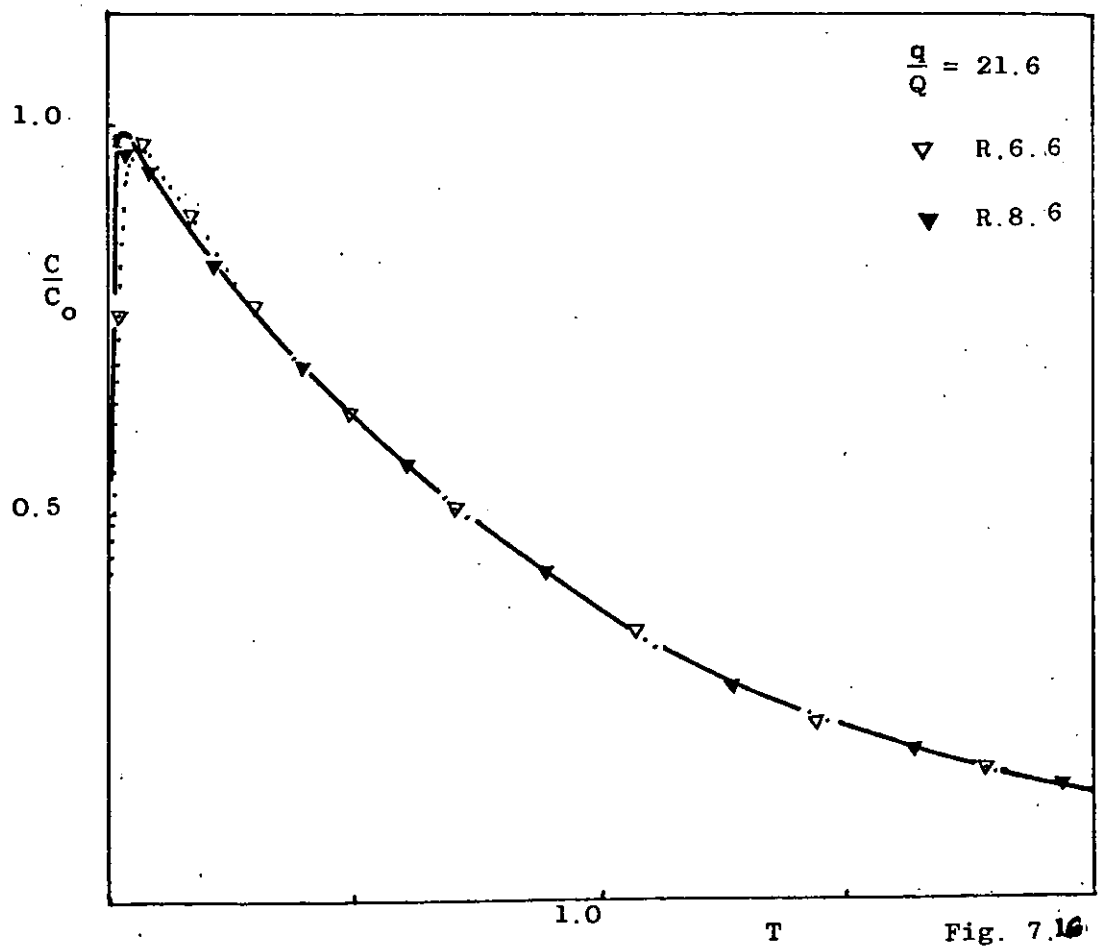

Fig. 7.16

7.2.3. The 2½"/9"/9" cylindrical system:- glycerol/water solution (2.5cp)

	Series R.9	Series R.10	Series R.11	Series R.12
Liquid Holdup (litres)	9.37	9.37	9.37	9.37
Flow Rate (litres/min)	1.0	1.0	1.0	1.0
Meantime (mins)	9.37	9.37	9.37	9.37
Inlet Position	Into Impeller	Into Loop	Into Impeller	Into Loop
Baffles	Unbaffled	UnBaffled	Baffled	Baffled

Figures 7.17 - 7.24 show the good comparison of the single and double loop model predictions with the experimental results for the 2.35 cp solution. The comparison is slightly worse in the lower range of (q/Q) than for the pure water and the 1.35 cp solution experiments, for both inlet feed positions. However, for $q/Q > 15$ the comparison between experimental results and theoretical predictions is still excellent. Previous comments on baffling apply in this section.

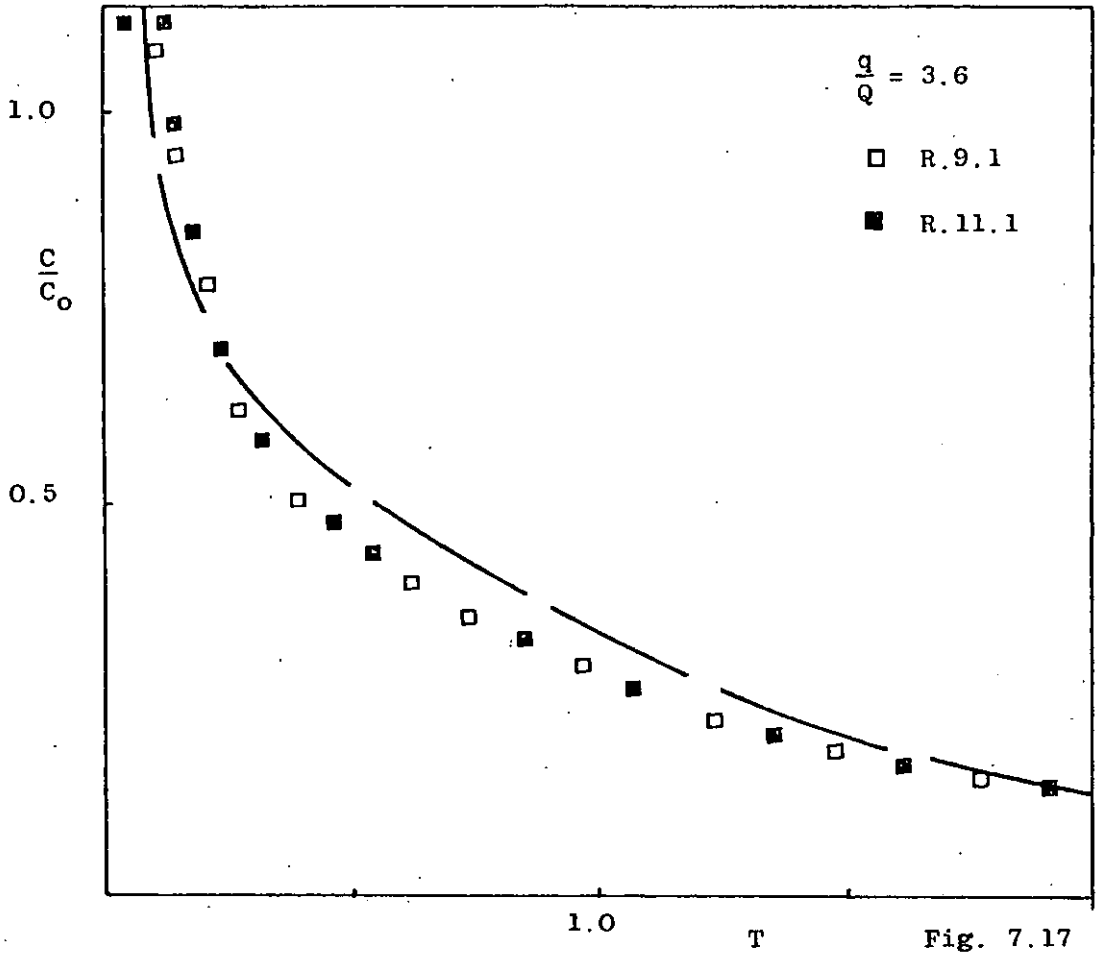

Fig. 7.17

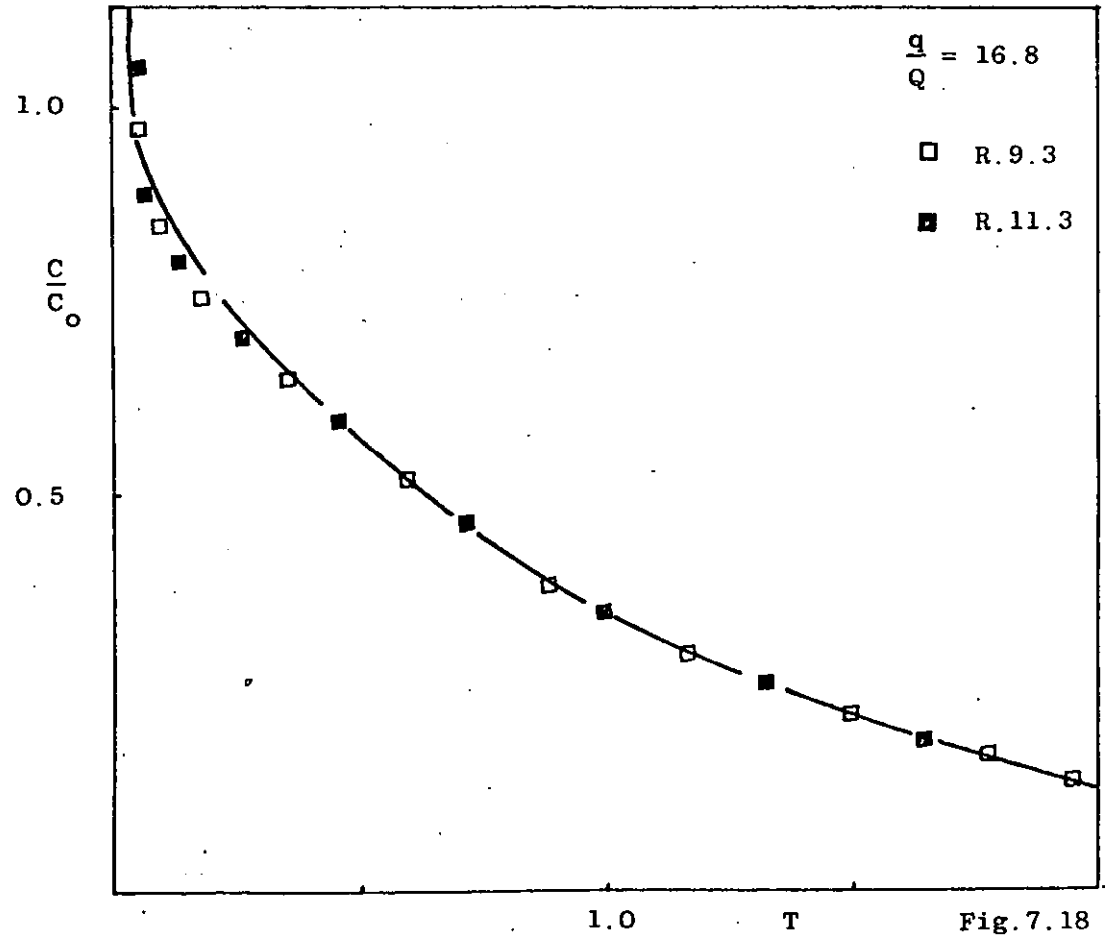

Fig.7.18

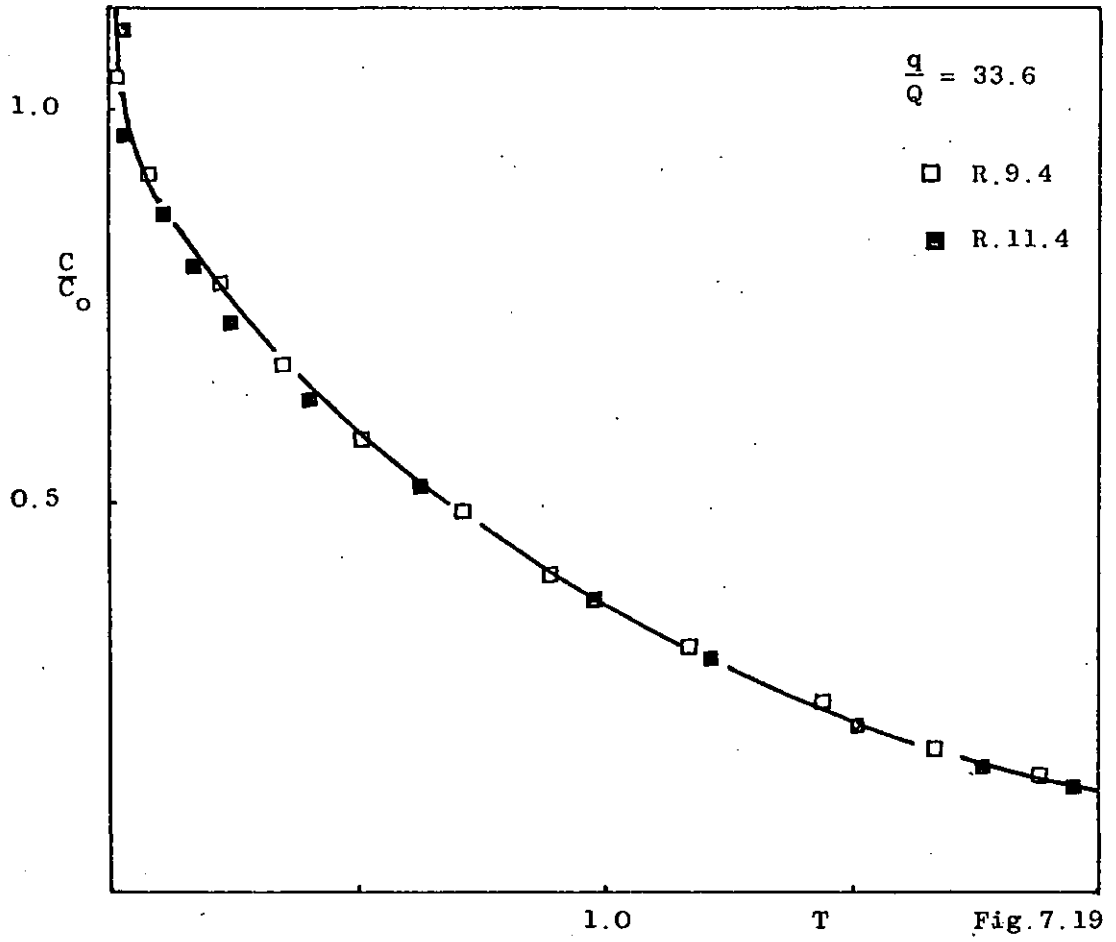

Fig.7.19

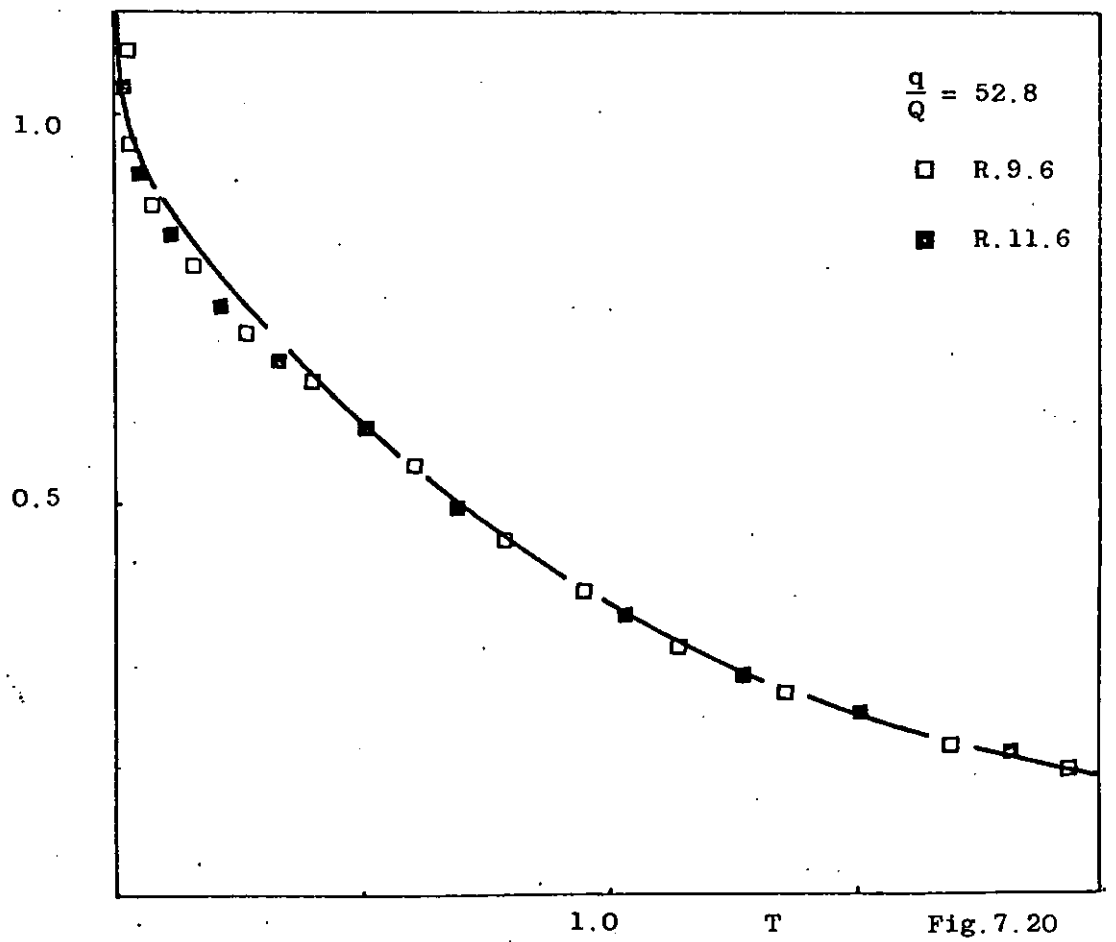

Fig.7.20

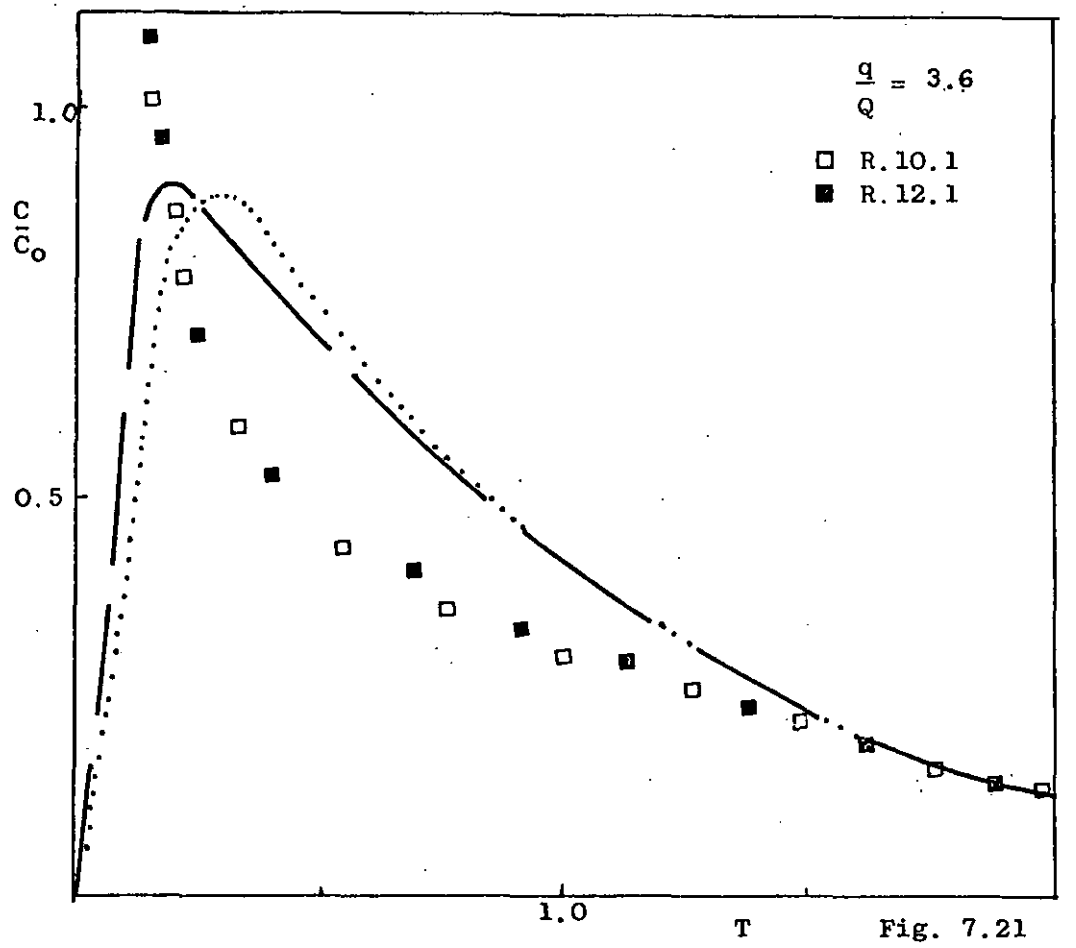

Fig. 7.21

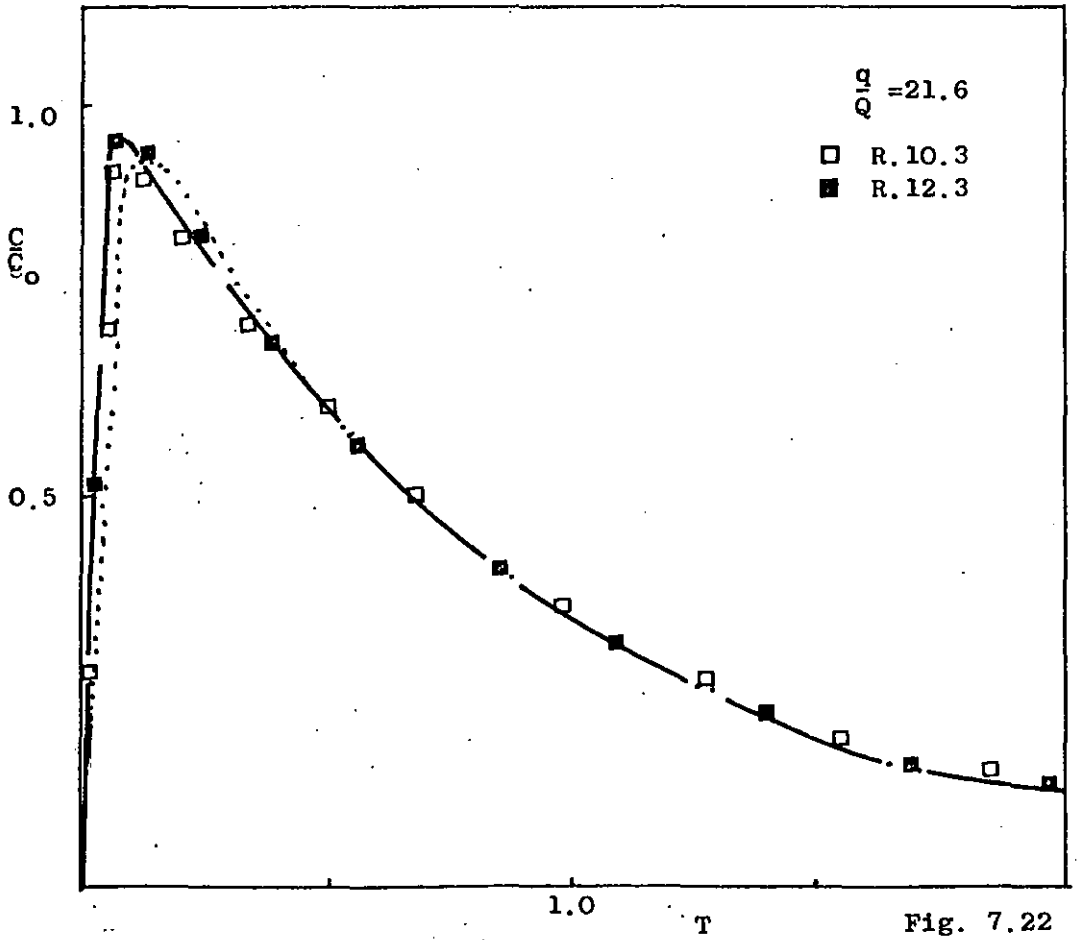

Fig. 7.22

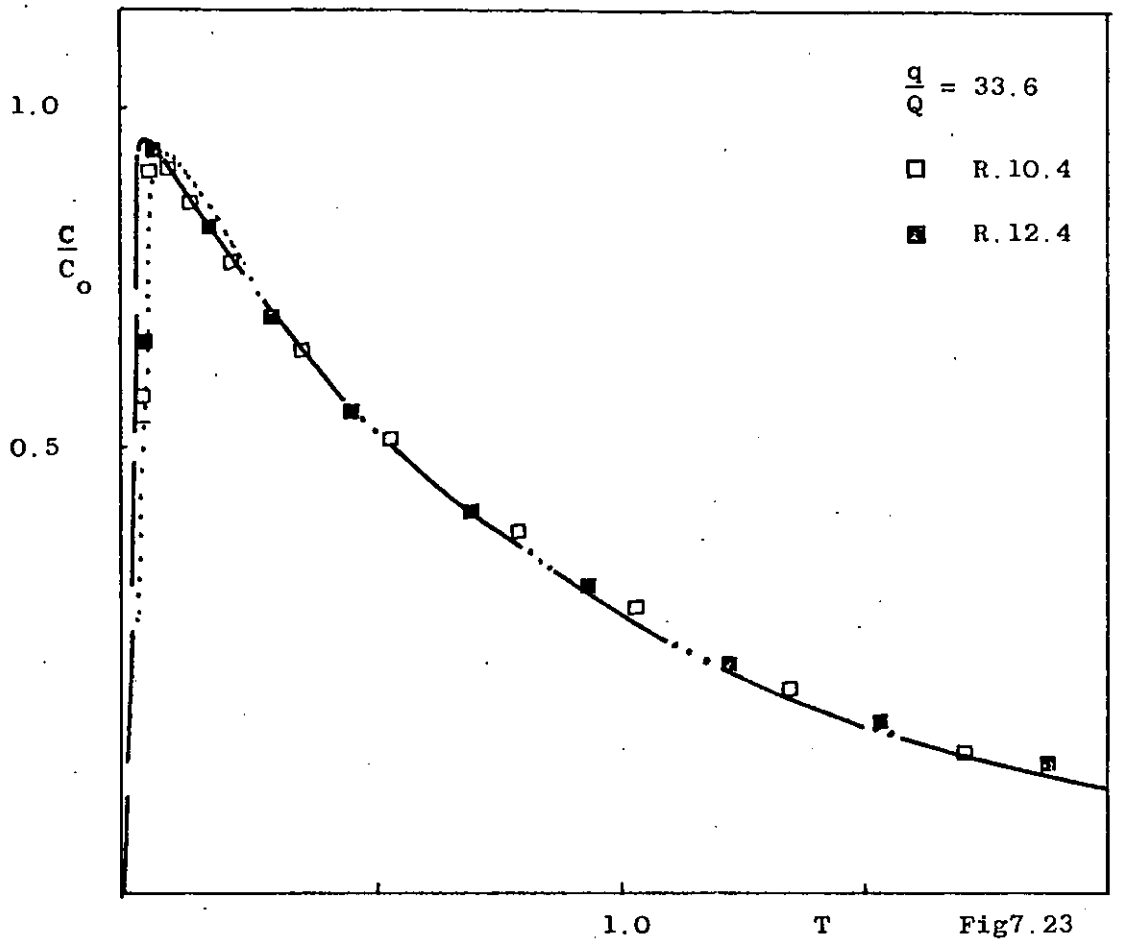

Fig7.23

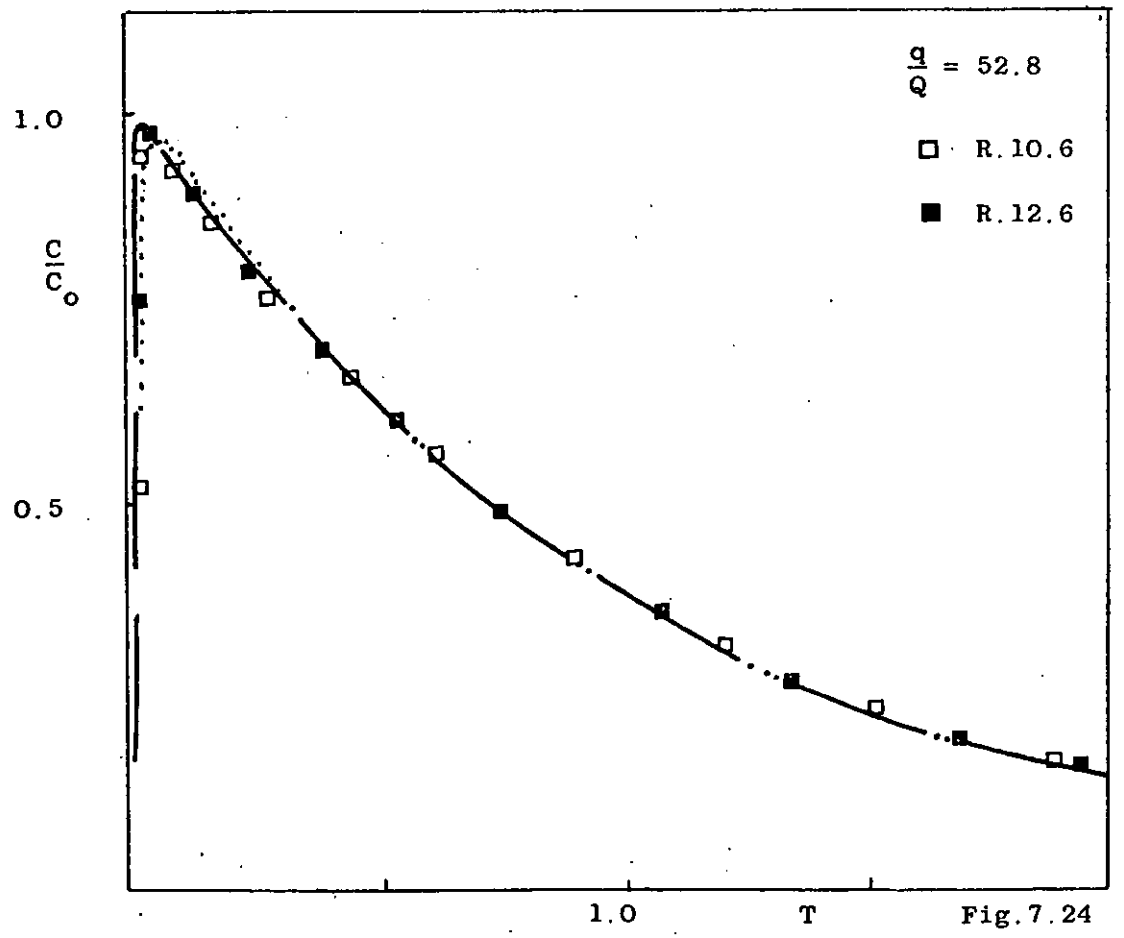

Fig.7.24

7.2.4. The 2½"/9"/9" cylindrical system:- glycerol/water solution (7.65 cp).

	Series R.13	Series R.14	Series R.15	Series R.16
Liquid Holdup (litres)	9.37	9.37	9.37	9.37
Flow Rate (litres/min)	1.0	1.0	1.0	1.0
Meantime (min)	9.37	9.37	9.37	9.37
Inlet Position	Into Impeller	Into Loop	Into Impeller	Into Loop
Baffles	Unbaffled	Unbaffled	Baffled	Baffled

In the case of the 7.65 cp glycerol/water system the comparison of experimental and theoretical responses is again very good for large values of (q/Q). However, when $(q/Q) < 15$, a bypassing effect predominates for both inlet feed to loop and feed to the impeller cases. Figures 7.25 and 7.32 illustrate this. Baffles are again found to have little effect on the impulse response of the system.

The residence time distribution curves, obtained for thin fluids agitated by a turbine impeller, yield a reasonable comparison with the predictions of the single and double loop models over a wide range of impeller speed. For low values of (q/Q), for the feed to loop condition a bypass effect is found. This disappears when the value of (q/Q) reaches a certain limit; the limit increases as the viscosity increases. Above this value an excellent comparison of theoretical and experimental curves is observed.

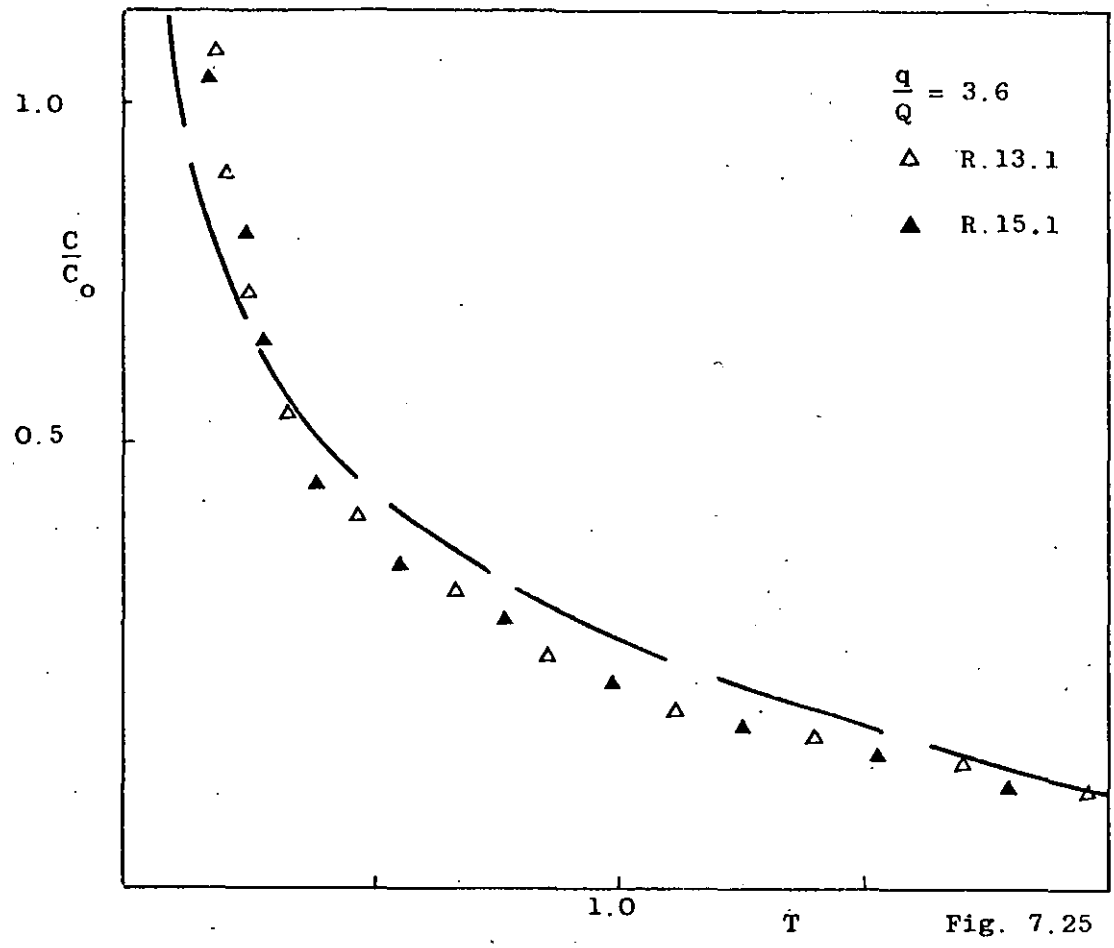

Fig. 7.25

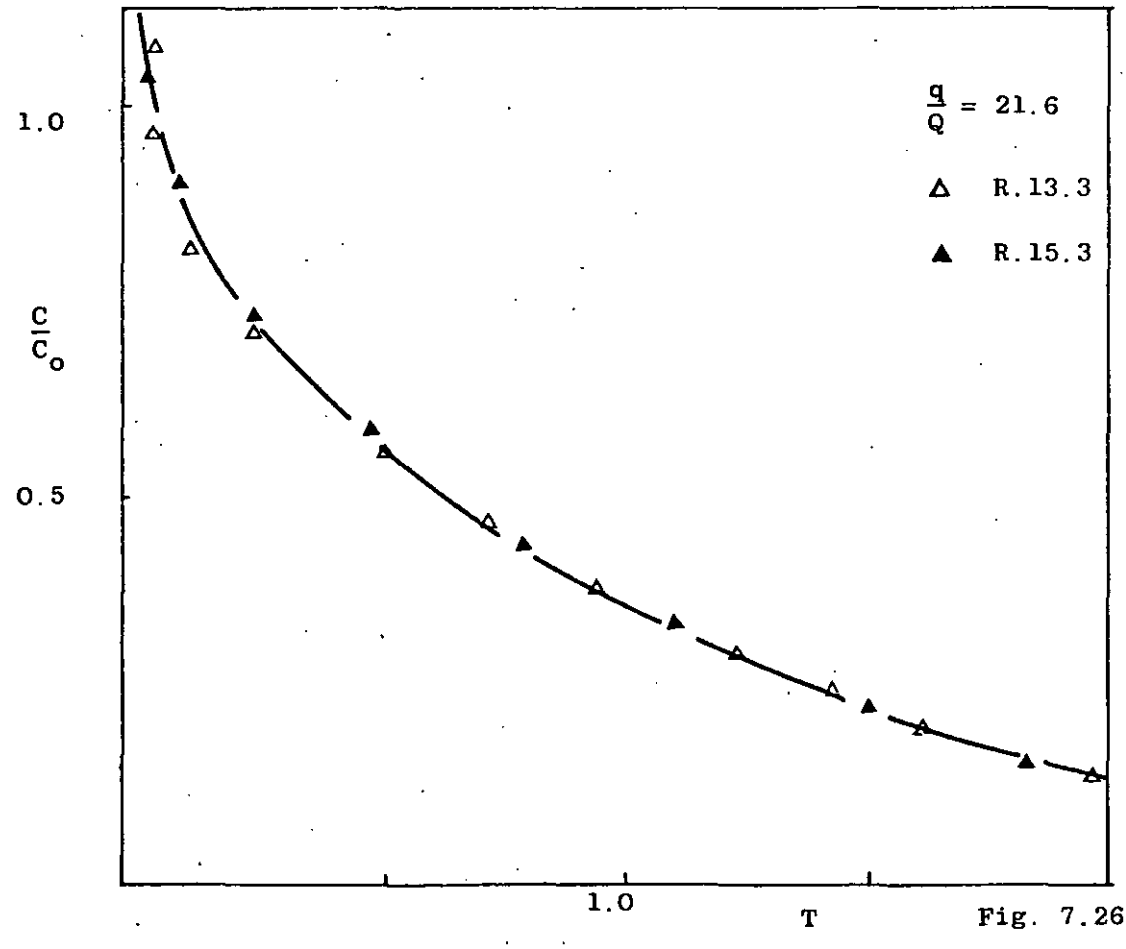

Fig. 7.26

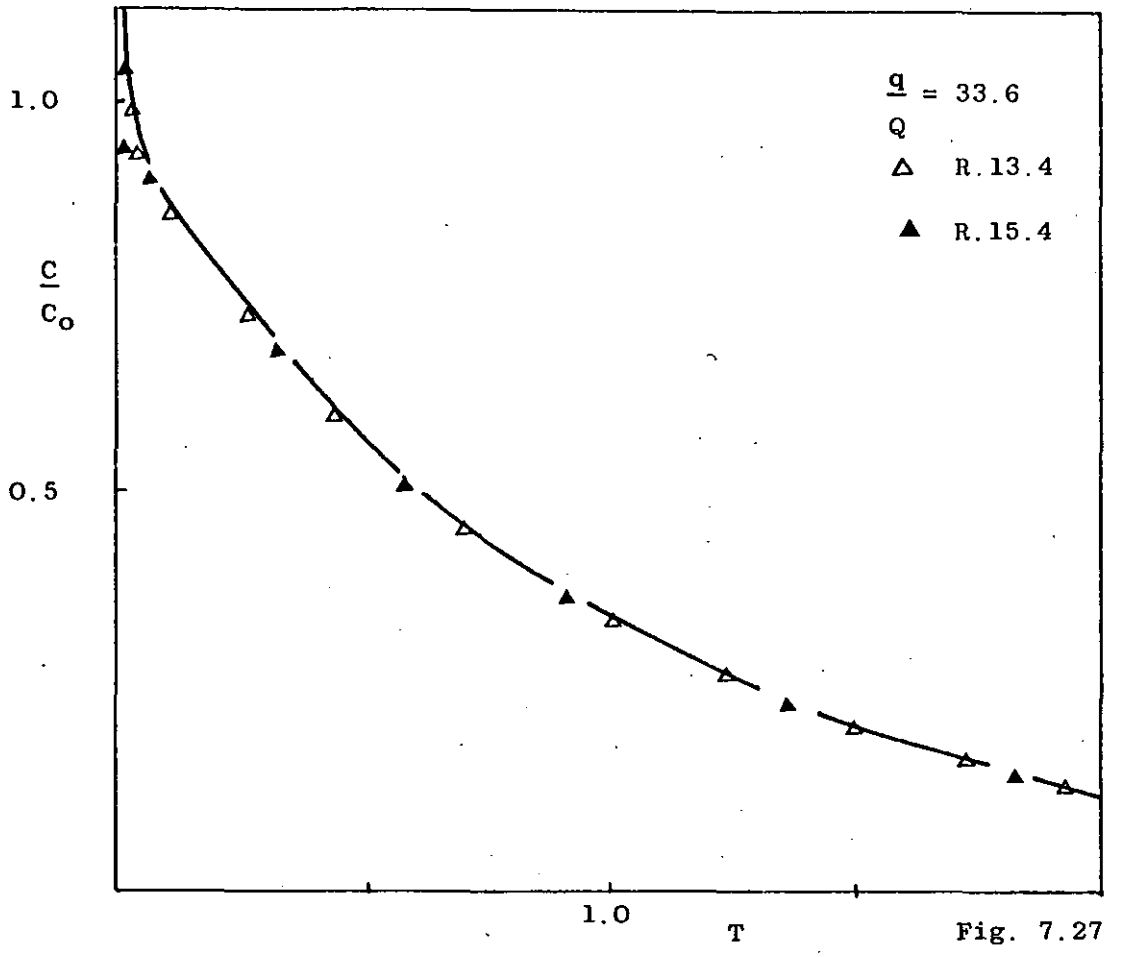

Fig. 7.27

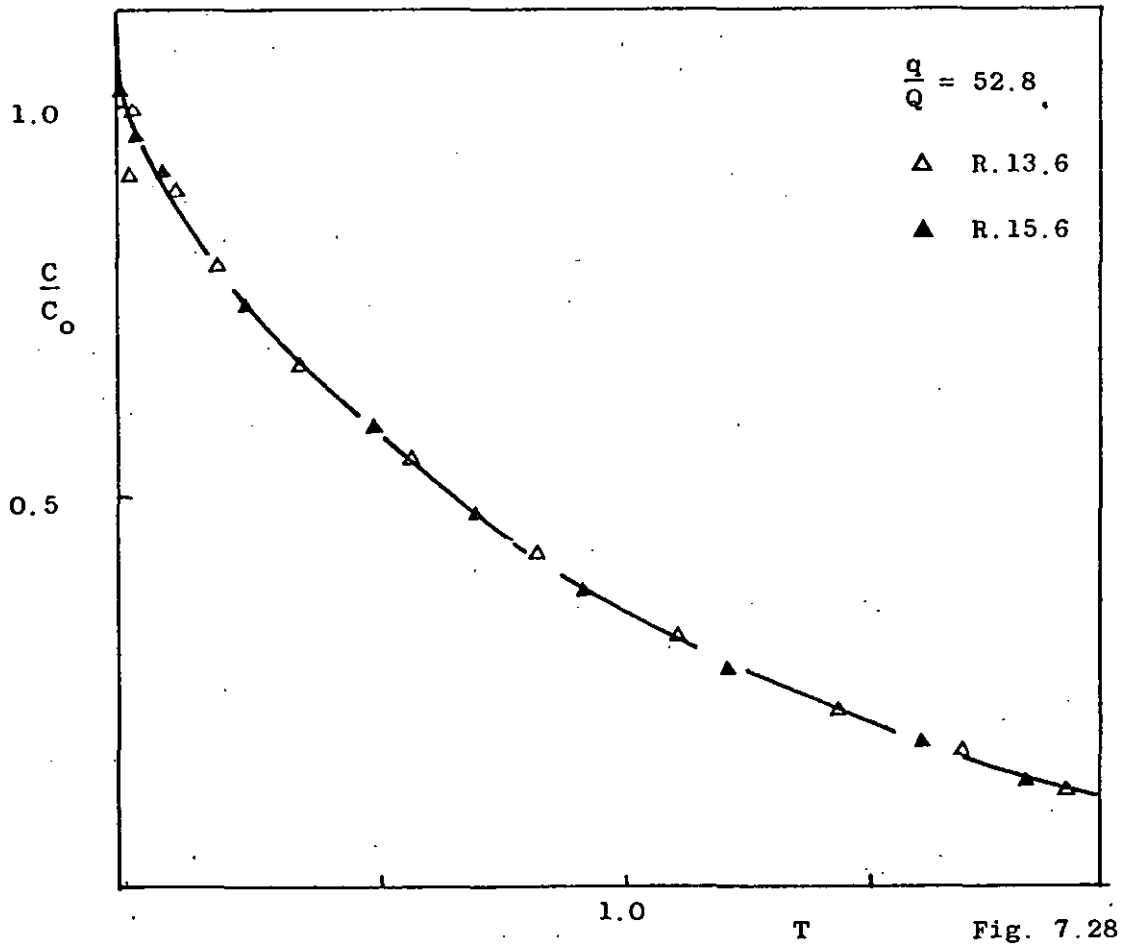

Fig. 7.28

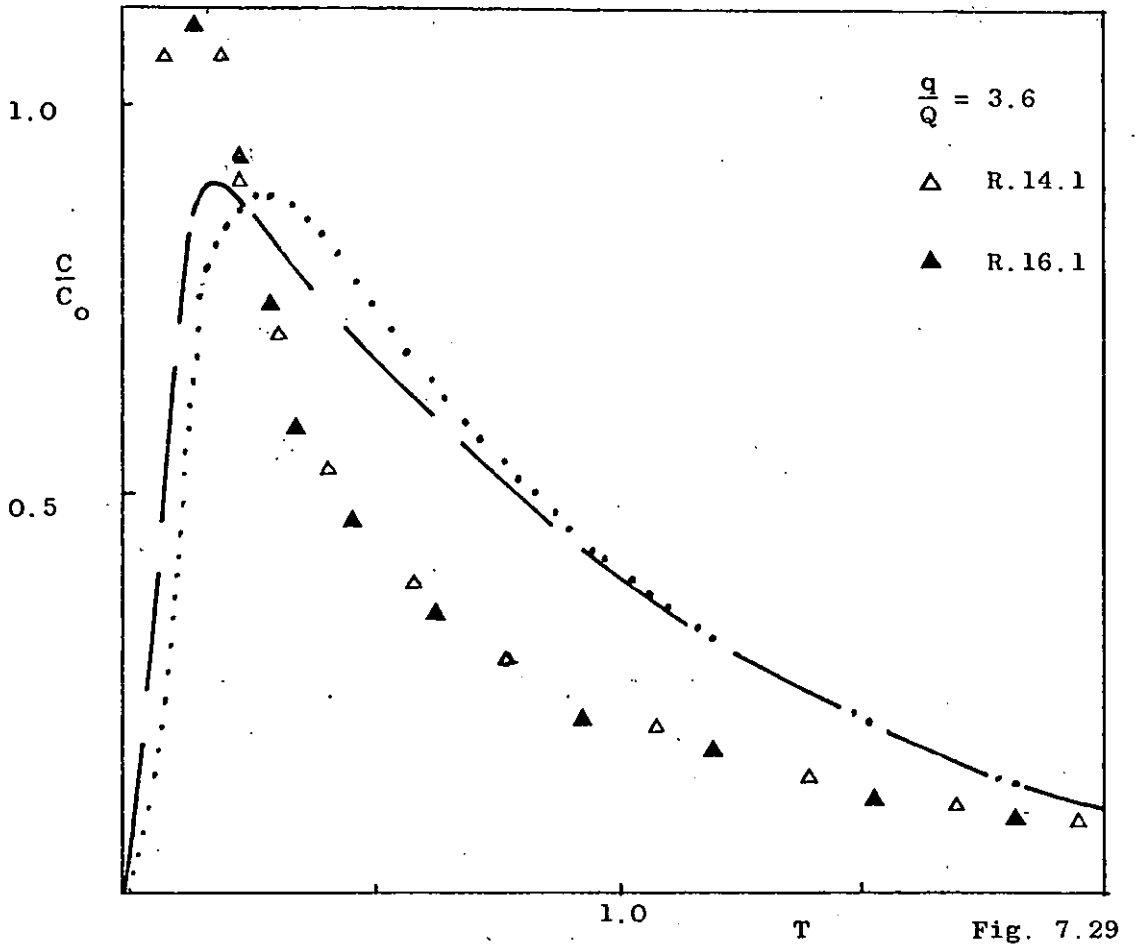

Fig. 7.29

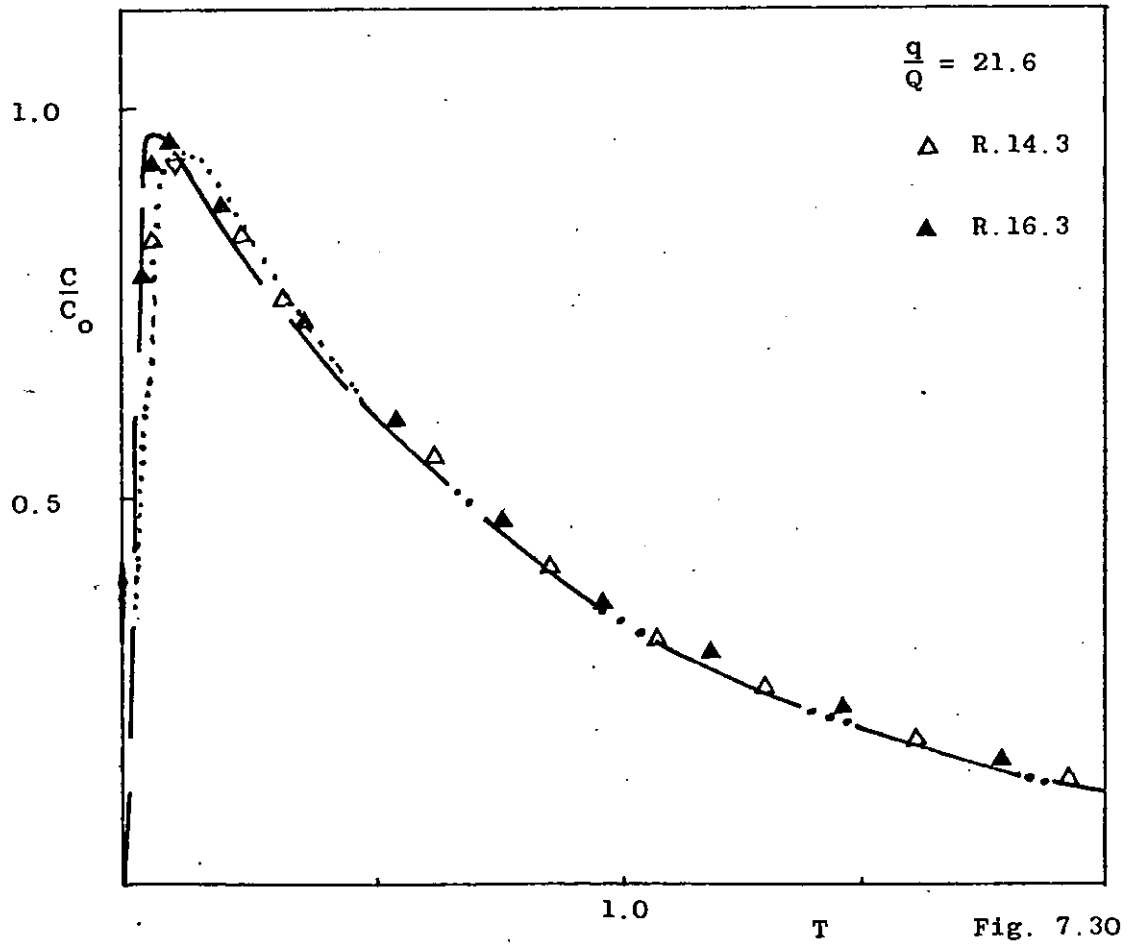

Fig. 7.30

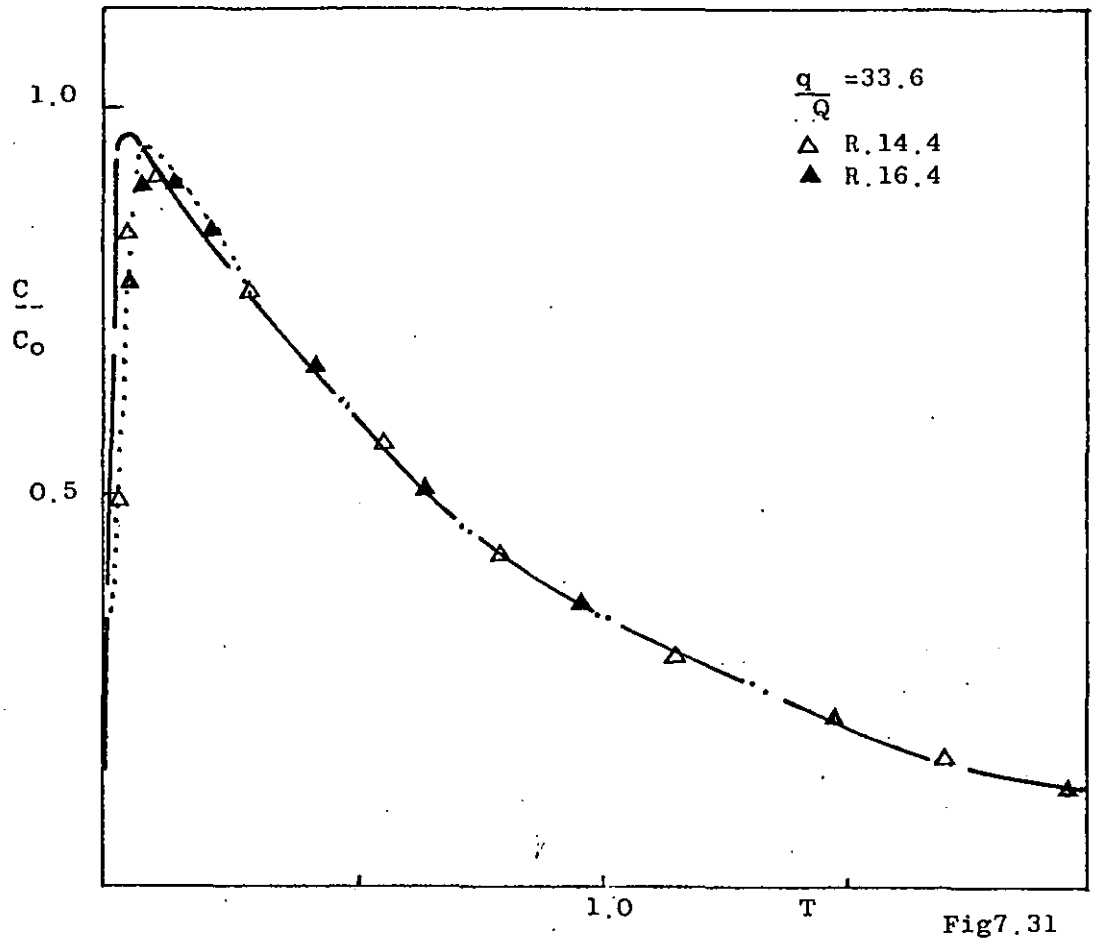

Fig7.31

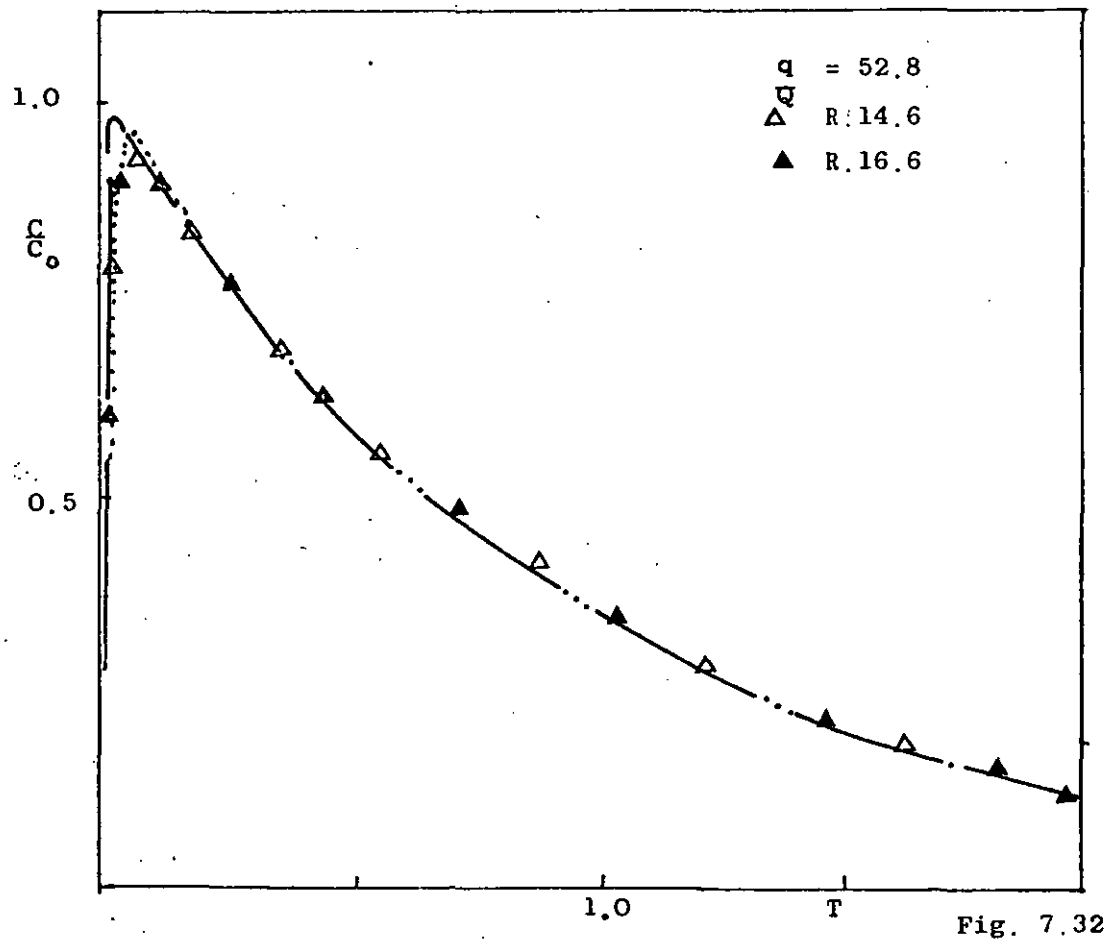

Fig. 7.32

7.2.5. The 4"/19"/19" cylindrical system:- water

Series R.20, 21, 22, 23 were conducted with a ¼" diameter feed line

Series R.24, 25, 26, 27 were conducted with a 1" diameter feed line

	Series R.20 R.24	Series R.21 R.25	Series R.22 R.26	Series R.23 R.27
Liquid Holdup (litres)	88.2	88.2	88.2	88.2
Flow Rate (litres/min)	5.2	5.2	5.2	5.2
Meantime (mins)	16.9	16.9	16.9	16.9
Inlet Position	Into Impeller	Into Loop	Into Impeller	Into Loop
Baffles	Unbaffled	Unbaffled	Baffled	Baffled

As the predicted normalised responses of the double loop and single loop models are almost identical for the feed to impeller condition, only the single loop response is shown in Figures 7.33 - 7.36 and Figures 7.41 - 7.44. As there is a distinct difference between the two model responses, for feed to the loop, each response is shown for this case Figures 7.37 - 7.40, Figures 7.45 - 7.50. The bold line depicts the single loop model solutions and the dotted line the double loop model predictions.

Figures 7.33 - 7.40 illustrate the comparison of experimental results for the 0.4" feed line and single loop model predictions. For low values of (q/Q) the "tail" of the experimental responses deviates slightly from the model solutions. Coupled with this is a higher degree of bypass in the initial parts of the response. This effect disappears when the 1" diameter feed line is substituted, Figures 7.41 - 7.48. The probable cause is the high inlet velocity of the ¼" feed line; producing a "jet effect". At high values of (q/Q) the circulation rate in the fluid is large enough to disperse the "jet" and thus reduce the deviation in residence time distribution.

However, the deviation is very small, and the comparison between the experimental results, for the 0.4" diameter feed, and the single loop model is reasonably good.

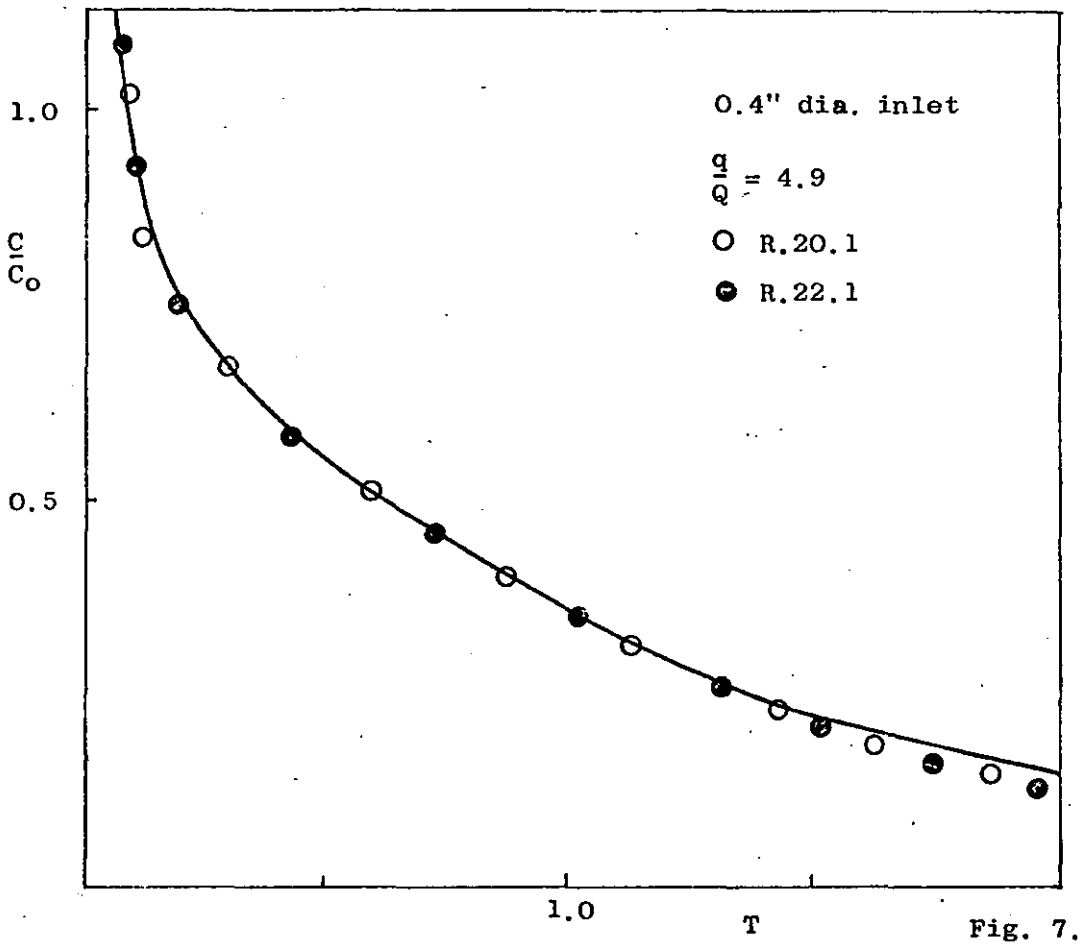

Fig. 7.33

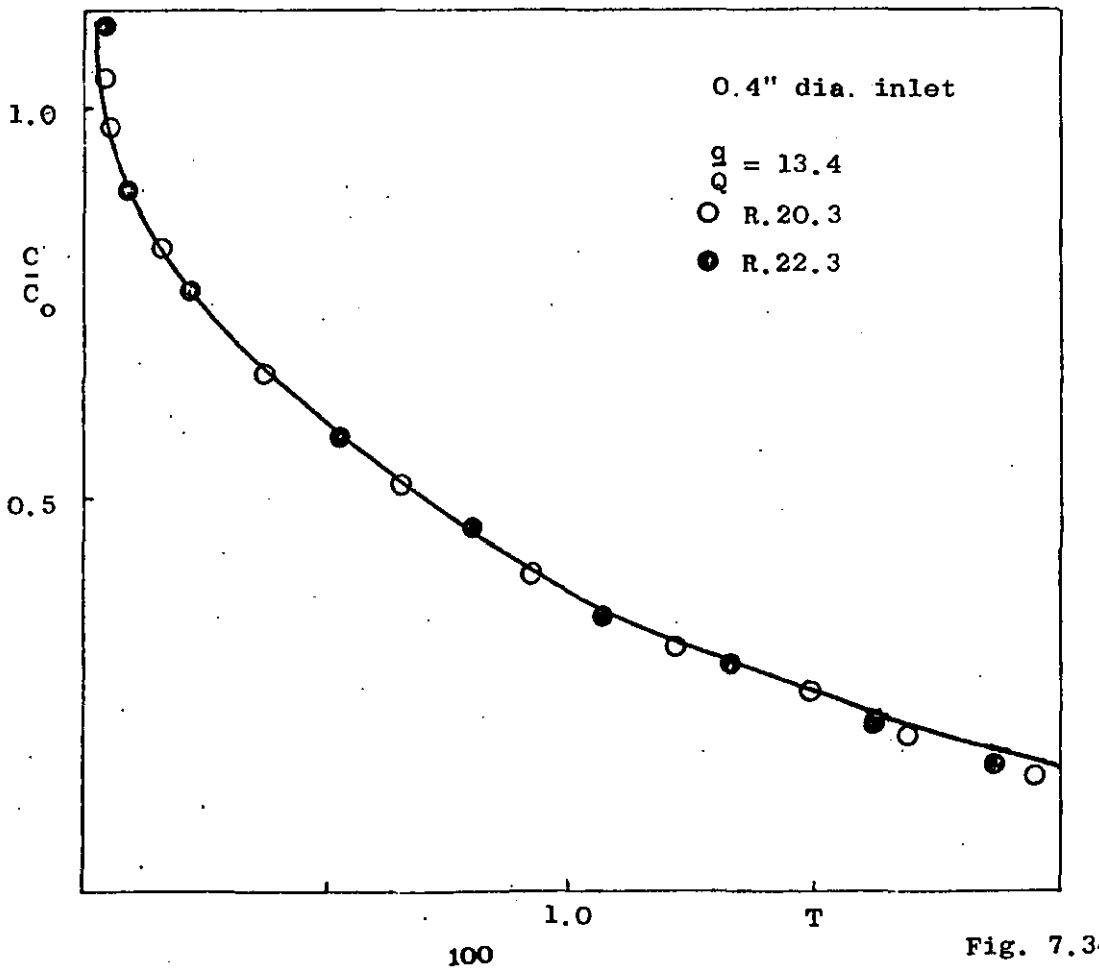

Fig. 7.34

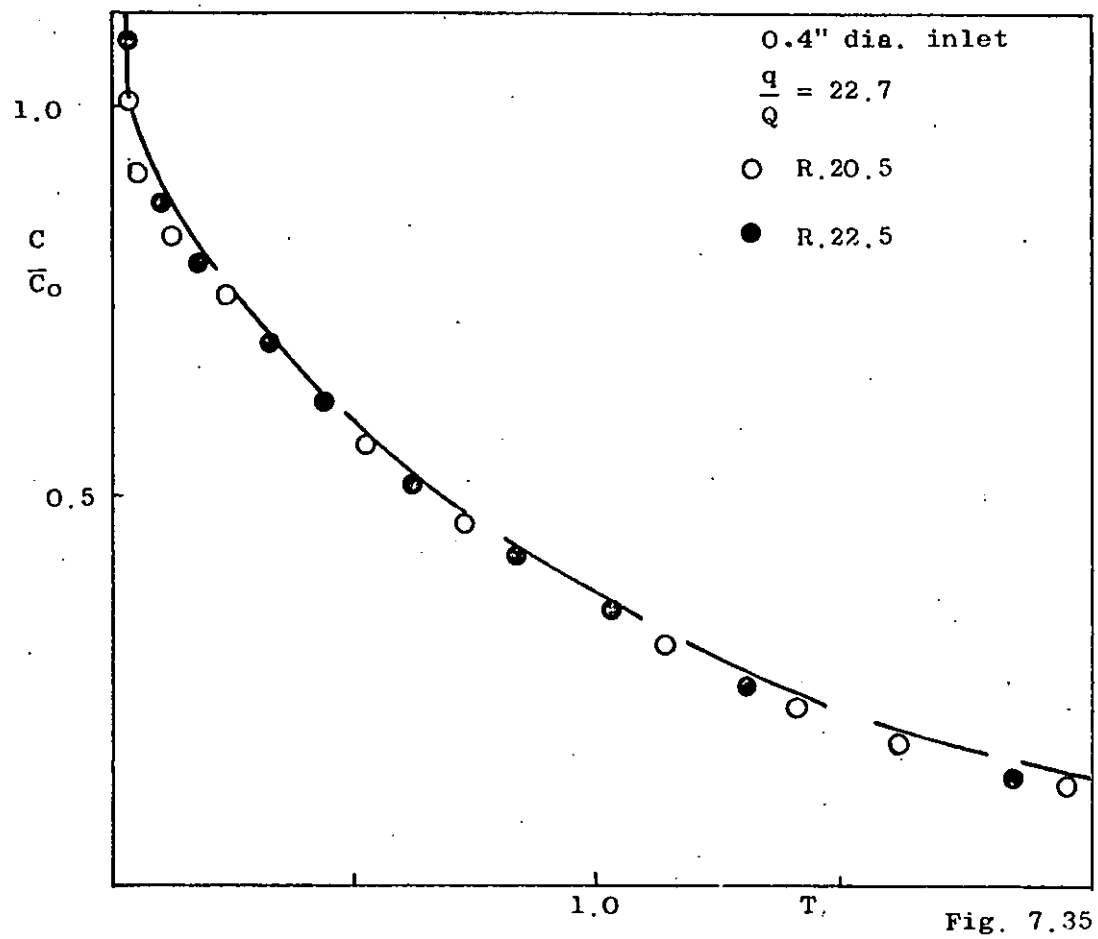

Fig. 7.35

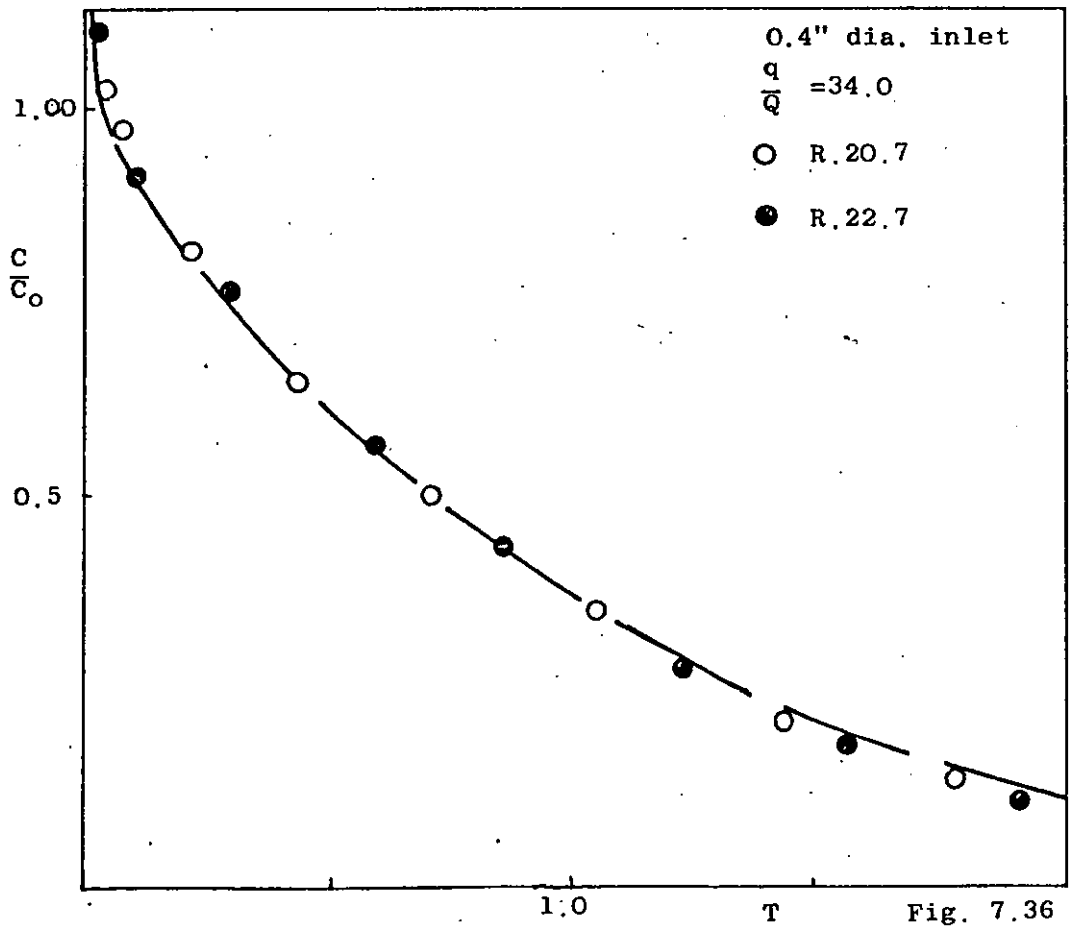

Fig. 7.36

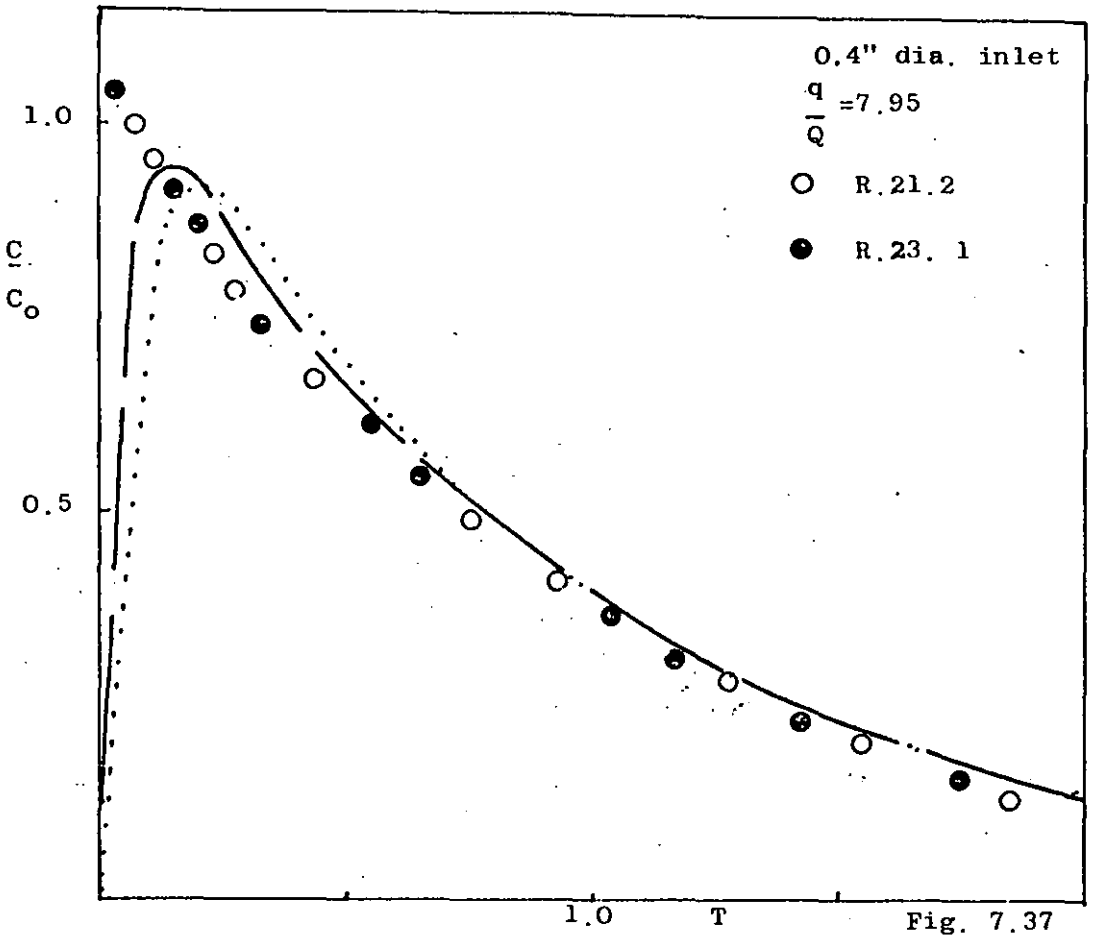

Fig. 7.37

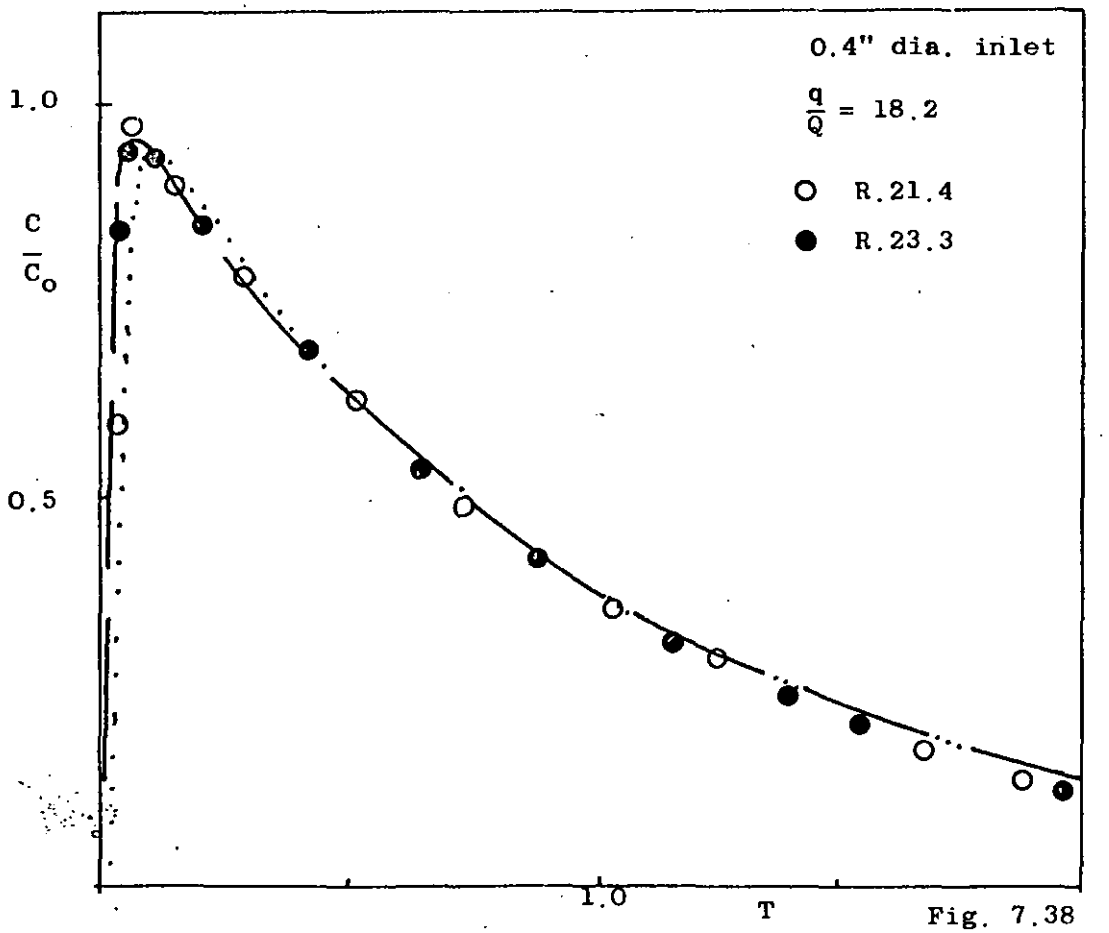

Fig. 7.38

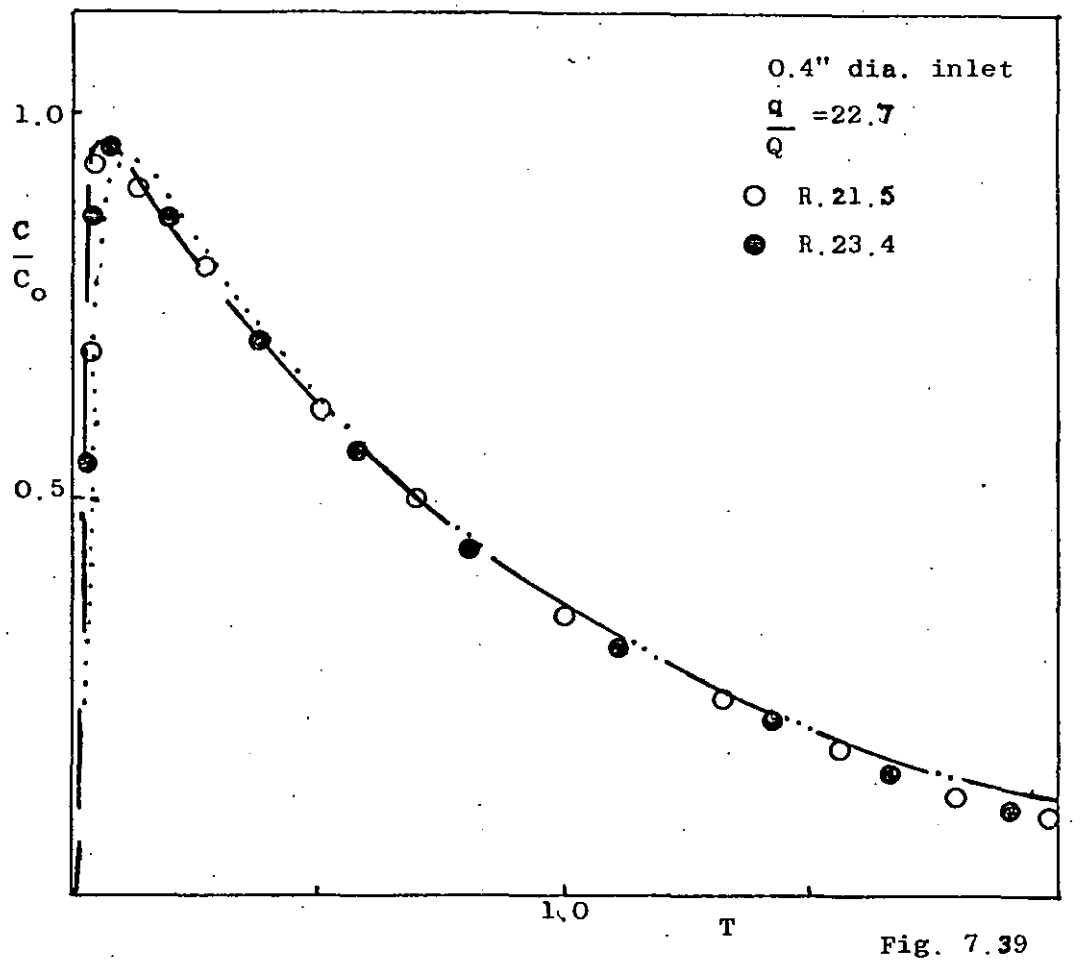

Fig. 7.39

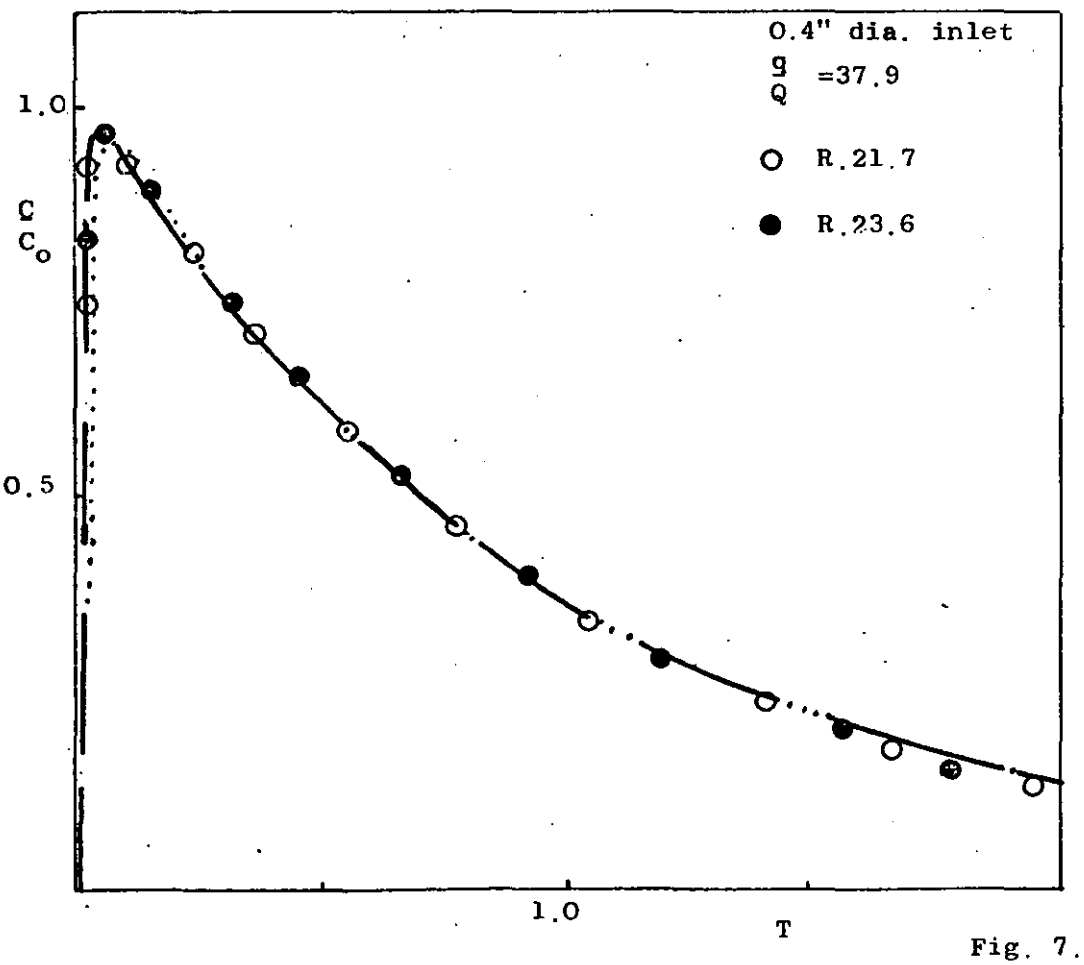

Fig. 7.40

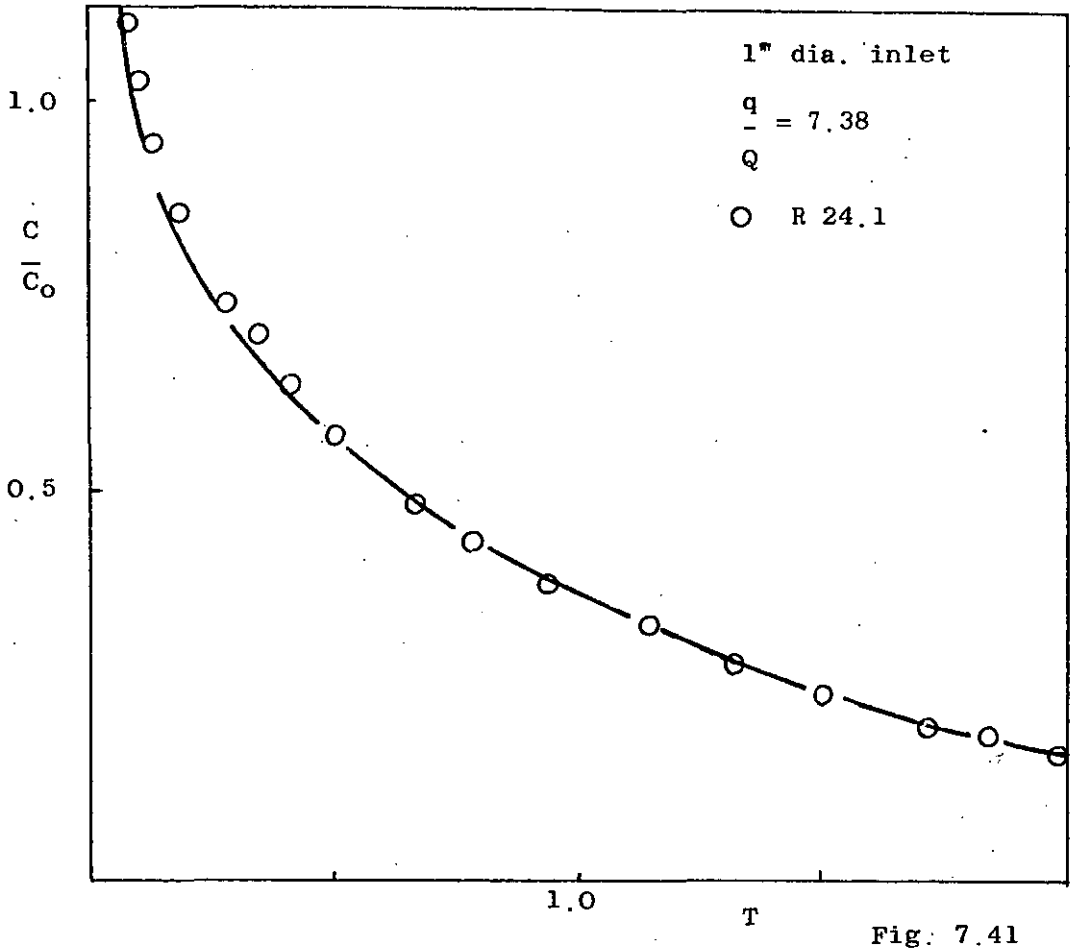

Fig. 7.41

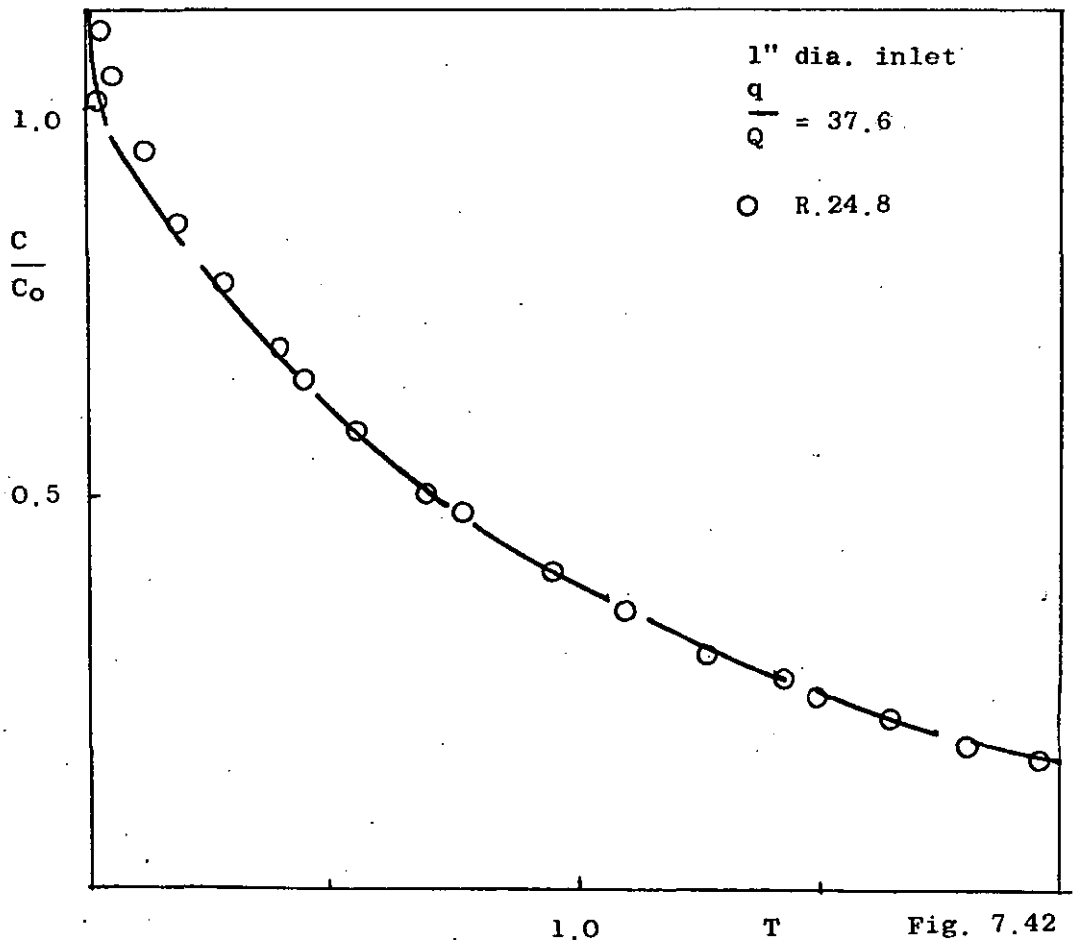

Fig. 7.42

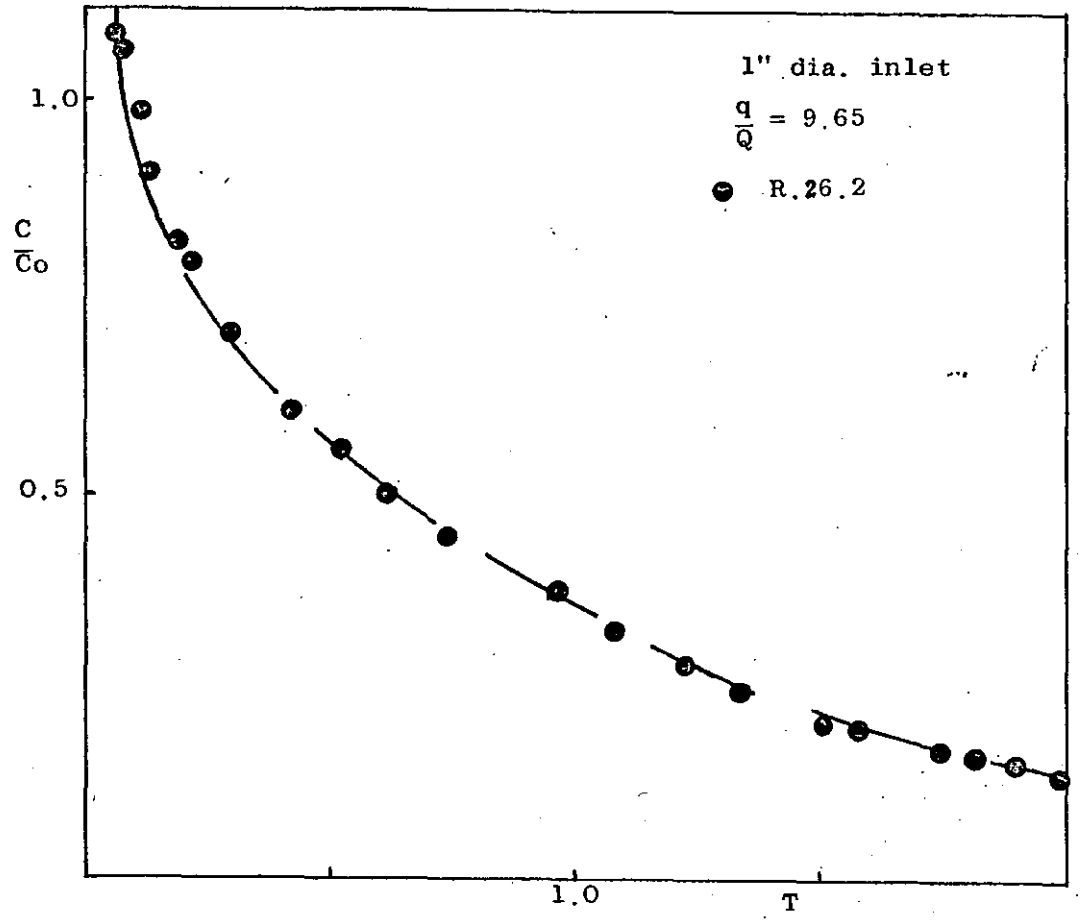

Fig. 7.43

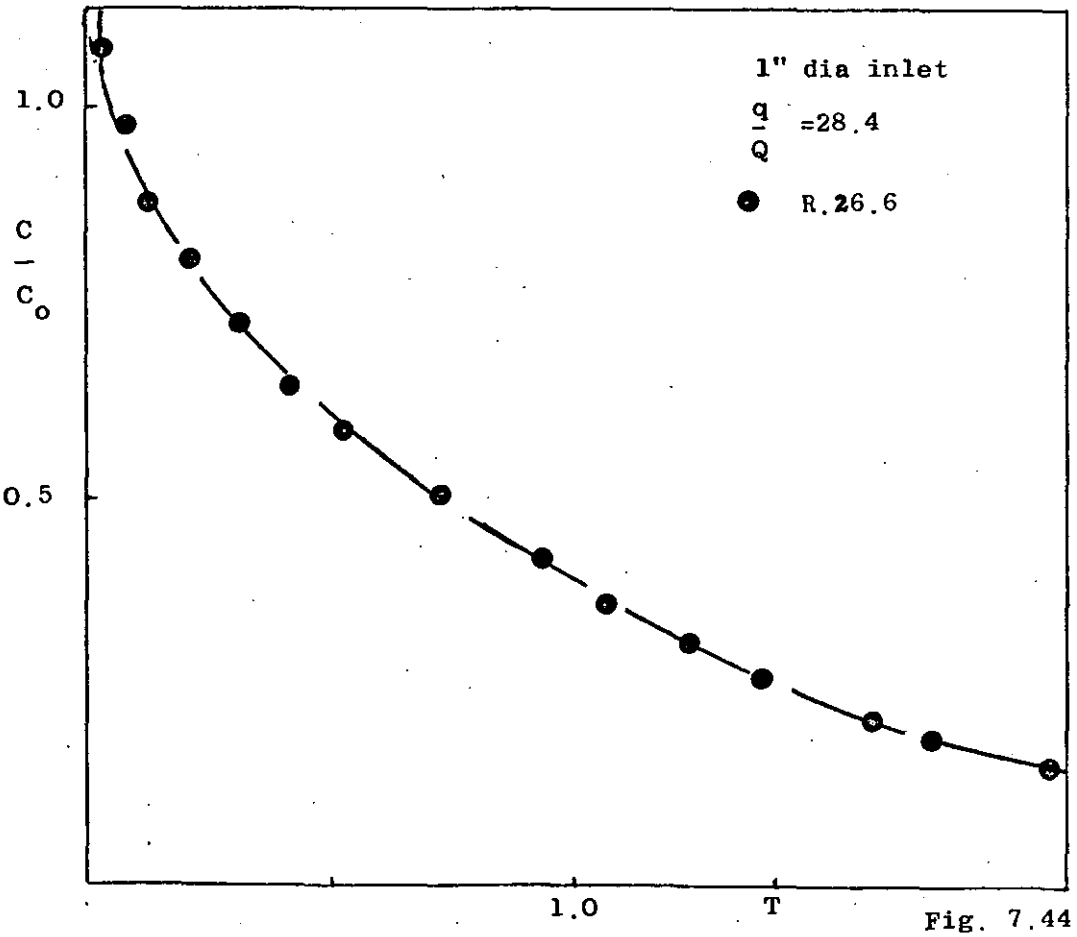

Fig. 7.44

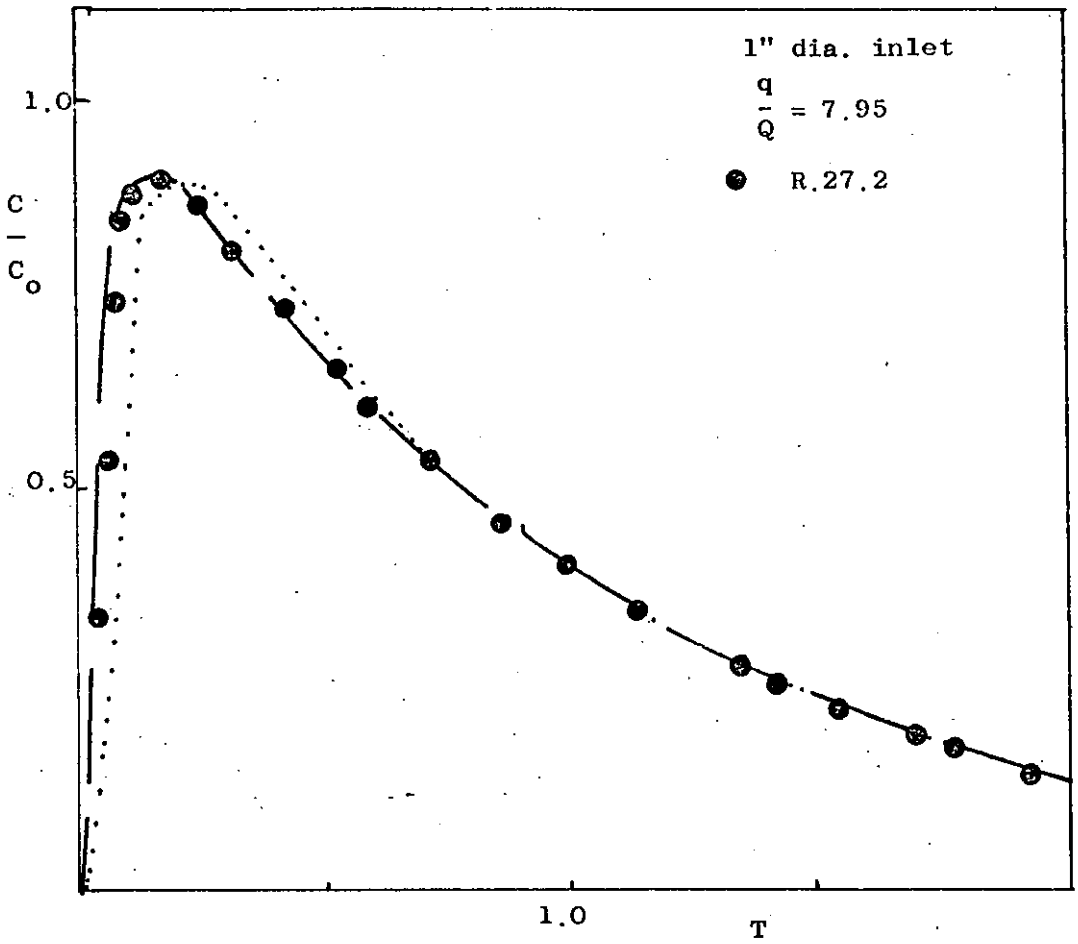

Fig. 7.45

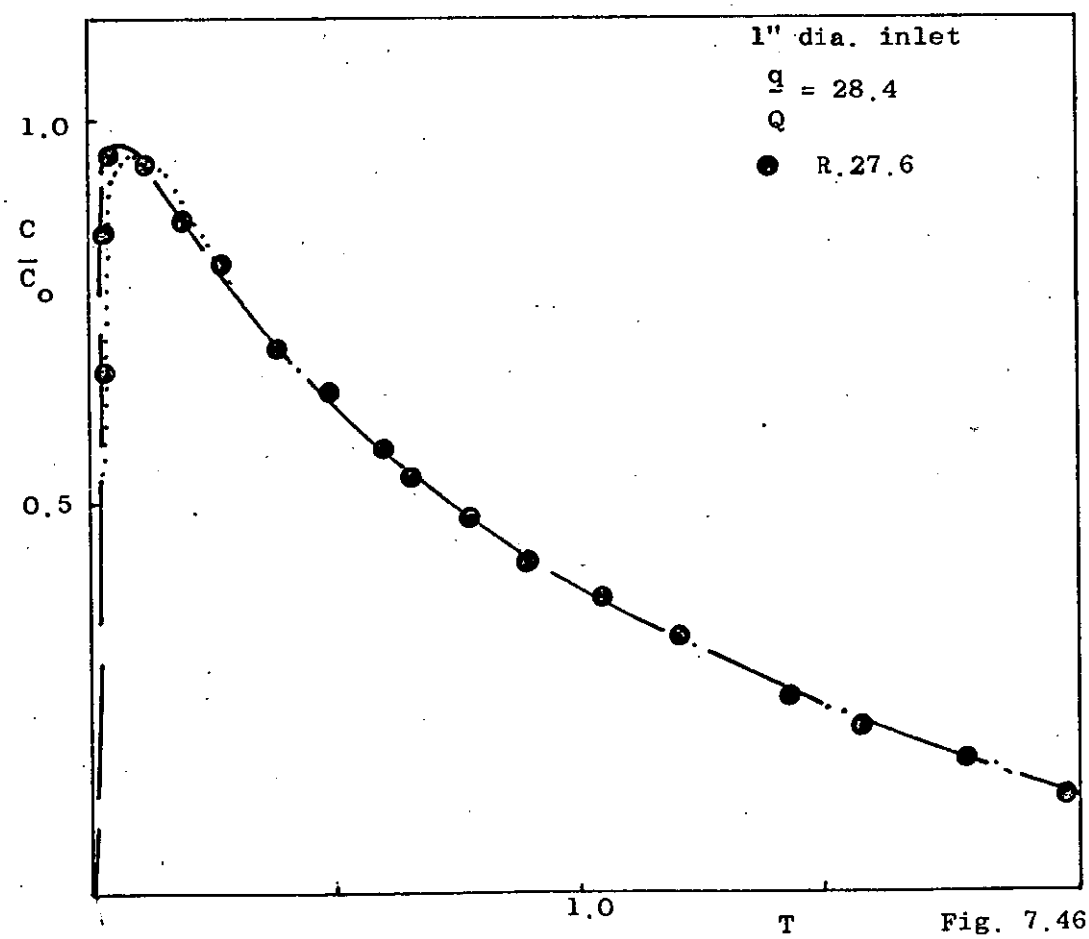

Fig. 7.46

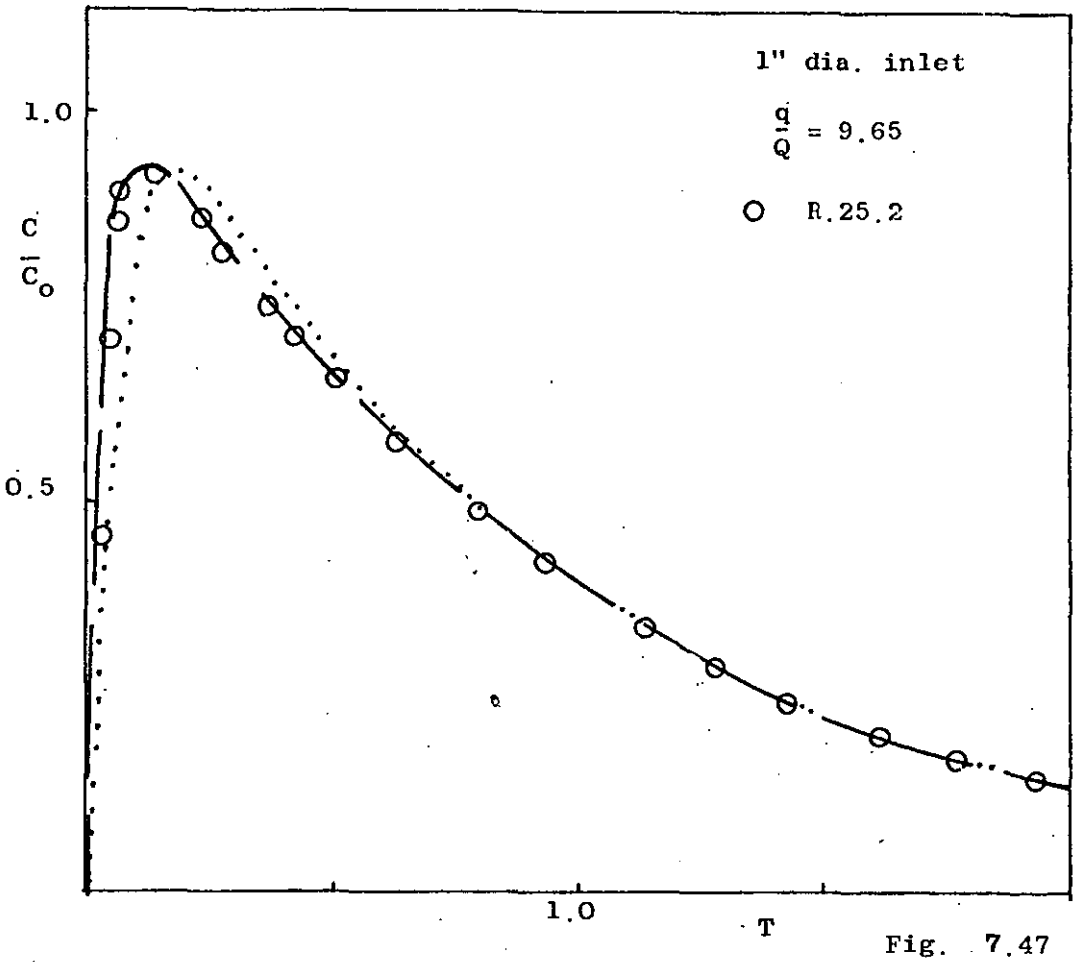

Fig. 7.47

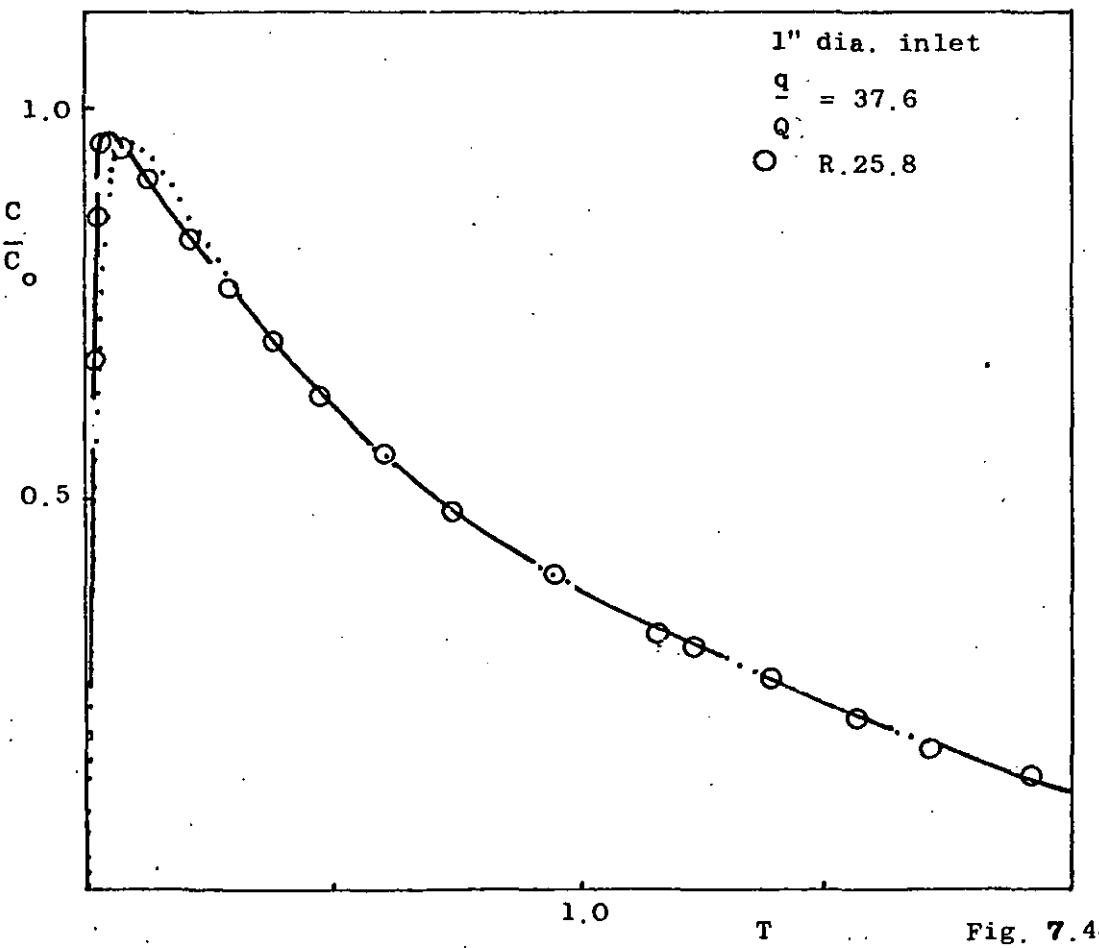

Fig. 7.48

7.2.6. The 8"/42"/42" cylindrical system:- water

	Series R.30	Series R.31
Liquid Holdup (litres)	960	960
Flow Rate (litres/min)	26.6	26.6
Meantime (mins)	36.0	36.0
Inlet Position	Into Impeller	Into Loop
Baffles	Unbaffled	Unbaffled

The figures 7.49 - 7.56 illustrate the comparison of experimental results and the theoretical single loop model predictions obtained for the large 42" diameter vessel. The similarity between the two is shown throughout the whole range of (q/Q) studied, and for both inlet feed positions. The baffled system was not considered.

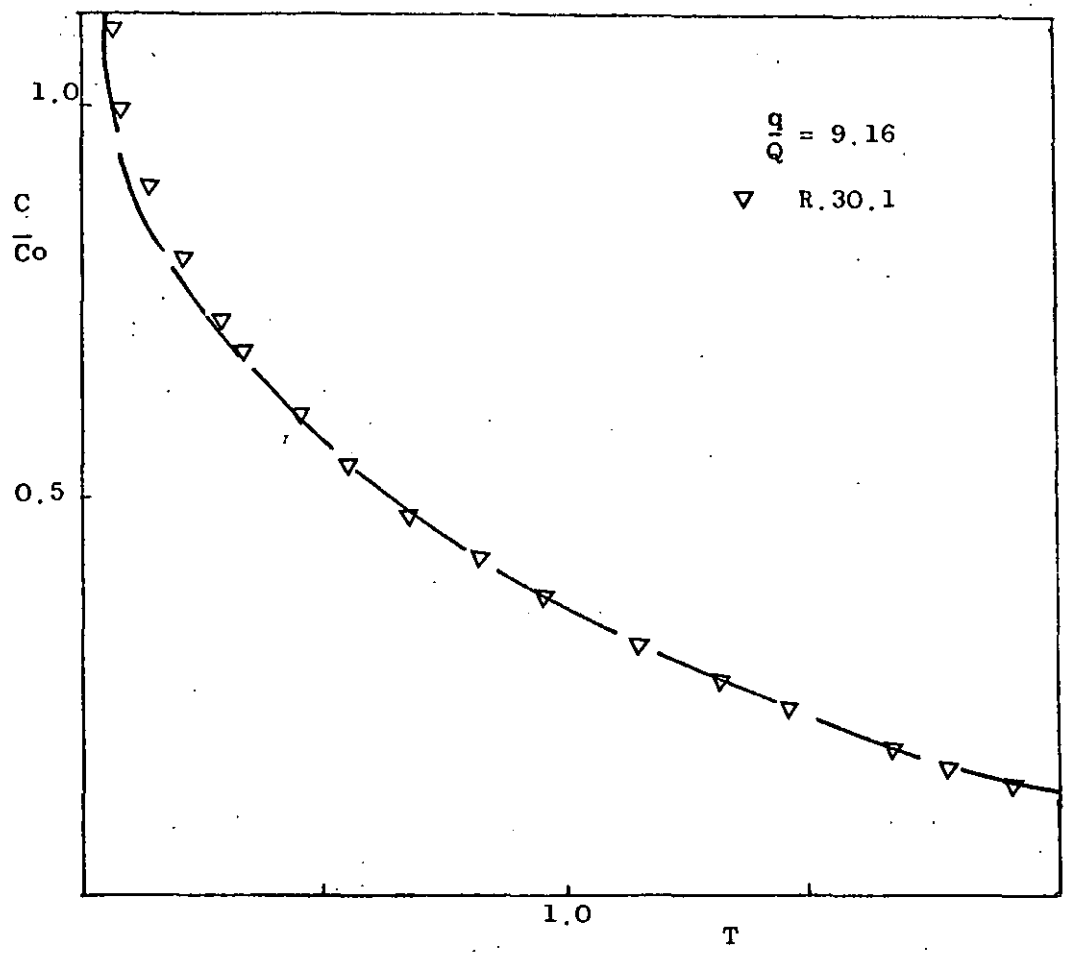

Fig. 7.49

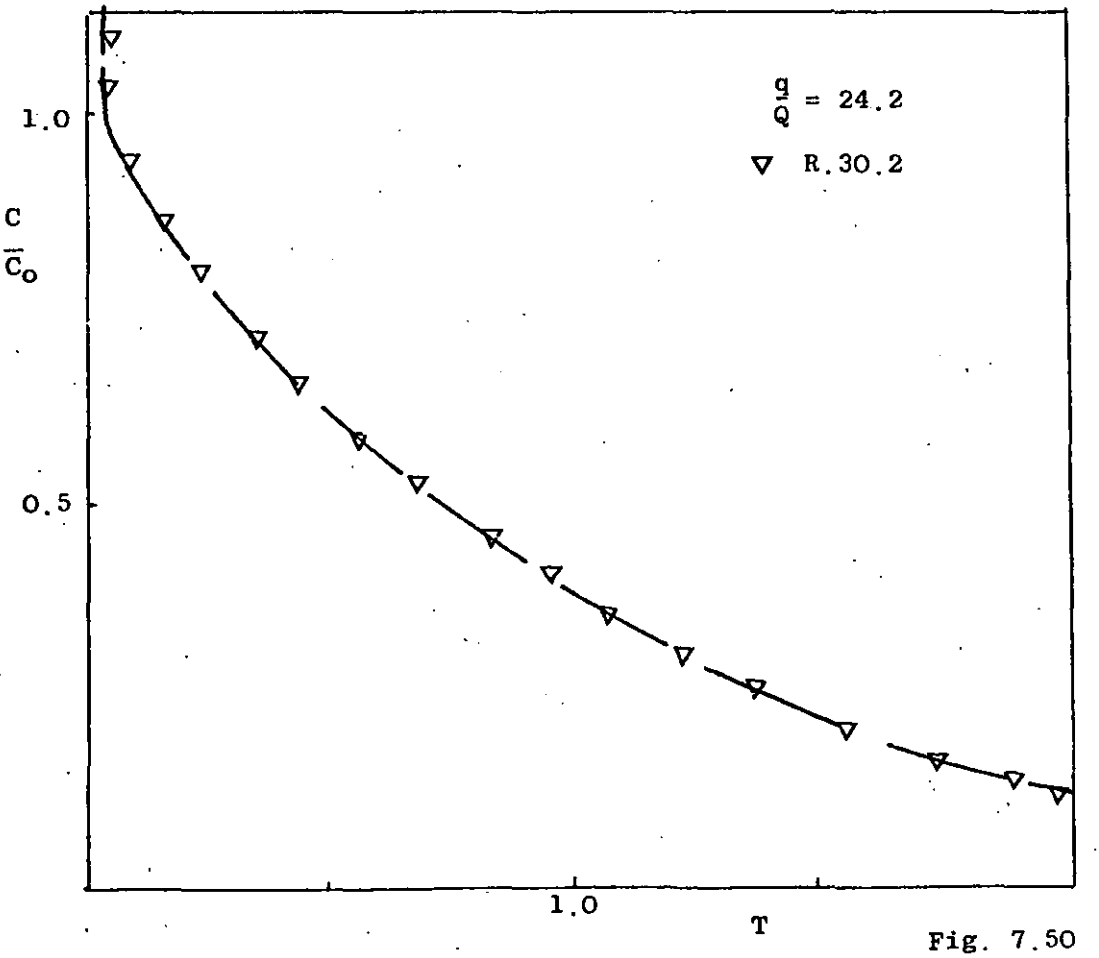

Fig. 7.50

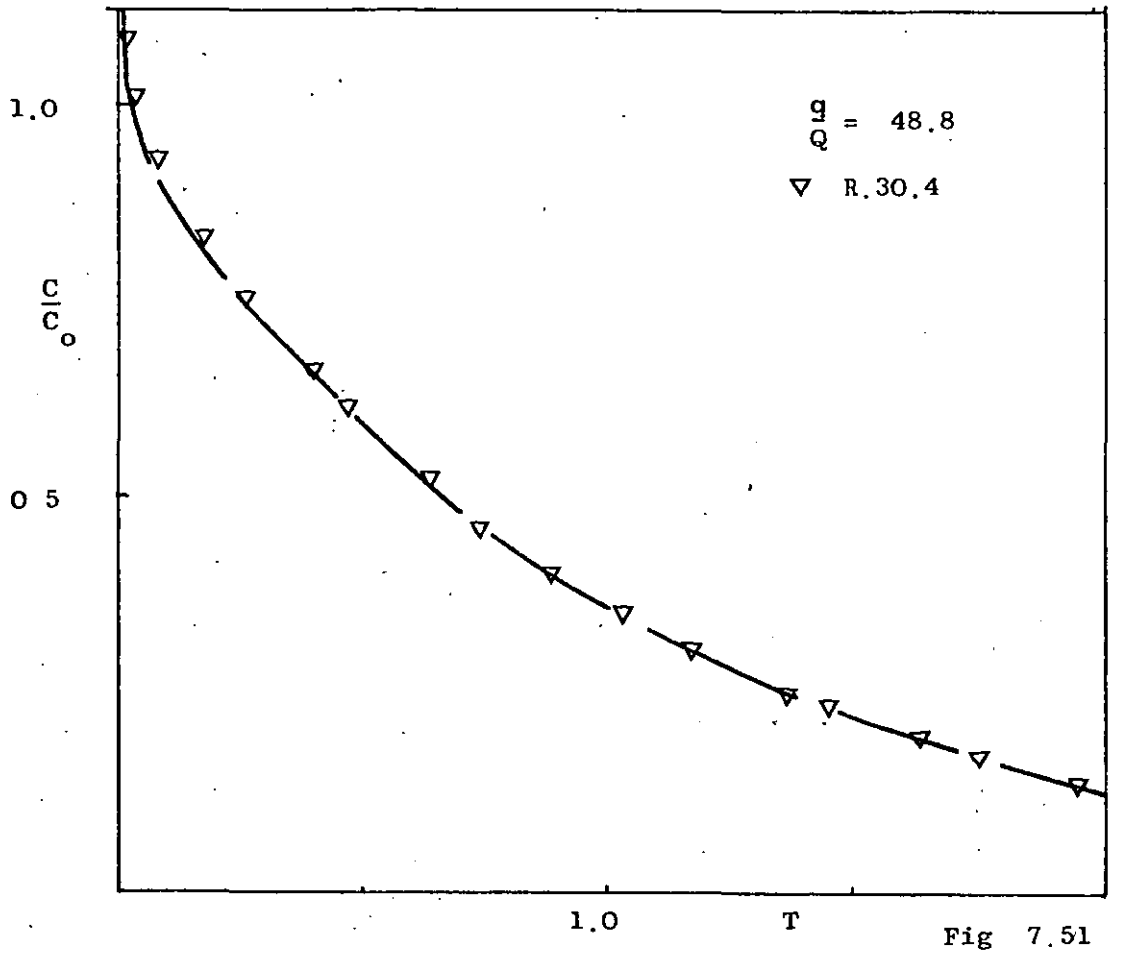

Fig 7.51

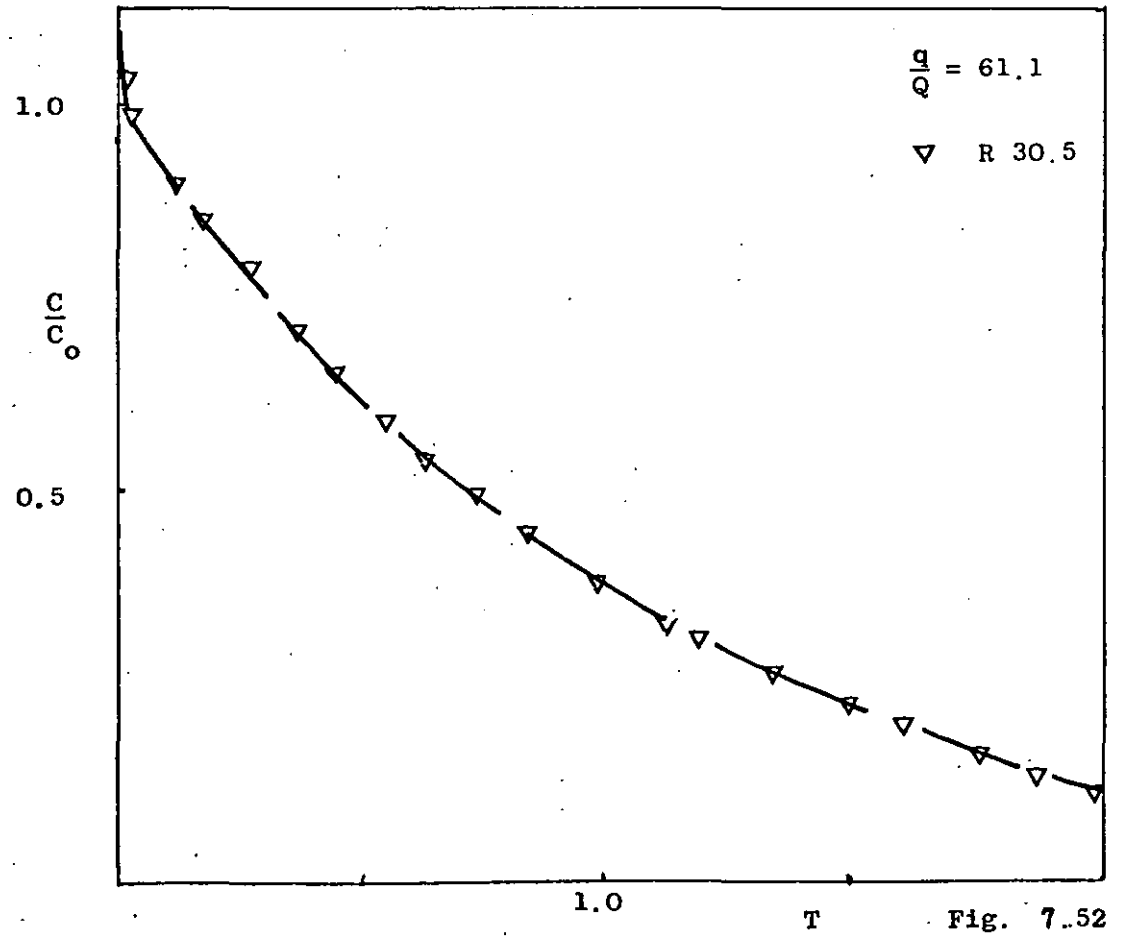

Fig. 7.52

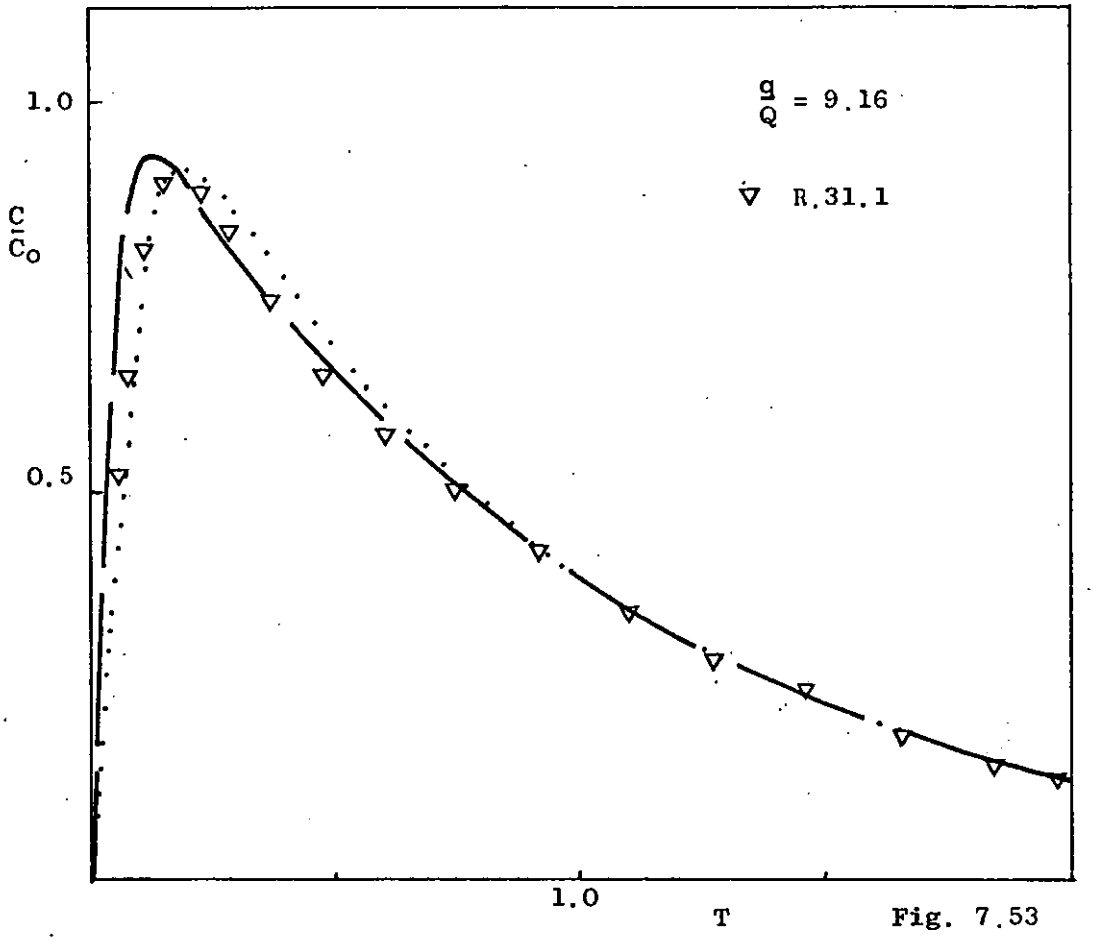

Fig. 7.53

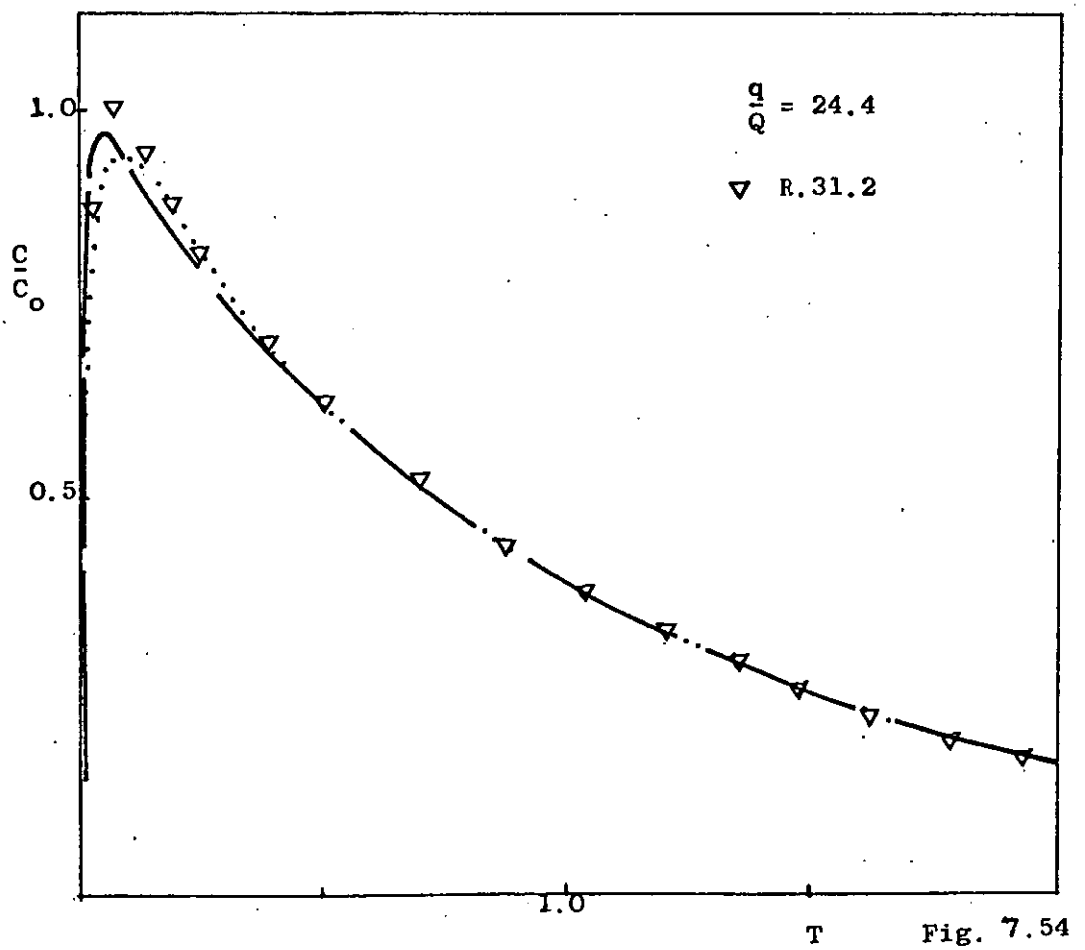

Fig. 7.54

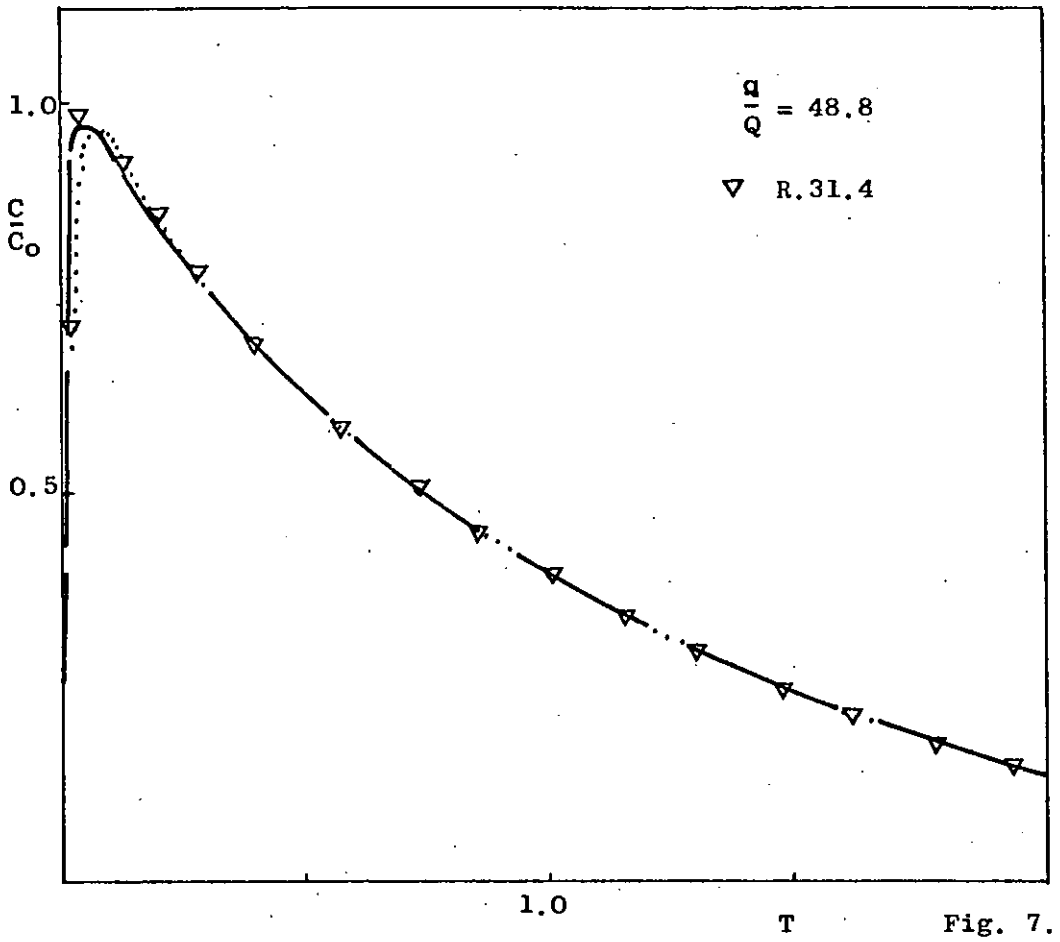

Fig. 7.55

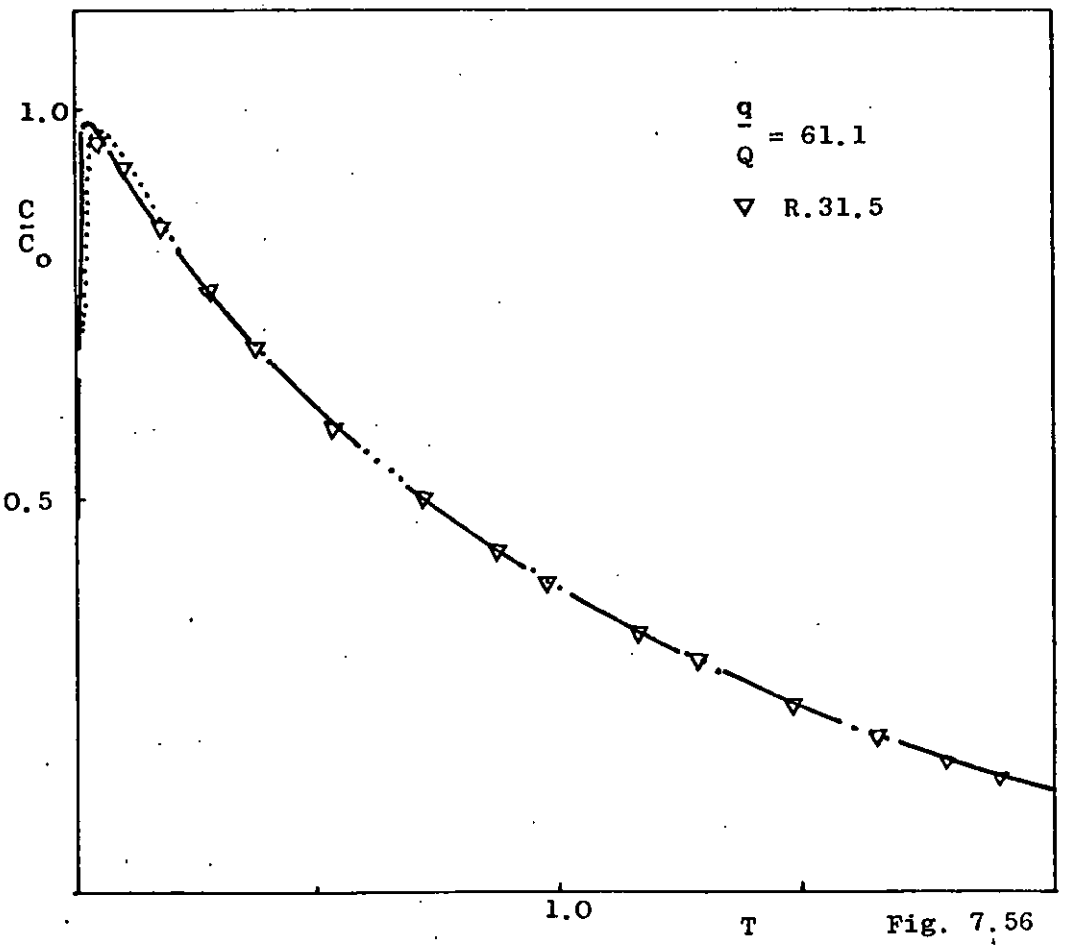

Fig. 7.56

7.3 Comparison of Propeller Impulse Response Results with Single Loop Model

The normalised experimental response results for the propeller experiments are presented in Appendix 1.2.

In the following sections the experimental responses of the propeller experiments are compared with the theoretical predictions of the single loop model discussed in Chapter 4. Tables are presented to indicate the vessel configuration, operating conditions and the variables investigated for each series of runs. The experiments were conducted for a wide range of impeller speeds for each inlet feed position. The baffles were 0.12D width.

The model parameter, propeller pumping capacity, was calculated using the relationship discussed in section 7.1; again comparison of experimental and theoretical responses curves was very good, and no further manipulation of this parameter was considered necessary.

The computer programme described in Appendix 2 was used to calculate all the normalised experimental responses. The Markov programme, Appendix 3, was used to obtain all model solutions.

7.3.1. The 2½"/9"/9" cylindrical system:- water

	Series P.1	Series P.2	Series P.3	Series P.4
Liquid Holdup (litres)	9.37	9.37	9.37	9.37
Flow Rate (litres/min)	2.26	2.26	2.26	2.26
Meantime (mins)	4.1	4.1	4.1	4.1
Inlet Position	Into Propeller	Into Loop	Into Propeller	Into Loop
Baffles	Unbaffled	Unbaffled	Baffled	Baffled

Excellent similarity exists between the theoretical single loop model predictions and the experimental impulse response results, for the range of model parameter studied. This comparison is illustrated in Figures 7.57 - 7.64. The predicted solutions of the model proposed by Marr and Johnson (44) for propeller agitated systems are also shown in Figures 7.57 - 7.60. The initial impulse at the origin,a feature of this model, is not shown. The figures show that the predictions of Marr and Johnson's model do not match experimental results in the lower range of (q/Q). In the higher range of model parameter ($q/Q > 25$), the fit is tolerable but the model completely ignores the initial bypass effect inherent in systems where the inlet feed is directed into the impeller.

The model of Marr and Johnson does not accommodate feed to the loop. The model predictions are completely different throughout the whole range of model parameter, Figures 7.61 - 7.64.

As the propeller induces an axial component of flow in the fluid the presence of baffles in the vessel should have very little effect on the flow patterns. Baffles are introduced into a vessel

in order to destroy any radial component of flow, and subsequently should have very little effect on the residence time distribution of a system which has a predominant axial component of flow. This fact was substantiated by the experimental curves for the unbaffled and baffled systems.

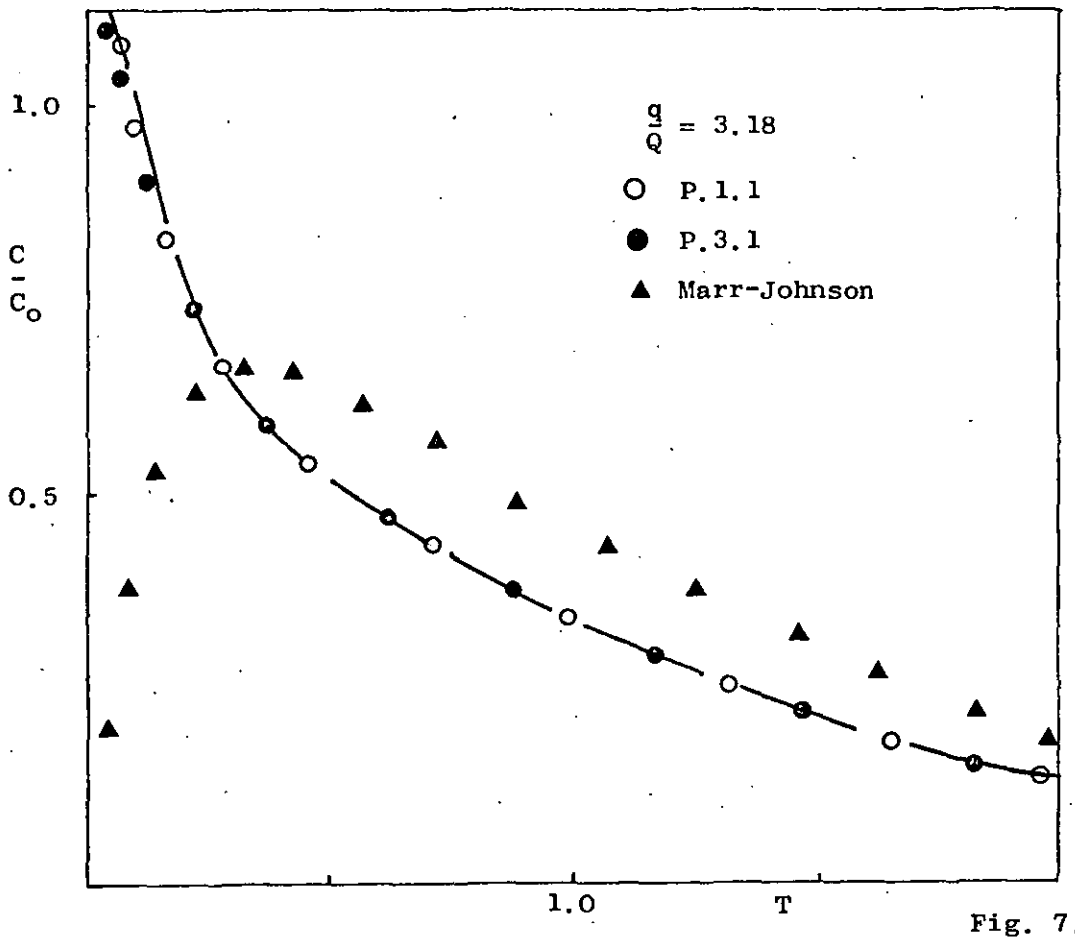

Fig. 7.57

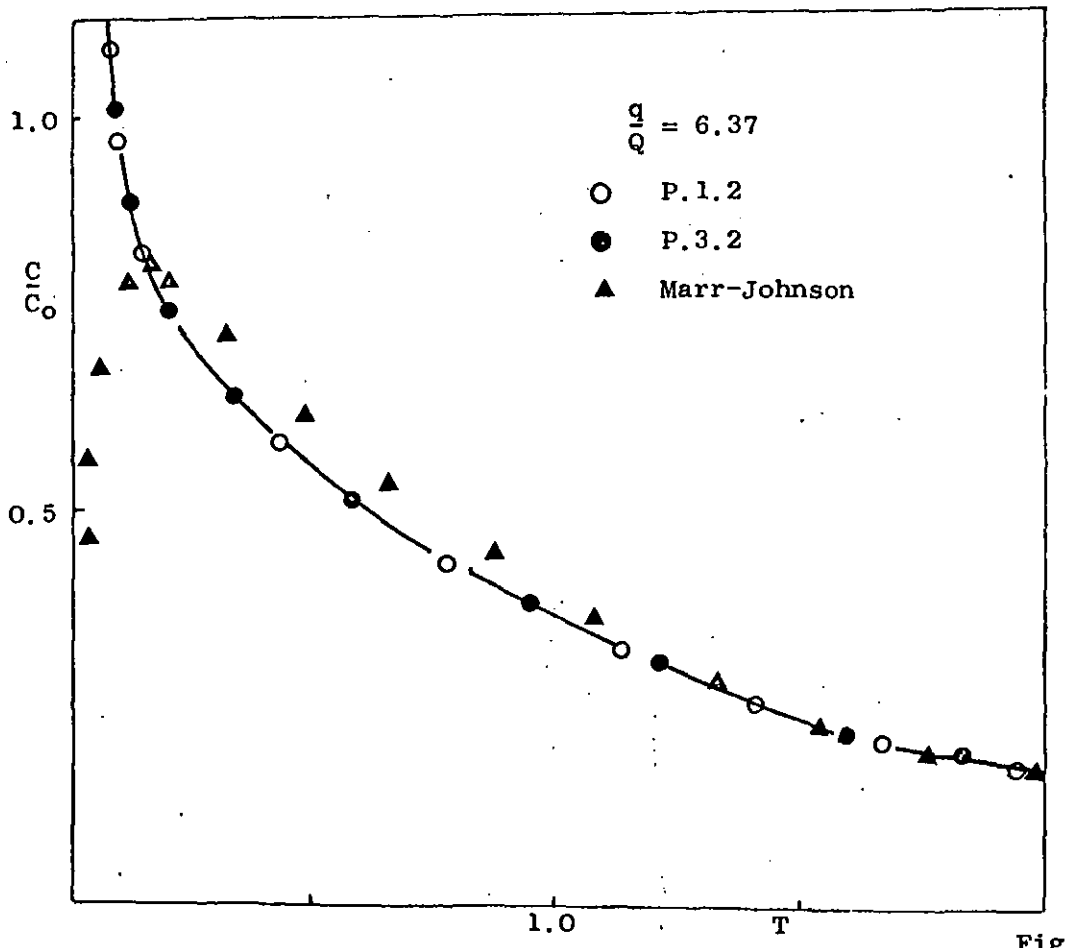

Fig. 7.58

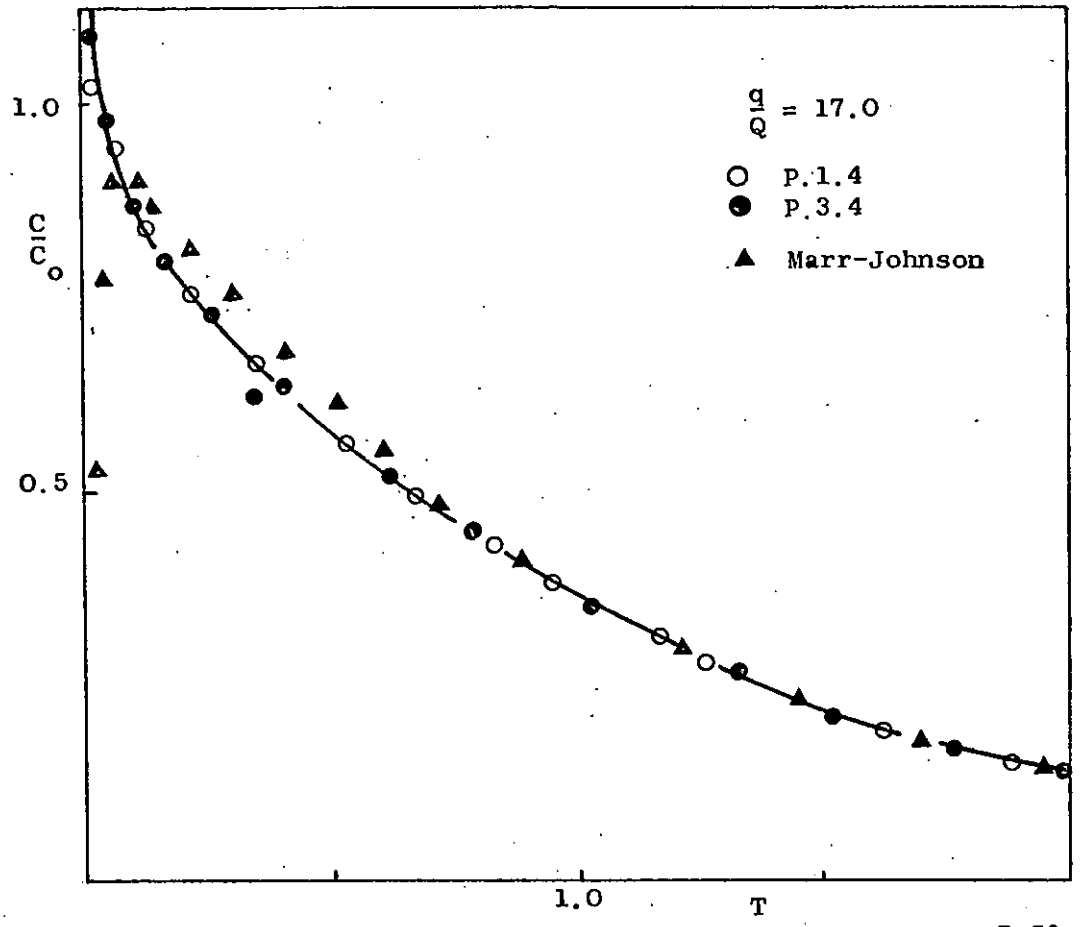

Fig. 7.59

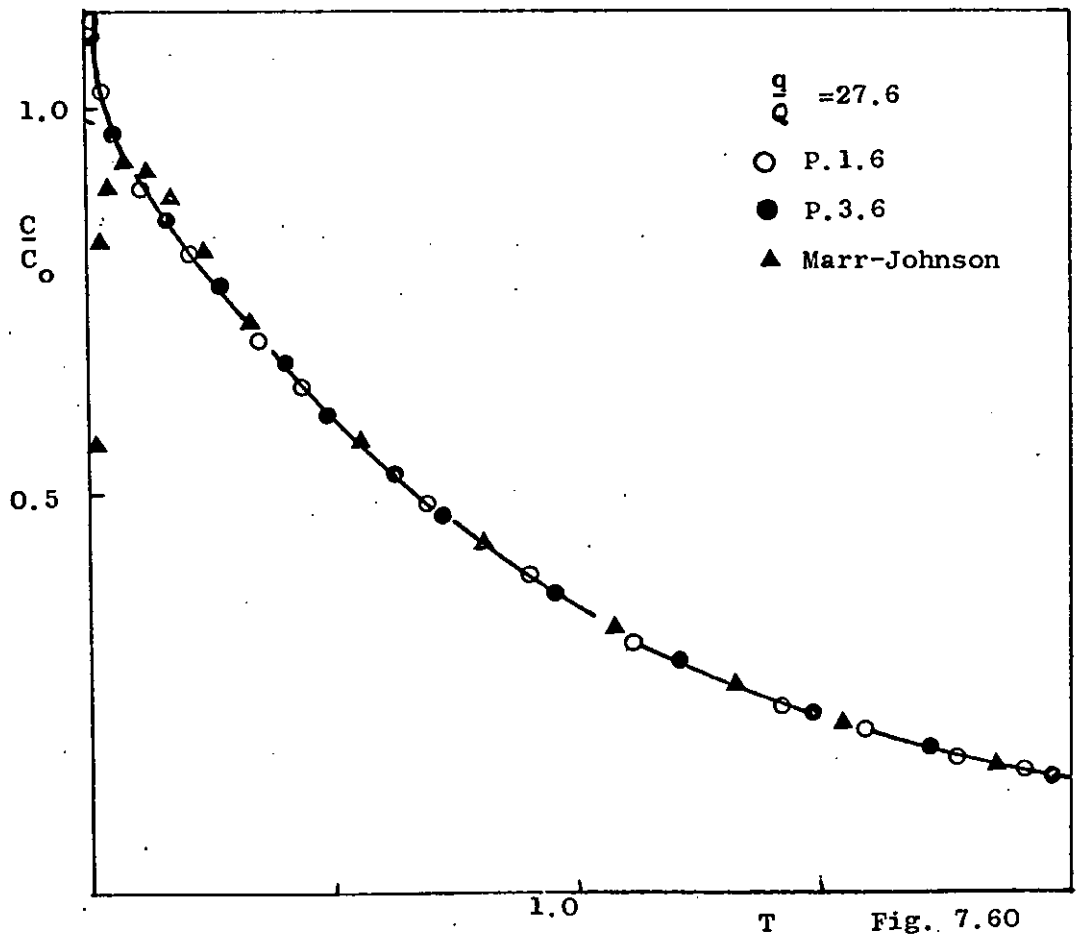

Fig. 7.60

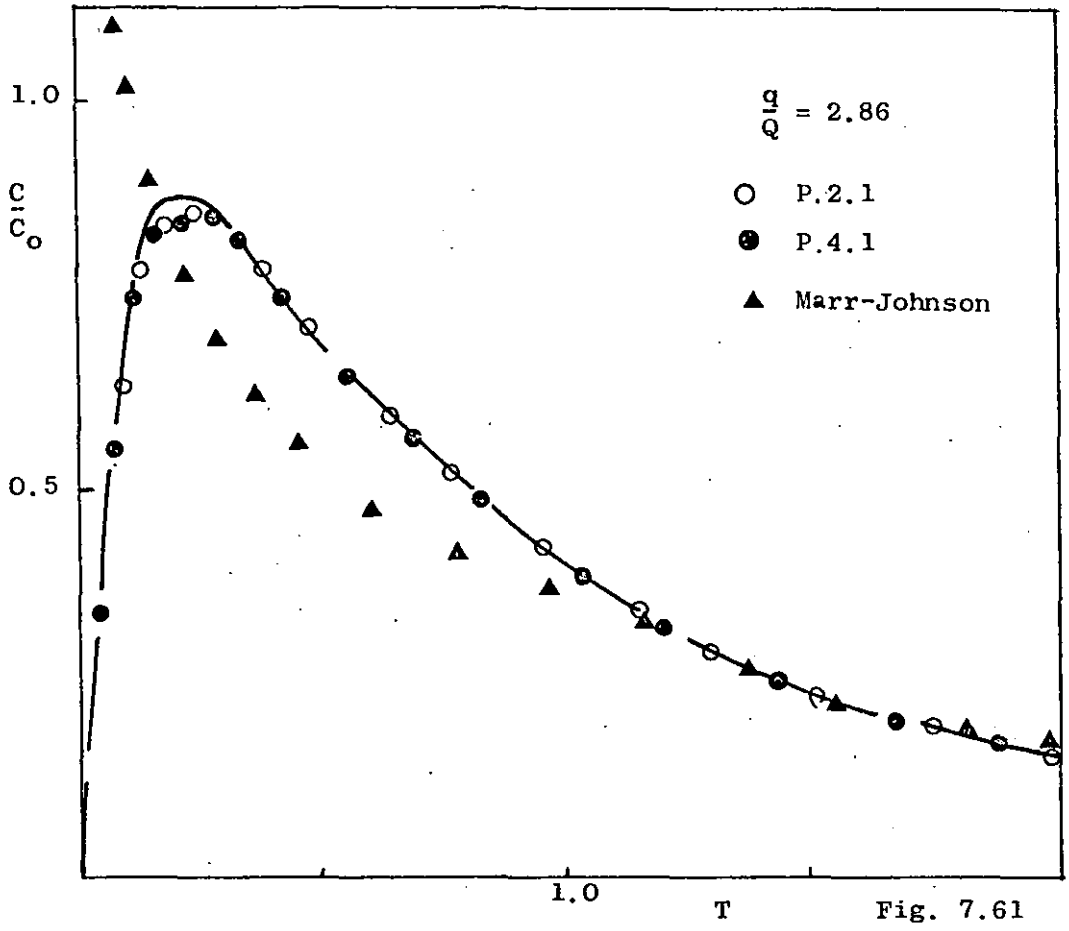

Fig. 7.61

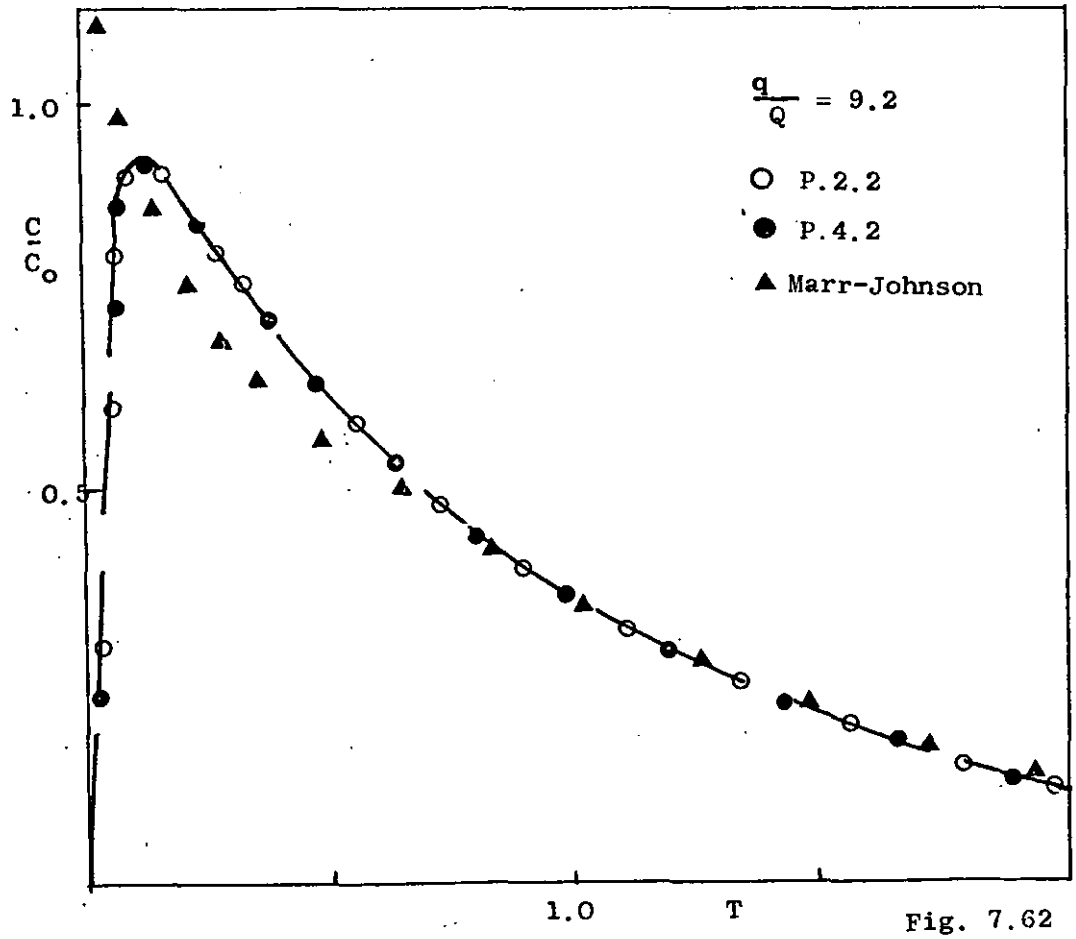

Fig. 7.62

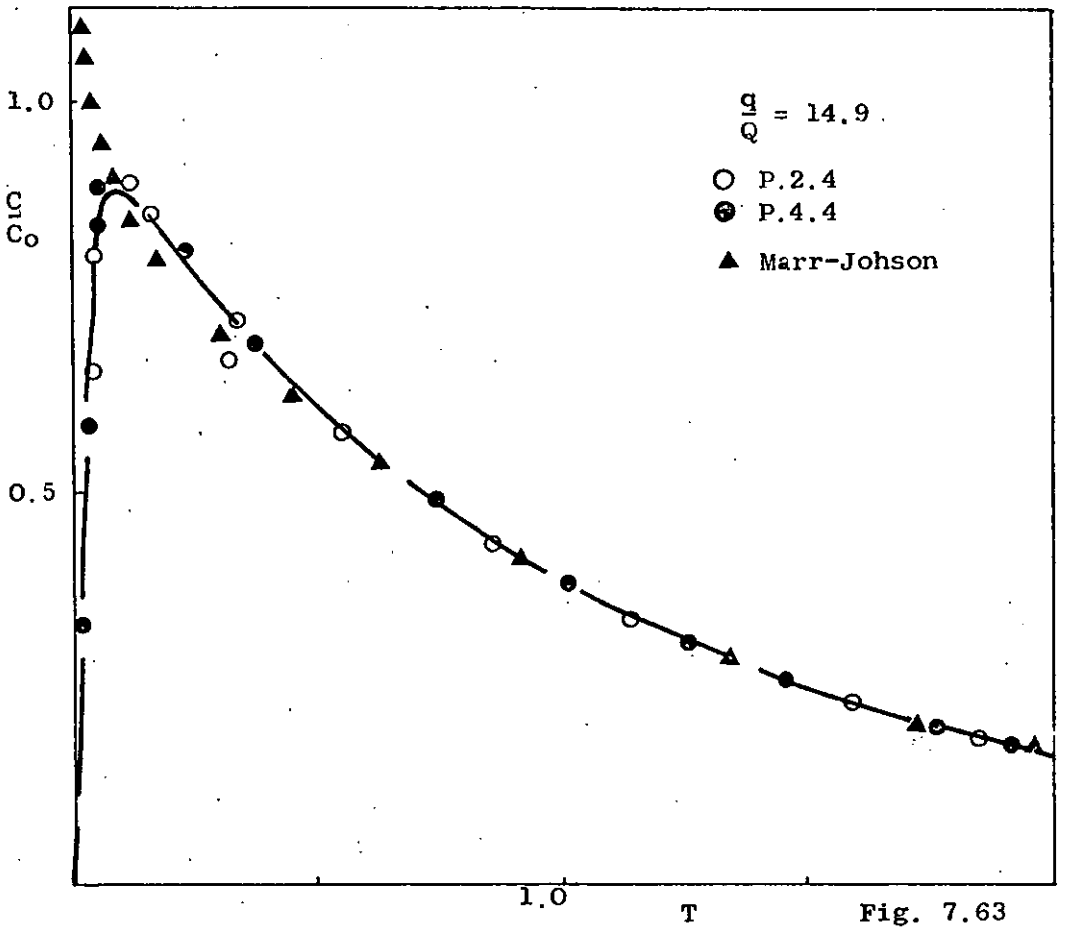

Fig. 7.63

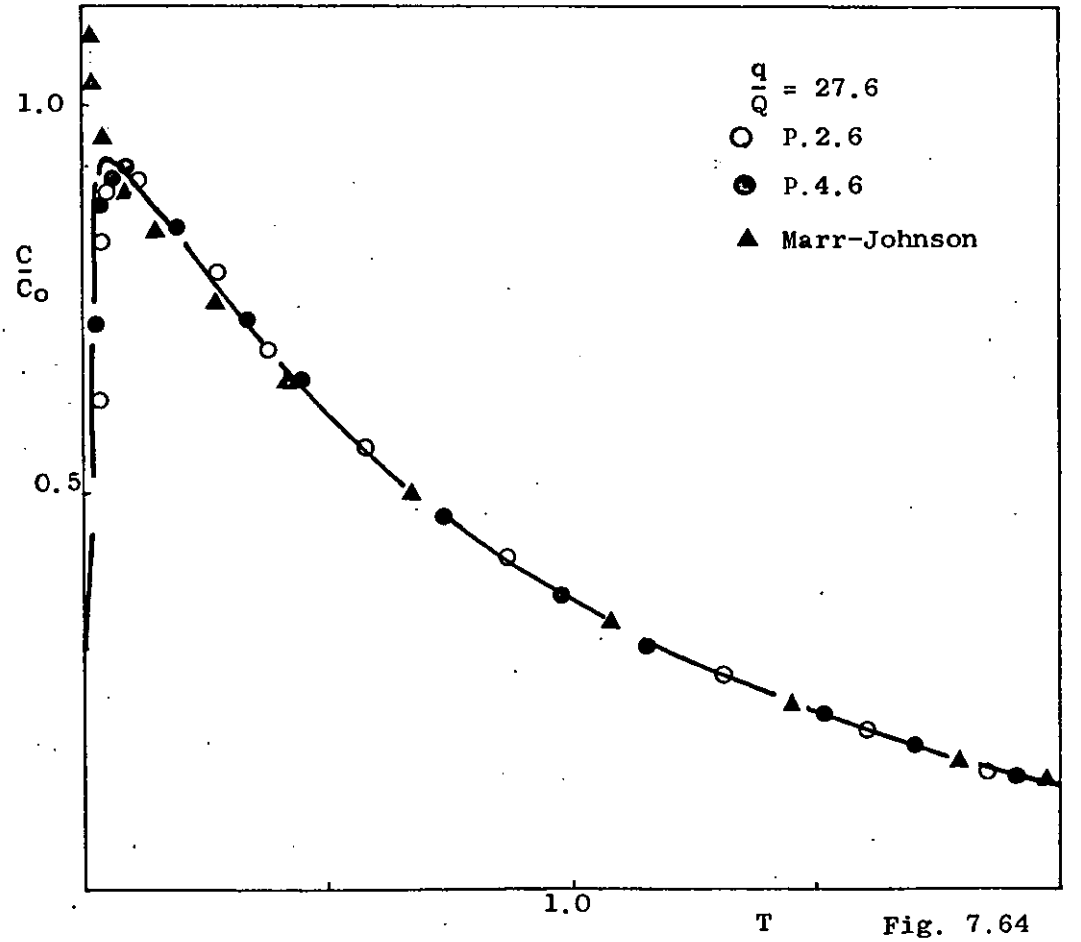

Fig. 7.64

7.3.2. The 4"/19"/19" cylindrical system:- water

	Series P.11	Series P.12	Series P.13	Series P.14
Liquid Holdup (litres)	88.2	88.2	88.2	88.2
Flow Rate (litres/min)	5.2	5.2	5.2	5.2
Meantime (mins)	16.9	16.9	16.9	16.9
Inlet Position	Into Impeller	Into Loop	Into Impeller	Into Loop
Baffles	Unbaffled	Unbaffled	Baffled	Baffled

Figures 7.65 - 7.72 illustrate the comparison between experimental results for the 4"/19"/19" system and the single loop model. The fit of experimental results and theoretical predictions is excellent for high valuesof the model parameter but for low values of (q/Q) the fit is slightly worse.

The predictions of the model of Marr and Johnson are again shown in the figures, for the feed to impeller case. The marked difference between these theoretical solutions and actual experimental results is again apparent.

The effect of baffles on the experimental normalised residence time distribution is again very small, as illustrated in the figures.

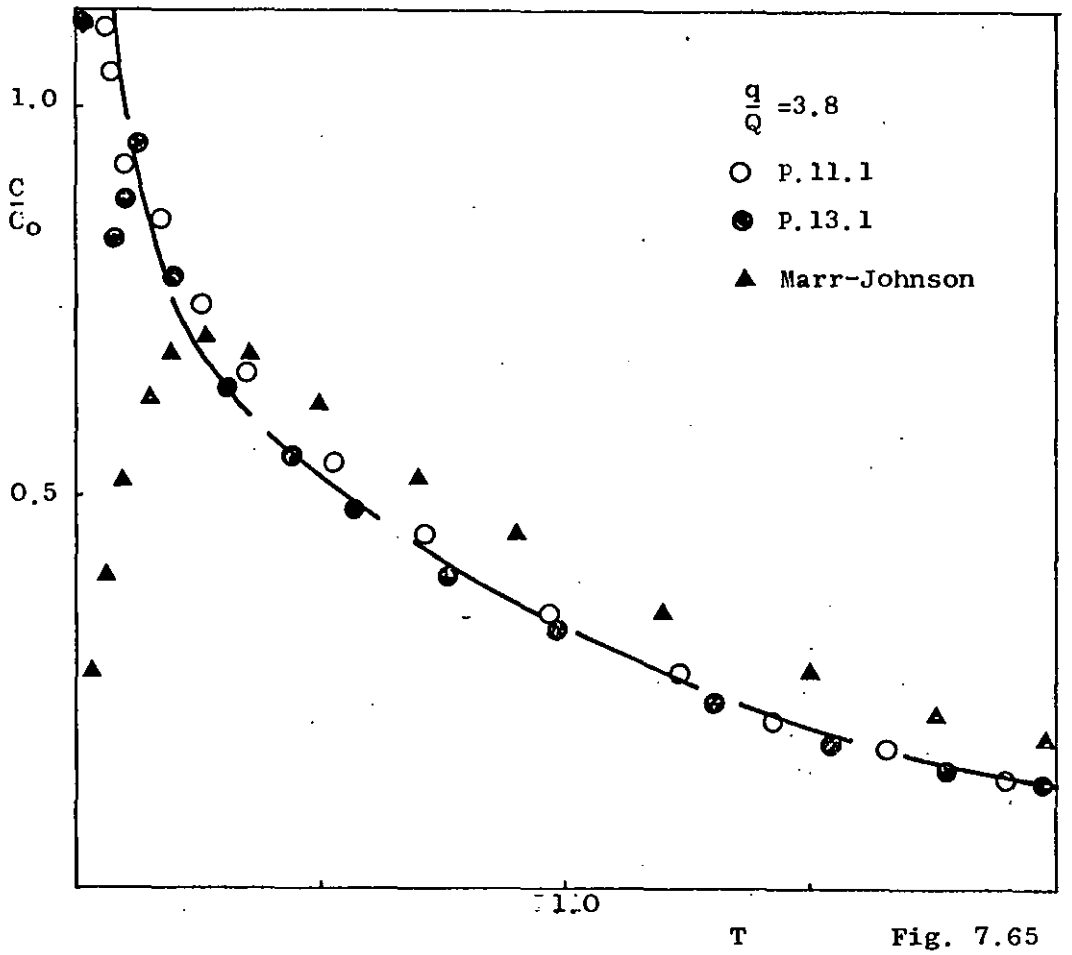

Fig. 7.65

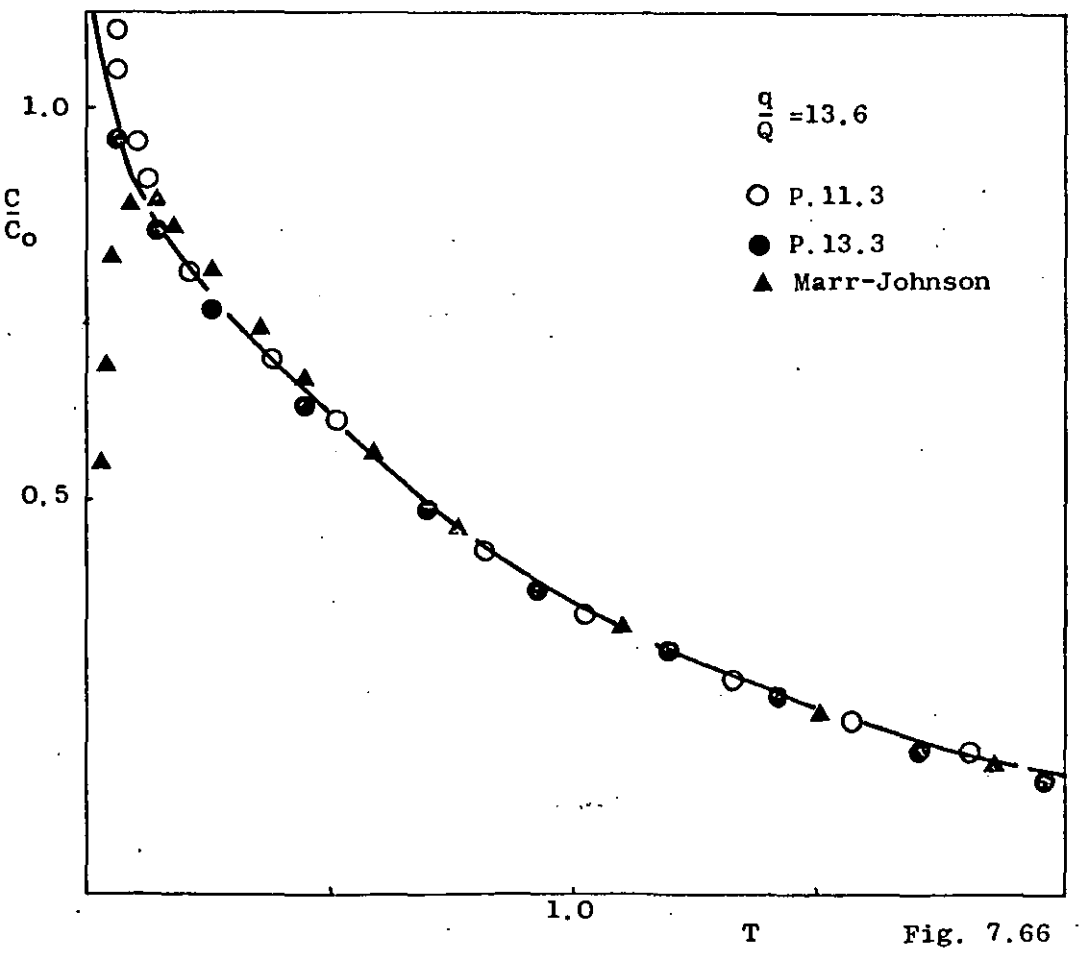

Fig. 7.66

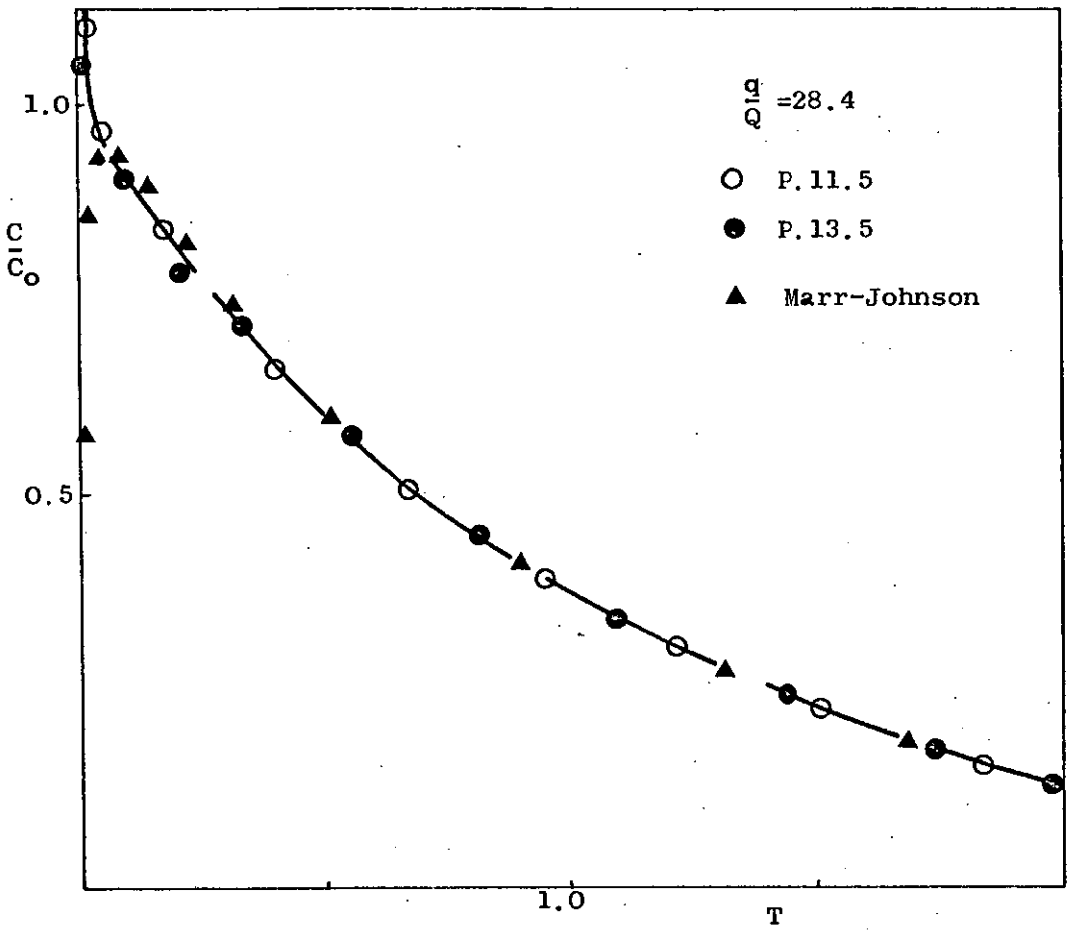

Fig. 7.67

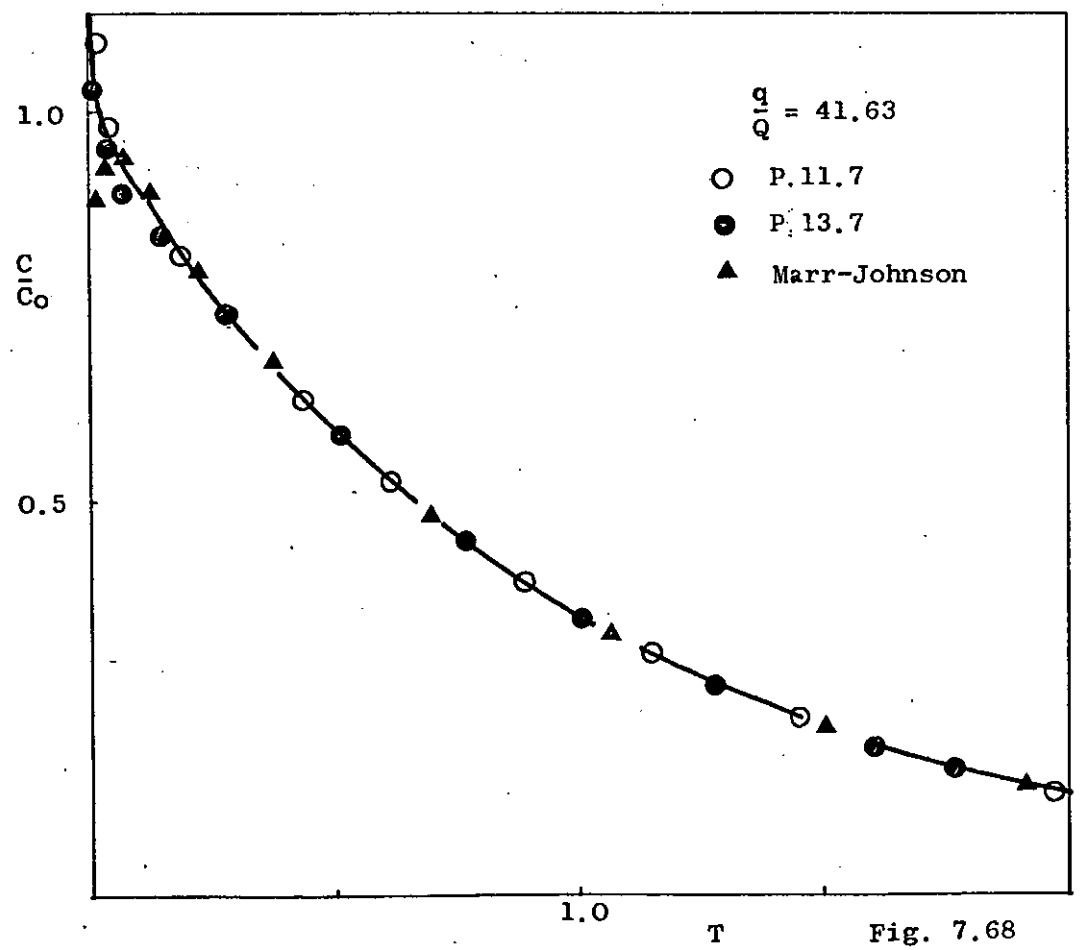

Fig. 7.68

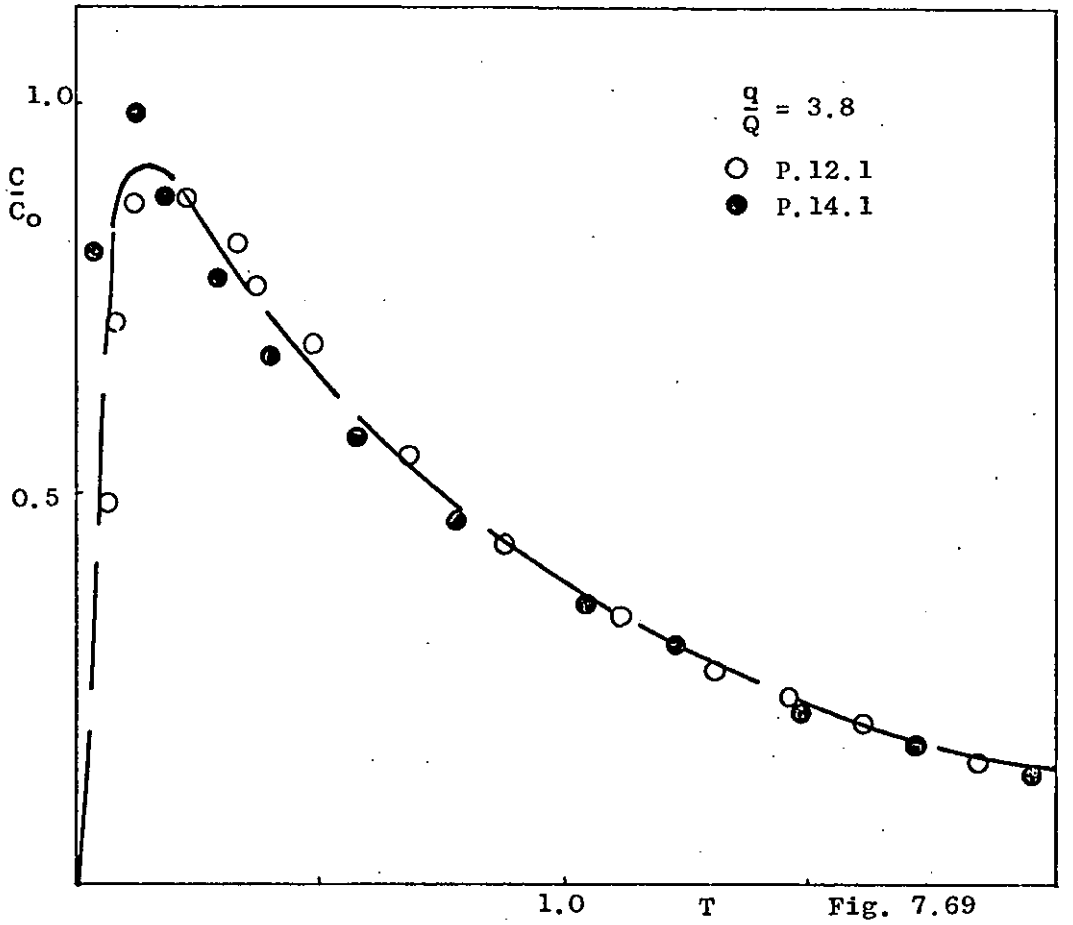

Fig. 7.69

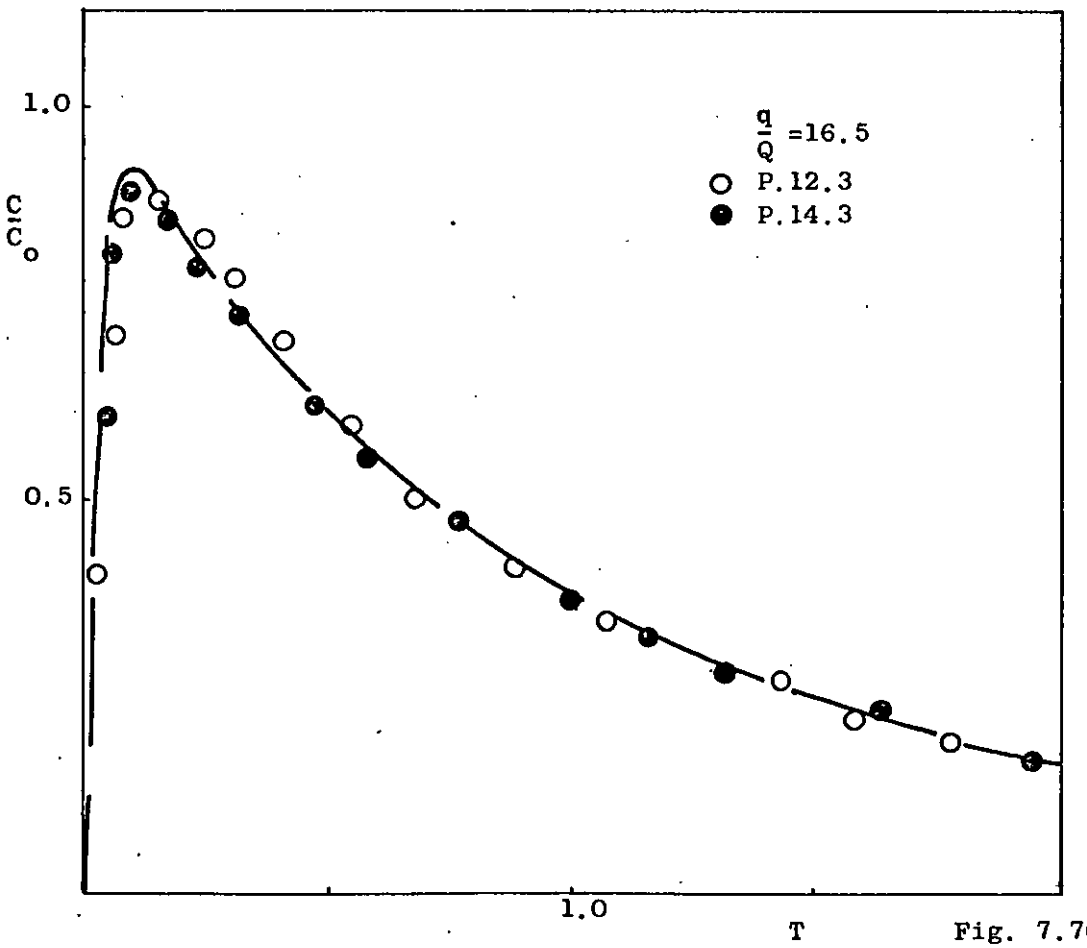

Fig. 7.70

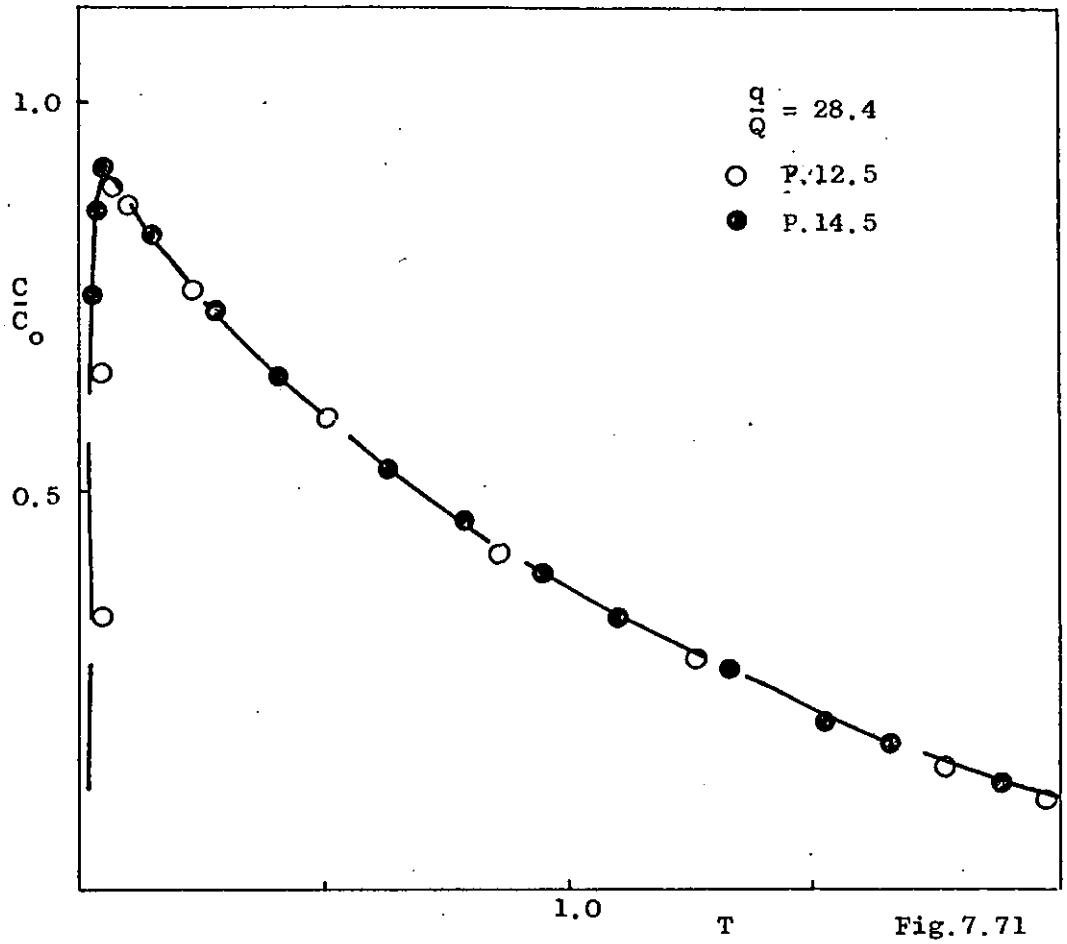

Fig.7.71

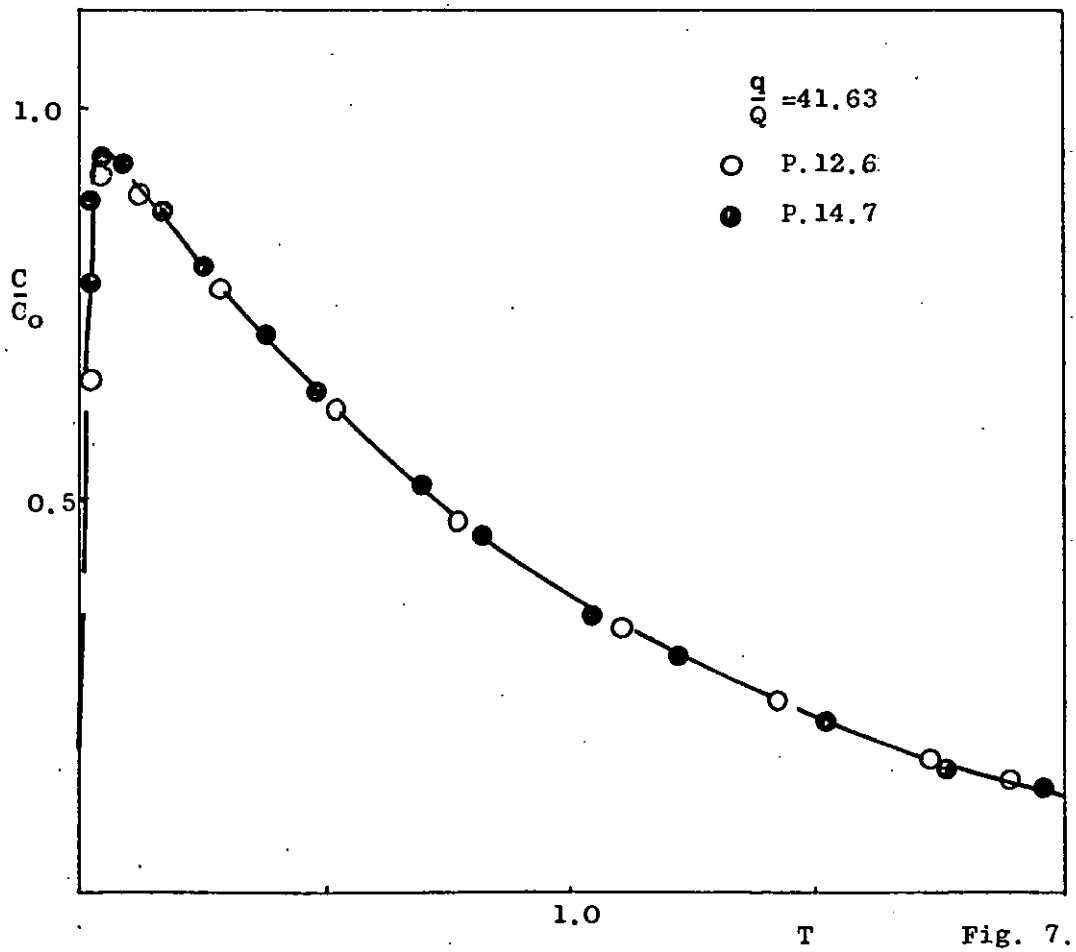

Fig. 7.72

7.4. Correlation of Gamma Function Model Parameter (n) with the Flow Model Parameter (q/Q) of the Single and Double Loop Models

Having verified the predictions of the theoretical flow models with experimental results, if is worthwhile to correlate the models' parameter (q/Q) of the single and double loop models, with the parameter (n) of the gamma function model. The gamma function model gives a quick and easy representation of the non-ideality of a continuous stirred tank. The correlation would give a broader base for design of turbine and propeller agitated vessels.

Using the least squares criteria, described in Appendix 4, the optimum value of (n) was computed for a wide range of (q/Q). This was achieved with the following modification of the programme described in Appendix 3. For a given value of (q/Q), the flow model predictions were computed and stored. The gamma function model solutions were then computed for the same time scale, for a particular value of (n). Then by repeated iteration of the gamma function model parameter (n), an optimum value of (n) was found, which gave the least sum of errors squared. This was repeated for various values of (q/Q) and for each of the least squares optimisation criteria.

Optimum values of the gamma function parameter (n) were also computed, for the experimental impulse response results of runs R.1, R.17, using the absolute criteria of Appendix 4. A simple programme which incorporated the same procedures as previously described was written to achieve this.

Figure 7.73 and Figure 7.74 show the resulting correlation of the gamma function model parameter (n) against the flow parameter (q/Q) of the single loop model for feed to the impeller and to the loop region respectively. Figures 7.75 - 7.76 illustrate similar

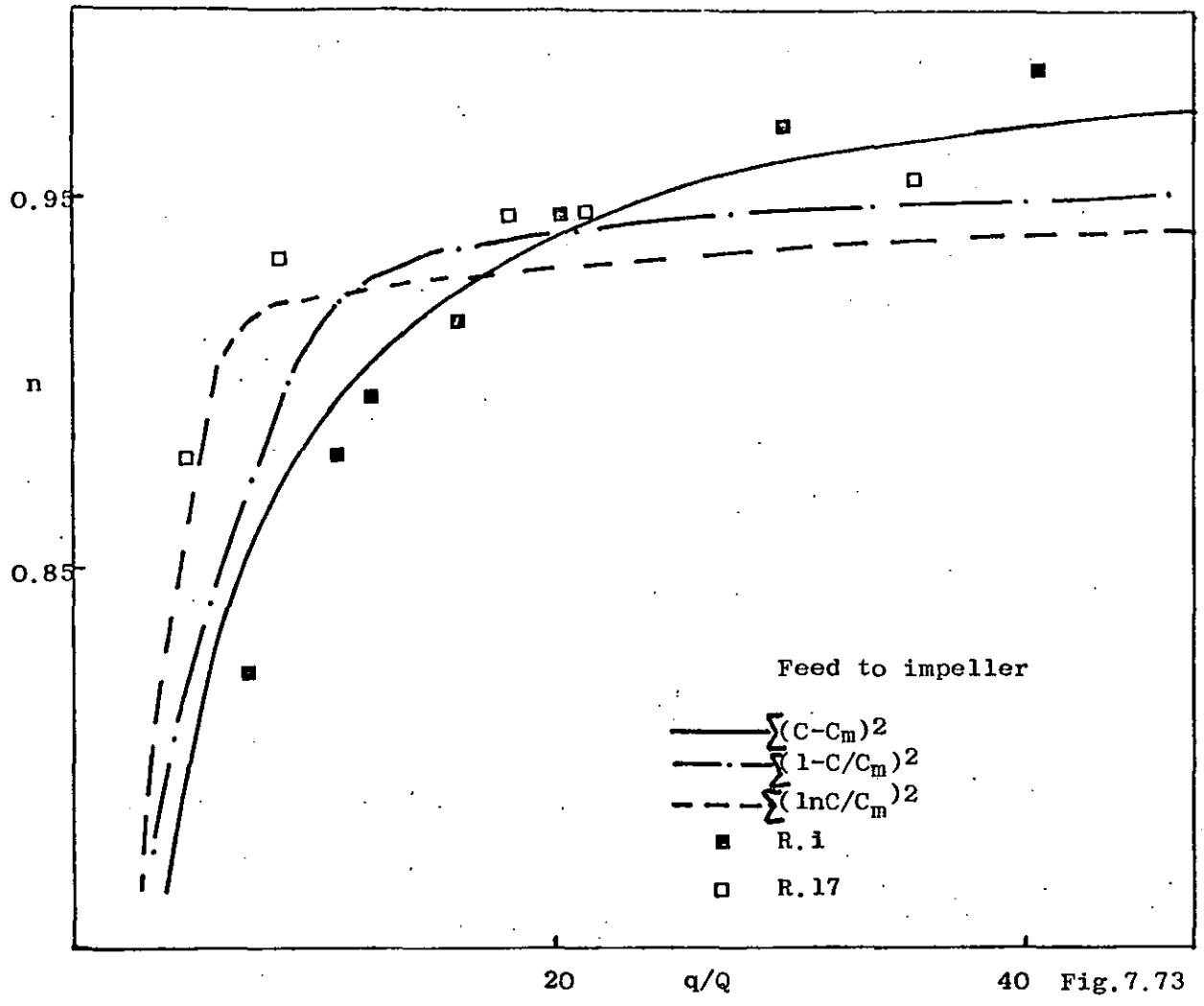

Fig.7.73 Gamma function model parameter n vs q/Q, Single loop model parameter

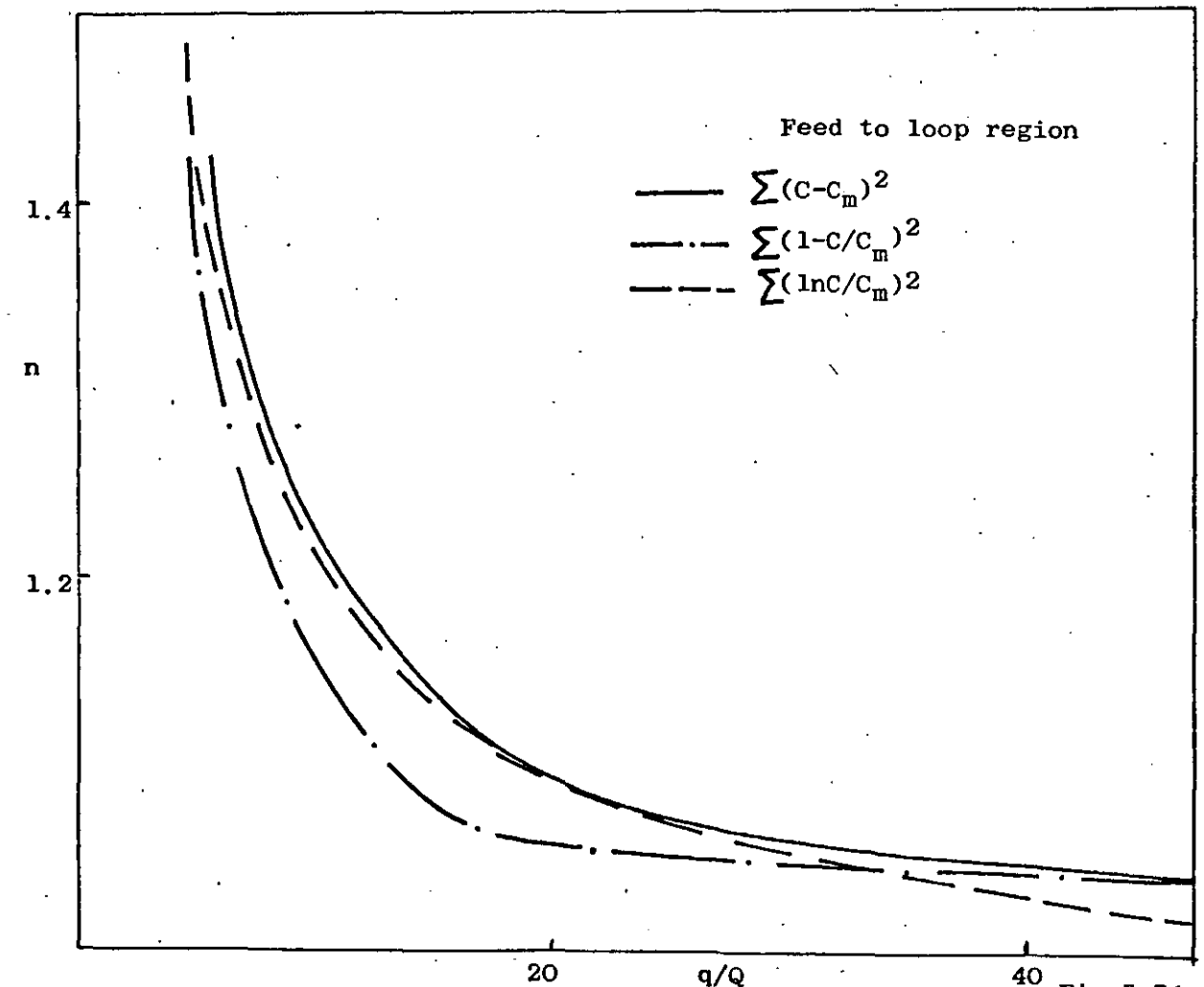

Fig.7.74

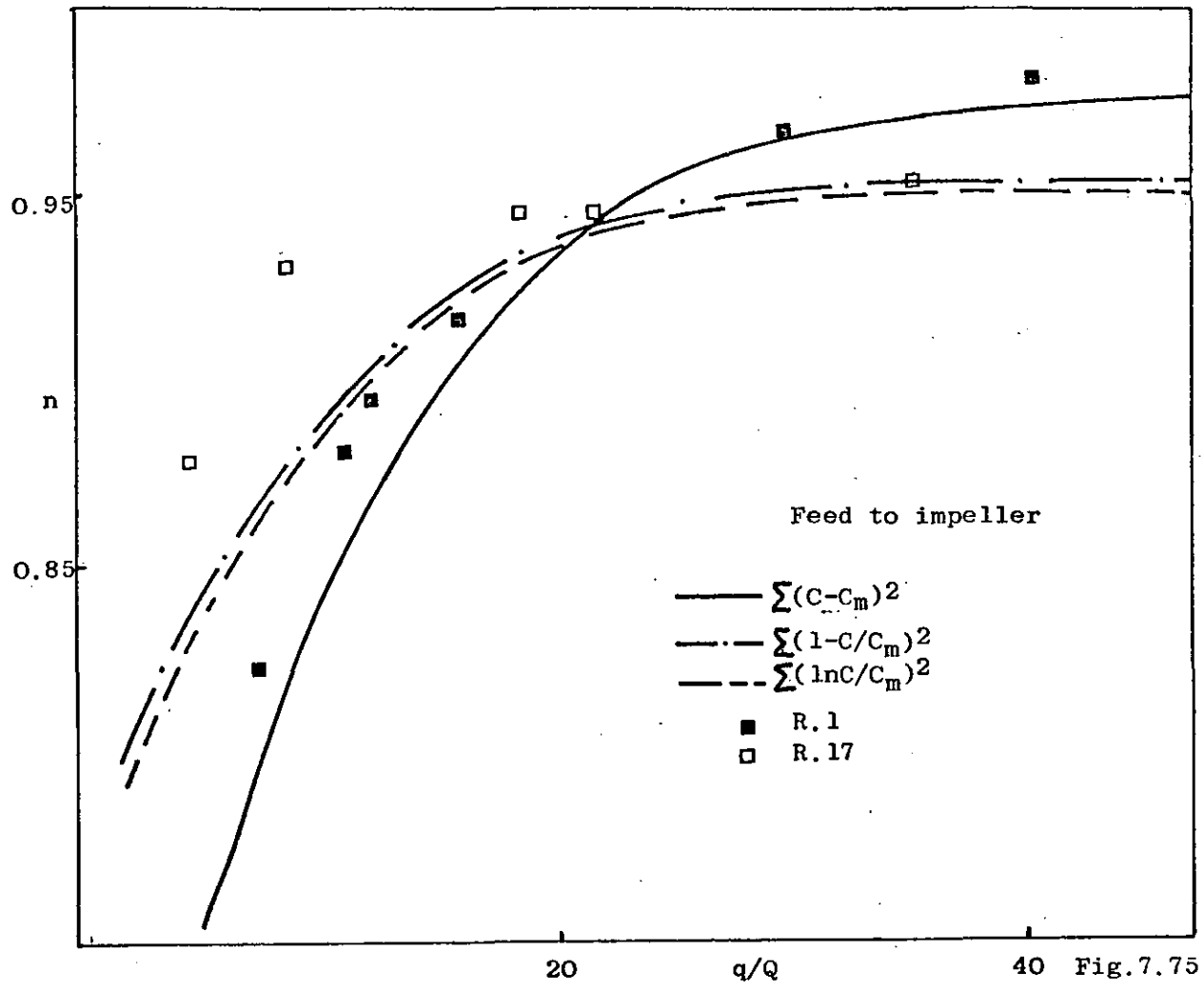

Fig.7.75 Gamma function model parameter n vs q/Q, Double loop model parameter

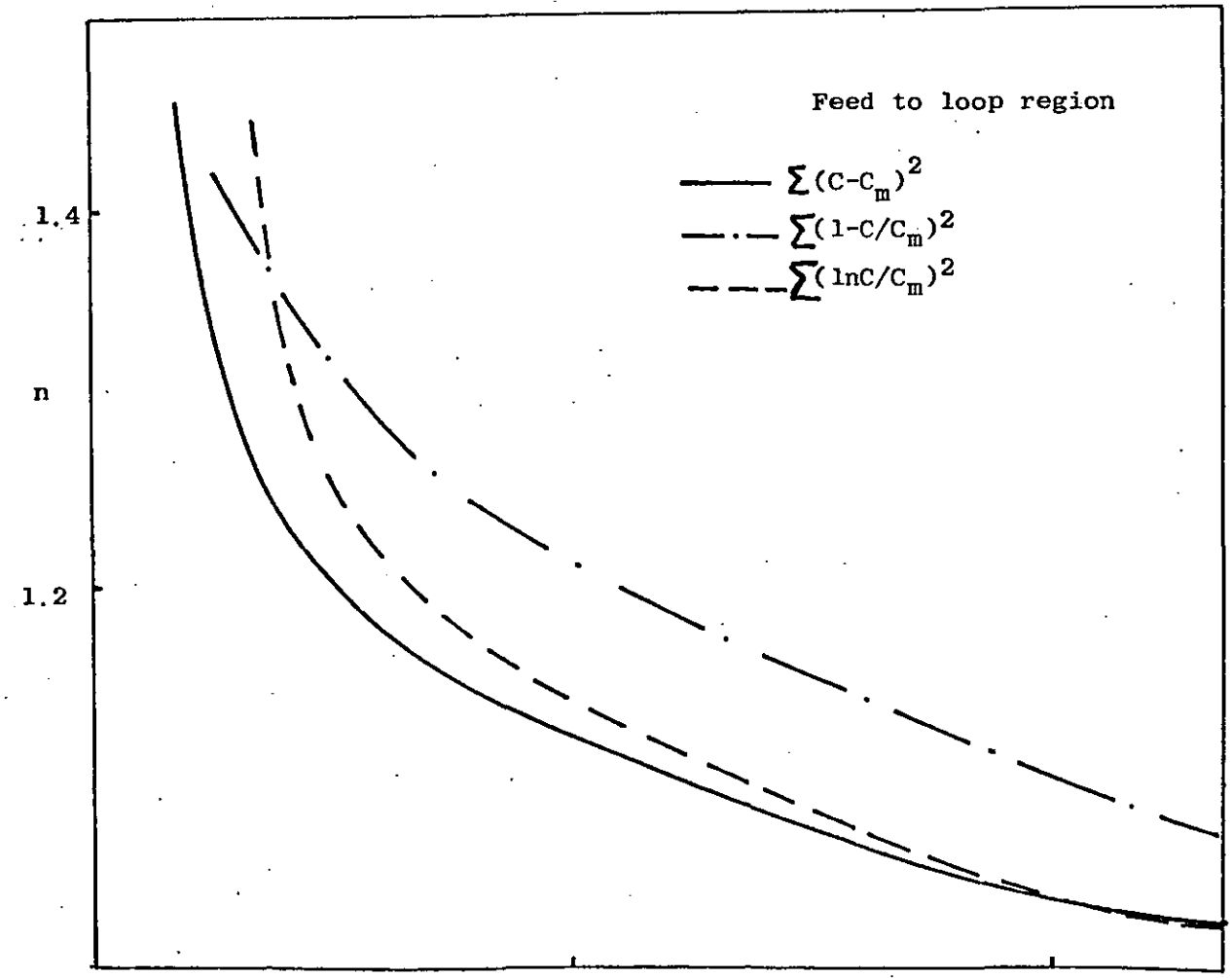

Fig. 7.76

correlations for the double loop model. Also shown are the optimum values of (n) computed for each of the experimental runs of R.1 and R.17.

A discrepancy appears in these figures, for as (q/Q) tends towards infinity the system should approach an ideal mixing vessel; consequently, the gamma function model parameter (n) should be unity. The figures show this not to be the case. However, the limiting value of (n) is close to unity for large values of (q/Q) for each optimisation criteria. The experimental results yield a similar phenomena.

Figures 7.77 - 7.84 illustrate predicted impulse responses of the single and double loop model and the equivalent gamma function model parameter (n); having obtained the value of (n) from the curves of Figures 7.73 - 7.76. The correspondence between the curves is excellent for the feed to the impeller case; the resulting sum of least squares was always small for this feed condition.

A marked difference in the predicted responses is apparent for the feed to the loop case for each optimisation criteria, Figures 7.79 - 7.80 and Figures 7.83 - 7.84. For low values of (q/Q) the deviation is most prominent, it becomes smaller as (q/Q) is increased.

The correspondence between experimental impulse response results and the computed least squares value of (n) leads to excellent correspondence for feed to the impeller and a somewhat less favourable comparison for feed to the loop case.

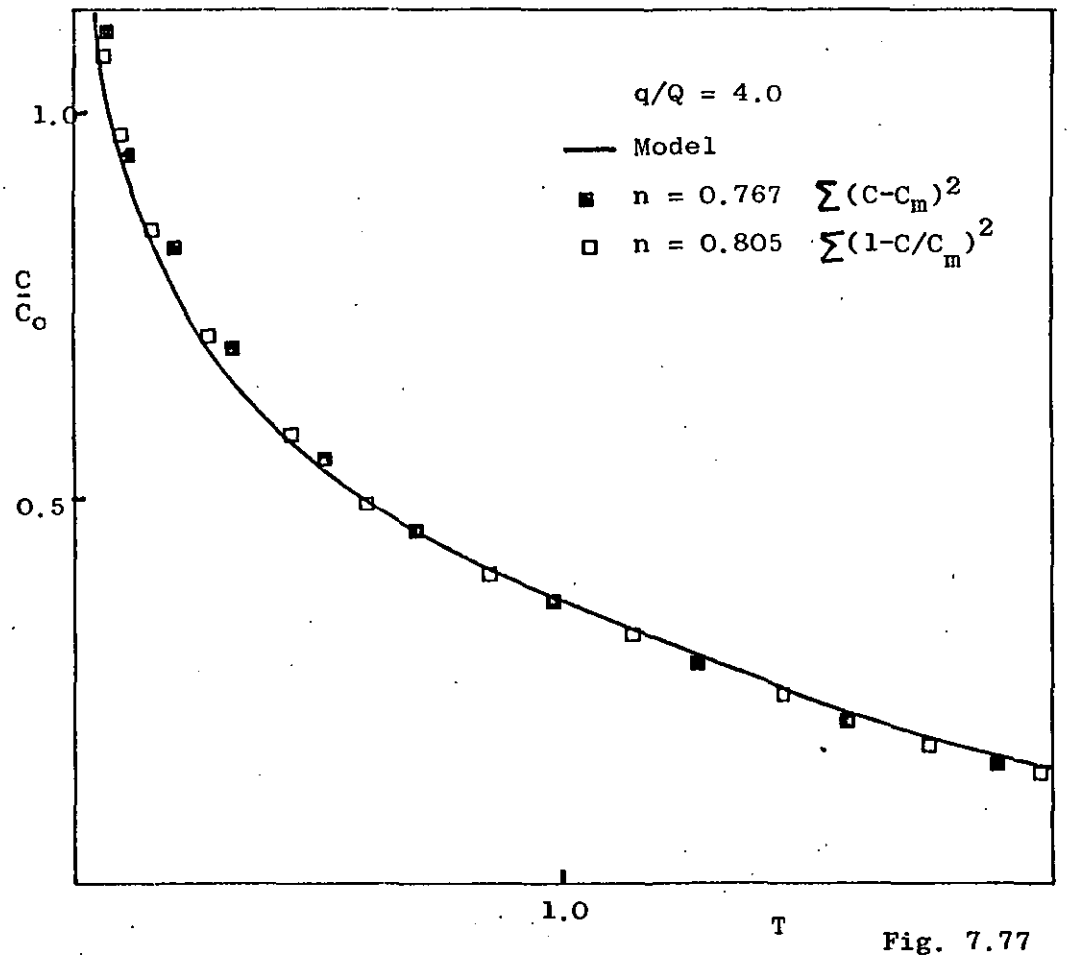

Fig. 7.77

Single loop parameter q/Q $\equiv$ Gamma function parameter n

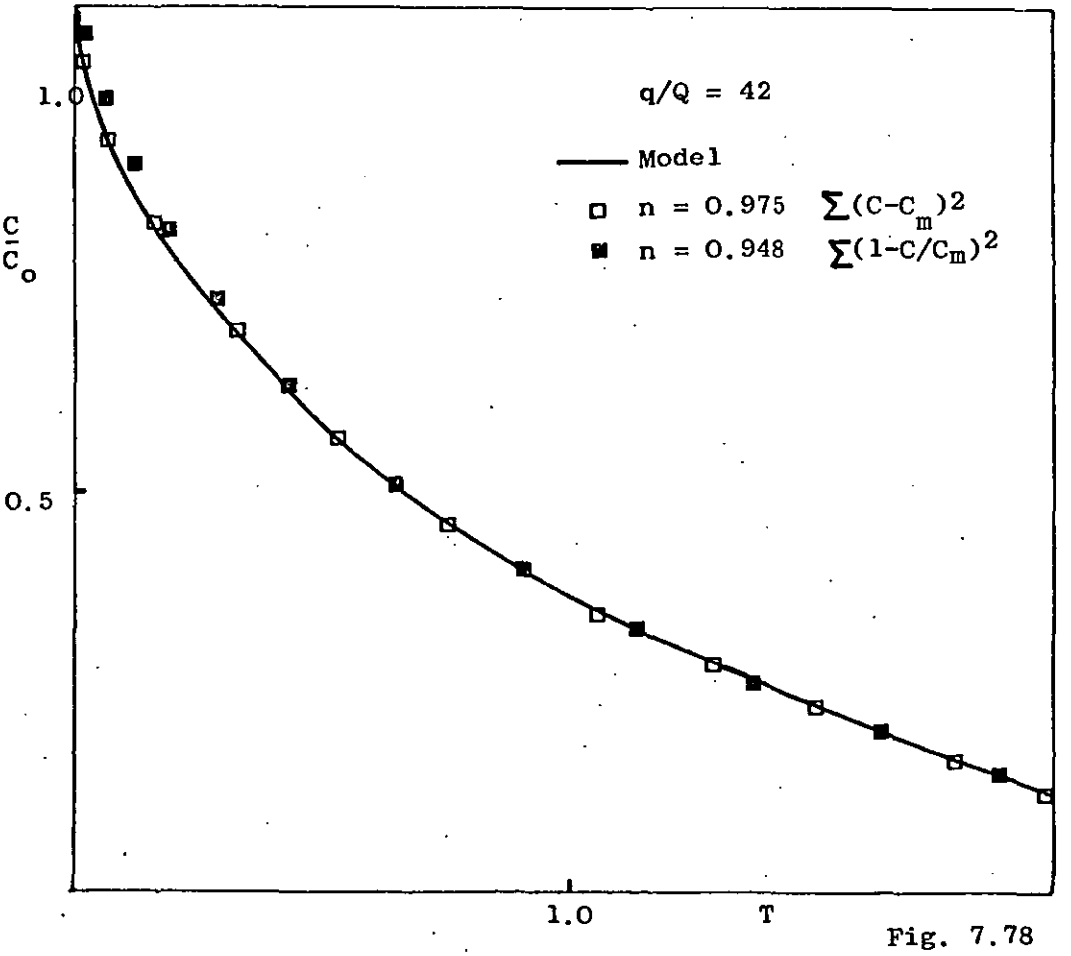

Fig. 7.78

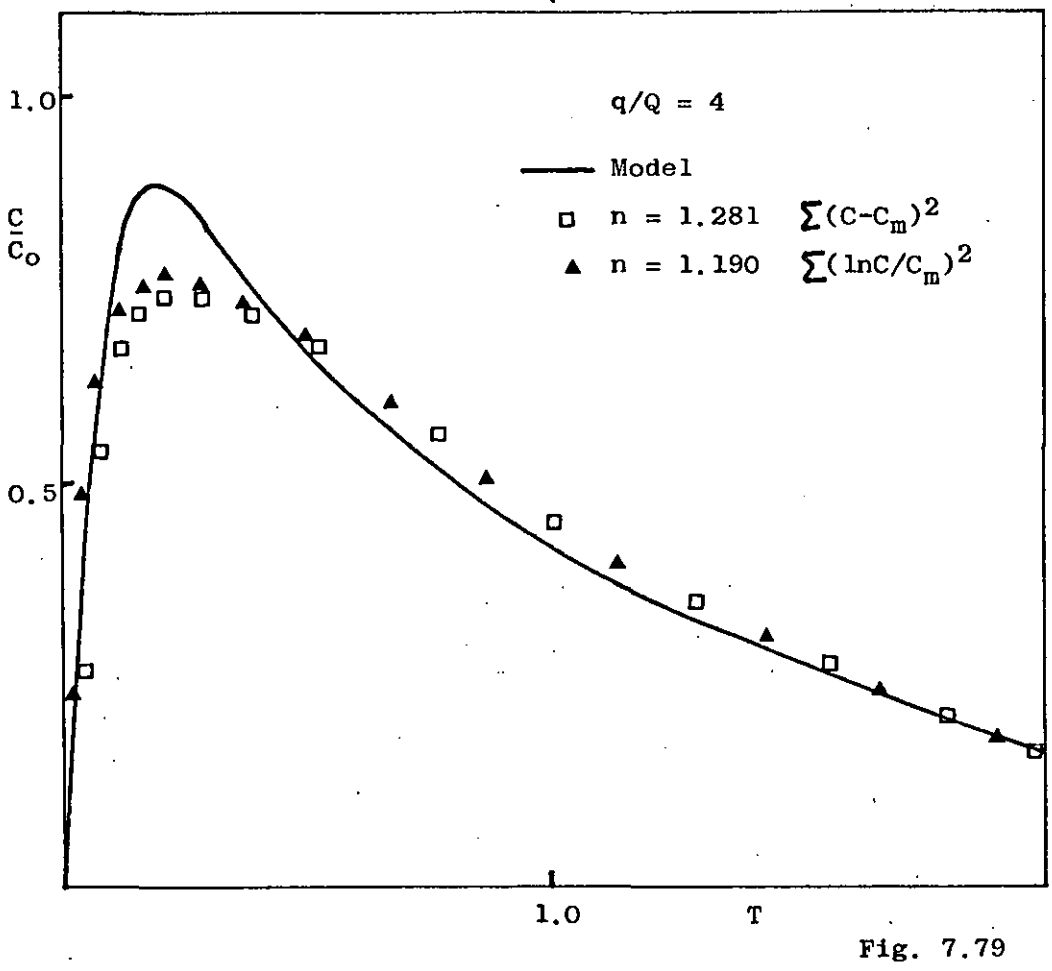

Fig. 7.79

Single loop parameter q/Q = Gamma function parameter n

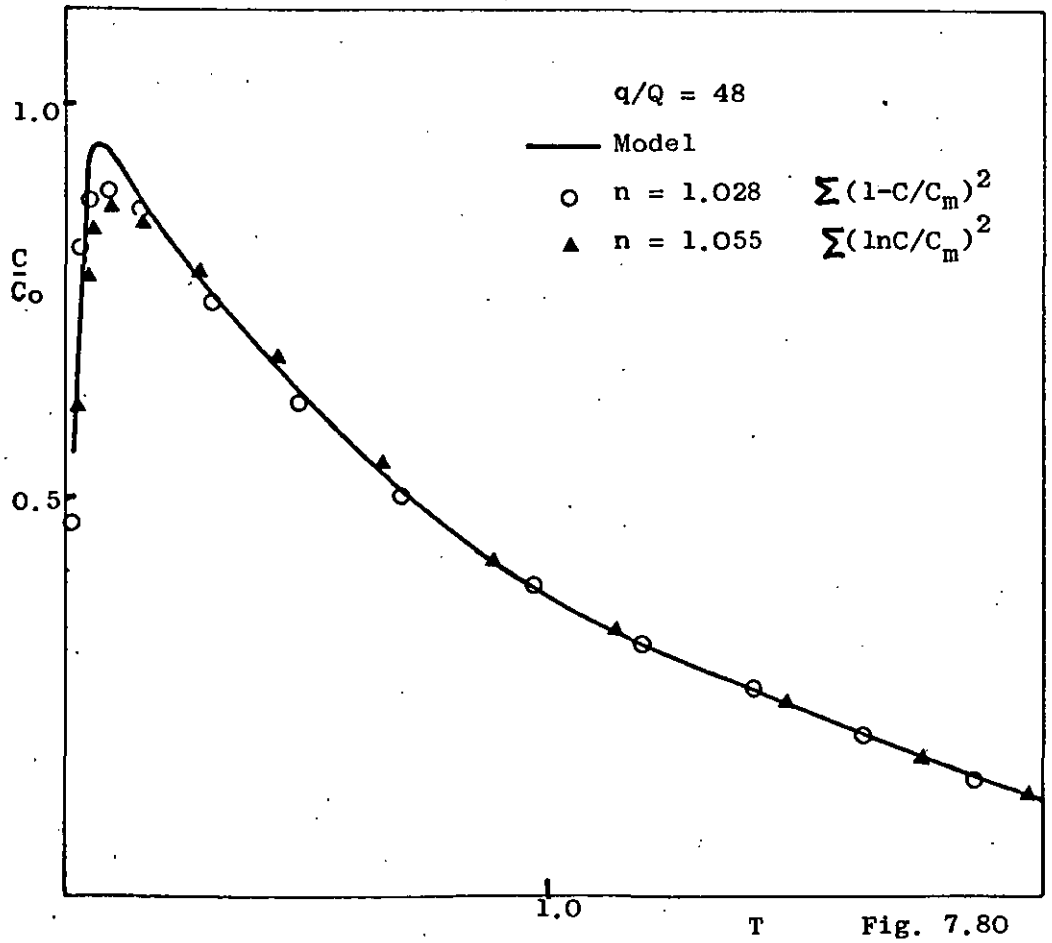

Fig. 7.80

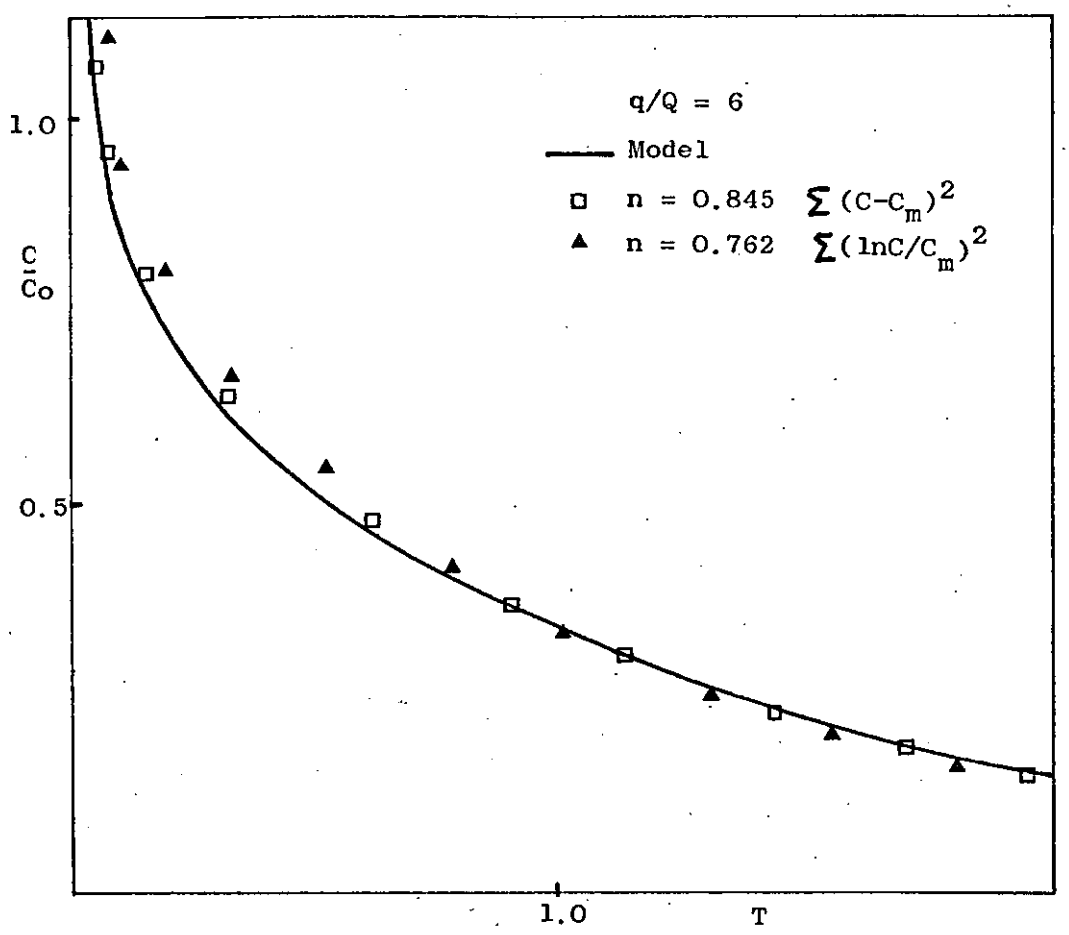

Fig. 7.81

Double loop parameter q/Q $\equiv$ Gamma function parameter n

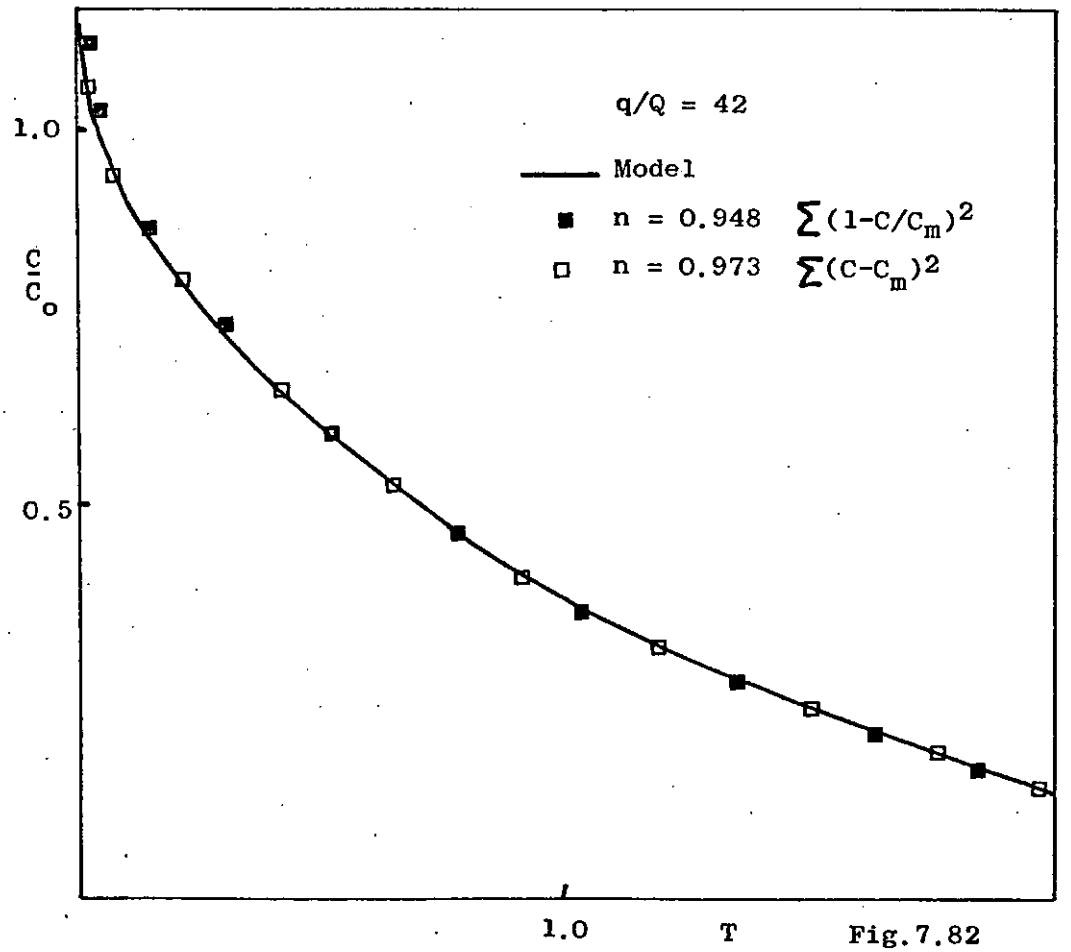

Fig.7.82

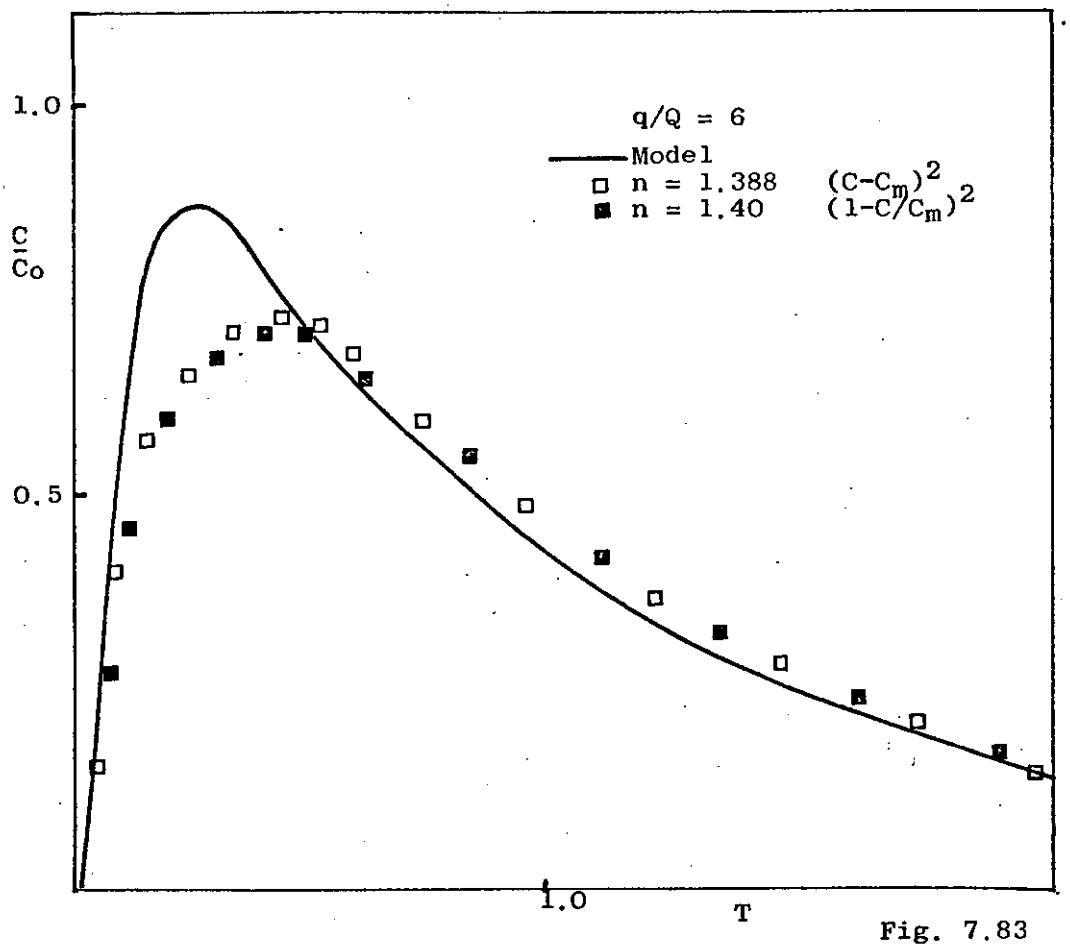

Fig. 7.83

Double loop parameter q/Q ≡ Gamma function parameter n

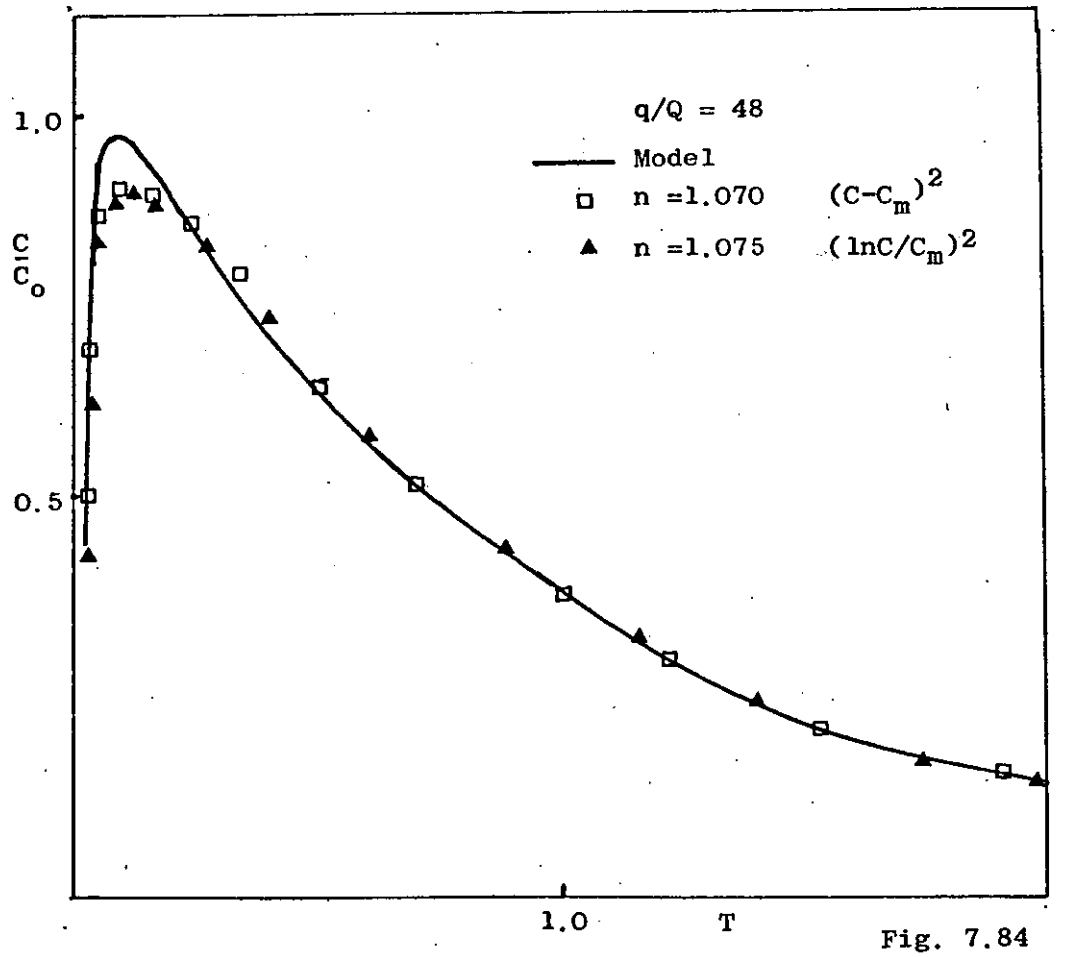

Fig. 7.84

7.5. Results of Turbine Batch Mixing Time Experiments

The results of the turbine batch mixing time experiments are presented in Appendix 13a.

In this section, experimental results are compared with the values derived from Metzner and Norwood's empirical relationship, and the predicted solutions of the analytical expression, equation 5.4. A homogenity level of 1.0%, $\delta = 0.01$, was found to match the analytical expression prediction with the experimental results. Figures 7.85 - 7.89 illustrate the comparisons for a variety of vessel and impeller diameters. For each vessel configuration the similarity between the experimental and the model predictions is most favourable; better comparison could be obtained by variation of the value of (δ) for each particular case. The solutions predicted from Metzner and Norwood's correlation, although following the trend of the experimental results, deviate greatly from the experimentally determined values, throughout the range of impeller speed studied and for each vessel arrangement. The values of batch mixing time obtained by this method were always shorter than those found experimentally.

Figure 7.85 shows the experimentally determined values, for a 2½" diameter turbine situated in a 10" diameter vessel ($Z/D = 1$), for the impeller positioned at Z/3, Z/2 respectively. It can be seen that impeller position has an effect on the experimentally determined batch mixing time, although both are well matched by the model solutions. Figure 7.86 illustrated similar phenomena for a 3" diameter turbine placed in a 10" diameter vessel ($Z/D = 1$). In Figures 7.87, 7.88 for the 13" diameter vessel, the effect of impeller position is more noticeable.

The introduction of baffles was found to have little effect on the experimental results as was the point of introduction of the acid

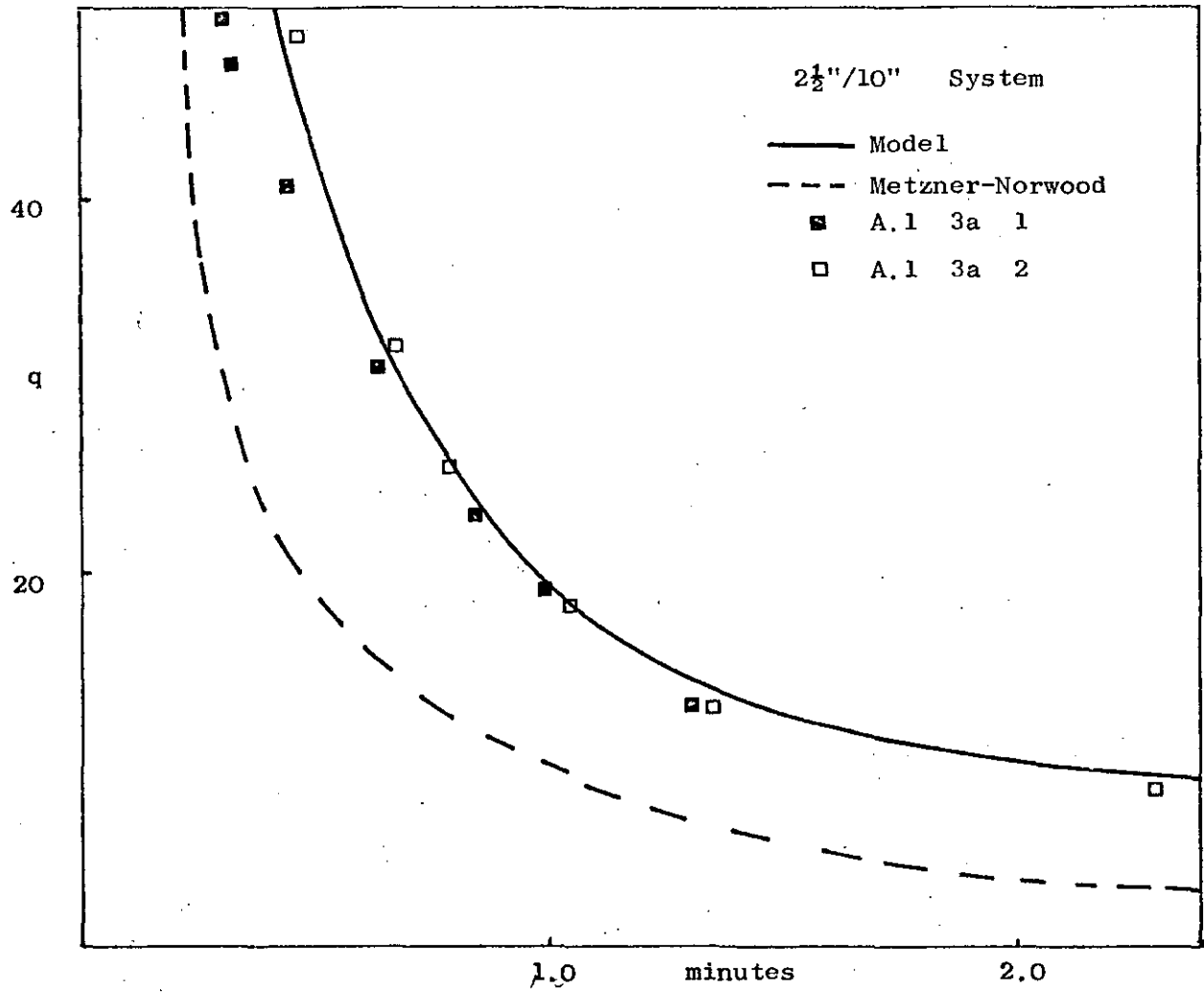

Fig. 7.85

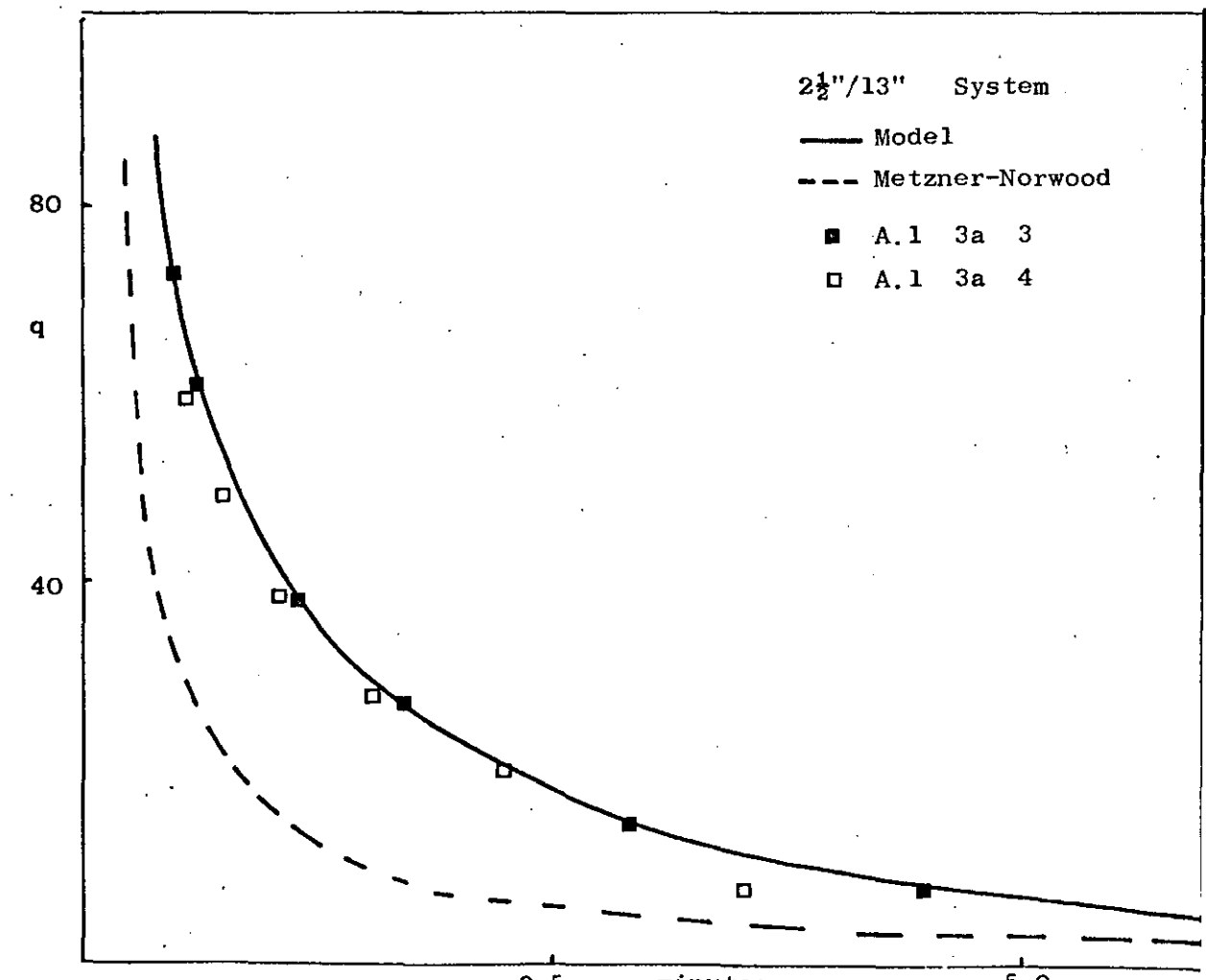

Fig. 7.86

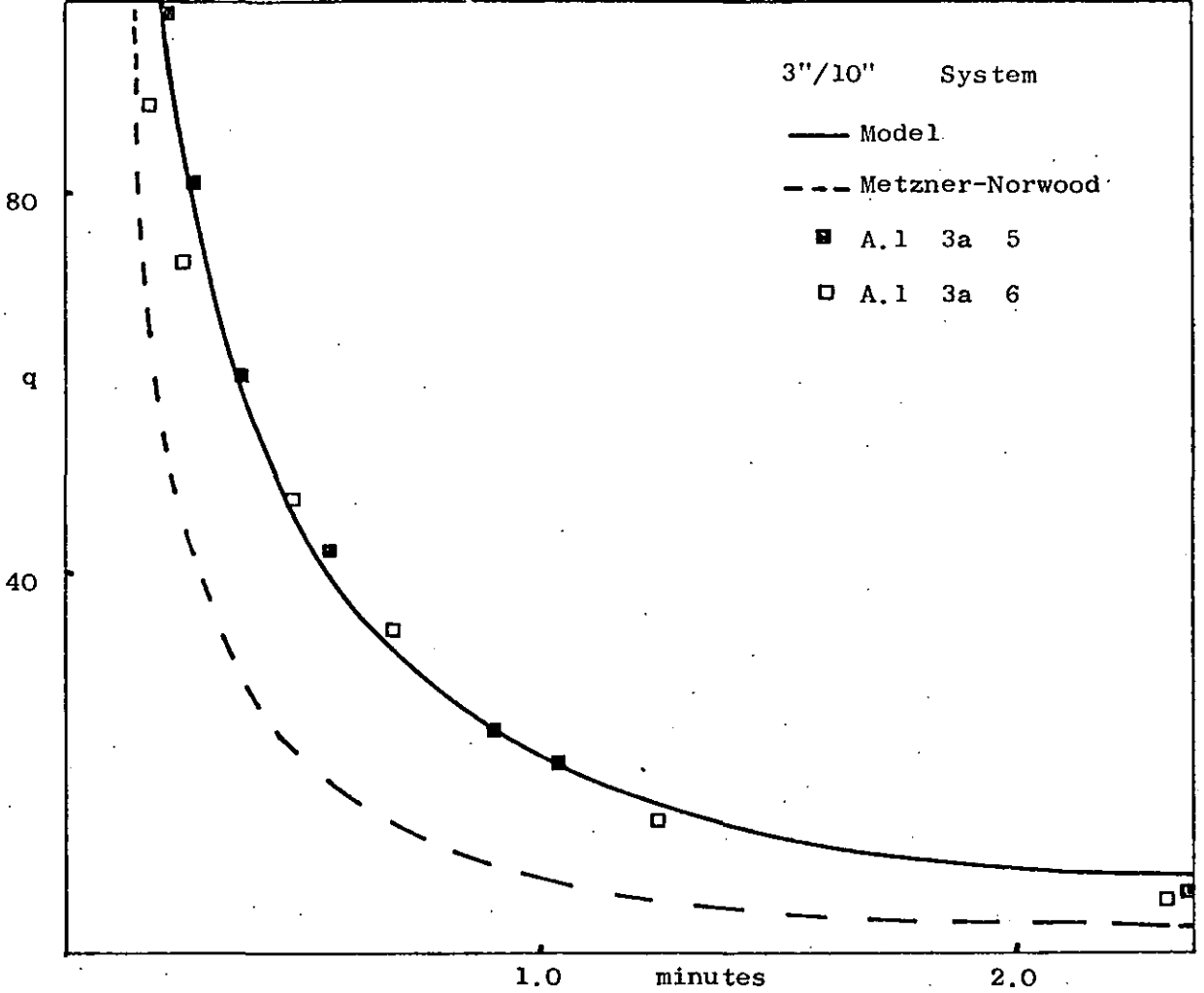

Fig. 7.87

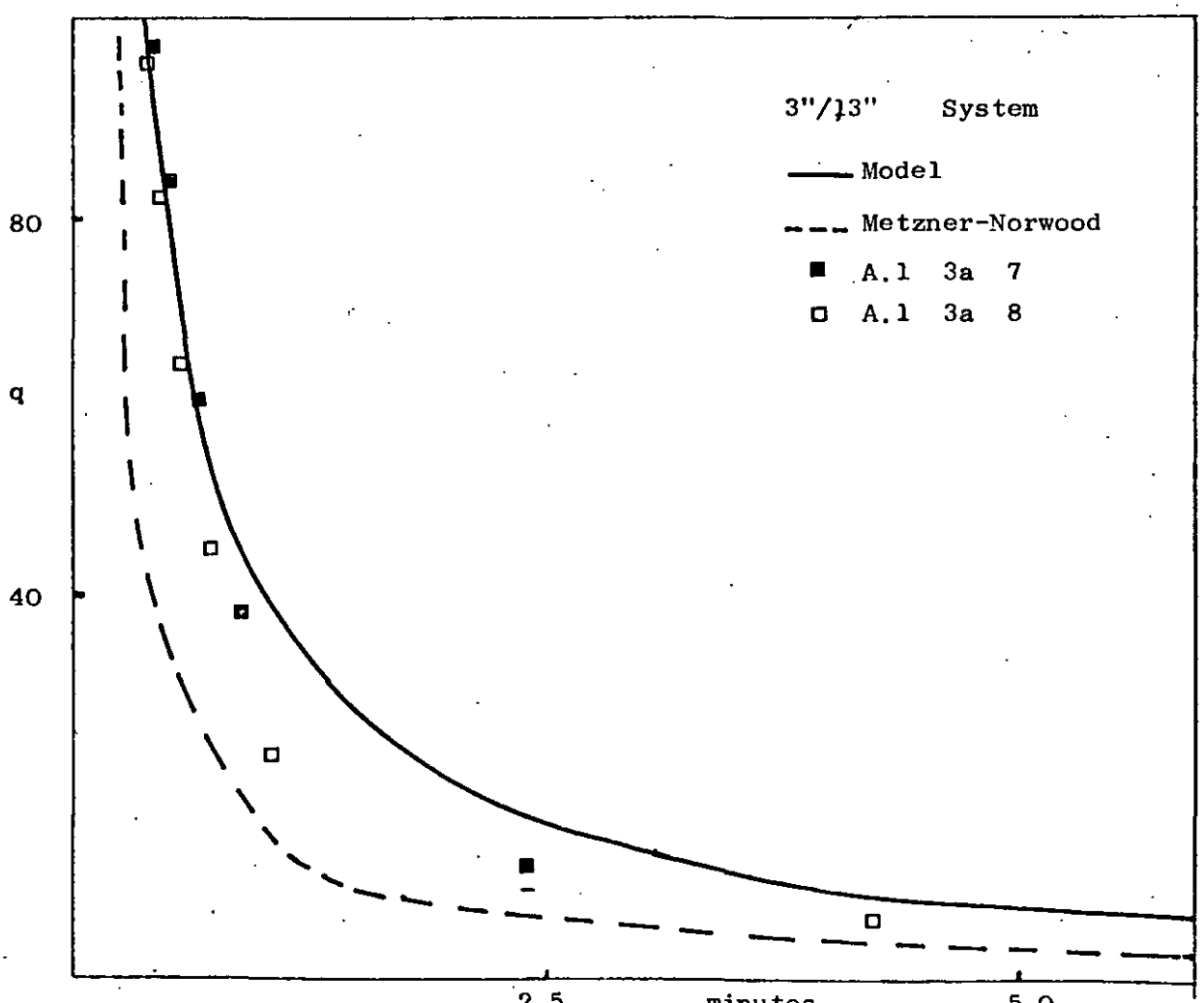

Fig. 7.88

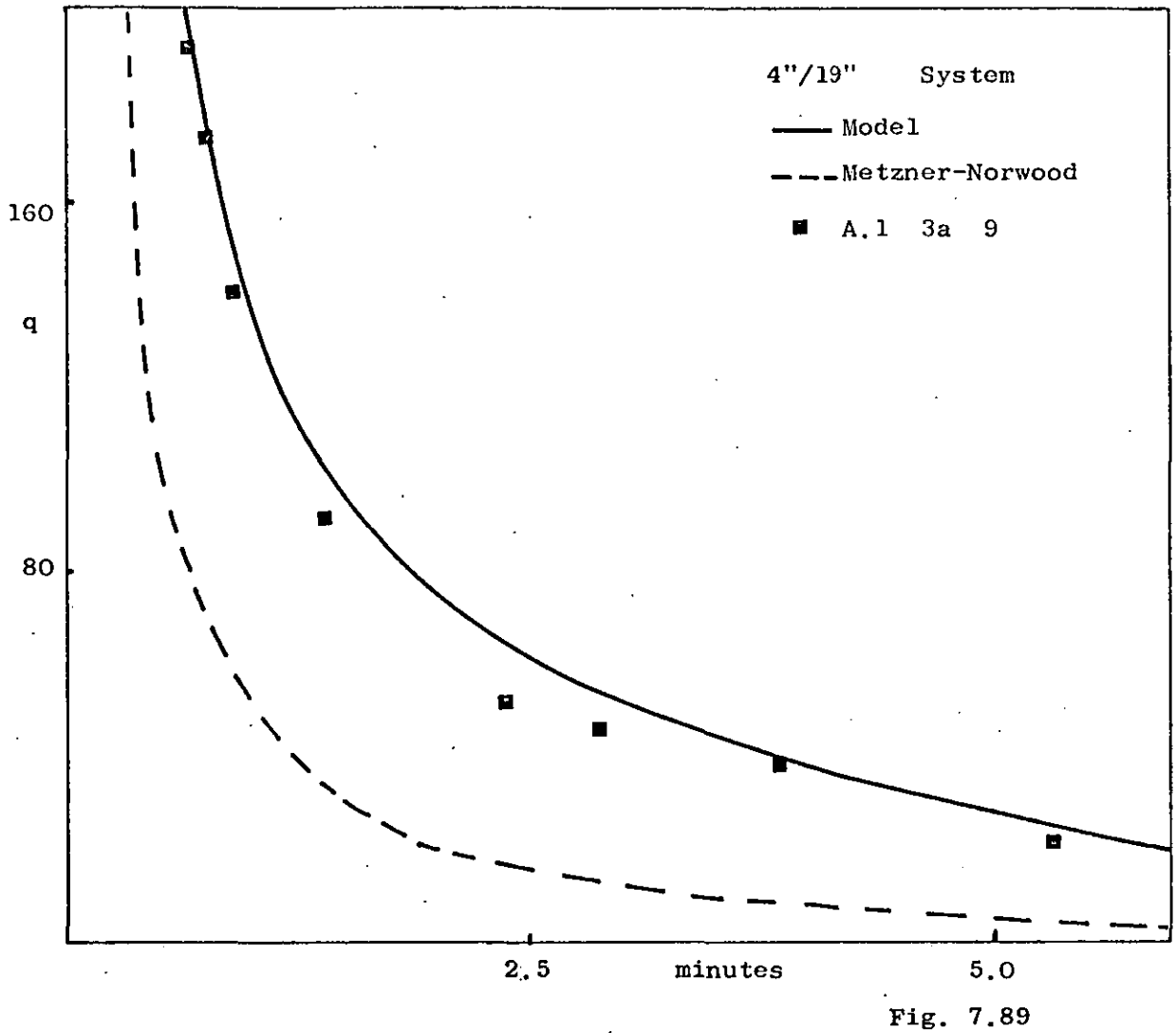
4"/19" System
Model
Metzner-Norwood
A.1 3a 9
160
q
80
2.5
minutes
5.0

Fig. 7.89

7.6. Results of Propeller Batch Mixing Time Experiments

The results of the propeller batch mixing time experiments are presented in Appendix 1.3b.

Figures 7.90 - 7.93 illustrate the comparison of experimental results and theoretical predictions of the empirical correlation of Fox and Gex and the analytical expression equation 5.4. A homogenity level of 0.1%, $\int = 0.001$, was found to match the analytical expression solutions with the experimental results throughout the range of impeller and vessel diameter studied. The predicted values of the model compare favourable with the experimental results, however, the batch mixing times derived from the correlation were always greater than the corresponding experimental results.

Figure 7.90 shows the experimental results for a $2\frac{1}{2}$" diameter propeller situated in a 10" diameter vessel, (Z/D = 1), for an impeller place at 1/3 of the liquid height from the base of the vessel. Figure 7.91 illustrates the results for a 3" diameter propeller in the same vessel. The effect of impeller position is shown in Figure 7.92 and Figure 7.93; $2\frac{1}{2}$", 3" diameter propeller in 13" diameter vessel respectively. The variation of propeller position, (Z/3, Z/2), has a little effect on the batch mixing time in vessels of this size.

As can be seen from the figures of the previous two sections the empirical correlations for batch mixing time are not sufficiently general for accurate determination of the batch mixing time, for systems, other than those from which they were originally developed. The deviation in results is probably caused by the impellers used in this work having different pumping capacities than those used to derive the correlations. This fact makes the correlations of a one-off nature.

The model predictions of the analytical expression are

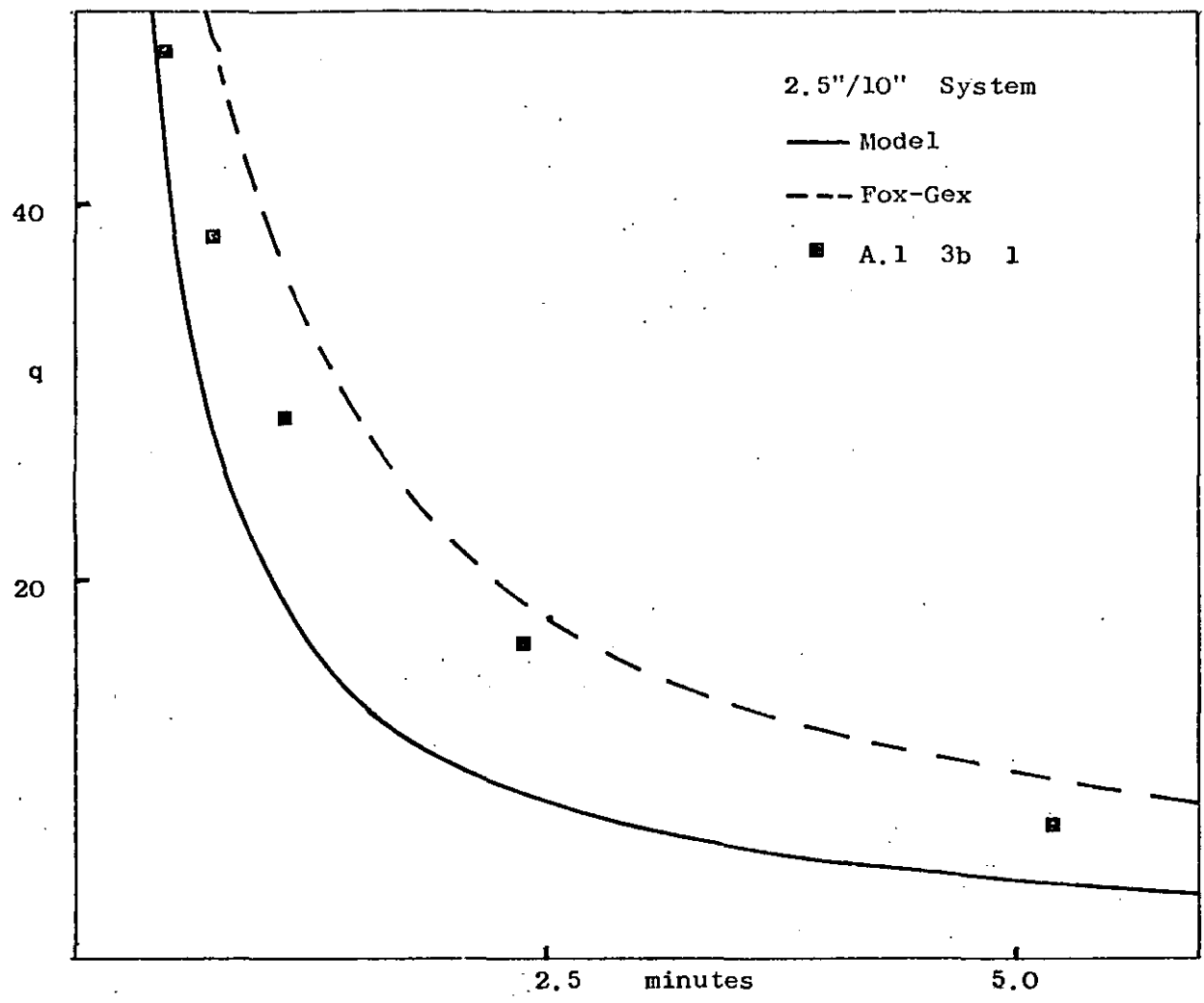

Fig. 7.90

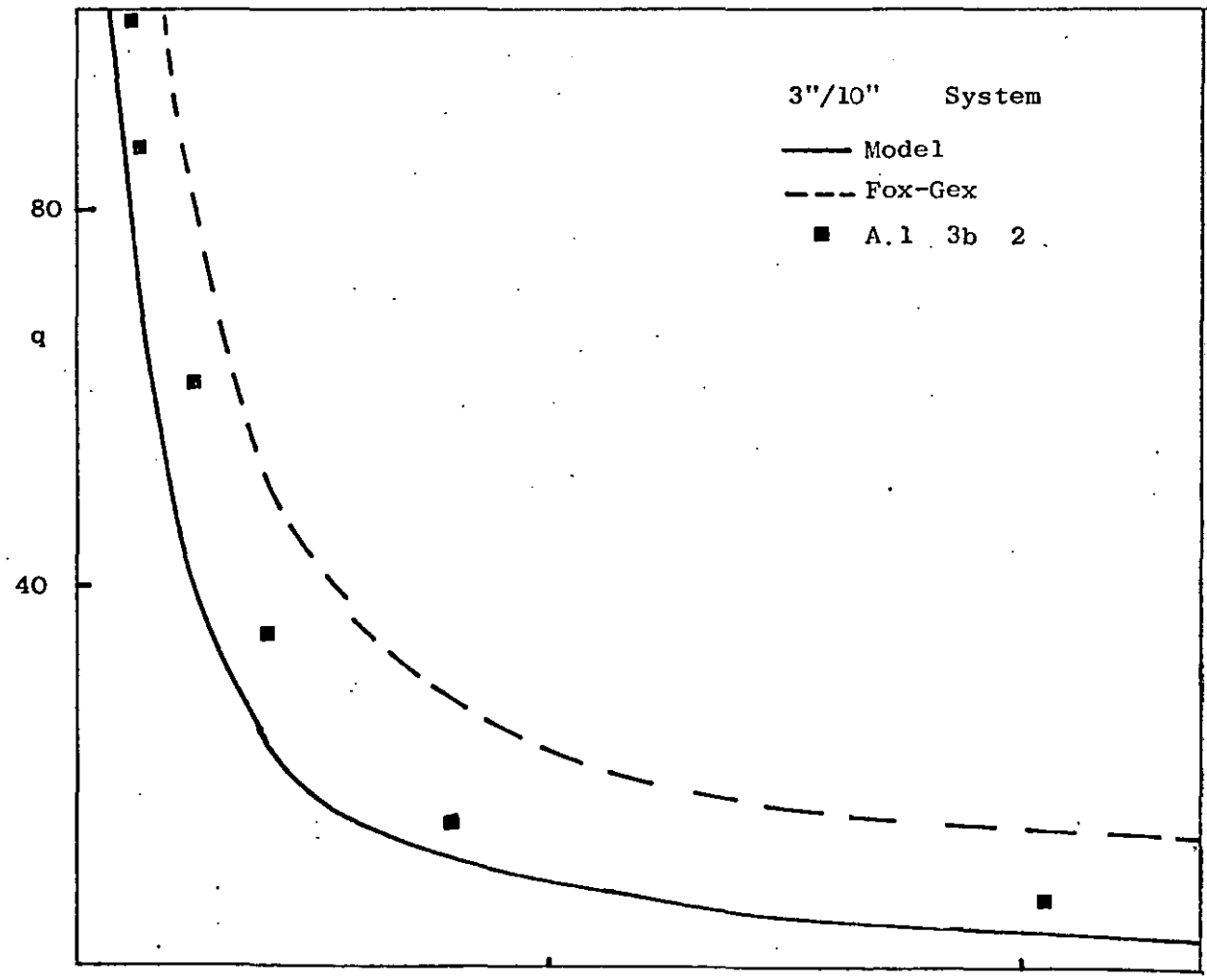

Fig. 7.91

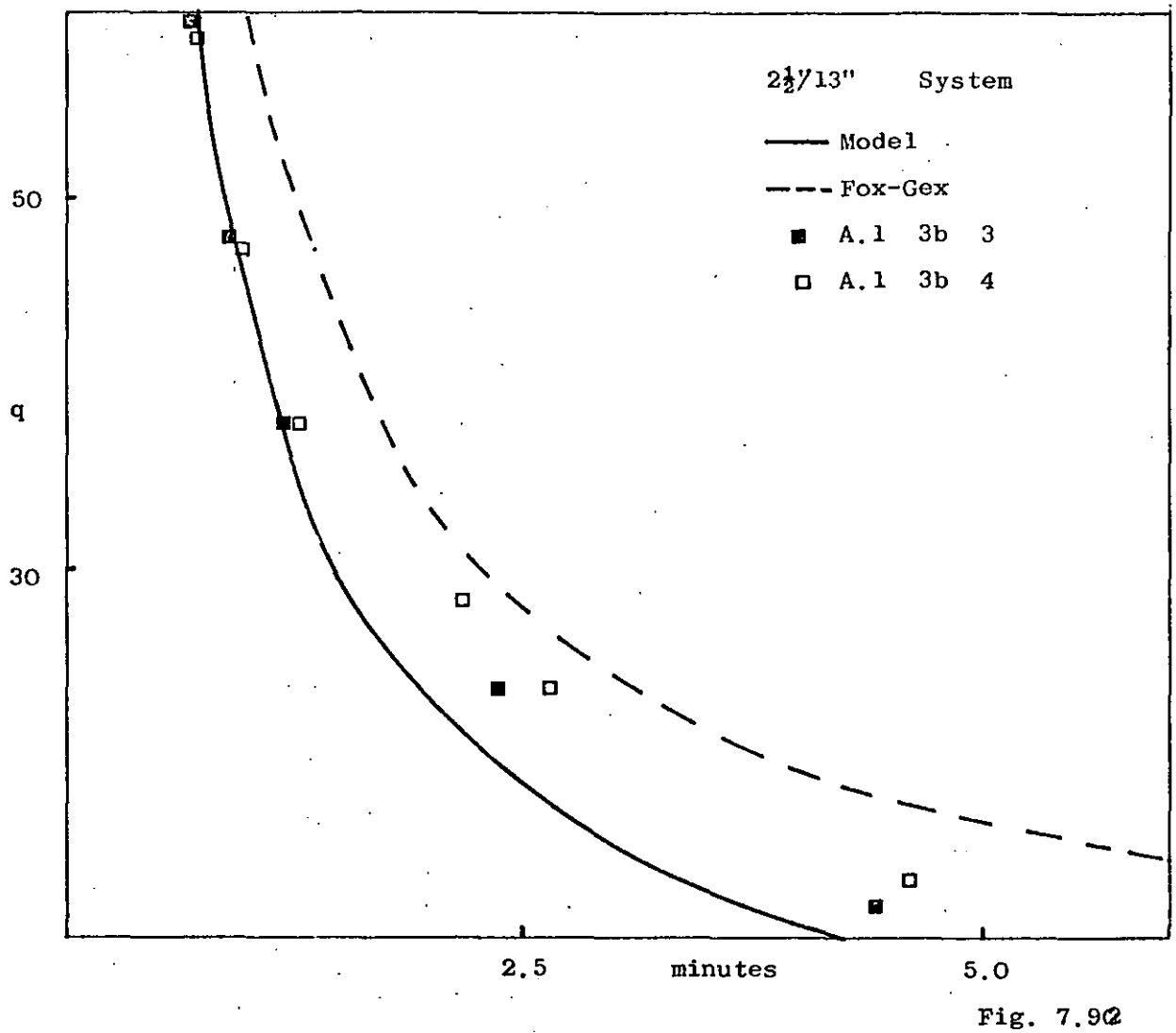

Fig. 7.92

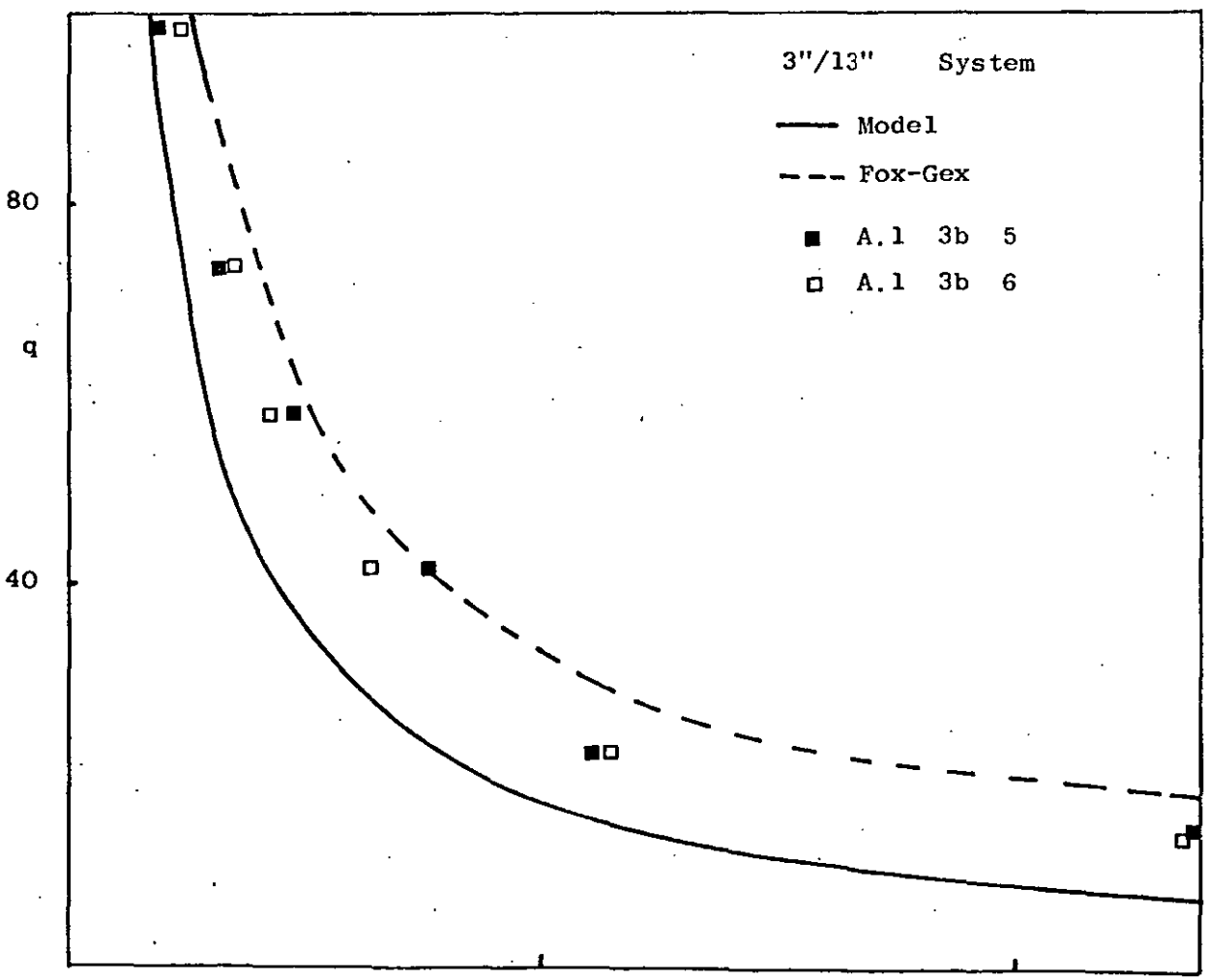

Fig. 7.93

dependent on the value of (δ), the homogenity level adopted. The solutions could be further justified if this level could be measured experimentally rather than relying on a visual judgment.

7.7. Relationship of Batch Mixing Time with Impeller Speed

The experimental batch mixing times of both the turbine and propeller agitated systems were found to be inversely proportional to the impeller speed. This is in agreement with the expression, equation5.4, derived in Chapter 5. Figure 7.94 shows typical plots of experimental results against the reciprocal impeller speed.

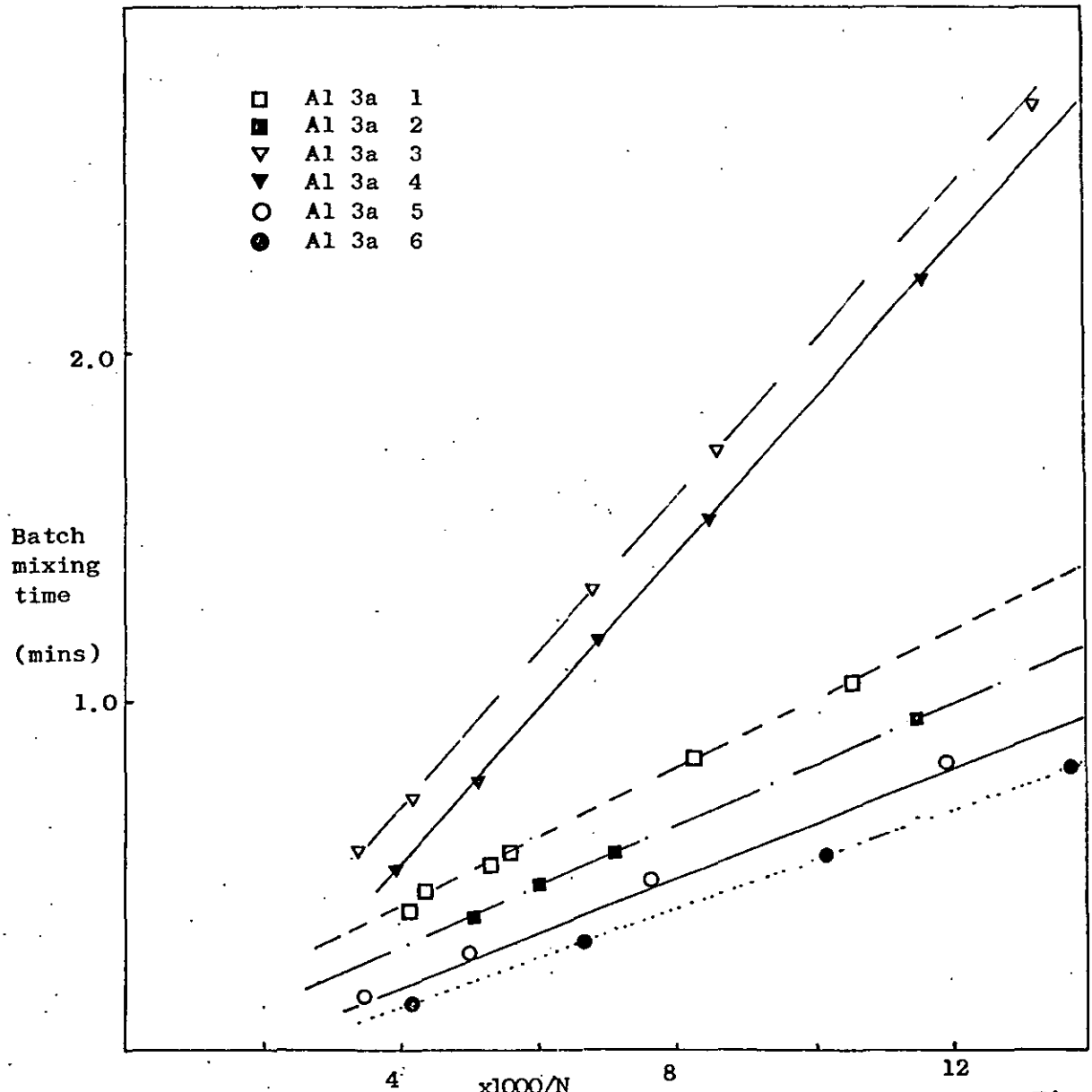

Fig. 7.94

8. ASSESSMENT OF SCALE-UP CRITERIA

8.1. A Dynamic Scale-Up Rule for Continuous Systems

A continuous blender mixes materials which enter over a period of time, so that the extent of product composition variation may be assessed from the residence time distribution. One way in which process characteristics may be matched is to preserve the same residence time distribution in the scale-up procedure. This apparently restrictive criteria leads to a useful design method in terms of a parameter based on the flows in the system.

As the predictions of the double loop and single loop models have been shown to match experimental results for a wide range of vessel diameters and operating conditions, the use of constant (q/Q), the ratio of impeller pumping capacity to vessel throughput, as a scale-up rule is justified. Scale-up of the impeller variable using this criterion would be accompanied by the assurance that the laboratory and pilot plant vessels would have identical normalised residence time distributions. Models based on the circulation loop concept have (q/Q) as the parameter, and thus it follows that scale-up on this basis should have a wide application.

In this chapter normalised residence time distribution curves of laboratory and pilot plant vessels are compared, after having scaled the impeller variable by the batch criteria discussed in Chapter 3. The pilot plant responses are computed using the single loop model.

8.2. Assessment of Scale-Up Criteria for Continuous Systems

The following batch scale-up criteria were assessed for scale-up of continuous blenders, Reynolds Number, tip speed, pumping capacity, recirculation time, mixing time and power per unit volume.

The assessment was made under various conditions:

i) Experimental conditions.

Using the ($2\frac{1}{2}$"/9") system as the laboratory vessel and the (4"/19") system for the pilot plant, the value of the stirrer variable was calculated for the same experimental operating conditions as those stated in Chapter 7. After having calculated the 4" diameter impeller speed to satisfy each scale-up, the pumping capacity was then obtained using the equations discussed in Chapter 7. The ratio of impeller pumping capacity to flow rate was then found. The normalised response for this value was then computed for the single loop model with the programme described in Appendix 3.

Figures 8.1 - 8.2 illustrate typical responses for the above conditions. The difference in normalised residence time distributions is apparent throughout the range of (q/Q) studied.

ii) Scale-up for scale ratio L and constant meantime.

Assuming complete geometric similarity and constant meantime in the laboratory and pilot plant vessels, the variation in residence time distributions for different scale-up ratios was investigated. Figures 8.3 - 8.6 illustrate the difference in predicted residence time distributions for a scale-up ratio of 2; Figures 8.7 - 8.10 for a scale-up ratio of 4 and Figures 8.11 - 8.14 for a scale-up ratio of 10. With the exception of scale-up using circulation time, it can be seen from the figures that scale-up using batch criteria will produce a marked difference between the residence time distribution of the laboratory vessel and pilot plant system; the deviation becoming more pronounced as the scale-up ratio is increased.

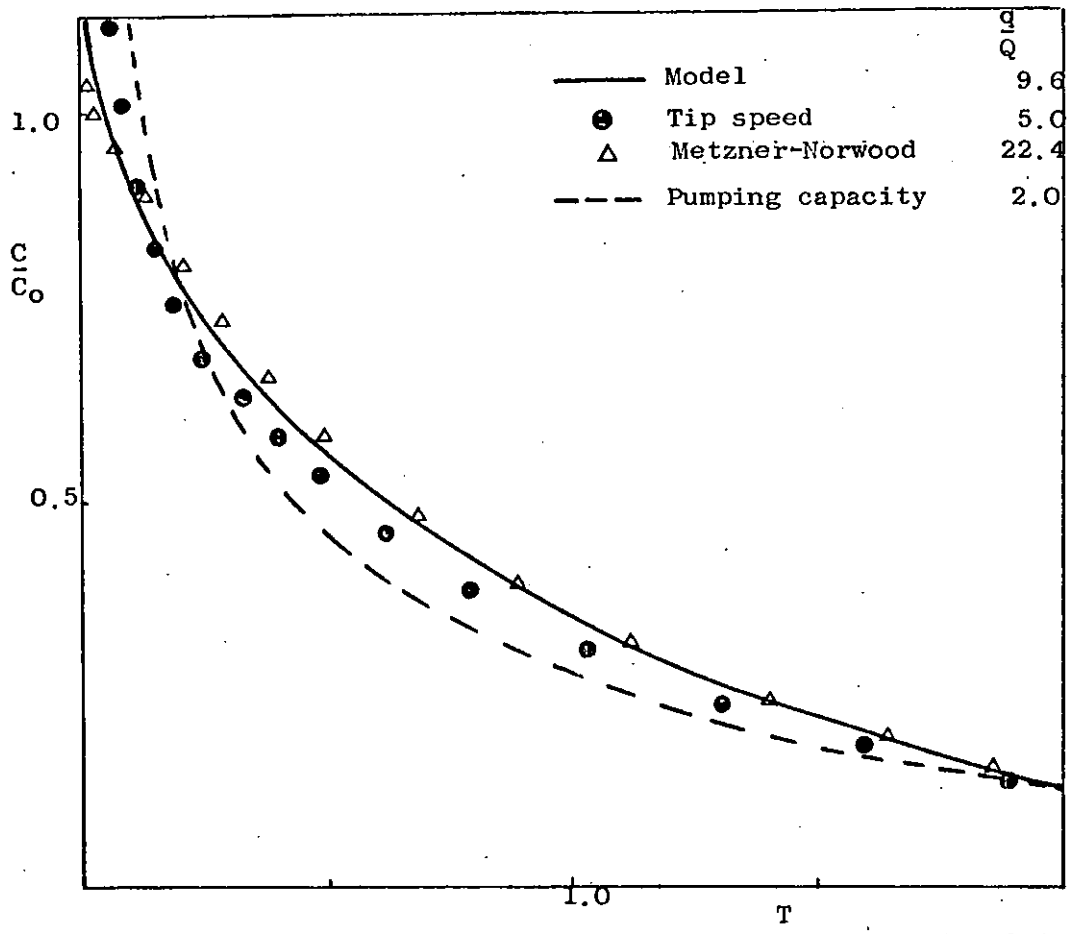
q/Q
Model 9.6
Tip speed 5.0
Metzner-Norwood 22.4
Pumping capacity 2.0
1.0
C/Co
0.5
1.0
T

Fig. 8.1

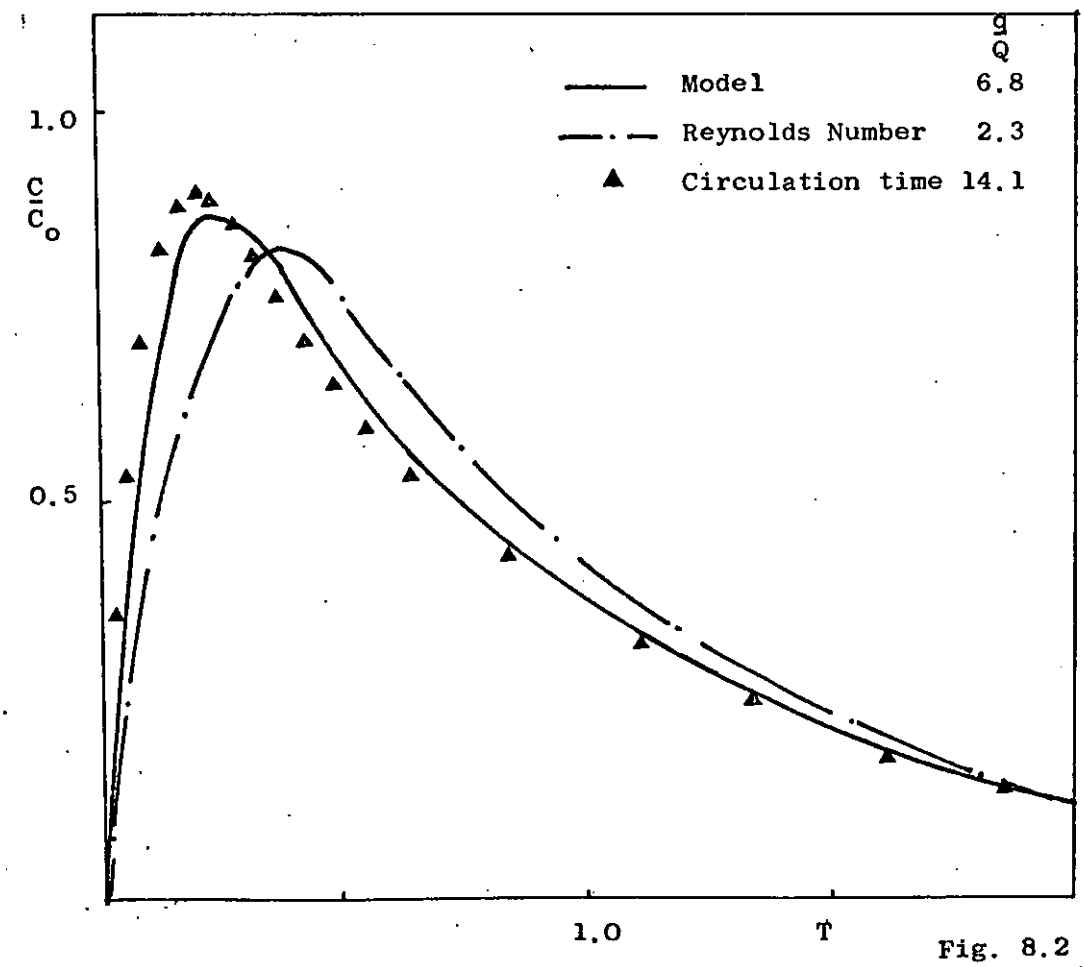
q/Q
Model 6.8
Reynolds Number 2.3
Circulation time 14.1
1.0
C/Co
0.5
1.0
T

Fig. 8.2

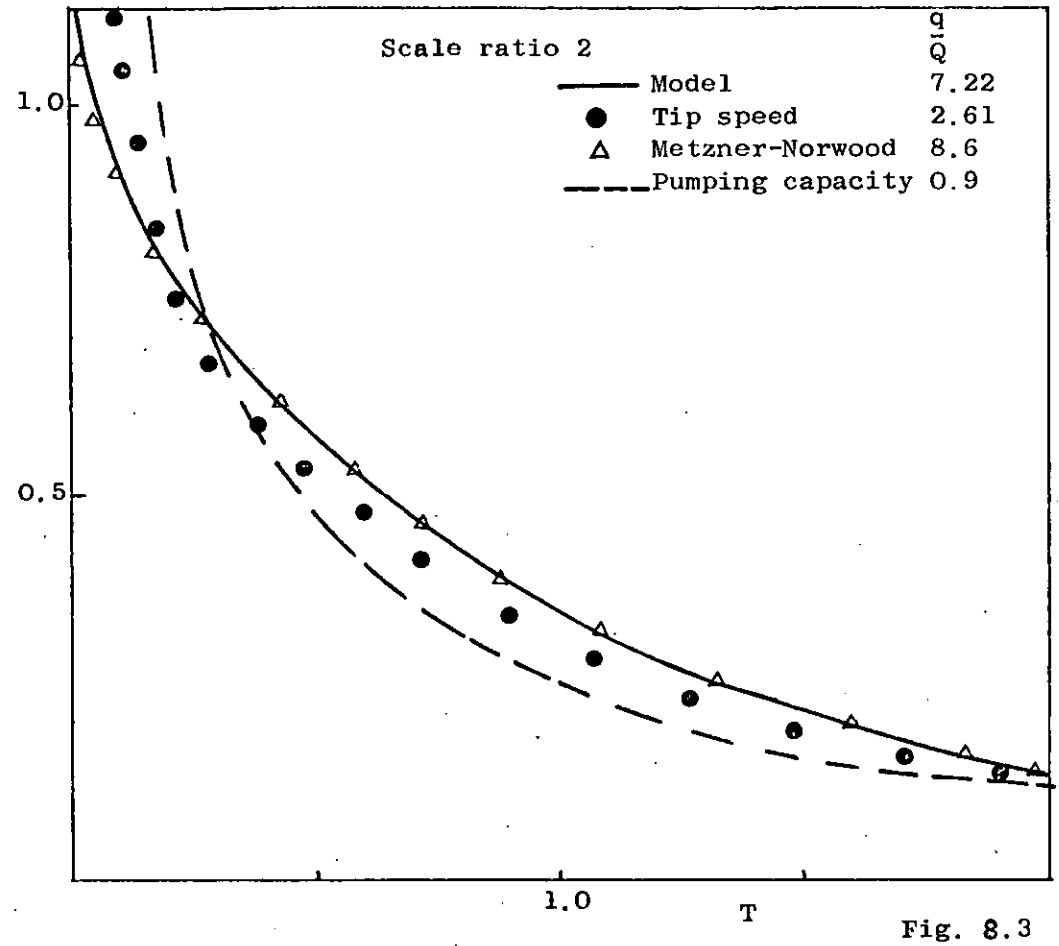
Scale ratio 2
q/Q
Model 7.22
Tip speed 2.61
Metzner-Norwood 8.6
Pumping capacity 0.9
1.0
0.5
1.0
T

Fig. 8.3

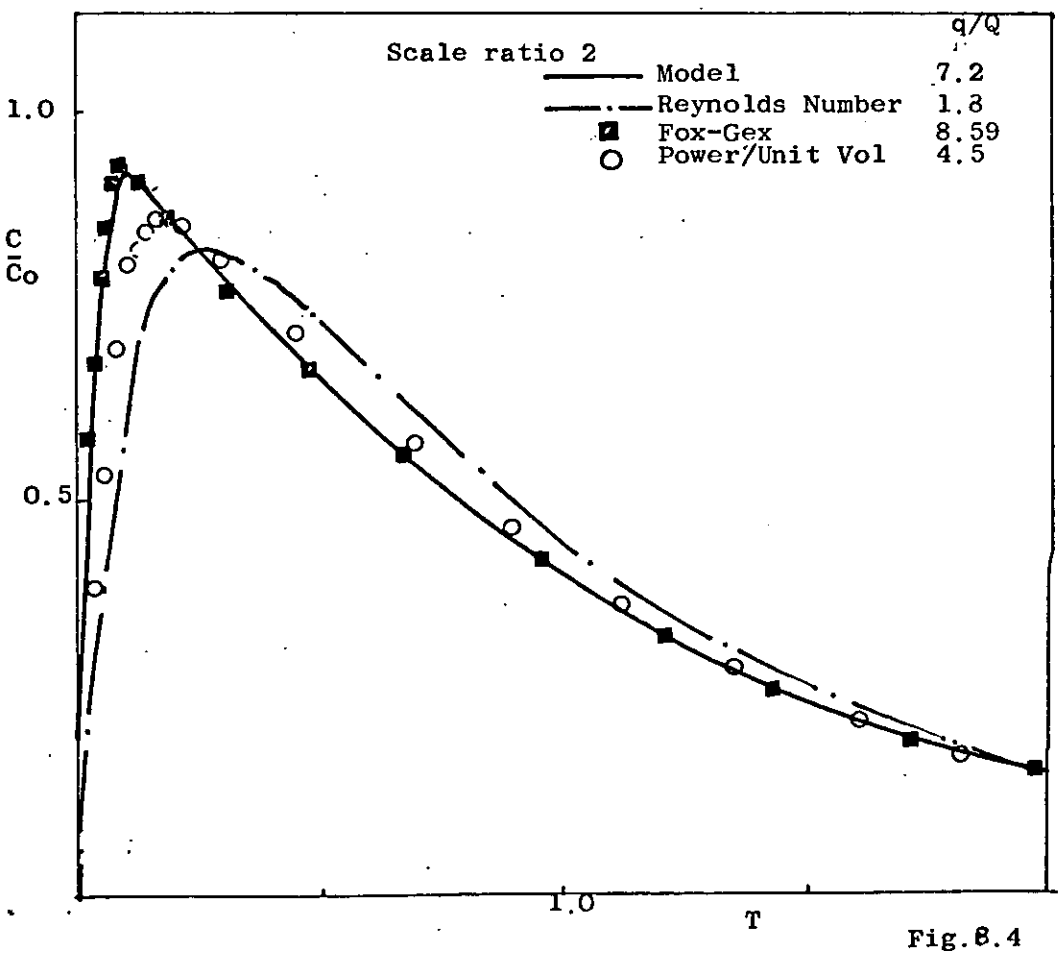
Scale ratio 2
q/Q
Model 7.2
Reynolds Number 1.8
Fox-Gex 8.59
Power/Unit Vol 4.5
1.0
C/Co
0.5
1.0
T

Fig. 8.4

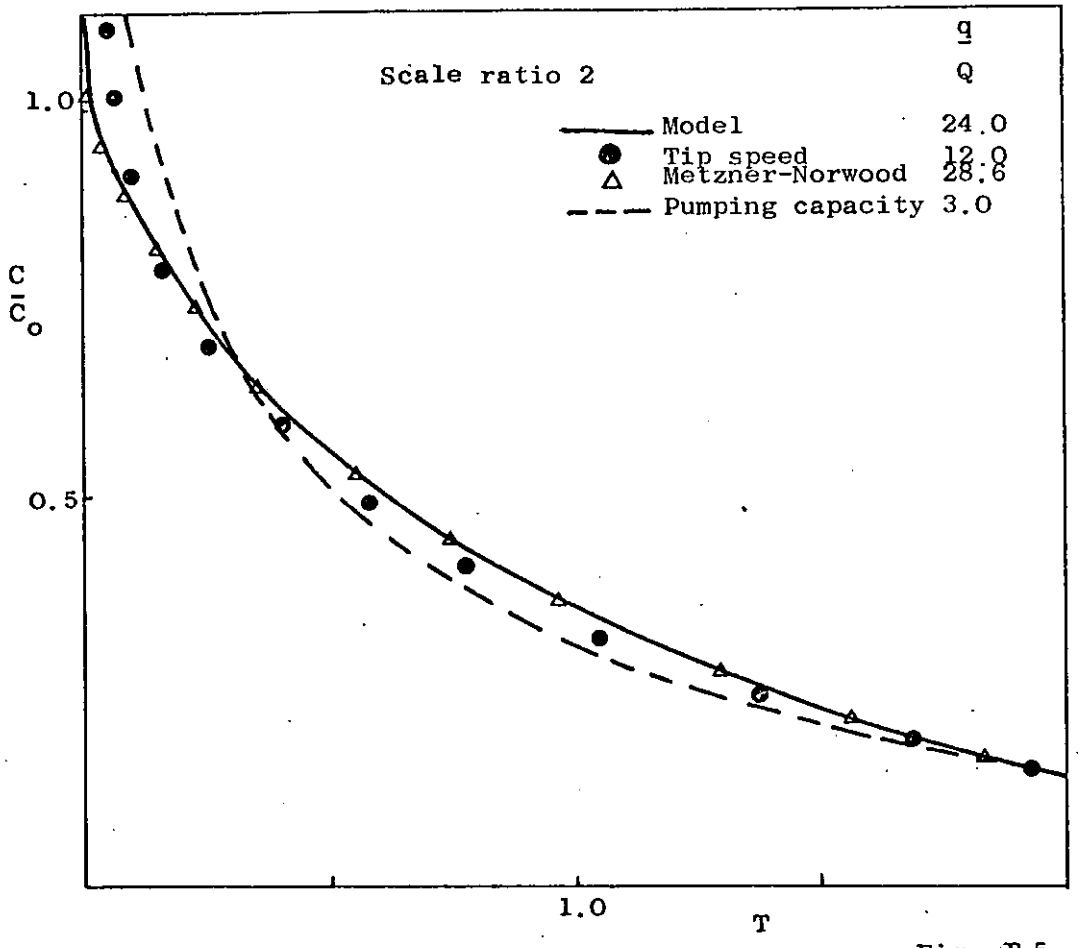
Scale ratio 2
q/Q
Model 24.0
Tip speed 12.0
Metzner-Norwood 28.6
Pumping capacity 3.0
C/C_o
1.0
0.5
1.0
T

Fig. 5

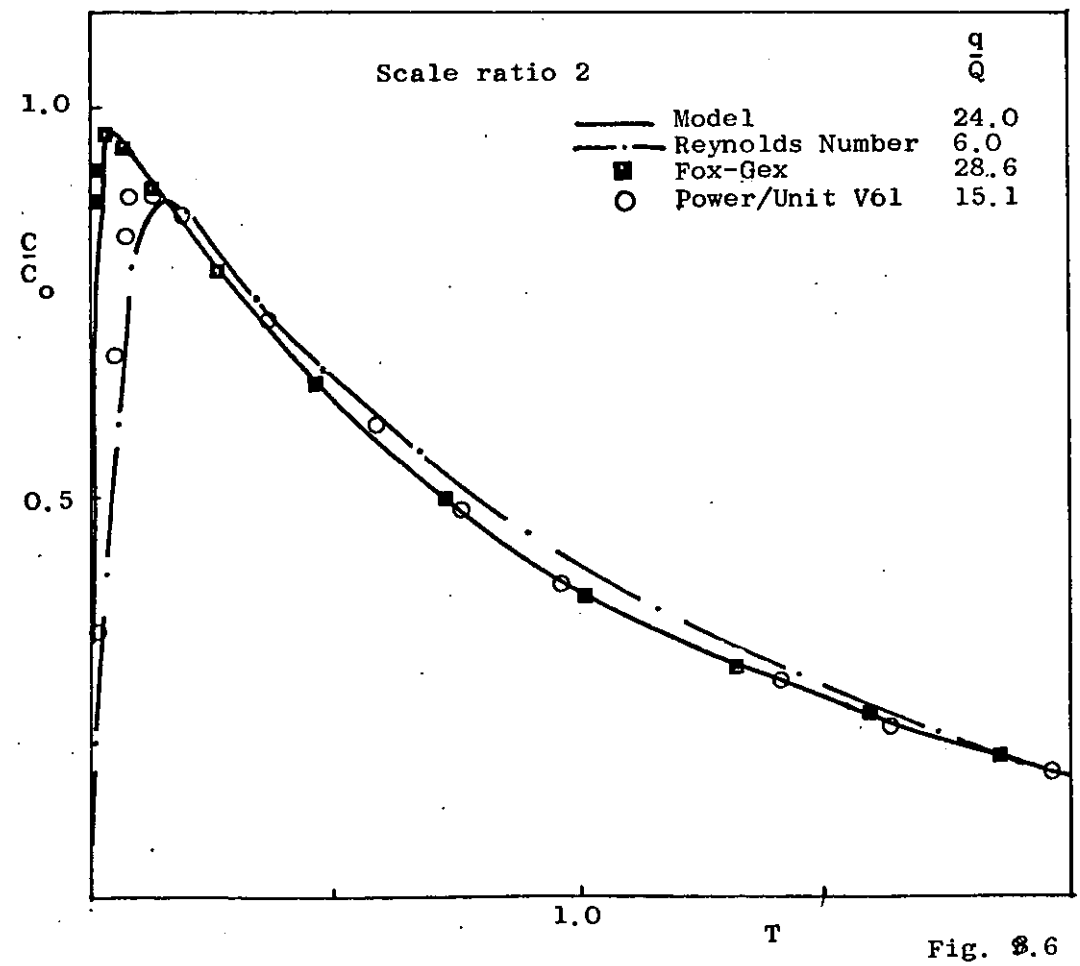
Scale ratio 2
q/Q
Model 24.0
Reynolds Number 6.0
Fox-Gex 28.6
Power/Unit V61 15.1
C/C_o
1.0
0.5
1.0
T

Fig. 6

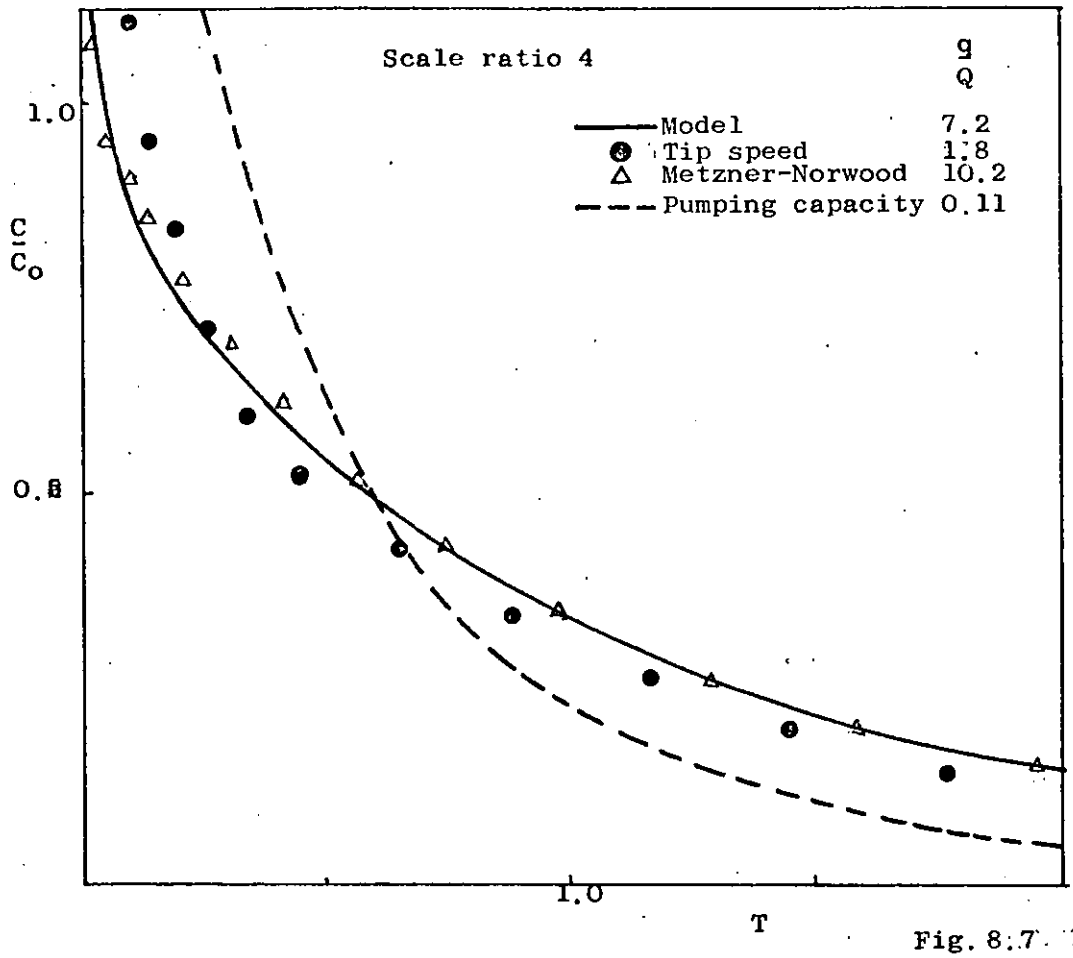
Scale ratio 4
q/Q
Model 7.2
Tip speed 1.8
Metzner-Norwood 10.2
Pumping capacity 0.11
1.0
C/Co
0.8
1.0
T

Fig. 8.7

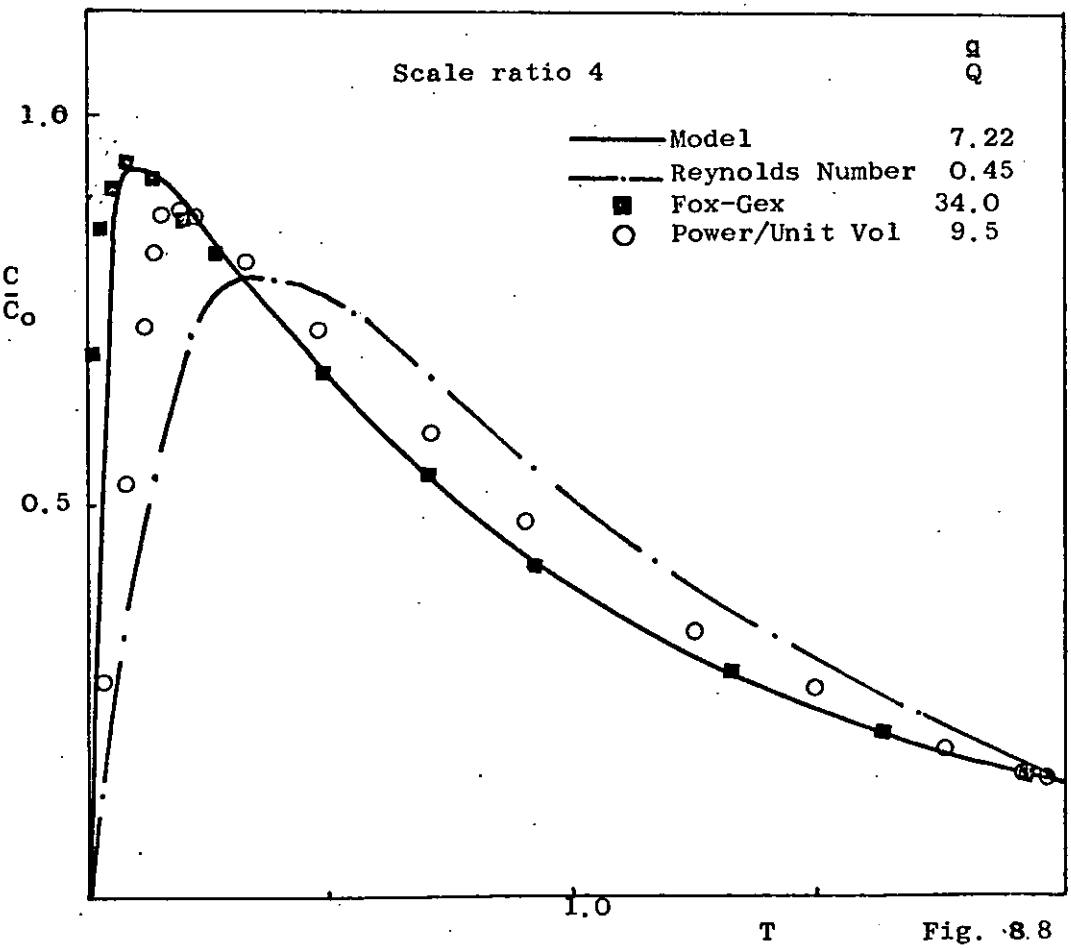
Scale ratio 4
q/Q
Model 7.22
Reynolds Number 0.45
Fox-Gex 34.0
Power/Unit Vol 9.5
1.0
C/Co
0.5
1.0
T

Fig. 8.8

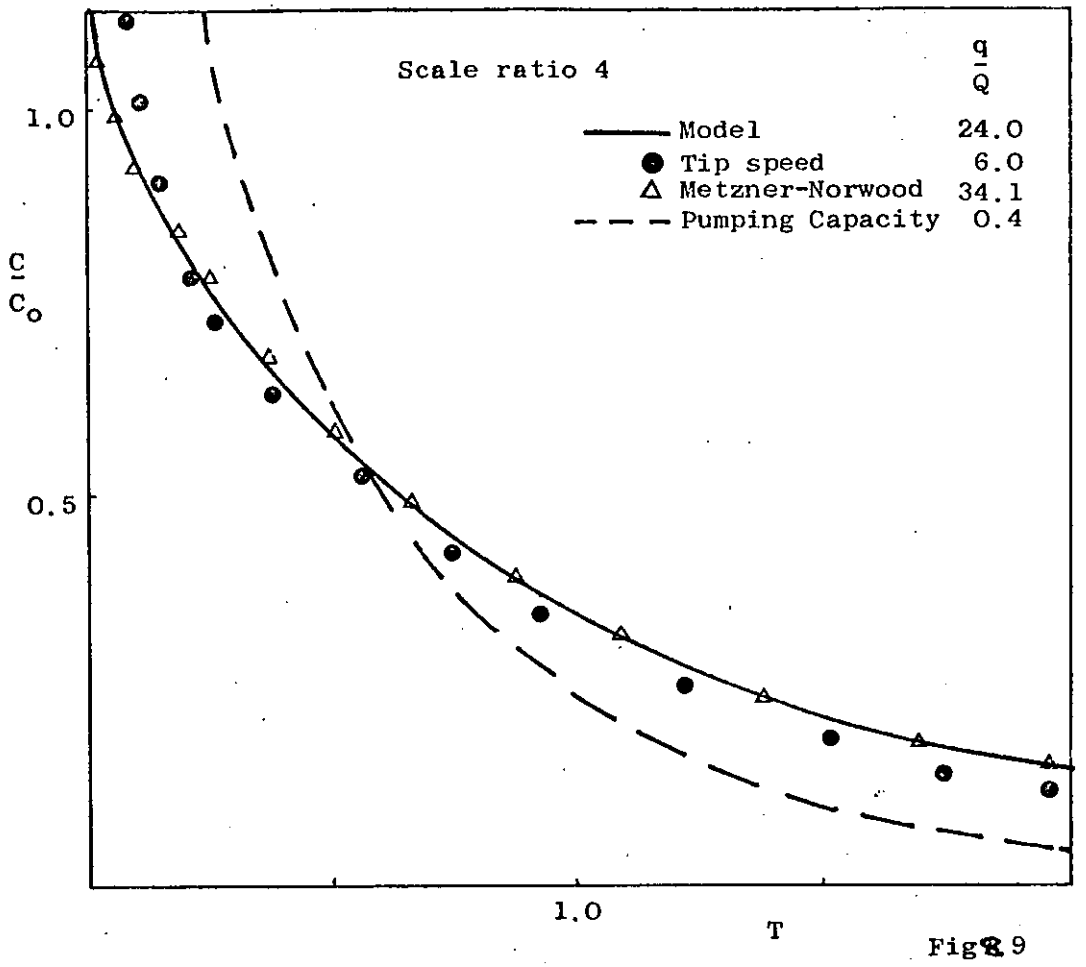
Scale ratio 4
q/Q
Model 24.0
Tip speed 6.0
Metzner-Norwood 34.1
Pumping Capacity 0.4
C/Co
1.0
0.5
1.0
T

Fig. 9

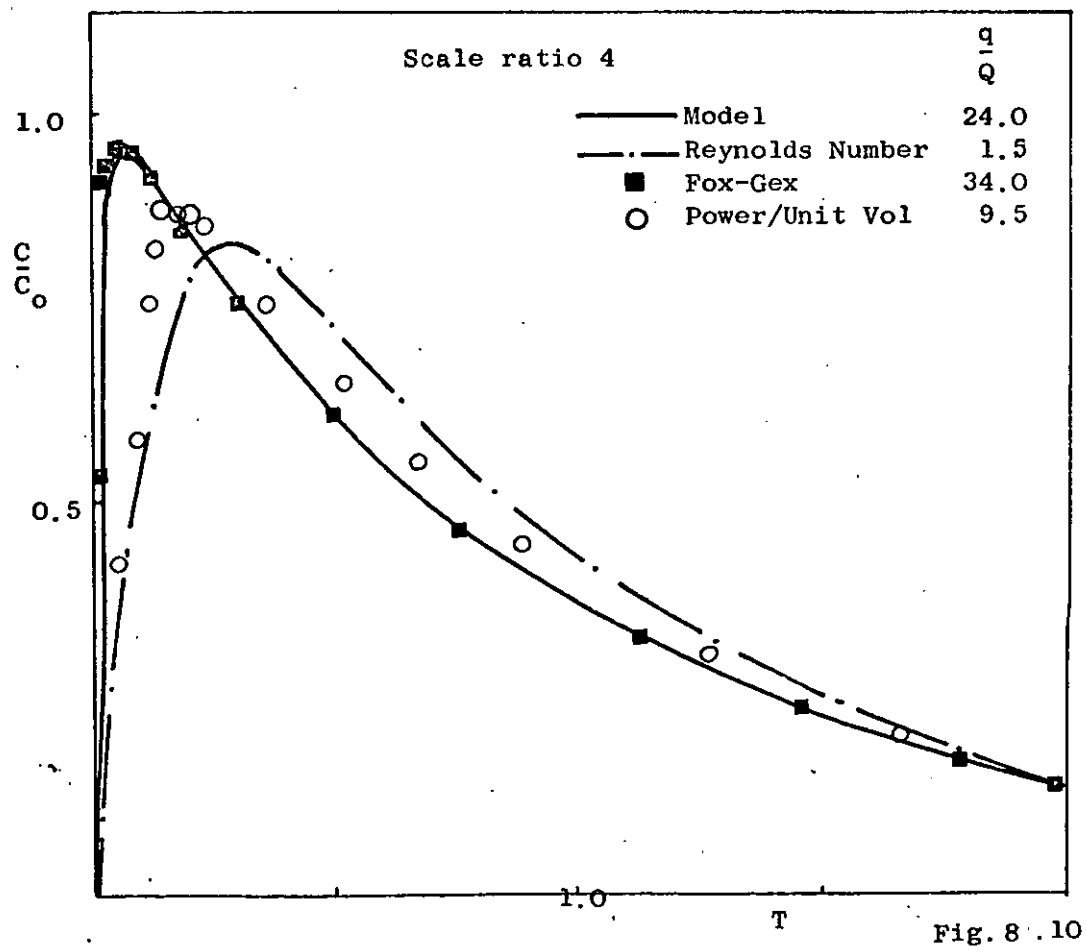
Scale ratio 4
q/Q
Model 24.0
Reynolds Number 1.5
Fox-Gex 34.0
Power/Unit Vol 9.5
C/Co
1.0
0.5
1.0
T

Fig. 8 .10

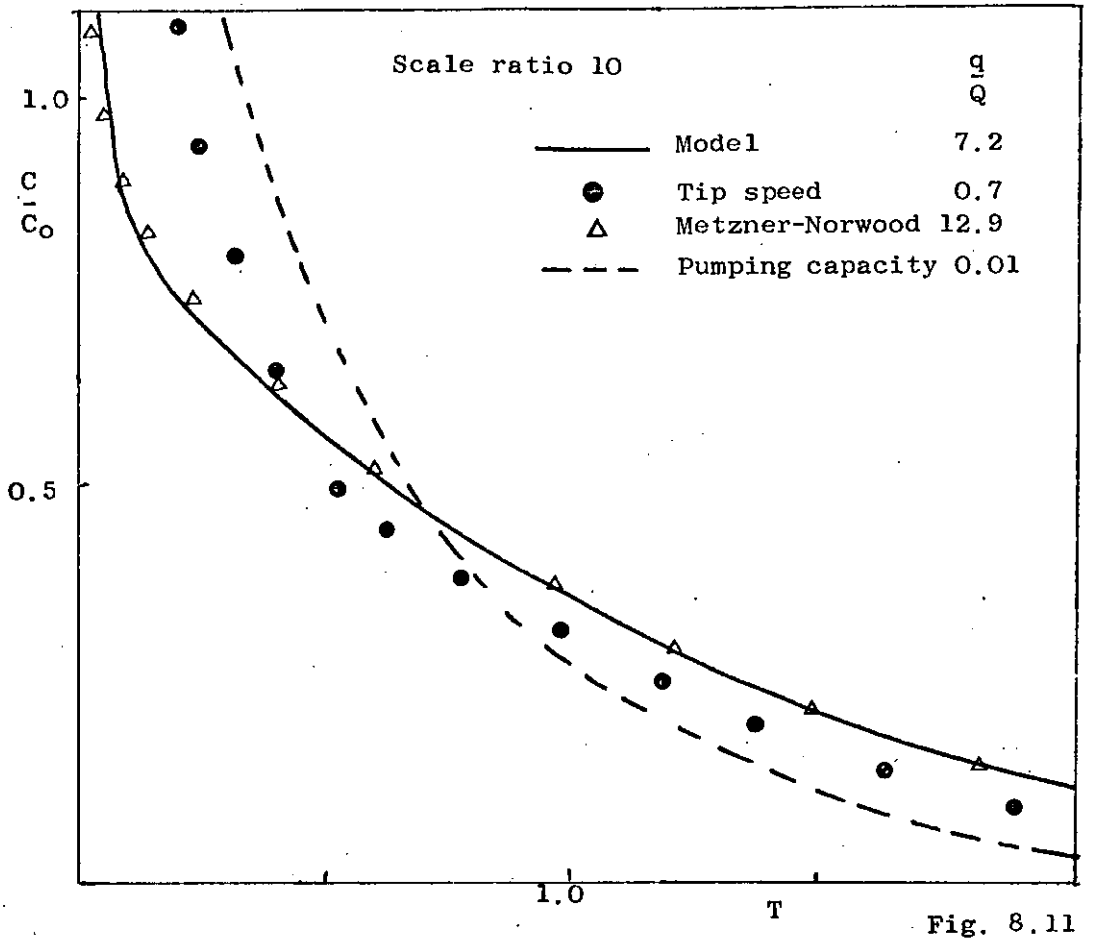

Fig. 8.11

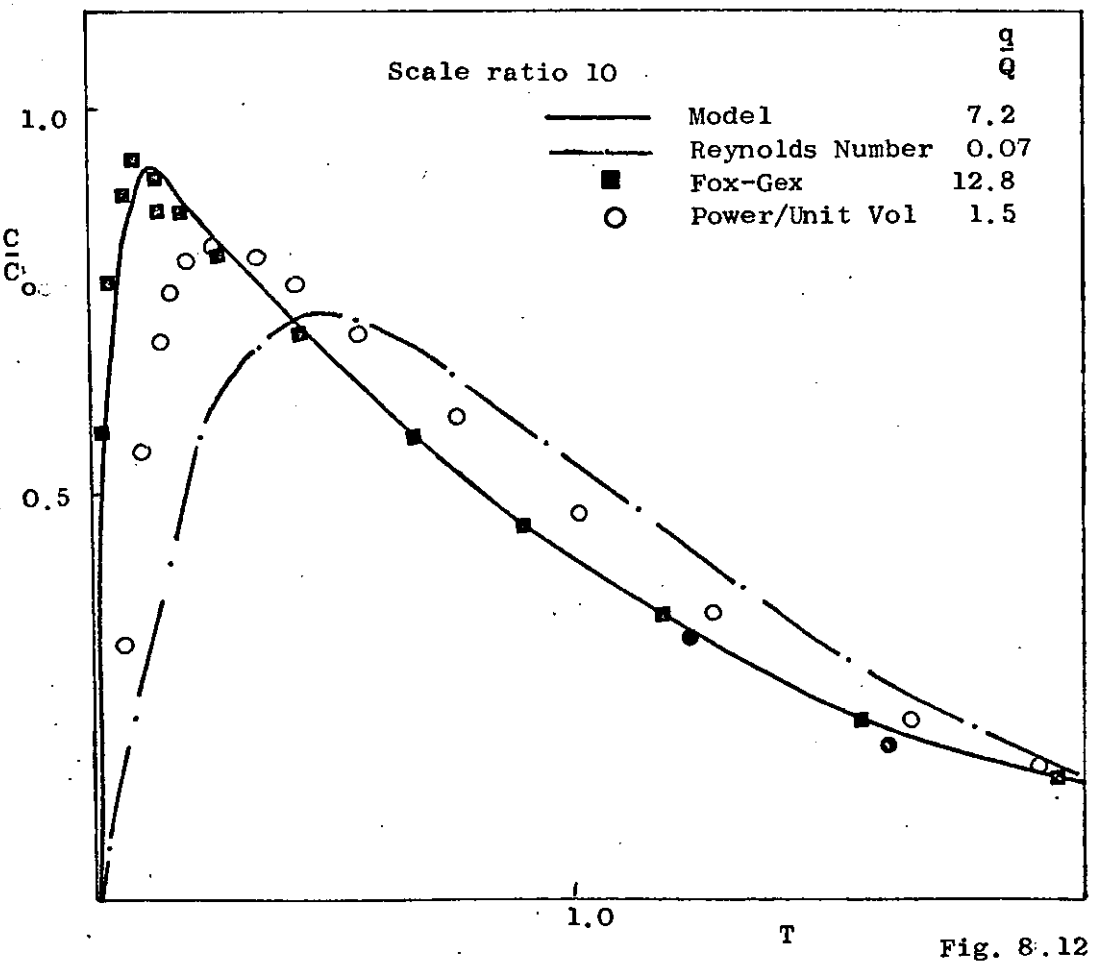

Fig. 8.12

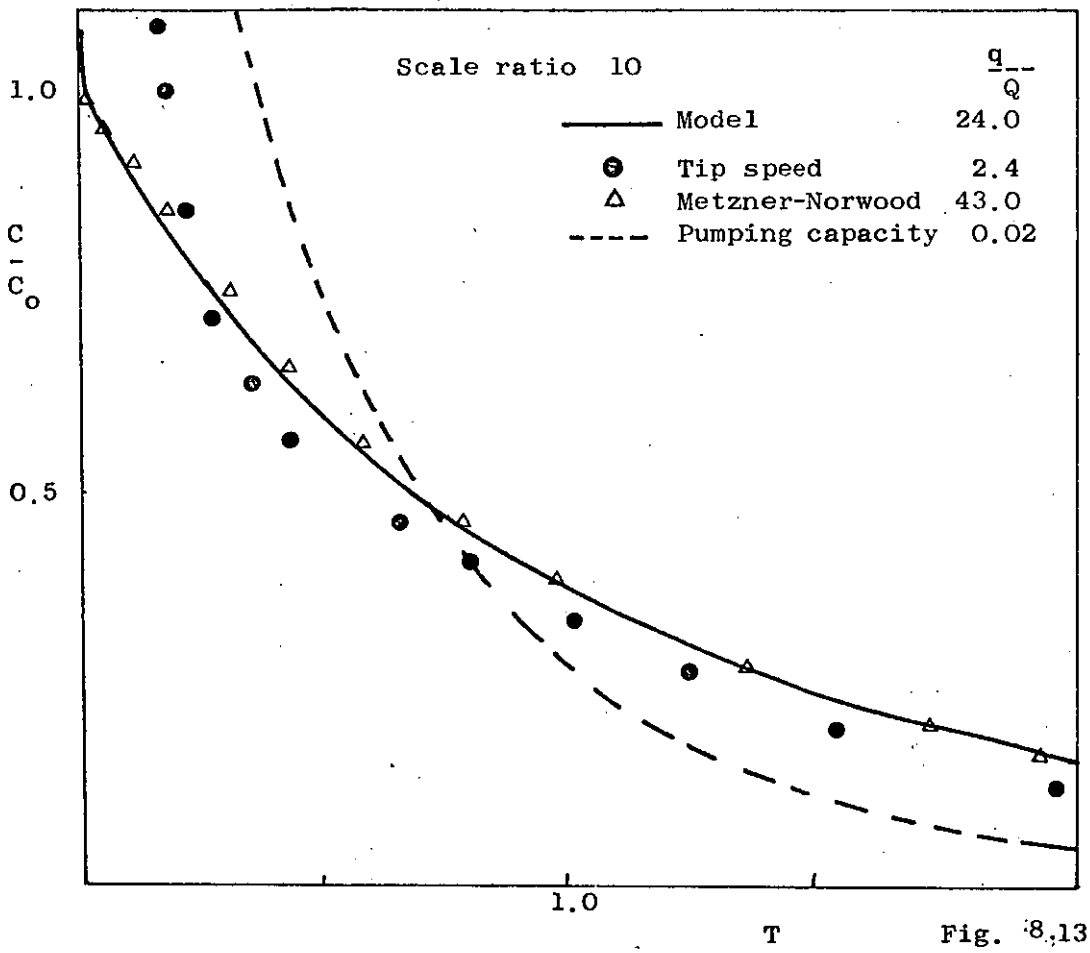

Fig. 8.13

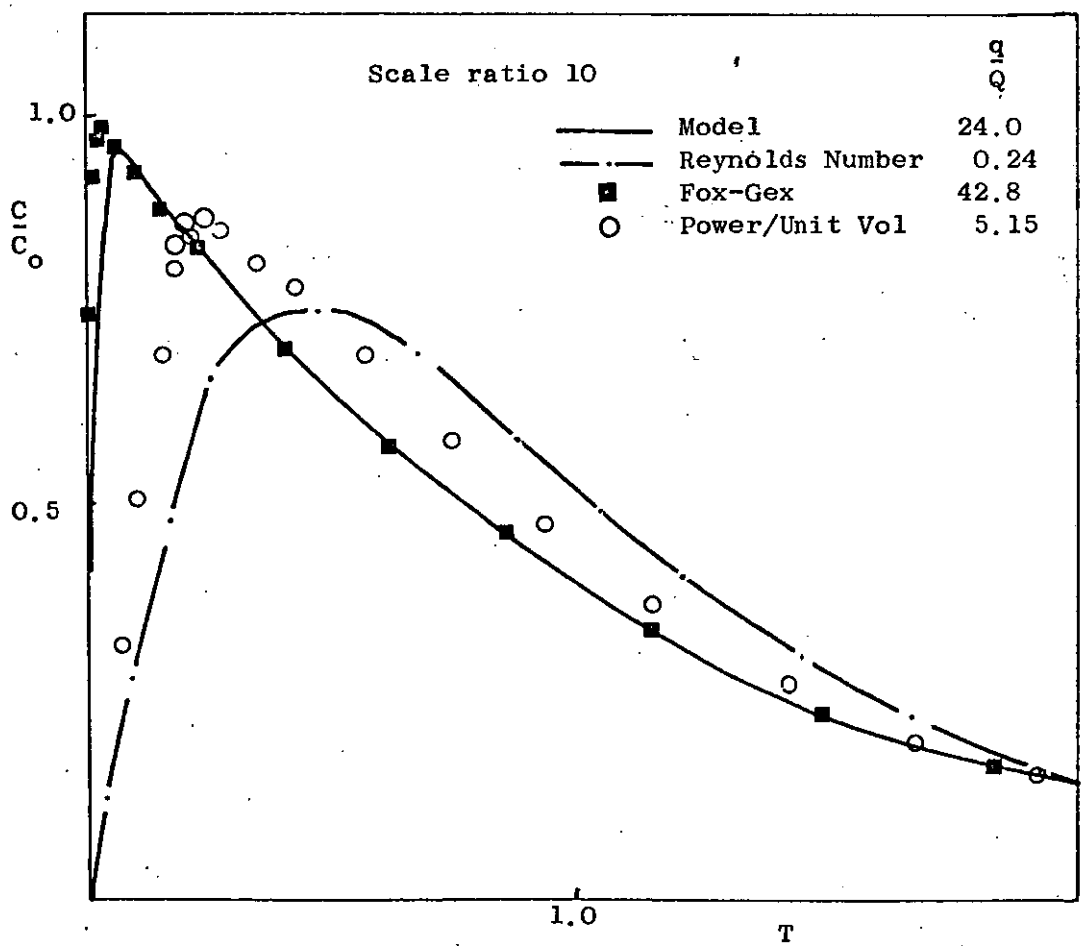

Fig. 8.14

The meantime of the scaled system was twice that of the smaller vessel for the responses shown in Figures 8.1, 8.2. Thus the deviation is correspondingly less marked than for the case using constant meantime. Geometric similarity was also not observed; length ratio 2:1, impeller diameter ratio 1.6:1. The effect of these factors is to further mask the difference in responses predicted by the following scale-up relationships. An indication of the difference between the unscaled residence time distribution and the corresponding scaled residence time distribution is described by the relationship of $(q/Q)_E$, the unscaled value, and $(q/Q)_S$, the scaled value of the model parameter. The following relationships are derived for geometrically similar systems, having the same meantime and a length scale-ratio of L.

Reynolds Number:- $(q/Q)_S = (q/Q)_E \cdot \frac{1}{L^2}$

Tip Speed:- $(q/Q)_S = (q/Q)_E \cdot \frac{1}{L}$

Pumping Capacity:- $(q/Q)_S = (q/Q)_E \cdot \frac{1}{L^3}$

Circulation Time:- $(q/Q)_S = (q/Q)_E \cdot \frac{1}{1}$

Mixing Time:-

Metzner-Norwood $(q/Q)_S = (q/Q)_E \cdot L^{1/8}$, $N_{Re} > 10^5$

Fox-Gex $(q/Q)_S = (q/Q)_E \cdot L^{1/4}$, $N_{Re} > 10^5$

van de Vusse $(q/Q)_S = (q/Q)_E \cdot L^{-1/6}$, $N_{Re} > 10^5$

Equation 5.4 $(q/Q)_S = (q/Q)_E \cdot 1$

Power/ Unit volume $(q/Q)_S = (q/Q)_E \cdot L^{-2/3}$, $N_{Re} > 10^5$

These relationships show that scale-up of a continuous system with Reynolds Number, tip speed, pumping capacity or power per unit volume will always produce a value of (q/Q)s which is less than the desired value to ensure identical residence time distributions. Scale-up with constant mixing time, calculated from the mixing time groups, will result in larger values of (q/Q)s than required to preserve the same residence time distribution. Constant circulation time and constant mixing time calculated from equation 5.4, give the same value of (q/Q) in the scaled and unscaled vessels and consequently identical residence time distributions.

If the value of (q/Q)s, calculated from the batch scale-up rules, is less than the experimental value, for the case of feed to the impeller, a greater degree of bypassing will result, this is shown in the initial section of the residence time distribution. For feed directed towards the loop region, the bulk of the fluid will reside longer in the vessel, due to the decrease in circulatory flow.

If the value of (q/Q)s is greater than the experimental value, i.e. scale-up using constant mixing time derived from the mixing time groups, greater circulation is available in the vessel. This reduces the bypassing effect for feed to the impeller, and distributes the elements of fluid more evenly for feed to loop.

As Reynolds Number and tip speed have only an indirect relationship with the mixing action of the fluid inside the vessel, it is not surprising that scale-up using these two as criteria should fall down in the continuous case. Likewise this discrepancy, between the process result of the laboratory and scaled vessels for these criteria, would also appear in the batch case.

The figures which show constant pumping capacity scale-up give the greatest difference between unscaled and scaled residence time distributions; constant pumping capacity scale-up should therefore not be attempted. Only if the throughput of the larger system is much smaller than the laboratory system should this criterion be used. As this seldom occurs practically, (the meantime of the larger system would be much greater than that of the smaller system), this scale-up rule has very little application.

Scale-up using either constant mixing time (equation 5.4) or constant circulation time, takes into consideration the fluid flow paths within the vessel. It would therefore be expected that scale-up using these criteria should give a closer comparison, between the laboratory and pilot plant residence time distributions than the previous rules.

The scale-up rules derived from the mixing time groups are only valid for $N_{Re} > 10^5$. For these figures the limits of their application has been extended to accommodate smaller Reynolds Numbers. As scale-up at constant mixing time has been proved to be identical with scale-up at constant circulation time, and both require scale-up with constant (q/Q), the use of the empirical mixing time groups for scale-up appears to be limited.

Scale-up using constant (q/Q) always ensures identical normalised residence time distributions. If the further restriction of constant system meantime is introduced, it will guarantee the same residence time distribution. Thus complicated reactions with involved kinetic problems could be overcome with this scale-up rule.

For systems of different meantime, responses have different time scales but normalisation of these responses will give identical response curves for the same (q/Q).

This new dynamic scale-up rule (q/Q) not only takes into account impeller characteristics and hence circulatory flow patterns but also the volumetric throughput of the system. This brings greater flexibility and a more sound foundation to the scale-up of continuous systems.

As the loop circulation concept has been adapted to a batch system, with the model parameter reducing to the pumping capacity; it follows from the above discussion that scale-up using constant circulation time would be most useful for this case.

9. DISCUSSION

9.1 Introduction

The introduction of the multiloop circulation models was an attempt to present an analogy between the model configuration and the paths taken by elements within the agitated fluid, i.e. the streamlines. If angular symmetry is assumed, it is readily seen that a reduction in the number of loops can be made when the information is based on input and output data only; the number of loops in the final model configuration being dependent on the degree of dissymmetry in the system. The operating conditions impose the dissymmetry, and consequently dictate the extent to which the multiloop representation may be simplified. The final model configuration depends upon the extent of baffling, and the inlet and outlet position in the continuous case, and the initial injection position in the batch case.

In a vessel in which the streamlines are described by a single loop Figure 3.1(b), symmetry reduces the multiloop interpretation to a single loop model for all operating conditions, Figures 4.2 - 4.3. However in a vessel in which a double loop streamline pattern is observed, Figure 3.1(a), the multiloop representation reduces to either a single, two or three loop model depending on the operating conditions, Figures 4.5, 4.6, 4.7. The batch system exhibits greatest symmetry. If the initial impulse is injected into the impeller region the double loop streamline pattern can be simulated by a single loop configuration. This has been proved mathematically, equations, 5.15 - 5.18.

The models proposed by Gibilaro (26,27) were based on the assumption that a turbine agitator, positioned one-third of the liquid height from the base of the vessel, produced two definite vortices in the fluid, one above and one below the impeller. However,

photography has shown that, for this turbine position, the induced flow pattern is not clearly defined and that the streamline paths are equally well described by single circulation loops. The streamlines produced by the propeller have also been shown to be of a single loop nature, for every impeller position. After incorporating this feature into the multiloop approach, symmetry produces the two new single loop recirculation models.

The salient feature of this research is the verification of the modified versions of the single loop circulation model, for the characterisation of turbine and propeller agitated systems, over a wide range of operating conditions. The main improvement of these models over their double loop counterparts is that the model parameter, (the pumping capacity), is treated as a complete entity in the single loop models. Whereas the double loop models are partly dependent on the assumption that the pumping capacity of the impeller is split in a ratio equal to the volume of liquid above the impeller to that below it, in order to give equal circulation times in the upper and lower loops.

The single loop model may be alternatively interpreted in the following fashion. Figure 9.1(a) shows the original single loop model configuration proposed for feed to the impeller. Figure 9.1(b) illustrates the same model presented in a more conventional fashion; this can be further amended to Figure 9.1(c).

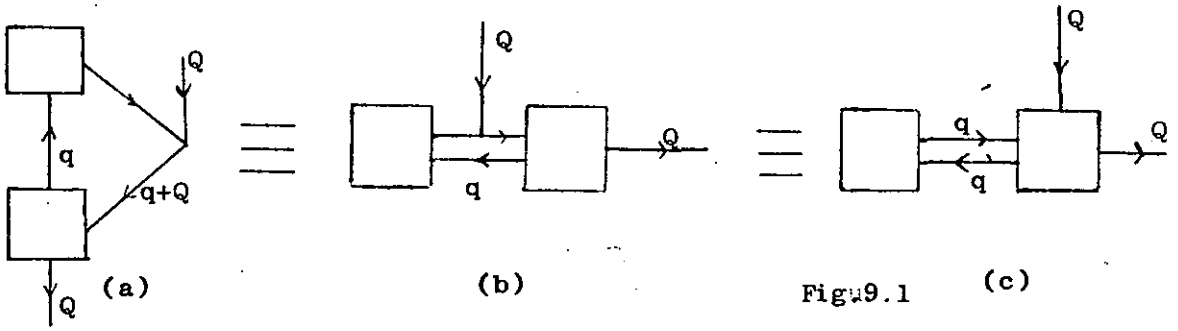

Fig 9.1

The analogy between the induced flow pattern and the model configuration is apparent in Figure 9.1(a), but quite hidden in Figures 9.1(b) and 9.1(c). The two stages in series with backflow

model of Figure 9.1(c) has been adopted by Levich et al (42) as the basis for the characterisation of flow through porous media. An alternative representation for the feed to loop region can be similarly derived, Figure 9.2(a) becoming Figure 9.2(b).

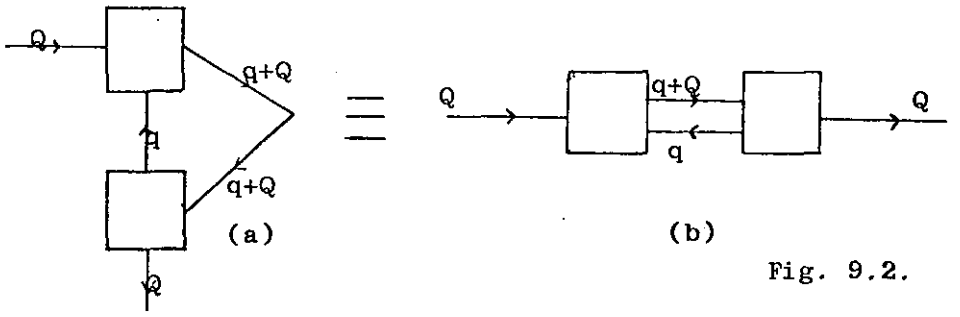

Fig. 9.2.

Figure 9.2(b) has received greater attention in past published work than its companion Figure 9.1(b). The two stages in series with back flow model has been the foundation of an abundance of research throughout the field of process dynamics.

9.2. Comparison of Single and Double Loop Models

The difference in predicted normalised residence time distribution responses of the two models is very small. For feed to the impeller the difference is marginal for all values of (q/Q): however for feed to the upper region the single loop model predictions always preceed the double loop model solutions. At low values of (q/Q) the distinction is quite marked but for (q/Q) greater than 25 the difference is again small.

In the following sections a further comparison is drawn between the two models by an investigation of their predicted steady state conversions, an analysis of the variance of the distribution and a comparison of intensity function distributions.

9.2.1. Steady state conversion for a first order reaction

The steady state conversion of a first order reaction may be predicted from the single loop and double loop transfer functions.

The ratio of the outlet transform to the inlet transform has been obtained for both models from a series of dynamic mass balances over each stage in the respective networks. It can easily be shown that the Laplace transform variable (s) can be replaced by the rate constant (k) for a first order reaction. Hence the ratio of Laplace transformed outlet/inlet concentration becomes, on substitution of (k) for (s), the ratio of actual outlet concentration to inlet concentration.

$$\frac{CA}{CA_0} = \int_0^\infty e^{-k_1 t} f(t) = \underset{s=k_1}{G(s)} = \int_0^\infty e^{-st} f(t)\, dt = \frac{\bar{C}o(s)}{\bar{C}i(s)}$$

For the normalised case of the ideal vessel the percentage conversion is:-

$$\frac{Ci-Co}{Ci} = R = \left(1 - \frac{1}{k+1}\right)100$$

Using a value of k = 3 for the rate constant, the steady state conversion for an ideal reactor is 75%. This value of k will now be used to obtain conversions for the single loop and the double loop model, for a range of the model parameter. The predicted percentage conversion for the single loop model is derived from equation 4.1 for the case of inflow to the impeller, Figure 4.2.

$$R = 100\left(1 - \frac{Q}{vk+q+Q - \dfrac{q^2}{vk+q}}\right)$$

For the same condition the double loop model (Figure 4.5), equation 4.5 reduces to:-

$$R = 100\left(1 + \frac{Q}{\dfrac{r^2}{r+vk} + \dfrac{2r^3(r+vk+Q)}{(r+vk)^2(Q+r)} - \dfrac{Q+3r(r+vk+Q)}{Q+r}}\right)$$

The effect of model parameter on the conversion for the two models is shown in Figure 9.3. At low impeller speeds the conversion for both models is below that of an ideal system but as the impeller speed increases the predicted conversion rapidly approaches the ideal value. There is a marked difference in the two predicted conversions up to a value of (q/Q) = 25.

For the case of inflow to the loop region the percentage conversion for the single loop model may be predicted using the following expression. Figure 4.3, equation 4.3.

$$R = 100\left(1 - \frac{Q}{\frac{(vk+q+Q)^2}{q+Q} - q}\right)$$

Similarly, the percentage conversion for the double loop model, Figure 4.6, equation 4.6 is given by:-

$$R = 100\left(1 - \frac{Qy}{\frac{(3r+Q-2ry)(Q+r+vK)}{r+Q} - \frac{r^2}{r+vK}}\right)$$

where $$y = \left(\frac{2r+Q}{2vk+2r+Q}\right)^2$$

Again the effect of model parameter on conversion for these operating conditions is illustrated, in Figure 9.4. Maximum conversion is obtained at zero impeller speed for both models. As the impeller speed increases both conversions approach that of the ideal system. There is however a difference in the conversions predicted by the models throughout a whole range of (q/Q).

Also shown in Figure 9.4 is the predicted steady state conversion for the baffled case of feed to the loop, for the double loop model. As the single loop model does not require modification to accommodate the baffled system, there is a major difference in the conversion predicted by the two models, for this inlet feed position and operating condition, over the range of (q/Q) studied. The double loop model predicts a definite peak at (q/Q) = 5, whereas the single loop decays from a maximum at (q/Q) = 0 to the ideal conversion at (q/Q) > 50. This phenomena detracts from the double

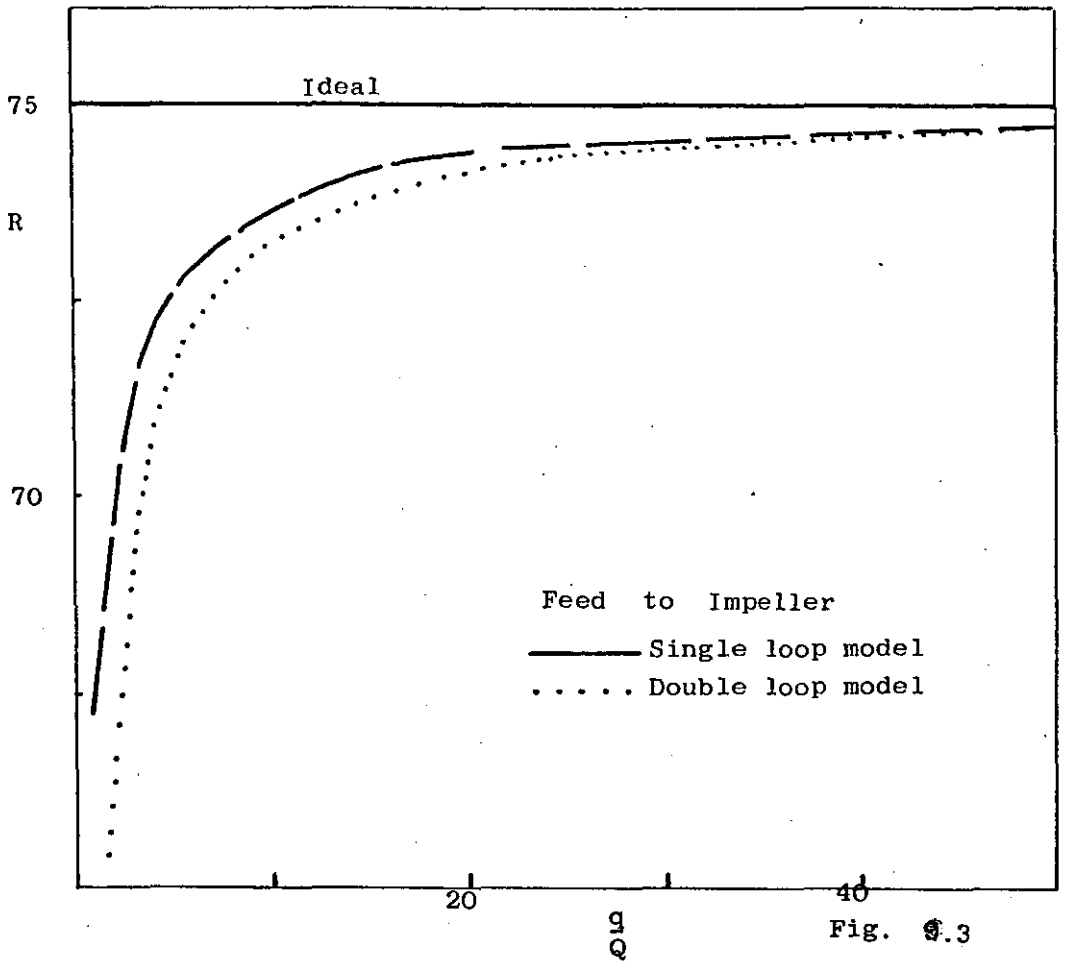
Ideal
75
R
70
Feed to Impeller
Single loop model
Double loop model
20
40
q/Q

Fig. 9.3

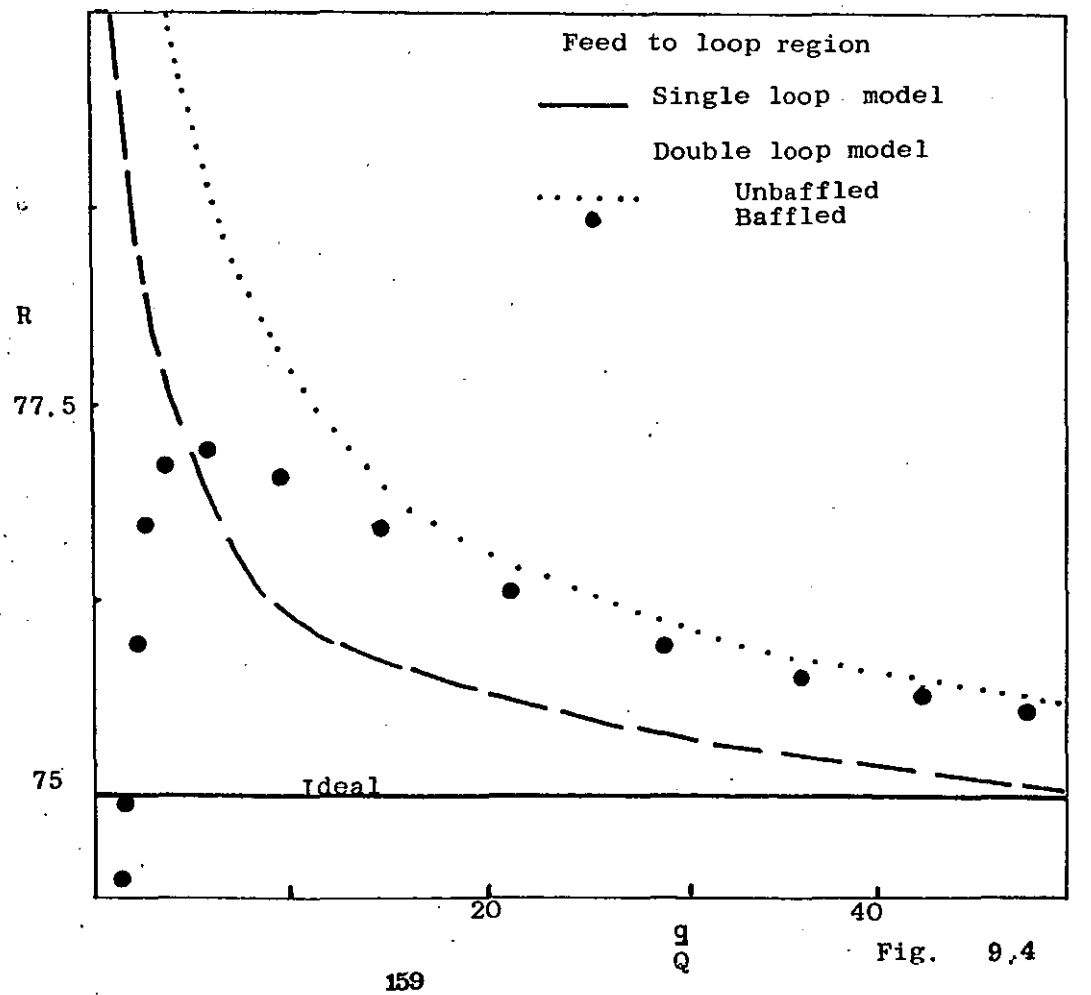
Feed to loop region
Single loop model
Double loop model
Unbaffled
Baffled
R
77.5
75
Ideal
20
40
q/Q

Fig. 9.4

loop simulation as it is hard to comprehend why the introduction of baffles should change the steady state conversion when the actual residence time distribution for the unbaffled/baffled cases are almost identical.

The expression used for prediction of the percentage conversion for the baffled case with the inflow into the loop region, (Figure 4.7), equation 4.7, is shown below:-

$$R = 100\left[1 - \frac{Qy}{\left[(qr+Q) - \frac{4r^3}{(r+kv)^2} - 2ry\right]\frac{3r+3kv+Q}{3r+Q} - \frac{3r^2}{r+kv}}\right]$$

9.2.2. Variance analysis

A variance analysis was conducted for the normalised distributions of the single and double loop flow models. The definition of variance is

$$\sigma^2 = \int_0^\infty f(t)^2 dt \qquad \text{for an impulse input.}$$

The variance was calculated numerically, using a modification of the programme described in Appendix 3, for various values of (q/Q). The value obtained depends upon the upper limit of integration and the integration interval used. These were dictated by available computer store space. However, the results obtained give a reasonable guide to the compatibility of the two models.

The results are compared with the ideal stirred tank for which the variance is derived below:-

$$\sigma^2 = \int_0^\infty f^2(\theta)\,d\theta = \int_0^\infty e^{-2\theta}\,d\theta = \frac{1}{2}$$

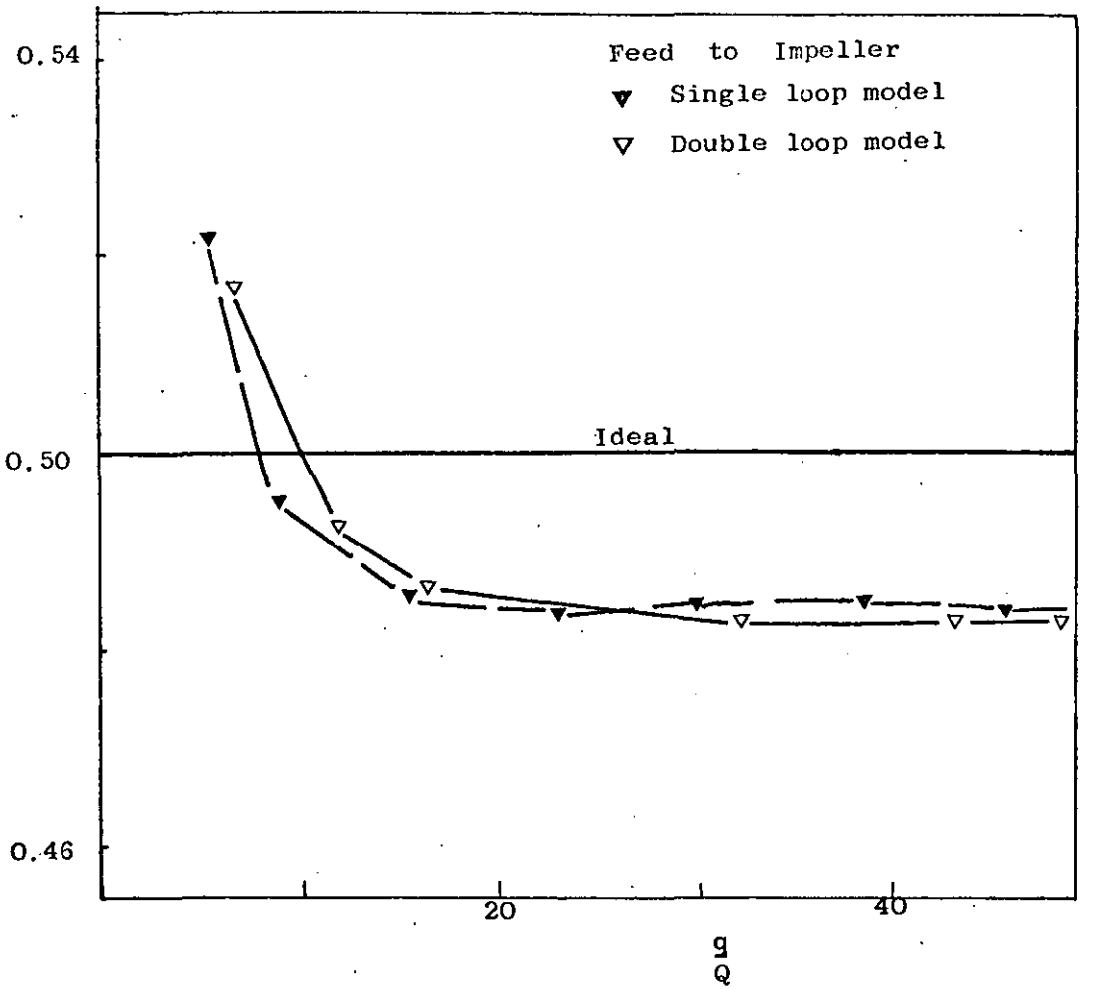

Fig. 9.5 : Variance vs $\frac{q}{Q}$

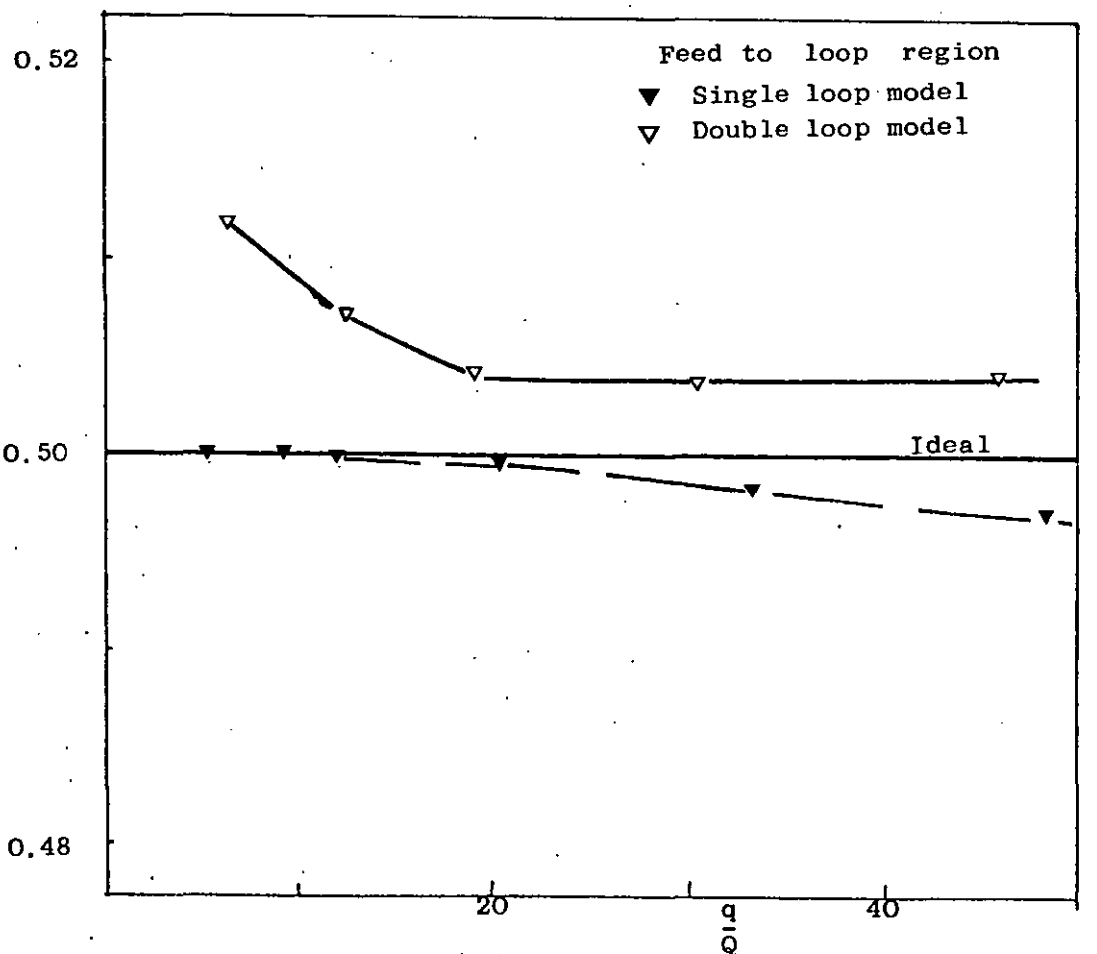

Fig. 9.6 : Variance vs $\frac{q}{Q}$

Figure 9.5 illustrates the reasonable comparison of the variance predicted by both models, for the feed to impeller condition. The comparison is slightly worse for the feed to loop case, Figure 9.6, as would be expected from the greater deviation in residence time distributions observed for this feed condition.

9.2.3. Intensity functions

The intensity functions of the single loop and double loop models were computed, using a modified version of the programme described in Appendix 3, for both inlet positions and for a range of values of the model parameter. Figures 9.7 - 9.8 illustrate various intensity functions.

For $(q/Q) < 12$, in the feed to impeller case, there is a marked difference in the intensity function predicted by each model; however above this value the intensity functions become almost identical, Figure 9.7. For feed to the loop region, Figure 9.8, there is a great difference in intensity function throughout the whole range of (q/Q) studied.

The intensity function is far more sensitive than the variance analysis and consequently gives a clearer definition of the difference in the two models.

9.3. Output Oscillations

Oscillations in the initial section of the output response were observed during experiments to determine the residence time distributions in the $2\frac{1}{2}$" turbine, 9" dia. vessel. A similar phenomena had previously been noted by Voncken et al (72) and Clegg and Coates (13). Figure 9.9 shows a typical set of responses obtained for a particular impeller speed. It can be seen that the frequency of oscillation is

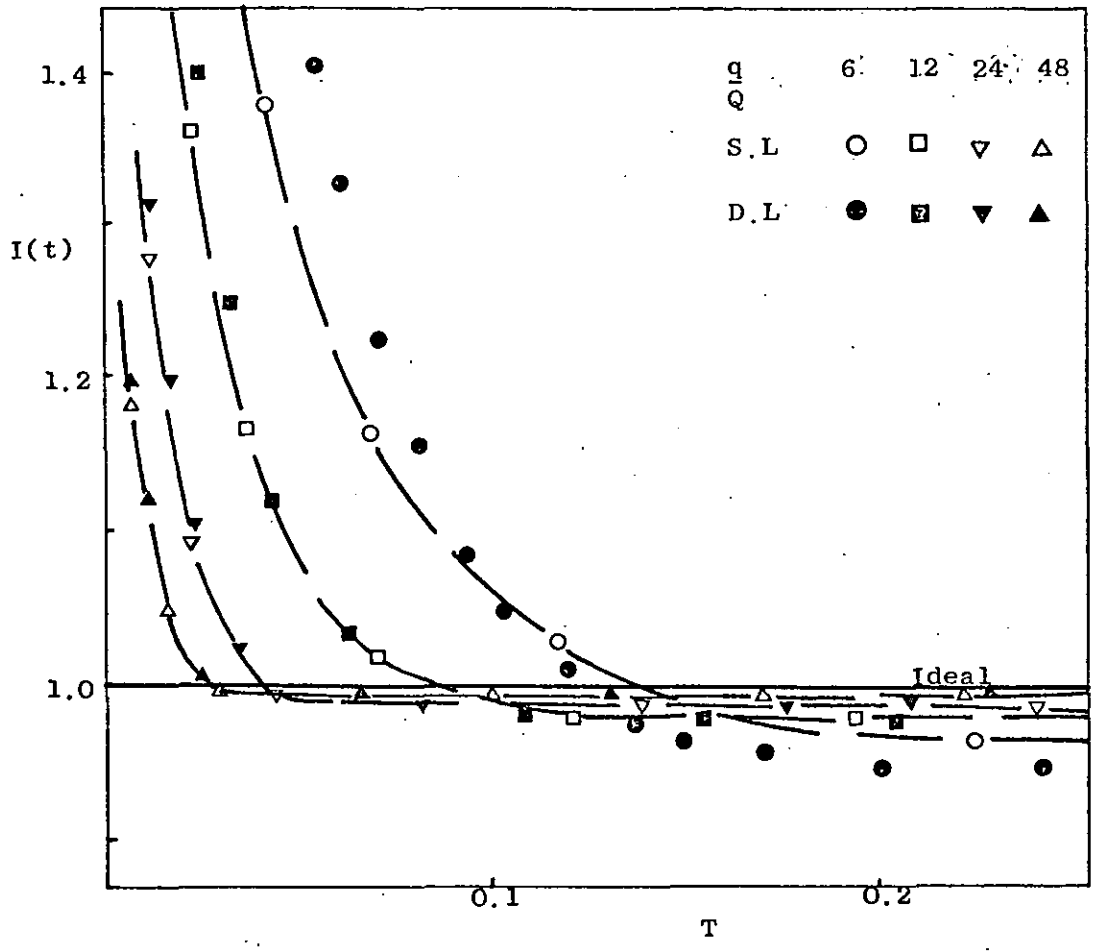

Fig. 9.7 Intensity Function curves for both models (feed to impeller region)

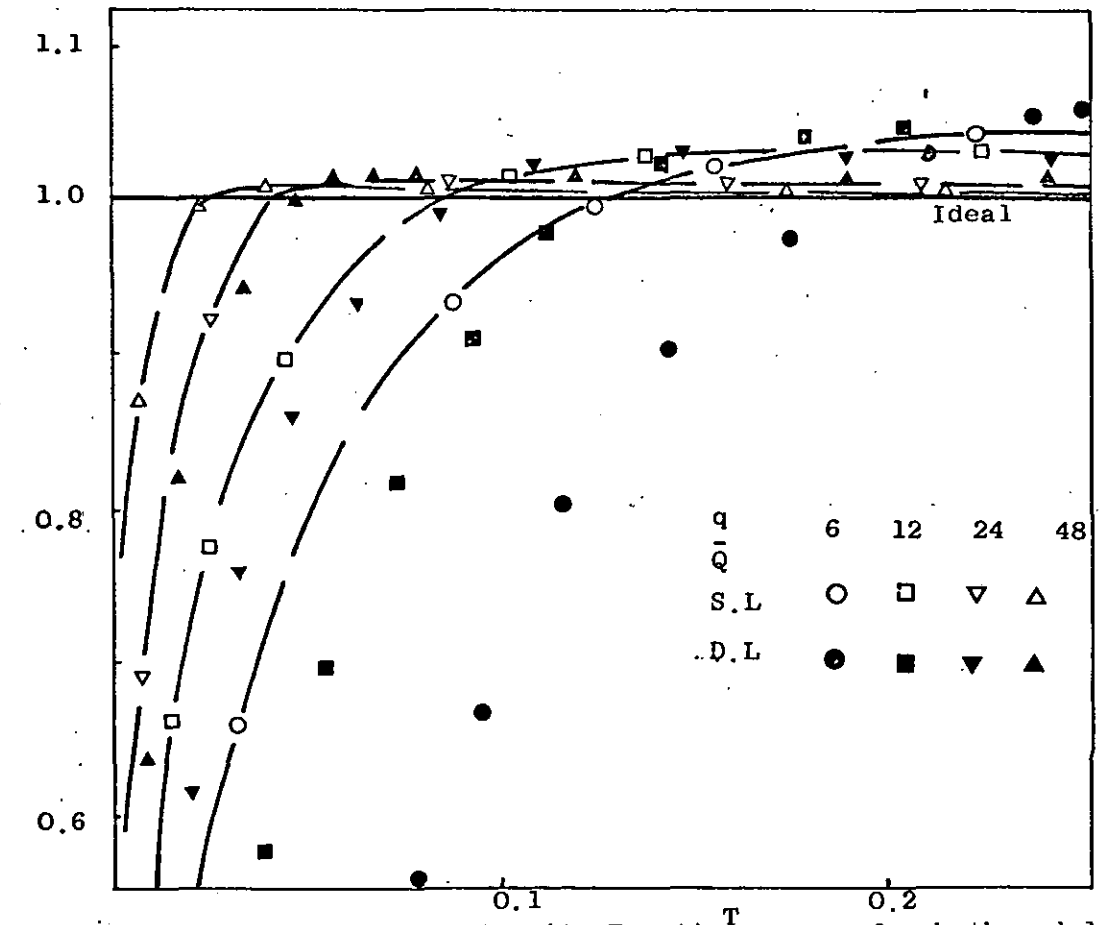

Fig. 9.8 Intensity Function curves for both models (feed to loop region)

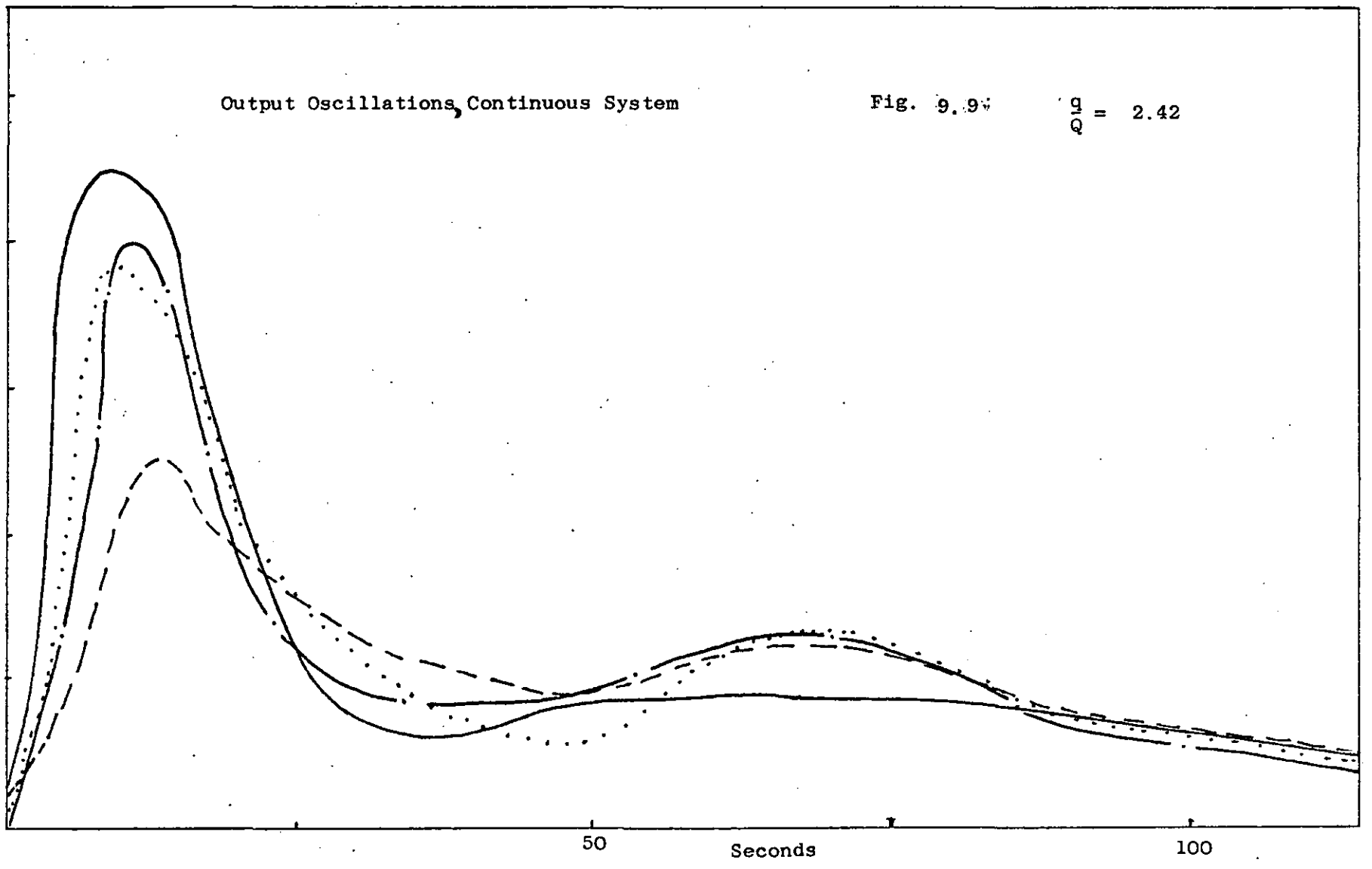
Output Oscillations, Continuous System
Fig. 9.9
$\frac{q}{Q}$ = 2.42
2.0
1.0
C/C_o
50
Seconds
100

reproducible but the amplitude of oscillation is not. This fact is in agreement with the results of both Voncken et al and Clegg and Coates. These workers each recorded upto four oscillations, in this work however two oscillations were the maximum observed. Further comparison with previous work is difficult. The oscillations measured by Voncken et al were recorded inside the vessel by a detecting device which surrounded the impeller, and the results of Clegg and Coates were obtained for a vessel without mechanical agitation. In this work the oscillations were measured by a device situated in the outlet line.

Figure 9.10 shows the values, averaged over four runs, for the distance between peak heights for various impeller pumping capacities. These results do not agree with the added momentum theory of Voncken as the distance between peaks varies directly with the pumping capacity. This suggests that the distance between peak heights is not a true indication of the circulation time in this continuous case, but rather a measure of the time taken for a fraction of the injected pulse, which has not been directly bypassed to the outlet, to travel around the shortest streamline path and back into the outlet stream. The oscillations were not observed above a value of q/Q > 25.

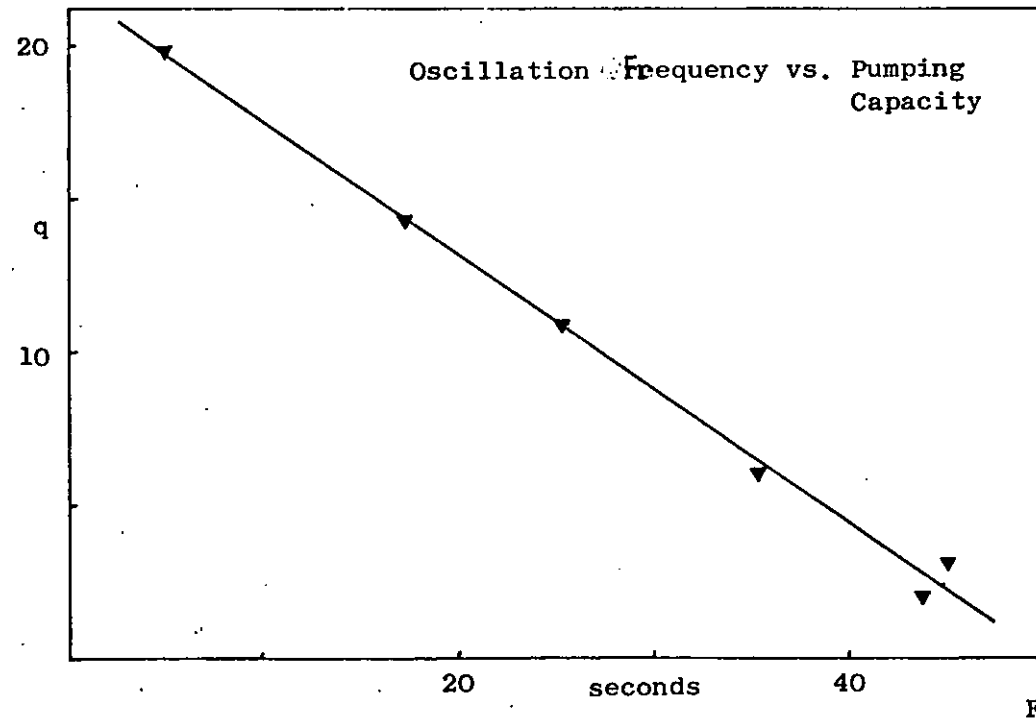

Fig. 9.10

9.4. Batch Mixing Time

The matrix technique for the solution of a network of ideal stirred tanks enables a swift calculation of the batch mixing time to be made. It has a wider application and flexibility than the restrictive approaches of previous research.

The experimental values of batch mixing time, found in this research, have been shown to be inversely proportional to the impeller speed; a result predicted by the equations derived in chapter 5. This conclusion has been noted by other workers (44, 67).

The expressions derived for batch mixing time are identical to those put forward by Marr and Johnson (45). This is to be expected for although the configuration of the single loop model developed in this work is different (changed outlet position), for the continuous case; it reduces to the same network for the batch case. The factor which governs the relationship derived for batch mixing time is the number of stages in series used to simulate the mixing in the circulation loop.

For an impulse to the impeller region, the upper and lower loops of the double loop network are symmetrical; reducing the double loop model to the single loop configuration. This is verified by the identical expressions derived from the two models for this feed condition. However, for the impulse to the loop condition, the double loop model lacks symmetry and thus cannot be simplified. This dissymmetry produces four different equations for the real time response of the stages in this network, equations 5.11 - 5.14. Figure 9.11 illustrates a typical series of curves, describing these equations for a particular value of impeller speed. Also shown are the responses derived from equations 5.15 - 5.18 for the feed to the impeller condition.

These curves were computed using a modification of the programme described in Appendix 3. The batch mxing time being the time required for each stage in the network to reach the same concentration level. Figure 9.11 shows that the feed to the loop produces a value of batch mixing time which is twice as long as the value predicted for feed to the impeller. Therefore from a theoretical standpoint it would be more advantageous in practice to mix into the impeller region.

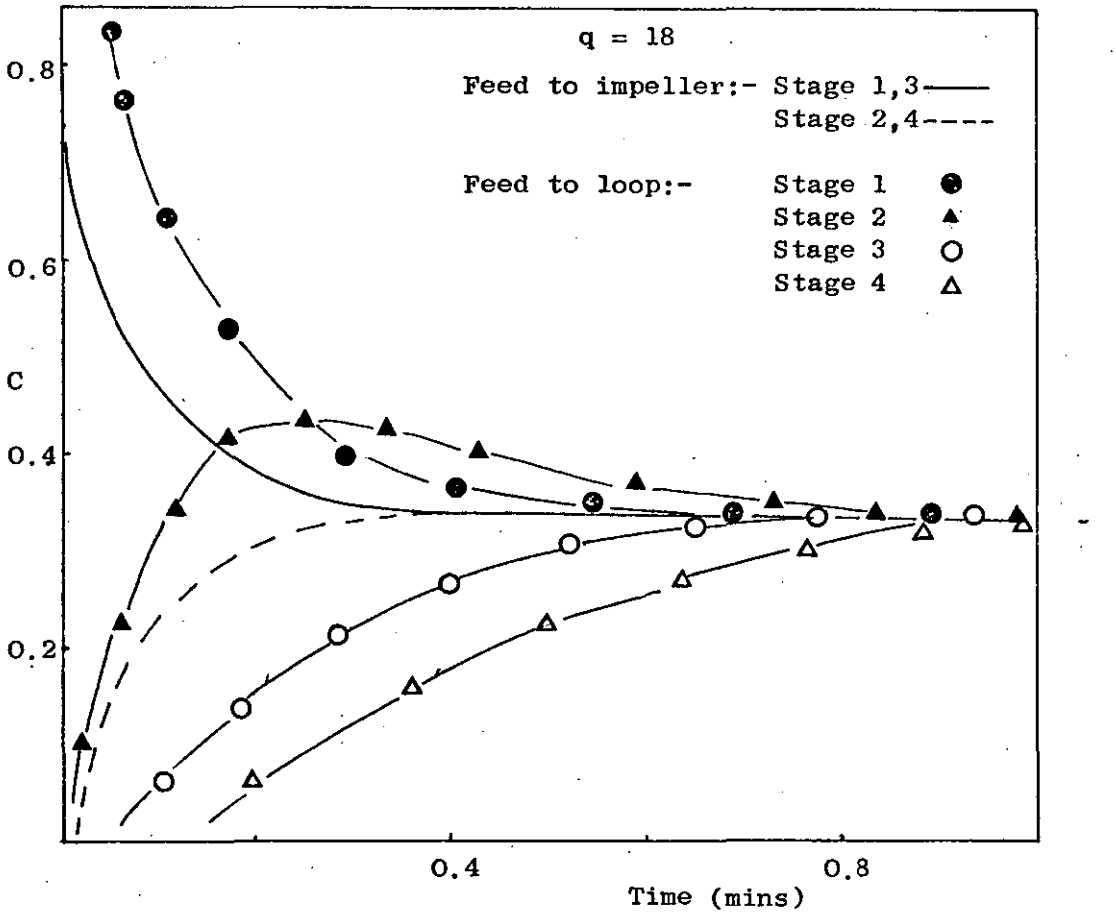

Fig. 9.11

The experimental results, however, do not substantiate this fact, as no apparent difference in batch mixing time was observed for the different impulse positions. In order to investigate this phenomena a more sophisticated experimental technique is required than the visual observation method. The single loop model predicts

the same value batch mixing time for both impulse injection positions.

The difference between the experimental-theoretical results and those calculated from the correlations of Metzner-Norwood and Fox-Gex, is due to the lack of generality of such correlations. Metzner-Norwood used a six bladed disk and vane type turbine, whereas in this work a straight flat bladed turbine was employed. This difference would produce different flow patterns in the two cases and subsequently different rates of mixing. The W/D ratio of the disk and vane turbines was 1/5, as compared with W/D = 1/8 for the turbines used in this work. Hence the impeller discharge rates of the two turbines would also be different. A similar argument holds for the propeller case; the propellers being of different pitch would produce different rates of discharge. It is apparent from the discussion that the batch mixing expressions supersede the empirical correlations.

9.5 Continuous Mixing Time

The use of the average value of the intensity function prediction and the semi-log solution appears to be a sound basis for the assessment of continuous mixing time. These criteria are independent of the inlet feed position whereas the tmax approach is only applicable for inlet feed to the loop. Marr and Johnson used the tmax approach to find an analytical expression which related continuous mixing time to system parameters. It was deduced by equating the derivative of the real time expression, of the continuous flow model, to zero. However, as the predictions of their recirculation model have been shown to deviate widely from experimental responses, this expression requires modification. Equation 9.1 is the expression derived for tmax, from the real time solution of the single loop model, feed to the loop, proposed in this work.

$$t_{max} = \frac{V_T}{4(q+Q)} \cdot \sqrt{\frac{q+Q}{q}} \ln \left(\frac{1 + \sqrt{\frac{q}{q+Q}}}{1 - \sqrt{\frac{q}{q+Q}}} \right) \qquad (9.1)$$

9.6. Economic Scale-up of Continuous Systems

The possible extension of Standarts approach (section 3.4), to the continuous case is complicated by the need for a diifferent design equation for this system. An expression is required which relates impeller speed, vessel diameter and concentration fluctuations at the outlet. As the objective of a continuous blender is to minimize the deviation of the output response from a specified value. The minimization of the sum of the $(\text{errors})^2$ would be a useful criterion for assessing the performance of a continuous blender.

$$J = \int_0^\infty e^2(t).dt.$$

Where e(t) is the error signal representing the difference between the desired and actual output signal.

The ease with which the above equation can be treated using transfer functions results from Parsevals Theorem (79) such that:-

$$\int_0^\infty f^2(t).dt. = \frac{1}{2\pi j}\int_{-j\infty}^{j\infty} F(s).F(-s).ds$$

When F(s) can be expressed as the ratio of two polynomials, that is, when F(s) is rational, the value of this complex integral has been tabulated (79) in terms of the polynomial coefficients of the system transfer function. From these tables it is possible to evaluate J.

The variance criterion adopted by Engh (22), to smooth out quality fluctuations in various combinations of plug flow and backmix regions, is also a useful criterion for assessing continuous blenders. It can, however, be shown to be equivalent to the minimization of the $(\text{errors})^2$ technique.

Engh:- $$\sigma^2 = \int_0^\infty f(t)^2 dt = \frac{1}{\pi} \int_0^\infty \left[h(j\omega) \right]^2 \, d\omega \qquad 9.2$$

$$\sum e^2 :- \quad J = \int_0^\infty f(t)^2 dt = \frac{1}{2\pi j} \int_{-j\infty}^{j\infty} F(s).F(-s).ds$$

now

$$s = j\omega, \quad ds = j d\omega$$

hence

$$\sum e^2, \quad J = \frac{1}{2\pi} \int_{-\infty}^{\infty} F(j\omega)\ F(-j\omega)\ d\omega$$

If $F(j\omega) = Re^{j\phi}$, $F(-j\omega) = Re^{-j\phi}$

$$J = \frac{1}{2\pi} \int_{-\infty}^{\infty} R^2 \, d\omega$$

As powers of ω are always even.

$$= \frac{1}{\pi} \int_0^\infty R^2 \, d\omega \qquad 9.3$$

Equation 9.3 is identical to equation 9.2.

The calculation of (σ^2) and (J) for the single loop model results in the following expressions:-

Inlet feed to the impeller, equation 4.1

$$J = \frac{1 + q/Q}{2q/Q + 1} \cdot \frac{1}{\bar{t}} \qquad 9.4$$

where $\bar{t} = \frac{V_T}{Q}$

as $q/Q \to \infty$, $J \to \frac{1}{\bar{t}\,2}$

as $q/Q \to 0$, $J \to \frac{1}{\bar{t}}$

Inlet feed to loop, from equation 4.3

$$J = \frac{1}{2\bar{t}} \quad , \quad \bar{t} = \frac{V_T}{Q}$$

9.5

$$\text{as } q/Q \longrightarrow \infty,\ J \longrightarrow \frac{1}{2\bar{t}} : q/Q \longrightarrow 0,\ J \longrightarrow \frac{1}{2\bar{t}}$$

Equation 9.4 shows that, for feed to impeller, the variance changes throughout the range of $(q/_Q)$. As $(q/_Q)$ tends to infinity i.e. to an ideal stirred tank, the variance assumes a value equivalent to the ideal case. With no circulation, $(q/_Q \Rightarrow 0)$, the variance of the distribution tends towards its maximum value. This is to be expected with the increased bypass effect at low circulation rates. Equation 9.5 shows that, for feed to the loop, the variance is independent of impeller speed. The variance, for the responses of this feed condition, is equivalent to the ideal case for all impeller speeds.

The above equations allow the optimum economic scale-up of continuous blenders to be examined. Adopting the same cost function as used by Standart, i.e. the sum of the power cost and capital depreciation cost.

$$£ = y_0 = K_1 N^3 D^5 + K_2 D^2 \qquad 9.6$$

Using the output variance as the characteristic of the system, the previous analysis has shown that a continuous system may be designed so that:-

$$J = \frac{Q}{2.V_T} \qquad 9.7$$

provided that $q/Q \geqslant K_3$ 9.8

The impeller pumping capacity may be described by:-

$$q = K_4 N D^3 \qquad 9.9$$

Equations 9.8 and 9.9 can be combined to form an inequality constraint and equation 9.7 which represents the output variance of a vessel to a unit impulse can be used as a final check to ensure that the optimum vessel will deal efficiently with possible input disturbances.

$$\text{Let} \qquad y_1 = \frac{K_3 Q}{K_4 N D^3} \ll 1 \qquad 9.10$$

Equations 9.6 and 9.10 are both polynomials of the form required for a simple optimum calculation by the method of geometric programming as described by Wilde and Beightler (81). The procedure is simply described in that for the optimum the global minimum of y_0 is equal to the maximum of d where d is a weighted geometric mean of the terms in the polynomials.

$$y_{0_{min}} = K_1 N_*^3 D_*^5 + K_2 D_*^2$$

$$= d_{max} = \left(\frac{K_1 N_*^3 D_*^5}{\omega_1}\right)^{\omega_1} \cdot \left(\frac{K_2 D_*^2}{\omega_2}\right)^{\omega_2} \cdot \left(\frac{K_3 Q}{\omega_3 K_4 N_* D_*^3}\right)^{\omega_3}$$

and it is found that, $\omega_1 = \frac{1}{3}$, $\omega_2 = \frac{2}{3}$, $\omega_3 = 1$

hence

$$y_{0_{min}} = \frac{K_1 N^3 D^5}{1/3} \qquad 9.11$$

$$y_{0_{min}} = \frac{K_2 D^2}{2/3} \qquad 9.12$$

Combining equations (9.11) and (9.12) gives

$$N^3 D^3 = \frac{K_2}{2 K_1} \qquad 9.13$$

$\therefore$ ND = constant

This is the same rule as that obtained by Standart for blending in a batch process. However the additional proviso of equation (9.8) as an equality must be satisfied. Therefore scale-up of the impeller for the laboratory and pilot plant vessels must be such that;-

$$\frac{K_{4s}}{K_{4u}} = \frac{D_s^2}{D_u^2} \qquad 9.14$$

In practice this equation may be satisifed by increasing the number of blades in the scaled case. For a linear scale ratio of L, i.e. $L_1 D_u = D_s$, and constant meantime in the two systems, constant tip speed and $(q/_Q)$ scale-up gives:-

$$K_{4s} = K_{4u} \cdot L \qquad 9.15$$

It may be noted that equation (9.14) may be an essential relationship, for the "design changes" mentioned by Bowers, necessary to ensure an equal scale of turbulence. Unfortunately Bowers has made no mention of the design changes used. This question is extremely important, because it could result in a practical solution of the problem of micromixing and macro-mixing (or segregation), where current practice has shown that for non first-order processes the residence time distribution alone does not adequately describe equipment performance.

9.7 Suggestions for Further Work

As the single loop recirculation model has been found to characterise the mixing of thin fluids agitated by turbine and propeller impellers, for a variety of vessel sizes, it would appear that any further impulse response tests with these systems would not be worthwhile. However, experiments with other impeller types, for various Z/T ratios and different fluid properties would be worthy of investigation so as to find the limits of the model's application.

An investigation into the effect of impulse injection position on batch mixing time in various diameter vessels, using a more sophisticated experimental technique, would be most valuable. A further extension would be to relate the theoretical approach to batch mixing time, to a derivation based on the scale and intensity of turbulence produced in batch systems. A series of experiments could be devised by which these relationships could be tested over a wide range of fluid properties.

The recent published work of Peters and Smith (80), using anchor agitators in viscoelastic fluids, lends itself to investigation with the techniques developed in this work. They found that differences in system geometry and fluid properties could be described in terms of vortex position and streamline deflection. Hence, after deriving a flow model to describe this system the approach discussed in chapter 5 could be applied. The results of the preceeding investigation would lead to a more comprehensive flow model for the continuous case.

An investigation into the use of constant (q/Q) as a scale-up rule, for systems in which reactions are taking place, would serve to test the validity of this scale-up criterion.

Previous research (6,7,8) has shown that scale-up at constant tip speed results in identical velocity contours in the scaled and unscaled batch systems when geometric similarity is maintained and identical turbulence contours after a "change in impeller design". The term "change in impeller design" is ambiguous for it is uncertain as to whether it refers to an increase in the number of blades, a change in the angle of inclination of the blades or a change of impeller. Thus, there remains the possibility that scale-up at constant tip speed, with (q/Q) also constant, would result in identical velocity and turbulence contours and the same residence time distribution in the laboratory and pilot plant vessels. As this research has also shown that scale-up

with constant impeller tip speed provides an economic optimum for the scale-up of continuous systems, this possibilty is worthy of further investigation.

A series of experiments, designed to measure the effect of number of blades, angle of inclination, blade width, on turbulence and velocity phenomena in different size continuous systems, would determine the potential of this suggested scale-up method. It would also lead to a greater insight into the problem of segregation.

9.8 Conclusions

A modified version of the single loop recirculation model was found to characterise the behaviour of propeller and turbine agitated systems, for various operating conditions in three different diameter vessels. The most significant factor associated with the response of each system was found to be the inlet position. The model however was able to accommodate this variation. This model supersedes the simplified versions of the multiloop model proposed by Gibilaro for turbine stirred tanks.

The matrix formulation of the network of ideal stirred tanks, used for the simulation of batch mixing, was found to be a useful approach for the derivation of batch mixing time relationships. The full potential of this technique can only be realised on more complicated networks. The empirical correlations for batch mixing time have been shown to be of a singular nature; the predictions being inaccurate for systems other than those from which they were derived.

The definition of intensity function promotes itself for use as a tool for the measurement of continuous mixing time. The average of the semilog and intensity function predictions is proposed as a conservative estimate of continuous mixing time.

The use of constant (q/Q) as a scale-up criterion for continuous blenders is shown to produce identical normalised residence time distributions in the laboratory and pilot plant vessels whereas, scale-up using other published criteria does not ensure this similarity.

Scale-up using constant impeller tip speed provides an economic optimum for the scale-up of continuous systems. Constant (q/Q) and constant tip speed scale-up can be observed simultaneously by increasing the number of blades on the scaled impeller.

For the batch system mixing into the impeller region has been shown to produce the best results. In the continuous case feed directed away from the impeller, i.e. into the loop, is more effective; the effectiveness being increased as the mean residence time of the system is increased.

BIBLIOGRAPHY

Bibliography

1. Babb, A.L., Bell, R.L., Chem. Eng. Sci. 1965 20. 1001

2. Bates, R.L., Fondy, P.L., Corpstein, R., Ind. Eng. Chem. Process Design And Development 1963 2. 310

3. Bates, R.L., Ind,Eng,Chem., 1959 51 1254

4. Berresford, H.I., Gibilaro, L.G., Kropholler, H.W., Spikins, D.J. Symposium on Mixing, Leeds 1968.

5. Biggs,R.D., A.I.Ch.E Journal 1963 9. 5. 636

6. Bowers, R.H., Symposium on Mixing, Leeds 1968.

7. Bowers, R.H., A.I.Ch.E. - I.Ch.E. Joint Meeting, London June 1965 6

8. Bowers,R.H., J.App. Chem. 1955 5. 542

9. Buffham,B., Gibilaro, L.G., A.I.Ch.E. Journal 1968 14.5.805

10. Buffham, B., Gibilaro, L.G., Chem Eng Sci 1968 23 1399

11. Chapman,F.S., Urban,W., Holland, F.A., Chem. & Proc. Eng. June 1965.

12. Chollet,A., Cloutier L. Can. J. Chem. Eng. 1959 37 105

13. Clegg. A., Coates, P., Chem. Eng. Sci. 1967 22 1117

14. Conover,J.A.,M.Sc. Research Thesis 1960. St. Louis University

15. Cooper, C., Wolf, R., Can. J. Chem. Eng. 1967 45 197

16. Corrigan, T.G., Lander, H.R., Shaefer,R., Dean, M.J, A.I.Ch. E. Journal 1967 13 1029

17. Corrsin, S., A.I.Ch.E. Journal 1957 3 329

18. Cutter, L.A. A.I.Ch.E. Journal 1966 12 35

19. Danckwerts, P.V., Chem. Eng. Sci. 1953 2. 1.

20. Danckwerts, P.V., Jenkins, J.W., Place, D., Chem. Eng. Sci. 1965 3 26

21. Douce, J.L., "An Introduction to the Mathematics of Servo-Mechanisms". E.U.P. 1963.

22. Engh, T.A., Trans. Inst. Ch. Eng. 1967 45 10

23. Fox. E., Gex, V. A.I.Ch.E. Journal 1956 2. 539

24. Gaskell, H., Whitehead, P., L.U.T. Chem.Eng.J. 1968 4 22

25. Gibilaro. L.G., L.U.T. Chem. Eng. J. 1961 1 3.

26. Gibilaro, L.G. Ph.D. Thesis "Models for Mixing in Stirred Vessels" 1967 Loughborough

27. Gibilaro, L.G., Kropholler, H.W., Spikins, D.J., Chem. Eng. Sci. 1967 22 517

28. Gianetto, A., Cazzulo, F., Chem. Eng. Sci., 1968 23 8

29. Gillespie, R., Carberry, J., Ind. Eng. Chem. Fundamentals 1966 2 164.

30. Gillespie, R., Carberry, J., Chem. Eng. Sci. 1966 21 472

31. Hixson, A.W., Ind. Eng. Chem. 1944 36 488

32. Holland, F., Chem. Eng. 1962 Nov 119

33. Holland, F., Chem. and Proc. Eng. 1964 March 141

34. Holmes, D., Voncken, R., Dekker, J.A., Chem. Eng. Sci. 1964 19 201

35. Howard, R.A., "Dynamic Programming and Markov Processes" Wiley New York 1960

36. Hyman, D., "Mixing and Agitation" Academic Press 1962

37. Johnstone, R.E., Thring, M.W., "Pilot Plants, Models and Scale-up Methods" McGraw Hill 1957

38. Kramers, H., Baars, G., Knoll, W., Chem. Eng. Sci. 1953 2 35

39. Krambeck, F.J., Shinnar, R., Katz, S., Ind. Eng. Chem. Fund. 1967 6 276

40. Levenspiel, O., "Chemical Reaction Engineering" Wiley 1962

41. Levenspiel, O., Can. J. Chem. Eng. 1963 41 132

42. Levich, V.G., Markin, V.S., Chismadzhiev, A., Chem. Eng. Sci. 1967 22 1357

43. Manning, F.S., Wolf, D., Keairns, D.L., A.I.Ch.E. Journal 11 4 723

44. Marr, G., Johnson. E., A.I.Ch.E. Journal 1963 9 383

45. Marr, G., Johnson. E., Chem. Eng. Prog. Symposium A.I.Ch.E 1961 57 109

46. Metzner, A.B., Feech, R.H., Ramos, H.L., Otto, R.E., Juthill, J.D A.I.Ch. E. Journal 1961 7 3

47. Nagata, S., Yamamoto, K., Hashimoto, K., Naruse, Y., M.F.E. Kyoto University 1959 21 260

48. Nagata, S., Yokoyama, T., M.F.E. Kyoto University 1955 17 253

49. Nagata, S., Yoshioka, N., Yokoyama, T., M.F.E. Kyoto University 1955 17 175

50. Norwood, K., Metzner, A., A.I.Ch.E. Journal 1960 6 432

51. Naor, P., Shinnar, R., Chem. Eng. Sci. 1967 22 1369

52. Naor, P., Shinnar, R., Ind. Eng. Chem. Fundamentals 1963. 2 4 278

53. Oldshue, J.V., Hirschland, H.E., Gretton, A.J., Chem. Eng, Prog. 1956 52 481

54. Peters, D.C., Smith,J.M., Symposium on Mixing. Leeds 1968

55. Procelli, O., Marr,G., Ind. Eng. Chem. Fundamentals 1962 1 3 172

56. Prochaka, J., Landau, J., Collections Czechoslav. Chem. Communs 1961 26 2961

57. Rippin, J., Ind. Eng. Chem. Fundamentals 1967 6 488

58. Rushton,J.H., Miller,F.D., Ind.Eng. Chem. 1944 36 499

59. Rushton,J.H., Ind. Eng. Chem. 1952 44 2931

60. Rushton,J.H., Chem. Eng. Sci. 1954 50 687

61. Rushton,J.H., Mack,D.E., Everitt, H., Trans. A.I.Ch.E. 1946 42 441

62. Rushton,J.H., Costich,E.W., Everitt,H.J., Chem.Eng.Prog. 1952 46 395,467

63. Rushton,J.H., Oldshue,J.V., A.I.Ch.E Journal Symposium Series 1959 55 181

64. Standart, G., Manchester University Chem. Eng. Journal 1968

65. Sterbacek,H., Tansk,C., "Mixing in the Chemical Industry" Pergammon 1965

66. Uhl, V., Gray,J., "Mixing Theory and Practice" Vols. 1& 2 Academic Press 1960

67. van de Vusse, J.G., Chem. Eng. Sci. 1955 4 178, 209

68. van de Vusse, J.G., Chem. Eng. Sci. 1964 10 507

69. van de Vusse, J.G., Joint Symposium - The Scaling up of Chemical Plant & Processes, London 1957

70. van de Vusse, J.G., Chem. Eng. Sci. 1966 21 611

71. van de Vusse, J.G., Chem. Eng. Sci. 1962 17 507

72. Voncken,R., Rotte,I., ten Houten,A.T., A.I.Ch.E. - Ind. Chem. Joint Meeting London June 1965

73. Weber, A.P., Chem.Eng. Prog. 1953 49 26

74. White, A.M., Brenner,E., Philips, G.A., A.I.Ch.E Trans. 1934 30 585

75. White, E.T., Can. Journal Chem. Eng. 1963 41 131

76. Wood, I.J., Nature 1961 191 563

77. Wolf,D., Resnick, W., Ind. Eng. Chem. Fundamentals 1963 2 4 287

78. Zwietering, T.N., Chem. Eng. Sci. 1959 11 1

79. Koppel,L.B., "Introduction to Control Theory with Applications to Process Control" Prentice-Hall 1968

80. Peters,D.C., Smith J.M., Tripartite Chem. Eng. Conference Montreal 1968.

81. Wilde, D.J., Beightler, C.S. "Foundations of Optimization" Prentice-Hall 1967.

APPENDICES

A.1. RESULTS OF EXPERIMENTAL WORK

A.1.1. TURBINE RESIDENCE TIME DISTRIBUTION EXPERIMENTS

Impulse Response Experiments

$2\frac{1}{2}$" dia. Turbine 9"/9" Cylindrical System

R.1. Unbaffled Feed to Impeller

	Normalised Concentration							
Run	1	2	3	4	5	6	7	8
N. Time	rpm 28	45	60	80	104	134	154	180
0.000	0.680	1.758	1.087	0.359	0.552	0.427	1.046	0.980
0.020	2.913	1.709	1.509	1.567	1.153	1.112	0.995	1.086
0.041	1.570	1.607	1.237	1.166	1.050	0.977	0.928	0.967
0.061	1.045	1.215	1.087	0.987	0.928	0.941	0.901	0.934
0.081	1.150	1.056	0.961	0.925	0.903	0.923	0.890	0.943
0.122	0.913	0.855	0.855	0.875	0.864	0.888	0.853	0.901
0.163	0.841	0.774	0.815	0.838	0.840	0.852	0.821	0.861
0.204	0.722	0.748	0.775	0.807	0.809	0.828	0.805	0.822
0.244	0.674	0.714	0.748	0.776	0.770	0.799	0.757	0.782
0.285	0.656	0.681	0.742	0.746	0.738	0.769	0.735	0.749
0.326	0.626	0.649	0.695	0.715	0.707	0.733	0.703	0.723
0.367	0.585	0.621	0.662	0.690	0.695	0.704	0.682	0.683
0.407	0.575	0.610	0.627	0.659	0.658	0.662	0.661	0.650
0.448	0.545	0.582	0.605	0.622	0.639	0.644	0.629	0.628
0.489	0.525	0.559	0.583	0.599	0.614	0.615	0.596	0.606
0.530	0.510	0.531	0.560	0.573	0.596	0.585	0.596	0.578
0.571	0.485	0.512	0.533	0.552	0.577	0.560	0.554	0.562
0.612	0.462	0.499	0.513	0.532	0.552	0.545	0.522	0.529
0.653	0.446	0.482	0.495	0.501	0.527	0.520	0.504	0.505
0.693	0.442	0.455	0.478	0.481	0.515	0.495	0.477	0.488
0.734	0.418	0.446	0.465	0.461	0.490	0.476	0.464	0.470
0.775	0.399	0.429	0.447	0.444	0.471	0.462	0.446	0.452
0.816	0.391	0.420	0.429	0.428	0.453	0.434	0.424	0.435
0.856	0.375	0.406	0.412	0.408	0.440	0.430	0.412	0.422
0.897	0.371	0.393	0.403	0.395	0.416	0.411	0.395	0.405
0.938	0.359	0.371	0.390	0.379	0.403	0.399	0.388	0.392
0.979	0.343	0.362	0.373	0.371	0.378	0.383	0.370	0.378
1.020	0.328	0.345	0.355	0.355	0.347	0.364	0.352	0.361
1.101	0.312	0.322	0.337	0.334	0.335	0.337	0.328	0.335
1.183	0.284	0.300	0.311	0.310	0.316	0.317	0.307	0.313
1.264	0.264	0.278	0.285	0.281	0.285	0.290	0.286	0.287
1.346	0.241	0.252	0.263	0.257	0.267	0.266	0.268	0.261
1.427	0.221	0.234	0.241	0.236	0.248	0.239	0.250	0.235
1.509	0.205	0.225	0.228	0.216	0.223	0.222	0.236	0.222
1.591	0.197	0.203	0.210	0.208	0.211	0.207	0.215	0.204
1.672	0.185	0.190	0.193	0.188	0.180	0.192	0.208	0.187
1.754	0.162	0.181	0.180	0.171	0.168	0.172	0.187	0.174
1.835	0.150	0.159	0.162	0.159	0.149	0.157	0.169	0.157
1.917	0.142	0.146	0.145	0.139	0.136	0.141	0.152	0.144
1.998	0.130	0.133	0.131	0.122	0.124	0.117	0.132	0.131
(q/Q)	6.1	9.81	13.1	14.44	22.7	29.2	33.6	39.66

Impulse Response Experiments

$2\frac{1}{2}$" dia. Turbine 9"/9" Cylindrical System

R.2 Unbaffled Feed to Loop

	Normalised Concentration							
Run	1	2	3	4	5	6	7	8
N.Time	rpm 10	30	45	80	104	134	150	180
0.000	0.000	0.000	0.000	0.000	0.000	0.000	0.000	0.000
0.20	0.000	0.000	0.463	0.348	0.196	0.572	0.480	0.777
0.041	0.116	0.387	0.801	0.727	0.754	0.902	0.806	0.971
0.061	0.218	1.136	0.788	0.883	0.915	0.955	0.974	0.958
0.081	0.583	1.088	0.858	0.935	0.961	0.949	0.904	0.958
0.122	1.034	0.979	0.921	0.949	0.948	0.922	0.849	0.921
0.163	1.063	0.938	0.927	0.920	0.915	0.889	0.818	0.883
0.204	1.012	0.897	0.896	0.883	0.883	0.876	0.793	0.852
0.244	0.953	0.856	0.864	0.838	0.851	0.829	0.762	0.821
0.285	0.923	0.815	0.832	0.816	0.818	0.789	0.737	0.790
0.326	0.857	0.775	0.794	0.771	0.780	0.756	0.706	0.752
0.367	0.821	0.761	0.750	0.734	0.741	0.743	0.694	0.715
0.407	0.769	0.713	0.725	0.702	0.721	0.696	0.657	0.696
0.448	0.732	0.679	0.706	0.677	0.676	0.663	0.625	0.659
0.489	0.681	0.643	0.668	0.646	0.644	0.628	0.602	0.628
0.530	0.669	0.620	0.624	0.621	0.615	0.606	0.576	0.599
0.571	0.632	0.598	0.602	0.584	0.588	0.583	0.555	0.573
0.612	0.602	0.569	0.576	0.564	0.567	0.566	0.535	0.552
0.653	0.577	0.541	0.549	0.540	0.540	0.528	0.504	0.510
0.693	0.548	0.522	0.512	0.510	0.518	0.505	0.484	0.490
0.734	0.533	0.499	0.492	0.491	0.495	0.487	0.467	0.477
0.775	0.509	0.481	0.476	0.466	0.473	0.470	0.451	0.453
0.816	0.485	0.459	0.455	0.451	0.456	0.452	0.439	0.436
0.856	0.470	0.441	0.442	0.432	0.439	0.434	0.422	0.420
0.897	0.451	0.423	0.417	0.417	0.422	0.417	0.410	0.407
0.938	0.432	0.414	0.405	0.398	0.405	0.408	0.398	0.387
0.979	0.412	0.391	0.388	0.383	0.392	0.386	0.381	0.379
1.020	0.398	0.378	0.365	0.368	0.375	0.373	0.373	0.366
1.101	0.359	0.342	0.339	0.334	0.345	0.340	0.349	0.333
1.183	0.325	0.310	0.304	0.309	0.316	0.322	0.328	0.304
1.264	0.296	0.288	0.279	0.280	0.286	0.294	0.308	0.272
1.346	0.272	0.261	0.250	0.255	0.260	0.268	0.287	0.247
1.427	0.247	0.238	0.225	0.236	0.239	0.246	0.262	0.232
1.509	0.223	0.220	0.209	0.216	0.217	0.224	0.241	0.210
1.591	0.199	0.202	0.196	0.196	0.200	0.202	0.221	0.202
1.672	0.175	0.180	0.175	0.177	0.179	0.184	0.205	0.183
1.754	0.155	0.162	0.159	0.162	0.157	0.162	0.184	0.173
1.835	0.141	0.144	0.150	0.147	0.149	0.149	0.176	0.148
1.917	0.126	0.130	0.130	0.137	0.141	0.132	0.167	0.132
1.998	0.117	0.121	0.113	0.123	0.124	0.123	0.160	0.123
(q/Q)	2.18	6.54	9.81	17.44	22.7	29.2	33.6	39.66

Impulse Response Experiments

$2\frac{1}{2}$" dia. Turbine 9"/9" Cylindrical System

R.3 Baffled Feed to Impeller

Run	Normalised Concentration 1	2	3	4	5	6	7
N.Time	rpm 28	45	80	104	134	154	180
0.000	2.160	1.521	1.461	1.236	1.187	1.106	1.067
0.020	1.610	1.484	1.373	1.150	1.112	0.970	1.186
0.041	1.320	1.261	1.097	1.007	0.977	0.947	0.997
0.061	1.160	1.167	1.001	0.934	0.941	0.923	0.980
0.081	1.060	0.989	0.961	0.902	0.916	0.908	0.956
0.122	0.923	0.900	0.895	0.852	0.878	0.880	0.921
0.163	0.861	0.810	0.840	0.836	0.849	0.850	0.861
0.204	0.761	0.756	0.780	0.801	0.810	0.821	0.822
0.244	0.694	0.720	0.736	0.761	0.767	0.769	0.771
0.326	0.630	0.661	0.706	0.710	0.726	0.703	0.723
0.367	0.594	0.627	0.680	0.695	0.701	0.682	0.683
0.407	0.582	0.609	0.657	0.659	0.664	0.662	0.650
0.448	0.553	0.592	0.622	0.637	0.642	0.627	0.627
0.489	0.531	0.563	0.598	0.608	0.615	0.599	0.603
0.530	0.521	0.529	0.576	0.590	0.586	0.590	0.580
0.571	0.493	0.509	0.553	0.578	0.576	0.556	0.567
0.612	0.468	0.488	0.534	0.553	0.547	0.522	0.529
0.653	0.450	0.482	0.507	0.526	0.523	0.507	0.513
0.693	0.438	0.465	0.482	0.510	0.499	0.487	0.499
0.734	0.420	0.447	0.470	0.493	0.486	0.467	0.493
0.775	0.389	0.430	0.449	0.473	0.466	0.457	0.483
0.816	0.380	0.421	0.430	0.460	0.438	0.444	0.461
0.856	0.378	0.406	0.410	0.444	0.432	0.438	0.438
0.897	0.378	0.393	0.400	0.426	0.419	0.427	0.428
0.938	0.361	0.372	0.381	0.403	0.399	0.407	0.409
0.979	0.337	0.362	0.367	0.379	0.384	0.380	0.391
1.020	0.337	0.342	0.347	0.356	0.368	0.369	0.371
1.101	0.303	0.321	0.327	0.316	0.327	0.339	0.341
1.183	0.281	0.300	0.306	0.306	0.307	0.326	0.326
1.264	0.267	0.281	0.287	0.286	0.286	0.306	0.300
1.346	0.261	0.261	0.262	0.259	0.278	0.283	0.281
1.427	0.241	0.239	0.241	0.234	0.247	0.256	0.261
1.509	0.219	0.225	0.229	0.219	0.226	0.229	0.236
1.591	0.206	0.204	0.201	0.207	0.204	0.210	0.222
1.672	0.189	0.188	0.189	0.192	0.199	0.186	0.210
1.754	0.168	0.172	0.173	0.182	0.188	0.180	0.190
1.835	0.152	0.157	0.160	0.163	0.168	0.163	0.176
1.917	0.149	0.140	0.147	0.153	0.152	0.148	0.153
1.998	0.136	0.129	0.136	0.140	0.137	0.133	0.139
(q/Q)	6.1	9.8	17.44	22.7	29.2	33.6	39.3

Impulse Response Experiments

$2\frac{1}{2}$" dia. Turbine 9"/9" Cylindrical System

R.4 Baffled Feed to Loop

	Normalised Concentration						
Run	1	2	3	4	5	6	7
N.Time	rpm 10	45	80	104	134	150	180
0.000	0.000	0.000	0.000	0.000	0.000	0.000	0.000
0.020	0.000	0.451	0.348	0.567	0.673	0.579	0.821
0.041	0.321	0.862	0.727	0.769	0.910	0.876	0.953
0.061	0.471	0.867	0.893	0.920	0.955	0.962	0.961
0.081	0.691	0.889	0.945	0.957	0.929	0.913	0.942
0.122	0.961	0.921	0.949	0.947	0.910	0.904	0.918
0.163	0.881	0.916	0.901	0.905	0.890	0.886	0.895
0.204	0.881	0.886	0.881	0.882	0.880	0.872	0.878
0.244	0.861	0.874	0.852	0.852	0.841	0.830	0.826
0.285	0.851	0.840	0.820	0.819	0.808	0.804	0.809
0.326	0.841	0.800	0.781	0.782	0.770	0.767	0.769
0.367	0.821	0.761	0.745	0.740	0.743	0.743	0.739
0.407	0.770	0.730	0.712	0.727	0.699	0.710	0.703
0.448	0.736	0.710	0.682	0.680	0.663	0.676	0.679
0.489	0.697	0.670	0.677	0.643	0.634	0.639	0.631
0.530	0.660	0.631	0.646	0.640	0.610	0.620	0.620
0.571	0.630	0.612	0.623	0.615	0.590	0.592	0.606
0.612	0.602	0.582	0.584	0.590	0.571	0.581	0.581
0.653	0.582	0.550	0.560	0.562	0.543	0.559	0.550
0.693	0.550	0.523	0.532	0.542	0.521	0.527	0.517
0.734	0.523	0.505	0.510	0.521	0.505	0.496	0.496
0.775	0.509	0.499	0.487	0.500	0.481	0.477	0.486
0.816	0.490	0.472	0.457	0.474	0.460	0.458	0.476
0.856	0.470	0.452	0.439	0.461	0.437	0.440	0.456
0.897	0.456	0.444	0.429	0.437	0.419	0.420	0.436
0.938	0.437	0.421	0.407	0.409	0.404	0.410	0.416
0.979	0.404	0.406	0.391	0.388	0.389	0.380	0.399
1.020	0.368	0.389	0.370	0.375	0.376	0.368	0.380
1.101	0.367	0.365	0.340	0.346	0.336	0.339	0.341
1.183	0.327	0.319	0.317	0.310	0.306	0.307	0.309
1.264	0.301	0.300	0.300	0.297	0.286	0.285	0.291
1.346	0.282	0.287	0.289	0.263	0.261	0.270	0.267
1.427	0.241	0.271	0.281	0.240	0.247	0.241	0.241
1.509	0.241	0.251	0.261	0.220	0.226	0.229	0.226
1.591	0.229	0.239	0.229	0.207	0.207	0.203	0.206
1.672	0.207	0.199	0.207	0.187	0.186	0.194	0.190
1.754	0.178	0.181	0.187	0.180	0.167	0.178	0.186
1.835	0.157	0.162	0.153	0.162	0.154	0.160	0.166
1.917	0.147	0.147	0.141	0.143	0.147	0.147	0.150
1.998	0.126	0.130	0.129	0.122	0.139	0.137	0.135
(q/Q)	2.18	9.81	17.4	22.7	29.2	32.7	39.3

Impulse Response Experiments

$2\frac{1}{2}$" dia. Turbine 9"/9" Cylindrical System. Viscosity 1.35 cp.

R.5 Unbaffled Feed to Impeller

	Normalised Concentration					
Run	1	2	3	4	5	6
N.Time	rpm 15	30	70	100	140	220
0.000	1.227	1.950	1.618	1.023	1.508	1.200
0.022	1.390	2.960	1.915	1.300	1.201	1.017
0.044	2.760	2.104	1.413	1.105	0.960	0.921
0.056	1.951	2.014	1.110	1.058	0.929	0.874
0.111	1.105	0.952	0.814	0.840	0.875	0.835
0.167	0.837	0.663	0.772	0.794	0.822	0.769
0.222	0.707	0.564	0.719	0.768	0.808	0.782
0.278	0.618	0.531	0.687	0.747	0.754	0.717
0.333	0.610	0.498	0.645	0.686	0.700	0.665
0.389	0.520	0.457	0.645	0.677	0.646	0.665
0.444	0.512	0.457	0.603	0.596	0.630	0.626
0.500	0.512	0.457	0.561	0.581	0.606	0.613
0.556	0.480	0.424	0.518	0.573	0.539	0.574
0.611	0.455	0.400	0.508	0.526	0.552	0.522
0.667	0.423	0.400	0.465	0.500	0.498	0.509
0.722	0.415	0.391	0.476	0.488	0.485	0.456
0.778	0.390	0.358	0.423	0.433	0.444	0.456
0.833	0.390	0.338	0.434	0.433	0.444	0.456
0.889	0.358	0.334	0.381	0.422	0.377	0.417
0.944	0.358	0.301	0.361	0.397	0.377	0.407
1.000	0.325	0.301	0.349	0.372	0.377	0.365
1.111	0.317	0.292	0.307	0.337	0.337	0.352
1.222	0.293	0.260	0.296	0.302	0.283	0.300
1.333	0.260	0.227	0.254	0.270	0.283	0.261
1.444	0.219	0.194	0.222	0.229	0.229	0.248
1.500	0.220	0.202	0.222	0.205	0.215	0.239
1.611	0.195	0.194	0.222	0.198	0.202	0.196
1.722	0.195	0.189	0.169	0.169	0.180	0.190
1.833	0.187	0.170	0.164	0.162	0.164	0.190
1.944	0.172	0.165	0.164	0.162	0.160	0.180
2.000	0.152	0.149	0.150	0.156	0.156	0.143
(q/Q)	3.6	7.2	16.8	24.0	33.6	52.8

Impulse Response Experiments

$2\frac{1}{2}$" dia. Turbine 9"/9" Cylindrical System. Viscosity 1.35cp.

R.6 Unbaffled Feed to Loop

Run	Normalised Concentration 1	2	3	4	5	6
N.Time	rpm 15	45	90	140	180	220
0.000	0.000	0.000	0.000	0.000	0.000	0.000
0.022	1.321	1.167	0.268	0.315	0.432	0.758
0.044	2.761	1.861	0.701	0.857	0.941	0.924
0.056	2.218	2.112	0.875	0.858	0.866	0.977
0.111	1.855	1.123	0.930	0.900	0.874	0.884
0.167	0.981	0.893	0.875	0.858	0.808	0.818
0.222	0.649	0.768	0.842	0.815	0.779	0.789
0.278	0.502	0.701	0.799	0.762	0.750	0.760
0.333	0.493	0.624	0.744	0.762	0.721	0.730
0.389	0.502	0.614	0.711	0.688	0.663	0.672
0.444	0.493	0.586	0.656	0.678	0.634	0.642
0.500	0.456	0.547	0.656	0.635	0.613	0.620
0.556	0.456	0.499	0.613	0.593	0.584	0.591
0.611	0.428	0.470	0.569	0.551	0.547	0.554
0.667	0.391	0.461	0.536	0.519	0.518	0.525
0.722	0.391	0.422	0.525	0.519	0.497	0.503
0.778	0.354	0.394	0.492	0.466	0.468	0.473
0.833	0.345	0.384	0.449	0.466	0.460	0.466
0.889	0.318	0.384	0.419	0.434	0.439	0.444
0.944	0.318	0.346	0.394	0.424	0.402	0.407
1.000	0.308	0.317	0.394	0.392	0.381	0.385
1.111	0.272	0.278	0.361	0.339	0.352	0.356
1.222	0.244	0.269	0.317	0.307	0.315	0.319
1.333	0.207	0.230	0.281	0.265	0.286	0.290
1.444	0.198	0.192	0.271	0.254	0.261	0.261
1.500	0.170	0.183	0.231	0.212	0.230	0.239
1.611	0.161	0.163	0.206	0.200	0.203	0.210
1.722	0.161	0.164	0.179	0.180	0.184	0.191
1.833	0.134	0.146	0.165	0.165	0.172	0.178
1.944	0.124	0.126	0.149	0.156	0.160	0.162
2.000	0.119	0.126	0.130	0.142	0.141	0.149
(q/Q)	3.6	10.8	21.6	33.6	43.2	52.8

Impulse Response Experiments

$2\frac{1}{2}$" dia. Turbine 9"/9" Cylindrical System. Viscosity 1.35cp.

R.7 Baffled Feed to Impeller

	Normalised Concentration					
Run	1	2	3	4	5	6
N.Time	rpm 15	30	70	100	140	220
0.000	1.402	0.200	0.000	0.000	1.451	1.170
0.022	0.711	1.293	1.223	1.367	1.072	1.072
0.044	1.765	1.033	1.226	1.228	0.948	0.948
0.056	1.565	1.147	1.271	1.129	0.948	0.863
0.111	1.076	1.045	0.797	0.881	0.882	0.802
0.167	0.742	0.999	0.739	0.852	0.844	0.780
0.222	0.652	0.740	0.673	0.788	0.806	0.724
0.278	0.644	0.666	0.640	0.739	0.730	0.703
0.333	0.611	0.601	0.606	0.710	0.692	0.688
0.389	0.587	0.592	0.565	0.682	0.683	0.647
0.444	0.546	0.564	0.540	0.625	0.616	0.619
0.500	0.546	0.555	0.507	0.597	0.616	0.591
0.556	0.522	0.518	0.507	0.561	0.569	0.563
0.611	0.489	0.490	0.473	0.533	0.541	0.528
0.667	0.481	0.453	0.440	0.511	0.503	0.500
0.722	0.448	0.444	0.432	0.483	0.493	0.472
0.778	0.416	0.407	0.407	0.455	0.465	0.451
0.833	0.416	0.399	0.399	0.426	0.427	0.444
0.889	0.391	0.399	0.365	0.398	0.417	0.423
0.944	0.350	0.370	0.341	0.369	0.379	0.388
1.000	0.359	0.370	0.341	0.362	0.379	0.378
1.111	0.318	0.333	0.333	0.338	0.331	0.360
1.222	0.293	0.296	0.299	0.297	0.313	0.339
1.333	0.261	0.268	0.266	0.256	0.275	0.311
1.444	0.253	0.222	0.241	0.247	0.228	0.283
1.500	0.228	0.222	0.233	0.199	0.201	0.251
1.611	0.220	0.222	0.216	0.199	0.189	0.226
1.722	0.196	0.157	0.180	0.178	0.176	0.199
1.833	0.163	0.148	0.162	0.157	0.159	0.184
1.944	0.163	0.111	0.135	0.137	0.147	0.170
2.000	0.147	0.111	0.127	0.119	0.141	0.152
(q/Q)	3.6	7.2	16.8	24.0	33.6	52.8

Impulse Response Experiments

$2\frac{1}{2}$" dia. Turbine 9"/9" Cylindrical System. Viscosity 1.35cp.

R.8 Baffled Feed to Loop

	Normalised Concentration					
Run	1	2	3	4	5	6
N.Time	rpm 15	45	90	140	180	220
0.000	0.000	0.000	0.000	0.000	0.000	0.000
0.022	0.000	0.000	0.186	0.321	0.420	0.520
0.044	1.616	1.261	0.506	0.716	0.867	0.962
0.056	2.617	1.786	0.961	0.892	0.953	0.924
0.111	1.389	1.003	0.876	0.857	0.953	0.924
0.167	0.935	0.817	0.826	0.821	0.894	0.861
0.222	0.794	0.735	0.769	0.786	0.858	0.821
0.278	0.641	0.681	0.734	0.741	0.846	0.790
0.333	0.527	0.620	0.712	0.706	0.811	0.766
0.389	0.507	0.593	0.677	0.670	0.761	0.734
0.444	0.481	0.573	0.620	0.644	0.704	0.695
0.500	0.421	0.546	0.591	0.608	0.669	0.671
0.556	0.447	0.512	0.561	0.599	0.621	0.632
0.611	0.401	0.491	0.534	0.573	0.609	0.600
0.667	0.374	0.464	0.513	0.528	0.574	0.576
0.722	0.347	0.430	0.477	0.493	0.527	0.576
0.778	0.340	0.403	0.456	0.496	0.515	0.505
0.833	0.320	0.383	0.446	0.422	0.479	0.505
0.889	0.314	0.376	0.427	0.422	0.420	0.474
0.944	0.287	0.356	0.392	0.395	0.420	0.450
1.000	0.267	0.329	0.392	0.360	0.385	0.408
1.111	0.240	0.293	0.342	0.351	0.337	0.379
1.222	0.214	0.268	0.306	0.315	0.325	0.347
1.333	0.187	0.247	0.278	0.289	0.278	0.324
1.444	0.160	0.220	0.249	0.253	0.243	0.292
1.500	0.160	0.220	0.221	0.244	0.231	0.241
1.611	0.127	0.186	0.199	0.208	0.203	0.203
1.722	0.127	0.166	0.181	0.187	0.181	0.185
1.833	0.110	0.162	0.170	0.172	0.172	0.175
1.944	0.110	0.154	0.156	0.157	0.154	0.165
2.000	0.106	0.137	0.141	0.143	0.149	0.152
(q/Q)	3.6	10.8	21.6	33.6	43.2	52.8

Impulse Response Experiments

$2\frac{1}{2}$" dia. Turbine 9"/9" Cylindrical System. Viscosity 2.55cp

R.9 Unbaffled Feed to Impeller

	Normalised Concentration					
Run	1	2	3	4	5	6
N.Time rpm	15	45	90	140	180	220
0.000	0.000	0.000	0.000	0.000	0.000	0.000
0.022	0.960	2.462	1.303	1.288	1.065	0.954
0.044	2.792	1.810	1.118	0.981	0.933	0.862
0.056	1.820	1.346	1.003	0.920	0.876	0.832
0.111	1.310	0.807	0.813	0.841	0.799	0.781
0.167	1.007	0.695	0.749	0.796	0.788	0.739
0.222	0.768	0.653	0.711	0.765	0.712	0.729
0.278	0.647	0.653	0.699	0.689	0.701	0.698
0.333	0.564	0.653	0.660	0.674	0.668	0.668
0.389	0.515	0.597	0.648	0.623	0.624	0.626
0.444	0.478	0.597	0.597	0.589	0.613	0.616
0.500	0.379	0.583	0.597	0.567	0.569	0.585
0.556	0.379	0.526	0.559	0.567	0.537	0.544
0.611	0.379	0.526	0.546	0.551	0.526	0.544
0.667	0.351	0.470	0.508	0.521	0.493	0.503
0.722	0.331	0.490	0.508	0.505	0.493	0.503
0.778	0.331	0.428	0.457	0.444	0.449	0.462
0.833	0.316	0.428	0.457	0.429	0.438	0.452
0.889	0.268	0.428	0.445	0.444	0.438	0.421
0.944	0.268	0.414	0.406	0.388	0.394	0.421
1.000	0.278	0.372	0.394	0.368	0.365	0.380
1.111	0.268	0.358	0.343	0.348	0.350	0.351
1.222	0.200	0.302	0.325	0.322	0.318	0.339
1.333	0.189	0.280	0.294	0.306	0.318	0.298
1.444	0.189	0.260	0.254	0.270	0.274	0.288
1.500	0.152	0.246	0.221	0.261	0.263	0.246
1.611	0.142	0.226	0.218	0.230	0.249	0.226
1.722	0.131	0.206	0.206	0.199	0.210	0.205
1.833	0.126	0.184	0.189	0.176	0.189	0.186
1.944	0.116	0.176	0.167	0.159	0.175	0.176
2.000	0.106	0.157	0.135	0.137	0.156	0.151
(q/Q)	3.6	10.8	21.6	33.6	43.2	52.8

Impulse Response Experiments

$2\frac{1}{2}$" dia. Turbine 9"/9" Cylindrical System. Viscosity 2.55cp.

R.10 Unbaffled Feed to Loop

	Normalised Concentration					
-Run	1	2	3	4	5	6
N.Time	rpm 15	45	90	140	180	220
0.000	0.000	0.000	0.000	0.000	0.000	0.000
0.022	1.671	0.046	0.170	0 320	0.470	0.702
0.044	2.350	1.480	0 460	0.720	0.818	0.910
0.056	2.201	1.498	0.653	0.897	0.923	0.886
0.111	1.555	0.957	0.828	0.876	0.830	0.828
0.167	1.002	0.871	0.828	0.816	0.809	0.782
0.222	0.726	0.818	0.773	0.779	0.769	0.736
0.278	0.541	0.742	0.737	0.779	0.755	0.736
0.333	0.541	0.699	0.740	0.730	0.701	0.702
0.389	0.553	0.688	0.697	0.670	0.647	0.644
0.444	0.553	0.645	0.642	0.633	0.647	0.644
0.500	0.450	0.602	0.610	0.625	0.553	0.564
0.611	0.490	0.590	0.566	0.577	0.540	0.552
0.667	0.443	0.516	0.555	0.536	0.540	0.506
0.722	0.403	0.516	0.512	0.517	0.499	0.506
0.778	0.403	0.473	0.523	0.501	0.486	0.472
0.833	0.397	0.473	0.479	0.487	0.445	0.472
0.889	0.357	0.441	0.468	0.438	0.445	0.426
0.944	0.369	0.430	0.426	0.426	0.432	0.414
1.000	0.323	0.398	0.381	0.390	0.378	0.380
1.111	0.311	0.344	0.338	0.341	0.337	0.322
1.222	0.277	0.301	0.294	0.319	0.283	0.288
1.333	0.265	0.269	0.270	0.280	0.283	0.288
1.444	0.219	0.258	0.268	0.243	0.243	0.242
1.500	0.219	0.258	0.250	0.223	0.218	0.220
1.611	0.184	0.226	0.218	0.203	0.196	0.197
1.722	0.162	0.195	0.198	0.183	0.179	0.186
1.833	0.138	0.172	0.170	0.170	0.167	0.170
1.944	0.138	0.172	0.161	0.151	0.153	0.149
2.000	0.126	0.149	0.148	0.127	0.137	0.129
(q/Q)	3.6	10.8	21.6	33.6	43.2	52.8

Impulse Response Experiments

$2\frac{1}{2}$" dia. Turbine 9"/9" Cylindrical System. Viscosity 2.55cp.

R.11 Baffled Feed to Impeller

	Normalised Concentration					
Run	1	2	3	4	5	6
N.Time	rpm 15	45	90	140	180	220
0.000	0.000	0.000	0.000	0.767	0.913	1.025
0.022	2.429	1.299	1.447	1.230	1.050	0.992
0.044	2.086	1.981	1.238	0.914	0.919	0.862
0.056	1.817	1.921	1.103	0.847	0.867	0.853
0.111	1.181	0.731	0.810	0.761	0.820	0.814
0.167	0.977	0.762	0.779	0.723	0.776	0.778
0.222	0.886	0.688	0.727	0.685	0.740	0.747
0.278	0.704	0.665	0.685	0.646	0.690	0.708
0.333	0.636	0.601	0.654	0.656	0.651	0.698
0.389	0.545	0.643	0.643	0.617	0.621	0.659
0.444	0.545	0.603	0.612	0.579	0.589	0.621
0.500	0.545	0.587	0.5700	0.579	0.560	0.591
0.556	0.432	0.561	0.559	0.541	0.539	0.582
0.611	0.432	0.521	0.518	0.503	0.513	0.543
0.667	0.454	0.503	0.518	0.503	0.503	0.514
0.722	0.432	0.468	0.476	0.464	0.480	0.475
0.778	0.432	0.468	0.444	0.464	0.461	0.475
0.833	0.393	0.432	0.434	0.426	0.428	0.436
0.889	0.393	0.412	0.392	0.416	0.421	0.436
0.944	0.363	0.412	0.392	0.416	0.400	0.398
1.000	0.343	0.383	0.361	0.380	0.386	0.388
1.111	0.293	0.361	0.320	0.349	0.332	0.320
1.222	0.281	0.307	0.277	0.302	0.301	0.310
1.333	0.250	0.271	0.277	0.311	0.278	0.281
1.444	0.220	0.243	0.224	0.263	0.260	0.242
1.500	0.203	0.218	0.235	0.235	0.234	0.233
1.611	0.180	0.201	0.225	0.205	0.213	0.204
1.722	0.169	0.184	0.193	0.187	0.197	0.194
1.833	0.152	0.159	0.169	0.158	0.180	0.179
1.944	0.147	0.143	0.154	0.147	0.160	0.162
2.000	0.137	0.129	0.139	0.132	0.142	0.151
(q/Q)	3.6	10.8	21.6	33.6	43.2	52.8

Impulse Response Experiments

$2\frac{1}{2}$" dia. Turbine 9"/9" Cylindrical System. Viscosity 2.55cp.

R.12 Baffled Feed to Loop

	Normalised Concentration					
Run	1	2	3	4	5	6
N.Time	rpm 15	45	90	140	180	220
0.000	0.000	0.000	0.000	0.000	0.000	0.000
0.022	2.534	0.048	0.547	0.407	0.433	0.466
0.044	2.339	1.647	0.957	0.921	0.911	0.937
0.056	2.222	1.467	0.929	0.895	0.867	0.885
0.111	1.339	0.929	0.780	0.855	0.847	0.853
0.167	1.091	0.843	0.780	0.814	0.805	0.799
0.222	0.770	0.776	0.745	0.784	0.762	0.757
0.278	0.653	0.737	0.699	0.743	0.720	0.725
0.333	0.585	0.699	0.687	0.692	0.710	0.714
0.389	0.507	0.661	0.652	0.661	0.678	0.682
0.444	0.429	0.613	0.641	0.651	0.625	0.629
0.500	0.390	0.613	0.594	0.621	0.593	0.629
0.556	0.341	0.584	0.559	0.570	0.593	0.597
0.611	0.390	0.536	0.547	0.539	0.540	0.544
0.667	0.351	0.507	0.512	0.488	0.508	0.501
0.722	0.341	0.469	0.512	0.488	0.508	0.501
0.778	0.312	0.469	0.466	0.458	0.466	0.501
0.833	0.273	0.421	0.454	0.448	0.466	0.469
0.889	0.273	0.421	0.454	0.417	0.424	0.426
0.944	0.302	0.383	0.408	0.407	0.424	0.426
1.000	0.263	0.354	0.373	0.381	0.384	0.384
1.111	0.224	0.316	0.373	0.366	0.339	0.373
1.222	0.195	0.306	0.326	0.326	0.326	0.330
1.333	0.195	0.268	0.314	0.285	0.285	0.288
1.444	0.185	0.239	0.280	0.254	0.286	0.288
1.500	0.156	0.230	0.268	0.244	0.254	0.245
1.611	0.156	0.230	0.268	0.244	0.244	0.245
1.722	0.146	0.201	0.221	0.204	0.201	0.204
1.833	0.127	0.163	0.183	0.173	0.169	0.184
1.944	0.107	0.153	0.161	0.163	0.157	0.163
2.000	0.107	0.148	0.151	0.153	0.150	0.147
(q/Q)	3.6	10.8	21.6	33.6	43.2	52.8

Impulse Response Experiments

$2\frac{1}{2}$" dia. Turbine 9"/9" CYlindrical System. Viscosity 7.65cp

R.13 Unbaffled Feed to Impeller

	Normalised Concentration					
Run	1	2	3	4	5	6
N.Time	rpm 15	45	90	140	180	220
0.000	0.000	0.000	0.000	0.000	0.000	0.000
0.022	0.601	0.672	0.780	0.880	0.760	0.680
0.044	1.971	1.342	1.056	0.968	1.002	0.931
0.056	2.952	i.561	0.903	0.945	0.933	0.870
0.111	2.166	0.878	0.831	0.876	0.907	0.866
0.167	1.424	0.900	0.793	0.845	0.863	0.831
0.220	0.864	0.974	0.771	0.802	0.794	0.778
0.278	0.708	0.703	0.722	0.746	0.768	0.742
0.333	0.569	0.657	0.683	0.702	0.699	0.707
0.389	0.517	0.635	0.634	0.671	0.664	0.672
0.444	0.469	0.584	0.617	0.628	0.620	0.636
0.500	0.469	0.522	0.600	0.603	0.586	0.605
0.556	0.399	0.516	0.546	0.572	0.560	0.565
0.611	0.395	0.454	0.508	0.547	0.516	0.552
0.667	0.360	0.454	0.486	0.503	0.490	0.512
0.722	0.343	0.432	0.464	0.472	0.482	0.495
0.778	0.308	0.381	0.442	0.472	0.456	0.464
0.833	0.291	0.387	0.420	0.429	0.421	0.446
0.889	0.273	0.387	0.398	0.404	0.377	0.429
0.944	0.261	0.364	0.370	0.404	0.361	0.411
1.000	0.243	0.313	0.354	0.379	0.361	0.389
1.111	0.226	0.296	0.305	0.329	0.317	0.353
1.222	0.204	0.268	0.283	0.304	0.273	0.318
1.333	0.191	0.251	0.239	0.273	0.247	0.283
1.444	0.174	0.229	0.220	0.249	0.213	0.252
1.500	0.156	0.206	0.205	0.230	0.204	0.234
1.611	0.152	0.178	0.198	0.198	0.199	0.216
1.722	0.139	0.155	0.156	0.174	0.167	0.199
1 833	0.139	0.138	0.151	0.174	0.156	0.177
1.944	0.122	0.138	0.129	0.149	0.149	0.163
2.000	0.122	0.128	0.134	0.144	0.1422	0.146
(q/Q)	3.6	10.8	21.6	33.6	43.2	52.8

Impulse Response Experiments

$2\frac{1}{2}$" dia. Turbine 9"/9" Cylindrical System Viscosity 7.65cp

R.14 Unbaffled Feed to Loop

	Normalised Concentration					
Run	1	2	3	4	5	6
N.Time	rpm15	45	90	140	180	220
0.000	0.000	0.000	0.000	0.000	0.000	0.000
0.022	0.006	0.002	0.042	0.237	0.416	0.512
0.044	1.500	1.200	0.953	0.553	0.725	0.777
0.056	2.375	1.482	0.953	0.702	0.806	0.825
0.111	2.987	1 000	0.953	0.856	0.863	0.883
0.167	1.811	0.865	0.888	0.851	0.845	0.825
0.220	1.117	0.845	0.842	0.808	0.815	0.777
0.278	0.733	0.760	0.814	0.766	0.756	0.729
0.333	0.567	0.740	0.768	0.729	0.736	0.699
0.389	0.442	0.70π	0.703	0.686	0.690	0.675
0.444	0.401	0.659	0.694	0.659	0.641	0.630
0.500	0.370	0.619	0.620	0.617	0.601	0.608
0.556	0.332	0.584	0.592	0.596	0.590	0.584
0.611	0.315	0.564	0 555	0.553	0.562	0.536
0.667	0.290	0.539	0.518	0.532	0.542	0.506
0.772	0.273	0.504	0.518	0.511	0.515	0.488
0.778	0.263	0.479	0.472	0.473	0.481	0.458
0.833	0.249	0.444	0.435	0.452	0.453	0.434
0.889	0.232	0.424	0.418	0.431	0.427	0.434
0.944	0.221	0.399	0.398	0.415	0.427	0.392
1.000	0.2o7	0.384	0.367	0.388	0.400	0.385
1.111	0.176	0.343	0.363	0.367	0.346	0.337
1.222	0.160	0.303	0.296	0.324	0.319	0.319
1.333	0.152	0.278	0.289	0.298	0.291	0.271
1.444	0.138	o.238	0.242	0.261	0.264	0.247
1.500	0.122	0.218	0.222	0.255	0.244	0.247
1.611	0.111	0.203	0.199	0.239	0.217	0.223
1.722	0.093	0.178	0.218	0.210	0.211	0.199
1.833	0.080	0.163	0.168	0.191	0.190	0.169
1.944	0.069	0.138	0.154	0.170	0.156	0.172
2.000	0.069	0.132	0.142	0.161	0.142	0.160
(q/Q)	3.6	10.8	21.6	33.6	43.2	52.8

Impulse Response Experiments

$2\frac{1}{2}$" dia Turbine 9"/9" Cylindrical System Viscosity 7.65cp

R.15 Baffled Feed to Impeller

		Normalised Concentration				
Run	1	2	3	4	5	6
N.Time	rpm15	45	90	140	180	220
0.000	0.000	0.000	0.000	0.000	0.000	0.000
0.022	0.230	1.558	0.320	0.994	0.956	0.848
0.044	0.980	1.644	1.049	0.899	0.929	0.966
0.056	1.517	2.293	0.953	0.915	0.935	0.882
0.111	1.794	1.619	0.928	0.866	0.874	0.882
0.167	1.479	1.010	0.877	0.811	0.846	0.823
0.220	1.277	0.807	0.827	0.783	0.789	0.776
0.278	1.075	0.690	0.770	0.748	0.764	0.743
0.333	0.646	0.629	0.725	0.692	0.708	0.716
0.389	0.568	0.589	0.700	0.665	0.688	0.663
0.444	0.631	0.548	0.649	0.644	0.633	0.644
0.500	0.769	0.507	0.624	0.609	0.605	0.610
0.556	0.558	0.482	0.599	0.581	0.571	0.564
0.611	0.585	0.447	0.567	0.553	0.550	0.537
0.667	0.555	0.426	0.523	0.532	0.523	0.504
0.722	0.318	0.406	0.497	0.504	0.495	0.484
0.778	0.366	0.381	0.472	0.477	0.468	0.451
0.833	0.328	0.365	0.466	0.442	0.440	0.431
0.889	0.255	0.340	0.440	0.421	0.413	0.425
0.944	0.194	0.320	0.396	0.393	0.385	0.398
1.000	0.167	0.304	0.390	0.393	0.381	0.378
1.111	0.152	0.279	0.345	0.358	0.351	0.325
1.222	0.139	0.244	0.320	0.303	0.296	0.299
1.332	0.114	0.223	0.288	0.275	0.268	0.272
1.444	0.117	0.198	0.263	0.248	0.241	0.239
1.500	0.114	0.183	0.244	0.247	0.22o	0.219
1.611	0.101	0.162	0.219	0.226	0.220	0.212
1.722	0.688	0.162	0.193	0.191	0.193	0.186
1.833	0.076	0.147	0.162	0.170	0.165	0.166
1.944	0.079	0.137	0.163	0.171	0.158	0.159
2.000	0.079	0.137	0.162	0.171	0.158	0.159
(q/Q)	3.6	10.8	21.6	33.6	43,2	52.8

Impulse Response Experiments

$2\frac{1}{2}$" dia. Turbine 9"/9" Cylindrical System Viscosity 7.65cp

R.16 Baffled Feed to Loop

Normalised Concentration						
Run	1	2	3	4	5	6
N.Time	rpm 15	45	90	140	180	220
0.000	0.000	0.000	0.000	0.000	0.000	0.000
0.022	0.342	0.000	0.000	0.060	0.586	0.350
0.044	2.445	0.945	0.589	0.918	0.849	0.787
0.056	2.878	1.193	0.782	0.918	0.876	0.823
0.111	1.810	1.173	0.844	0.896	0.896	0.917
0.167	1.175	1.172	0.867	0.867	0.851	0.870
0.220	0.928	0.964	0.844	0.806	0.815	0.823
0.278	0.780	0.879	0.813	0.769	0.770	0.777
0.333	0.671	0.777	0.751	0.717	0.734	0.749
0.389	0.578	0.707	0.713	0.687	0.694	0.701
0.444	0.490	0.657	0.689	0.649	0.648	0.677
0.500	0.424	0.622	0.651	0.620	0.628	0.631
0.556	0.381	0.572	0.620	0.567	0.592	0.607
0.611	0.359	0.536	0.589	0.537	0.552	0.566
0.667	0.327	0.507	0.534	0.500	0.527	0.543
0.722	0.320	0.457	0.534	0.500	0.491	0.514
0.778	0.293	0.429	0.496	0.470	0.466	0.491
0.833	0.277	0.400	0.472	0.448	0.446	0.450
0.889	0.255	0.364	0.434	0.411	0.430	0.426
0.944	0.249	0.364	0.410	0.388	0.410	0.397
1.000	0.233	0.336	0.403	0.381	0.390	0.380
1.056	0.205	0.314	0.379	0.357	0.370	0.374
1.111	0.205	0.307	0.341	0.321	0.349	0.356
1.222	0.211	0.250	0.310	0.299	0.309	0.304
1.333	0.183	0.229	0.279	0.269	0.289	0.286
1.444	0.189	0.200	0.256	0.239	0.248	0.257
1.500	0.162	0.193	0.256	0.239	0.243	0.257
1.611	0.162	0.171	0.225	0.209	0.223	0.216
1.722	0.145	0.136	0.194	0.179	0.203	0.187
1.833	0.118	0.114	0.194	0.179	0.182	0.164
1.944	0.118	0.107	0.155	0.142	0.162	0.164
2.000	0.118	0.107	0.147	0.138	0.147	0.151
(q/Q)	3.6	10.8	21.6	33.6	43.2	52.8

Impulse Response Experiments

4" dia. Turbine 19"/19" Cylindrical System

R.20 Unbaffled ½"dia. Inlet Feed to Impeller

	Normalised Concentration						
Run	1	2	3	4	5	6	7
N.Time	rpm26	51	71	101	120	150	180
0.000	0.000	0.000	0.000	0.487	0.593	1.784	1.521
0.020	1.361	1.515	1.561	1.211	1.165	1.131	1.060
0.041	1.047	0.831	0.990	0.861	0.871	0.952	0.992
0.062	0.941	0.914	0.941	0.817	0.861	0.931	0.965
0.082	0.817	0.878	0.851	0.827	0.827	0.827	0.948
0.122	0.790	0.830	0.800	0.793	0.795	0.837	0.918
0.204	0.732	0.750	0.747	0.733	0.742	0.802	0.845
0.285	0. 671	0.703	0.705	0.699	0.689	0.736	0.782
0.367	0.616	0.643	0.649	0.643	0.636	0.685	0.723
0.449	0.586	0.595	0.609	0.600	0.604	0.634	0.664
0.530	0.528	0.548	0.556	0.555	0.553	0.583	0.609
0.612	0.506	0.500	0.524	0.518	0.508	0.544	0.565
0.693	0.458	0.464	0.492	0.476	0.479	0.496	0.521
0.775	0.421	0.432	0.437	0.439	0.425	0.455	0.476
0.856	0.383	0.404	0.405	0.405	0.393	0.420	0.432
0.938	0.361	0.368	0.383	0.362	0.369	0.382	0.399
1.020	0.332	0.341	0.352	0.348	0.338	0.353	0.355
1.101	0.305	0.305	0.330	0.317	0.306	0.318	0.325
1.183	0.276	0.277	0.291	0.283	0.284	0.292	0.296
1.264	0.254	0.257	0.259	0.260	0.255	0.267	0.266
1.347	0.227	0.241	0.245	0.237	0.231	0.241	0.241
1.427	0.208	0.213	0.224	0.215	0.212	0.216	0.211
1.509	0.186	0.193	0.195	0.203	0.191	0.200	0.194
1.591	0.169	0.181	0.181	0.178	0.167	0.174	0.167
1.672	0.147	0.163	0.173	0.158	0.156	0.152	0.152
1.754	0.140	0.149	0.150	0.147	0.138	0.139	0.121
1.835	0.118	0.139	0.131	0.124	0.124	0.126	0.126
1.917	0.108	0.132	0.121	0.113	0.106	0.111	0.107
1.998	0.096	0.13o	0.110	0.101	0.095	0.099	0.098
(q/Q)	4.9	9.65	13.4	19.11	22.7	28.4	34.0

Impulse Response Experiments

4" dia. Turbine 19"/19" Cylindrical System

R.21 Unbaffled ½"dia. Inlet Feed to Loop

	Normalised Concentration						
Run	1	2	3	4	5	6	7
N.Timerpm	26	42	68	96	120	160	200
0.000	0.000	0.000	0.000	0.000	0.000	0.000	0.000
0.020	0.898	0.761	0.510	0.621	0.681	0.721	0.810
0.041	1.288	1.114	0.920	0.945	0.954	0.935	0.960
0.062	0.987	0.978	0.952	0.930	0.960	0.929	0.951
0.082	0.878	0.920	0.951	0.898	0.970	0.901	0.936
0.122	0.890	0.876	0.882	0.865	0.921	0.867	0.903
0.204	0.820	0.811	0.812	0.804	0.845	0.803	0.810
0.285	0.760	0.767	0.746	0.787	0.787	0.737	0.748
0.367	0.697	0.692	0.701	0.697	0.725	0.690	0.702
0.449	0.645	0.640	0.654	0.677	0.677	0.631	0.640
0.530	0.599	0.594	0.607	0.589	0.616	0.598	0.597
0.612	0.550	0.553	0.553	0.550	0.576	0.549	0.550
0.693	0.510	0.503	0.496	0.511	0.530	0.516	0.517
0.775	0.473	0.468	0.450	0.464	0.478	0.482	0.469
0.856	0.427	0.434	0.424	0.435	0.442	0.440	0.425
0.938	0.391	0.398	0.401	0.383	0.405	0.405	0.392
1.020	0.354	0.347	0.371	0.357	0.356	0.373	0.370
1.101	0.314	0.333	0.344	0.327	0.322	0.346	0.337
1.183	0.280	0.292	0.310	0.305	0.284	0.322	0.302
1.264	0.265	0.268	0.276	0.265	0.284	0.287	0.267
1.346	0.231	0.235	0.244	0.246	0.295	0.261	0.262
1.427	0.207	0.224	0.222	0.217	0.200	0.245	0.239
1.509	0.191	0.184	0.207	0.185	0.231	0.231	0.217
1.591	0.167	0.173	0.153	0.190	0.178	0.221	0.201
1.672	0.154	0.159	0.138	0.170	0.160	0.201	0.187
1.754	0.130	0.148	0.111	0.151	0.195	0.179	0.170
1.835	0.118	0.129	0.111	0.131	0.125	0.161	0.149
1.917	0.108	0.116	0.103	0.112	0.108	0.136	0.132
1.998	0.102	0.106	0.099	0.102	0.100	0.119	0.116
(q/Q)	4.9	7.95	13.4	18.4	22.7	30.3	37.9

Impulse Response Experiments

4"dia. Turbine 19"/19" Cylindrical System

R.22 Baffled ½"dia. Inlet Feed to Impeller

	Normalised Concentration						
Run	1	2	3	4	5	6	7
N. Timerpm	26	51	71	101	120	150	180
0.000	0.000	0.000	0.000	0.000	0.000	0.693	0.730
0.020	0.601	1.200	1.402	1.130	1.100	1.661	1.062
0.041	1.175	0.671	1.286	0.944	0.887	0.915	0.938
0.062	1.014	1.110	0.960	0.900	0.842	0.905	0.912
0.082	0.808	0.810	0.863	0.844	0.805	0.856	0.896
0.122	0.791	0.792	0.790	0.835	0.774	0.820	0.844
0.204	0.740	0.720	0.732	0.764	0.730	0.775	0.798
0.285	0.674	0.680	0.691	0.716	0.674	0.725	0.731
0.367	0.626	0.631	0.648	0.656	0.626	0.657	0.692
0.449	0.584	0.590	0.600	0.607	0.584	0.621	0.641
0.530	0.546	0.553	0.560	0.571	0.546	0.573	0.585
0.612	0.509	0.510	0.517	0.515	0.506	0.535	0.524
0.693	0.456	0.471	0.479	0.491	0.463	0.488	0.498
0.775	0.429	0.443	0.443	0.453	0.454	0.444	0.459
0.856	0.383	0.403	0.419	0.405	0.413	0.408	0.420
0.938	0.354	0.371	0.368	0.370	0.386	0.381	0.394
1.020	0.332	0.343	0.358	0.349	0.355	0.349	0.365
1.101	0.303	0.323	0.317	0.310	0.333	0.322	0.326
1.183	0.274	0.301	0.297	0.278	0.305	0.289	0.300
1.264	0.247	0.271	0.254	0.283	0.275	0.275	0.277
1.346	0.235	0.244	0.257	0.230	0.253	0.251	0.261
1.427	0.208	0.224	0.237	0.215	0.242	0.227	0.225
1.509	0.186	0.204	0.216	0.183	0.222	0.206	0.222
1.591	0.169	0.191	0.168	0.165	0.194	0.195	0.196
1.672	0.147	0.181	0.176	0.159	0.185	0.171	0.174
1.754	0.137	0.161	0.166	0.123	0.165	0.156	0.161
1.835	0.128	0.144	0.153	0.122	0.155	0.135	0.144
1.917	0.111	0.131	0.143	0.116	0.135	0.123	0.133
1.998	0.096	0.111	0.125	0.103	0.124	0.116	0.126
(q/Q)	4.9	9.65	13.4	19.1	22.7	28.4	34.6

Impulse Response Experiments

4" dia. Turbine 19"/19" Cylindrical System

R.23 Baffled ½"dia. Inlet Feed to Loop

	Normalised Concentration						
Run	1	2	3	4	5	6	7
N.Time	rpm42	68	96	120	160	200	
0.000	0.000	0.000	0.000	0.000	0.000	0.000	
0.020	0.650	0.897	0.526	0.550	0.806	0.808	
0.041	1.154	0.987	1.038	0.982	0.948	0.959	
0.061	0.985	0.987	0.965	0.970	0.946	0.973	
0.081	0.950	0.964	0.956	0.967	0.938	0.931	
0.122	0.892	0.916	0.919	0.928	0.906	0.921	
0.204	0.827	0.842	0.843	0.872	0.838	0.850	
0.285	0.769	0.787	0.788	0.799	0.766	0.790	
0.367	0.703	0.724	0.736	0.747	0.722	0.720	
0.449	0.659	0.696	0.677	0.662	0.681	0.681	
0.489	0.629	0.647	0.649	0.665	0.644	0.653	
0.612	0.553	0.564	0.573	0.567	0.573	0.579	
0.693	0.520	0.517	0.526	0.543	0.528	0.537	
0.775	0.484	0.462	0.482	0.482	0.493	0.484	
0.856	0.443	0.416	0.439	0.442	0.455	0.442	
0.938	0.396	0.393	0.395	0.408	0.413	0.400	
1.020	0.363	0.370	0.373	0.359	0.386	0.368	
1.101	0.331	0.322	0.319	0.323	0.337	0.324	
1.183	0.309	0.291	0.288	0.283	0.324	0.314	
1.264	0.279	0.267	0.256	0.263	0.286	0.259	
1.346	0.246	0.233	0.231	0.222	0.259	0.241	
1.427	0.224	0.210	0.201	0.200	0.233	0.213	
1.509	0.199	0.187	0.187	0.173	0.215	0.213	
1.591	0.180	0.165	0.166	0.152	0.191	0.189	
1.672	0.166	0.142	0.146	0.136	0.171	0.157	
1.754	0.144	0.127	0.133	0.121	0.155	0.145	
1.835	0.122	0.111	0.114	0.114	0.142	0.137	
1.917	0.114	0.117	0.108	0.106	0.128	0.119	
1.998	0.101	0.105	0.097	0.100	0.116	0.101	
(q/Q)	7.95	13.4	18.2	22.7	30.3	37.9	

Impulse Response Experiments

4" dia Turbine 19"/19" Cylindrical System

R.24 Unbaffled 1"dia. Inlet Feed to Impeller

	Normalised Concentration							
Run	1	2	3	4	5	6	7	8
N.Time	39	55	71	93	112	143	168	198
0.000	0.000	0.000	0.000	0.116	0.000	0.000	0.069	0.079
0.020	1.558	1.391	1.741	2.388	1.757	1.493	1.079	0.967
0.041	1.558	1.146	1.195	1.200	1.035	1.045	0.945	1.004
0.061	1.153	0.993	1.076	1.049	1.02o	0.958	0.929	1.004
0.081	1.083	0.926	0.904	0.961	0.967	0.933	0.913	0.986
0 122	0.930	0.796	0.868	0.912	0.893	0.887	0.873	0.958
0.204	0.807	0.764	0.823	0.843	0.808	0.824	0.809	0.864
0.285	0.721	0.725	0.749	0.765	0.747	0.722	0.745	0.789
0 367	0.644	0.662	0.698	0.698	0.686	0.699	0.673	0.733
0.448	0.606	0.591	0.638	0.633	0.634	0.636	0.609	0.652
0.489	0.586	0.576	0.609	0.617	0.608	0.605	0.593	0.652
0.530	0.550	0.553	0.579	0.584	0.582	0.580	0.569	0.614
0.612	0.496	0.521	0.538	0.536	0.530	0.529	0.530	0.575
0.693	0 488	0.489	0.491	0.486	0.486	0.504	0.491	0.522
0.775	0.449	0.438	0.449	0.451	0.455	0.462	0.445	0.460
0.856	0.418	0.412	0.412	0.426	0.434	0.445	0.399	0.439
0.938	0.387	0.386	0.388	0.406	0.399	0 412	0.393	0.408
1.020	0.364	0.347	0 347	0.368	0.371	0.378	0 353	0.377
1.101	0.325	0.332	0.317	0.335	0.343	0.353	0.332	0.346
1.183	0 302	0 311	0.308	0.316	0.322	0.328	0.300	0 315
1.264	0.286	0 296	0.278	0.297	0.294	0.393	0.274	0.297
1.346	0.271	0.275	0.264	0.271	0.273	0.269	0.264	0.259
1.427	0 240	0 254	0 244	0.258	0 252	0.252	0.248	0.359
1.509	0.225	0.248	0.220	0.232	0.224	0 227	0.221	0.235
1.591	0 217	0.218	0 205	0.213	0.203	0.210	0.200	0.216
1.672	0.194	0.215	0.195	0.200	0.189	0.185	0.190	0.198
1.754	0.186	0.207	0.176	0.191	0.175	0.185	0.179	0.179
1.835	0.176	0.180	0.161	0.175	0.167	0 170	0.169	0.164
1.917	0.154	0.171	0.153	0.161	0.139	0.162	0.158	0.149
1.998	0.119	0.152	0.137	0.147	0.139	0.152	0.149	0.149
(q/Q)	7.38	10.4	13.4	17.8	21.2	27.2	32.0	37.0

Impulse Response Experiments

4"dia Turbine 19"/19" Cylindrical System

R.25 Unbaffled 1"dia Inlet Feed to Loop

	Normalised Concentration							
Run	1	2	3	4	5	6	7	8
N.Time rpm	39	55	71	93	112	142	164	198
0.000	0.000	0.000	0.000	0.000	0.000	0.000	0.000	0.000
0.020	1.273	0.563	0.580	0.382	0.300	0.659	0.409	0.682
0.041	1.044	0.739	0.906	0.967	0.706	0.919	0.893	0.933
0.061	0.950	0.926	0.899	0.976	0.868	0.944	0.939	0.933
0.081	0.913	0.909	0.913	0.992	0.881	0.919	0.924	0.941
0.122	0.883	0.938	0.906	0.983	0.857	0.906	0.901	0.897
0.204	0.813	0.883	0.848	0.903	0.799	0.780	0.825	0.814
0.285	0.761	0.797	0.783	0.823	0.718	0.755	0.764	0.756
0.367	0.702	0.731	0.725	0.742	0.662	0.679	0.680	0.707
0.448	0.650	0.659	0.667	0.670	0.616	0.639	0.642	0.663
0.530	0.604	0.624	0.617	0.605	0.606	0.619	0.602	0.617
0.612	0.551	0.554	0.556	0.553	0.541	0.578	0.543	0.570
0.693	0.499	0.519	0.515	0.501	0.504	0.537	0.518	0.509
0.775	0.461	0.482	0.474	0.448	0.476	0.487	0.468	0.478
0.856	0.429	0.446	0.432	0.408	0.448	0.456	0.449	0.441
0.938	0.397	0.418	0.415	0.372	0.420	0.426	0.399	0.395
1.020	0.364	0.397	0.385	0.345	0.373	0.395	0.368	0.380
1.101	0.338	0.368	0.349	0.329	0.354	0.365	0.347	0.339
1.264	0.298	0.297	0.301	0.287	0.308	0.335	0.307	0.290
1.346	0.276	0.283	0.286	0.260	0.295	0.294	0.294	0.281
1.427	0.259	0.269	0.277	0.239	0.261	0.274	0.281	0.257
1.509	0.237	0.248	0.248	0.207	0.252	0.264	0.261	0.241
1.591	0.225	0.234	0.229	0.196	0.233	0.243	0.231	0.233
1.672	0.207	0.220	0.219	0.191	0.214	0.223	0.221	0.212
1.754	0.190	0.205	0.200	0.171	0.205	0.206	0.201	0.196
1.835	0.175	0.180	0.187	0.162	0.187	0.175	0.185	0.172
1.911	0.156	0.170	0.181	0.151	0.170	0.160	0.173	0.157
1.998	0.142	0.151	0.142	0.139	0.143	0.130	0.148	0.139
(q/Q)	7.38	10.8	13.4	17.8	21.2	27.1	31.6	37.6

Impulse Response Experiments

4" dia Turbine 19"/19" Cylindrical System

R.26 Baffled 1"dia.Inlet Feed to Impeller

	Normalised Concentration						
Run	1	2	3	4	5	6	7
N.Time	rpm 26	51	88	100	120	150	180
0.000	0.000	0.000	0.000	1.214	0.000	0.063	1.323
0.021	1.761	1.610	1.410	1.702	0.940	1.078	1.321
0.042	1.802	1.046	0.979	0.951	0.889	0.958	0.813
0.061	1.210	0.921	0.941	0.900	0.840	0.945	0.851
0.081	1.172	0.909	0.937	0.779	0.852	0.875	0.786
0.122	0.968	0.838	0.891	0.779	0.820	0.850	0.753
0.204	0.853	0.785	0.835	0.719	0.761	0.788	0.703
0.285	0.765	0.745	0.783	0.679	0.697	0.726	0.659
0.367	0.688	0.691	0.713	0.624	0.653	0.668	0.614
0.448	0.624	0.638	0.671	0.598	0.632	0.633	0.572
0.530	0.548	0.612	0.543	0.567	0.576	0.567	0.538
0.612	0.510	0.566	0.573	0.523	0.522	0.546	0.510
0.693	0.459	0.518	0.518	0.463	0.472	0.502	0.468
0.775	0.421	0.460	0.490	0.437	0.462	0.470	0.447
0.856	0.382	0.428	0.434	0.417	0.433	0.437	0.413
0.938	0.344	0.411	0.416	0.382	0.388	0.401	0.395
1.020	0.332	0.375	0.378	0.362	0.373	0.379	0.374
1.101	0.293	0.357	0.364	0.322	0.343	0.349	0.354
1.183	0.255	0.322	0.308	0.297	0.324	0.328	0.333
1.264	0.242	0.304	0.277	0.282	0.295	0.295	0.312
1.346	0.215	0.286	0.249	0.256	0.269	0.281	0.301
1.427	0.204	0.250	0.238	0.261	0.269	0.251	0.289
1.509	0.179	0.228	0.224	0.236	0.239	0.229	0.270
1.591	0.166	0.210	0.193	0.221	0.190	0.216	0.270
1.672	0.153	0.192	0.179	0.201	0.209	0.194	0.250
1.754	0.141	0.175	0.145	0.176	0.194	0.183	0.234
1.835	0.123	0.157	0.137	0.161	0.175	0.175	0.230
1.917	0.115	0.157	0.137	0.156	0.160	0.153	0.164
1.998	0.102	0.139	0.123	0.136	0.149	0.142	0.153
(q/Q)	4.9	9.65	.16.7	18.9	22.7	28.4	34.1

Impulse Response Experiments

4" dia. Turbine 19"/19" Cylindrical System

R.27 Baffled 1"dia. Inlet Feed to Loop

	Normalised Concentration						
Run	1	2	3	4	5	6	7
N. Time	rpm 17	42	71	100	120	150	180
0.000	0.000	0.000	0.000	0.000	0.000	0.000	0.000
0.020	0.720	0.310	0.610	0.710	0.865	0.906	0.960
0.041	0.920	0.641	0.811	0.944	0.948	0.976	0.971
0.061	0.908	0.821	0.881	0.899	0.966	0.956	0.968
0.081	0.778	0.887	0.917	0.878	0.952	0.962	0.909
0.122	0.767	0.848	0.853	0.838	0.910	0.892	0.882
0.204	0.708	0.892	0.784	0.781	0.836	0.834	0.803
0.285	0.661	0.854	0.730	0.709	0.766	0.762	0.752
0.326	0.625	0.815	0.713	0.696	0.742	0.749	0.725
0.448	0.563	0.677	0.635	0.632	0.665	0.643	0.643
0.530	0.531	0.526	0.596	0.589	0.618	0.594	0.598
0.612	0.490	0.500	0.537	0.539	0.569	0.552	0.557
0.693	0.453	0.521	0.514	0.499	0.519	0.519	0.520
0.775	0.427	0.463	0.473	0.458	0.479	0.465	0.465
0.856	0.406	0.420	0.432	0.458	0.445	0.436	0.434
0.938	0.375	0.392	0.405	0.428	0.408	0.410	0.397
1.020	0.344	0.369	0.375	0.391	0.375	0.376	0.369
1.101	0.323	0.326	0.348	0.375	0.346	0.347	0.328
1.183	0.292	0.308	0.311	0.351	0.316	0.312	0.297
1.264	0.271	0.295	0.307	0.321	0.288	0.294	0.273
1.346	0.250	0.269	0.284	0.294	0.255	0.260	0.256
1.427	0.240	0.256	0.257	0.268	0.229	0.231	0.230
1.509	0.219	0.231	0.240	0.231	0.216	0.218	0.225
1.591	0.198	0.192	0.213	0.201	0.191	0.200	0.198
1.672	0.188	0.192	0.203	0.187	0.185	0.189	0.178
1.754	0.167	0.179	0.189	0.174	0.186	0.150	0.151
1.834	0.156	0.167	0.173	0.147	0.165	0.165	0.161
1.917	0.146	0.134	0.149	0.124	0.143	0.137	0.123
1.998	0.134	0.134	0.149	0.124	0.143	0.137	0.111
(q/Q)	3.2	7.9	13.4	18.9	22.7	28.4	34.1

Impulse Response Experiments

8" dia. Turbine 42"/42" Cylindrical System

R.30 Unbaffled Feed to Impeller

	Normalised Concentration				
-Run	1	2	3	4	5
N.Time	rpm 30	80	120	160	200
0.000	0.000	1.098	1.077	1.100	1.056
0.045	2.046	0.972	0.994	0.978	0.961
0.090	0.970	0.915	0.960	0.950	0.876
0.135	0.880	0.885	0.937	0.925	0.840
0.180	0.850	0.848	0.918	0.890	0.810
0.225	0.825	0.809	0.861	0.856	0.780
0.300	0.760	0.760	0.781	0.790	0.745
0.350	0.735	0.730	0.740	0.750	0.700
0.400	0.690	0.690	0.689	0.710	0.666
0.500	0.630	0.640	0.580	0.613	0.603
0.600	0.550	0.580	0.490	0.561	0.546
0.700	0.508	0.519	0.444	0.500	0.496
0.800	0.457	0.465	0.404	0.450	0.449
0.900	0.400	0.420	0.381	0.392	0.406
1.000	0.365	0.367	0.344	0.344	0.364
1.100	0.320	0.332	0.314	0.290	0.330
1.200	0.285	0.290	0.280	0.230	0.302
1.300	0.260	0.260	0.260	0.200	0.274
1.400	0.230	0.232	0.237	0.190	0.248
1.500	0.220	0.214	0.217	0.180	0.220
1.600	0.200	0.196	0.200	0.170	0.200
1.700	0.180	0.180	0.180	0.155	0.180
1.800	0.160	0.170	0.170	0.140	0.167
1.900	0.132	0.128	0.135	0.118	0.137
2.000	0.130	0.120	0.125	0.118	0.117
(q/Q)	9.16	24.4	36.6	48.8	61.0

Impulse Response Experiments

8"dia. Turbine 42"/42" Cylindrical System

R.31 Unbaffled Feed to Loop

	Normalised Concentration				
Run	1	2	3	4	5
N.Time	rpm 30	80	120	160	200
0.000	0.000	0.000	0.000	0.000	0.000
0.045	0.616	0.960	1.064	1.040	1.030
0.090	0.838	1.030	0.988	0.980	0.952
0.135	0.878	0.970	0.940	0.896	0.910
0.180	0.858	0.920	0.910	0.839	0.865
0.225	0.840	0.884	0.860	0.800	0.820
0.300	0.788	0.810	0.750	0.742	0.750
0.350	0.715	0.760	0.660	0.716	0.720
0.400	0.665	0.720	0.570	0.686	0.684
0.500	0.610	0.640	0.560	0.620	0.619
0.600	0.570	0.580	0.528	0.563	0.560
0.700	0.510	0.530	0.488	0.519	0.506
0.800	0.468	0.490	0.450	0.476	0.460
0.900	0.435	0.440	0.411	0.431	0.414
1.000	0.404	0.392	0.363	0.391	0.362
1.100	0.371	0.341	0.343	0.362	0.342
1.200	0.342	0.300	0.308	0.320	0.302
1.300	0.310	0.270	0.269	0.286	0.278
1.400	0.290	0.240	0.250	0.257	0.251
1.500	0.270	0.220	0.230	0.230	0.228
1.600	0.230	0.210	0.215	0.197	0.206
1.700	0.210	0.197	0.199	0.181	0.186
1.800	0.190	0.180	0.180	0.180	0.169
1.900	0.170	0.160	0.150	0.152	0.153
2.000	0.150	0.126	0.135	0.136	0.132
(q/Q)	9.2	24.4	36.6	48.8	61.0

A.1.2 PROPELLER RESIDENCE TIME DISTRIBUTION EXPERIMENTS

Impulse Response Experiments

$2\frac{1}{2}$" dia. Propeller 9"/9" Cylindrical System

P.1 Unbaffled Feed to Impeller

Run	Normalised Concentration					
	1	2	3	4	5	6
N.Time	rpm 30	60	116	160	200	260
0.000	1.251	1.276	0.601	1.104	1.476	1.356
0.027	1.009	1.414	1.431	1.017	1.149	1.195
0.062	0.925	0.981	1.211	0.969	0.976	0.967
0.100	0.888	0.884	1.085	0.922	0.946	0.930
0.154	0.823	0.836	0.960	0.866	0.897	0.870
0.309	0.697	0.696	0.714	0.725	0.779	0.713
0.463	0.591	0.595	0.620	0.615	0.664	0.608
0.618	0.507	0.489	0.515	0.558	0.559	0.512
0.772	0.436	0.428	0.441	0.481	0.471	0.447
0.927	0.371	0.367	0.372	0.411	0.381	0.396
1.082	0.324	0.311	0.329	0.346	0.333	0.341
1.235	0.288	0.271	0.277	0.288	0.281	0.294
1.390	0.250	0.244	0.242	0.237	0.234	0.249
1.544	0.220	0.215	0.205	0.198	0.195	0.212
1.699	0.195	0.191	0.173	0.170	0.169	0.176
1.853	0.169	0.167	0.142	0.140	0.143	0.151
2.000	0.152	0.148	0.121	0.119	0.124	0.130
2.162	0.135	0.132	0.103	0.101	0.105	0.110
2.316	0.119	0.116	0.087	0.084	0.094	0.096
2.471	0.106	0.104	0.074	0.072	0.075	0.084
2.625	0.093	0.092	0.065	0.060	0.060	0.073
2.780	0.085	0.080	0.055	0.050	0.056	0.064
2.934	0.072	0.072	0.049	0.040	0.048	0.057
(q/Q)	3.2	6.4	12.2	17.0	21.2	27.6

Impulse Response Experiments

$2\frac{1}{2}$" dia. Propeller 9"/9" Cylindrical System

P.2 Unbaffled Feed to Loop

	Normalised Concentration					
Run	1	2	3	4	5	6
N.Time	rpm 27	86	110	140	200	260
0.000	0.000	0.000	0.000	0.000	0.000	0.000
0.027	0.164	0.677	0.650	0.414	0.545	0.755
0.062	0.492	0.853	0.861	0.861	0.803	0.867
0.100	0.670	0.936	0.947	0.938	0.990	0.913
0.154	0.814	0.936	0.921	0.855	0.994	0.887
0.309	0.823	0.771	0.781	0.783	0.792	0.767
0.463	0.714	0.632	0.647	0.668	0.668	0.665
0.618	0.608	0.546	0.549	0.563	0.556	0.568
0.772	0.508	0.465	0.471	0.468	0.475	0.482
0.926	0.435	0.407	0.407	0.423	0.403	0.420
1.081	0.371	0.357	0.359	0.364	0.349	0.373
1.235	0.298	0.302	0.312	0.315	0.301	0.349
1.390	0.261	0.266	0.268	0.267	0.256	0.295
1.544	0.220	0.215	0.218	0.224	0.215	0.242
1.699	0.187	0.182	0.189	0.188	0.178	0.211
1.853	0.164	0.157	0.165	0.163	0.150	0.179
2.007	0.142	0.135	0.138	0.137	0.129	0.150
2.162	0.125	0.113	0.117	0.116	0.109	0.132
2.316	0.108	0.098	0.098	0.104	0.093	0.115
2.471	0.094	0.086	0.086	0.089	0.081	0.100
2.625	0.082	0.074	0.077	0.080	0.072	0.087
2.780	0.072	0.066	0.067	0.070	0.061	0.078
2.934	0.060	0.058	0.060	0.061	0.054	0.066
(q/Q)	2.8	9.2	11.7	14.9	21.2	27.6

Impulse Response Experiments

$2\frac{1}{2}$" dia. Propeller 9"/9" Cylindrical System

P.3 Baffled Feed to Impeller

	Normalised Concentration					
Run	1	2	3	4	5	6
N.Time rpm	30	60	116	160	200	260
0.000	1.451	1.351	1.315	0.752	1.049	1.143
0.027	1.100	1.070	1.215	0.812	1.018	1.018
0.062	0.980	0.960	1.148	0.998	0.997	0.965
0.100	0.903	0.900	1.016	0.937	0.955	0.926
0.154	0.822	0.843	0.916	0.876	0.891	0.862
0.309	0.698	0.706	0.735	0.752	0.777	0.713
0.463	0.600	0.603	0.626	0.640	0.658	0.626
0.618	0.502	0.489	0.523	0.548	0.558	0.534
0.772	0.436	0.425	0.450	0.479	0.465	0.459
0.927	0.375	0.362	0.381	0.416	0.395	0.398
1.082	0.324	0.309	0.332	0.354	0.329	0.345
1.235	0.280	0.271	0.285	0.295	0.279	0.293
1.390	0.257	0.242	0.242	0.247	0.230	0.250
1.544	0.226	0.215	0.205	0.207	0.194	0.210
1.699	0.196	0.189	0.172	0.176	0.170	0.179
1.853	0.169	0.167	0.145	0.147	0.146	0.154
2.007	0.152	0.147	0.130	0.126	0.123	0.131
2.162	0.136	0.132	0.104	0.109	0.107	0.112
2.316	0.118	0.116	0.087	0.094	0.091	0.097
2.471	0.107	0.102	0.075	0.083	0.075	0.086
2.625	0.092	0.090	0.065	0.071	0.063	0.075
2.780	0.085	0.085	0.057	0.060	0.047	0.065
2.934	0.071	0.072	0.048	0.051	0.041	0.057
(q/Q)	3.2	6.4	12.2	17.0	21.2	27.6

Impulse Response Experiments

$2\frac{1}{2}$" dia. Propeller 9"/9" Cylindrical System

P.4 Baffled Feed to Loop

	Normalised Concentration					
Run	1	2	3	4	5	6
N.Time	rpm 27	86	110	140	200	260
0.000	0.000	0.000	0.000	0.000	0.000	0.000
0.027	0.227	0.638	0.610	0.383	0.504	0.783
0.062	0.523	0.853	0.861	0.669	0.803	0.884
0.100	0.746	0.935	0.947	0.779	0.999	0.915
0.154	0.823	0.935	0.906	0.857	0.994	0.869
0.309	0.823	0.782	0.810	0.805	0.792	0.757
0.463	0.714	0.638	0.642	0.669	0.678	0.648
0.618	0.608	0.546	0.552	0.570	0.556	0.553
0.772	0.507	0.468	0.470	0.487	0.475	0.477
0.927	0.432	0.411	0.412	0.428	0.408	0.410
1.081	0.362	0.357	0.358	0.369	0.352	0.350
1.235	0.298	0.305	0.301	0.316	0.301	0.294
1.390	0.257	0.263	0.273	0.268	0.256	0.243
1.544	0.224	0.218	0.218	0.225	0.217	0.208
1.699	0.187	0.182	0.186	0.189	0.180	0.179
1.853	0.161	0.157	0.162	0.152	0.150	0.150
2.007	0.142	0.135	0.137	0.137	0.129	0.131
2.162	0.125	0.113	0.114	0.117	0.107	0.116
2.361	0.106	0.099	0.100	0.102	0.093	0.101
2.471	0.094	0.086	0.099	0.090	0.082	0.087
2.625	0.079	0.074	0.086	0.080	0.072	0.076
2.780	0.070	0.066	0.072	0.070	0.061	0.066
2.934	0.060	0.058	0.061	0.059	0.054	0.059
(q/Q)	2.9	9.2	11.7	14.9	21.2	27.6

Impulse Response Experiments

4" dia. Propeller 19"/19" Cylindrical System

P.11 Unbaffled 1"dia. Inlet Feed to Impeller

	Normalised Concentration						
Run	1	2	3	4	5	6	7
N.Time	rpm 20	50	72	110	150	180	22
0.000	1.583	0.000	0.000	0.000	0.174	0.898	1.1
0.030	1.337	1.458	1.444	1.104	1.333	1.324	1.1
0.060	0.961	1.326	1.115	0.999	1.045	0.979	0.9
0.090	0.951	0.956	1.015	0.876	0.890	0.888	0.8
0.121	0.941	0.979	0.910	0.866	0.871	0.828	0.8
0.211	0.842	0.844	0.804	0.808	0.778	0.768	0.7
0.271	0.773	0.758	0.753	0.757	0.737	0.728	0.7
0.331	0.721	0.751	0.712	0.696	0.686	0.686	0.6
0.392	0.694	0.704	0.664	0.672	0.655	0.648	0.6
0.452	0.629	0.647	0.617	0.634	0.624	0.608	0.6
0.512	0.591	0.612	0.579	0.590	0.583	0.578	0.5
0.573	0.547	0.567	0.547	0.559	0.553	0.538	0.5
0.633	0.529	0.532	0.518	0.511	0.512	0.498	0.5
0.693	0.500	0.498	0.477	0.488	0.481	0.468	0.4
0.753	0.451	0.463	0.442	0.457	0.451	0.438	0.4
0.814	0.419	0.422	0.427	0.419	0.421	0.408	0.4
0.874	0.392	0.391	0.398	0.396	0.389	0.378	0.3
0.934	0.371	0.367	0.369	0.371	0.362	0.354	0.3
0.994	0.355	0.359	0.358	0.355	0.369	0.341	0.3
1.115	0.314	0.327	0.320	0.314	0.313	0.313	0.3
1.236	0.281	0.295	0.285	0.286	0.279	0.288	0.2
1.356	0.261	0.226	0.271	0.258	0.257	0.259	0.2
1.477	0.214	0.211	0.239	0.231	0.231	0.225	0.2
1.597	0.191	0.187	0.215	0.209	0.209	0.209	0.2
1.718	0.176	0.180	0.199	0.188	0.188	0.191	0.1
1.838	0.157	0.164	0.173	0.174	0.174	0.171	0.1
1.959	0.140	0.141	0.159	0.153	0.146	0.153	0.1
(q/Q)	4.9	9.6	13.6	20.8	26.7	34.1	41.

Impulse Response Experiments

4" dia. Propeller 19"/19" Cylindrical System

P.12 Unbaffled 1"dia. Inlet Feed to Loop

	Normalised Concentration					
Run	1	2	3	4	5	6
N.Time	rpm 20	45	80	110	150	220
0.000	0.000	0.000	0.000	0.000	0.000	0.000
0.030	0.007	0.823	0.749	0.505	0.397	0.666
0.060	0.237	0.895	0.504	0.745	0.612	0.921
0.090	0.500	0.919	0.781	0.818	0.786	0.901
0.121	0.868	0.991	0.856	0.860	0.858	0.881
0.211	0.908	0.990	0.923	0.871	0.848	0.812
0.271	0.858	0.943	0.899	0.830	0.806	0.772
0.331	0.808	0.909	0.781	0.766	0.755	0.732
0.392	0.768	0.863	0.707	0.714	0.704	0.682
0.452	0.709	0.809	0.653	0.672	0.663	0.642
0.512	0.669	0.729	0.611	0.630	0.622	0.612
0.573	0.609	0.621	0.568	0.588	0.581	0.573
0.633	0.560	0.551	0.525	0.557	0.541	0.533
0.693	0.540	0.501	0.493	0.526	0.511	0.503
0.753	0.511	0.483	0.461	0.494	0.469	0.473
0.814	0.481	0.442	0.429	0.452	0.438	0.443
0.874	0.440	0.400	0.397	0.421	0.411	0.403
0.934	0.403	0.371	0.365	0.390	0.390	0.380
0.994	0.371	0.341	0.333	0.369	0.369	0.359
1.115	0.321	0.307	0.301	0.313	0.334	0.325
1.236	0.291	0.281	0.271	0.285	0.299	0.298
1.356	0.257	0.241	0.269	0.256	0.272	0.272
1.477	0.221	0.217	0.247	0.235	0.244	0.244
1.597	0.202	0.201	0.219	0.220	0.223	0.224
1.718	0.181	0.181	0.184	0.185	0.202	0.203
1.838	0.153	0.158	0.164	0.171	0.181	0.182
1.959	0.142	0.137	0.141	0.151	0.157	0.153
(q/Q)	4.9	8.2	15.2	20.8	27.6	41.8

Impulse Response Experiments

4"dia. Propeller 19"/19" Cylindrical System

P.13 Baffled 1"dia. Inlet Feed to Impeller

	Normalised Concentration						
Run	1	2	3	4	5	6	7
N.Time	rpm 20	45	72	110	150	180	220-
0.000	0.000	0.009	0.762	1.563	1.873	1.920	1.94
0.030	2.036	1.948	1.291	0.940	1.083	0.967	0.98
0.060	0.763	1.307	0.946	0.947	0.897	0.897	0.85
0.090	0.813	1.147	0.916	0.817	0.864	0.871	0.84
0.121	0.854	0.960	0.856	0.842	0.832	0.844	0 83
0.211	0.771	0.819	0.771	0.768	0.767	0.783	0.79
0.271	0.713	0.752	0.719	0.702	0.726	0.748	0.7
0.331	0.638	0.711	0.677	0.670	0.686	0.696	0.67
0.392	0.621	0.666	0.642	0.645	0.649	0.652	0.64
0.452	0.557	0.605	0.603	0.596	0.597	0.610	0.6
0.512	0.531	0.572	0.570	0.562	0.597	0.569	0.56
0.573	0.485	0.540	0.543	0.536	0.536	0.548	0.53
0.633	0.472	0.507	0.516	0.504	0.523	0.521	0.51
0.693	0.440	0.481	0.483	0.485	0.485	0.494	0.49
0.753	0.400	0.455	0.456	0.459	0.466	0.473	0.47
0.814	0.394	0.436	0.429	0.440	0.447	0.452	0.44
0.874	0.368	0.410	0.402	0.401	0.409	0.418	0.42
0.934	0.342	0.390	0.387	0.382	0.390	0.391	0.4
0.994	0.329	0.365	0.356	0.363	0.371	0.377	0.38
1.115	0.277	0.339	0.315	0.324	0.339	0.322	0.34
1.236	0.251	0.289	0.268	0.278	0.288	0.288	0.3
1.356	0.226	0.257	0.237	0.253	0.263	0.240	0.28
1.477	0.213	0.234	0.210	0.219	0.221	0.222	0.24
1.597	0.187	0.189	0.196	0.201	0.199	0.201	0.2
1.718	0.169	0.171	0.178	0.179	0.182	0.182	0.19
1.838	0.147	0.149	0.148	0.162	0 166	0.160	0.17
1.959	0.138	0.142	0.141	0.147	0.151	0·152	0.14
(q/Q)	4.9	8.2	13.6	20.8	27.6	34.1	41.8

Impulse Response Experiments

4"dia. Propeller 19"/19" Cylindrical System

P.14 Baffled 1"dia Inlet Feed to Loop

	Normalised Concentration					
Run	1	2	3	4	5	6
N.Time	rpm 20	45	80	110	150	180
0.000	0.004	0.000	0.000	0.000	0.000	0.000
0.030	0.829	0.696	0.521	0.721	0.907	0.903
0.060	1.442	1.495	1.039	0.977	0.908	0.978
0.090	1.039	1.695	0.928	0.901	0.898	0.911
0.121	1.077	0.889	0.873	0.881	0.883	0.868
0.211	0.855	0.817	0.818	0.808	0.811	0.811
0.271	0.740	0.772	0.770	0.763	0.772	0.774
0.331	0.719	0.735	0.731	0.719	0 719	0.714
0.392	0.678	0.682	0.699	0.683	0.680	0.677
0.452	0.644	0.637	0.652	0.638	0.649	0.641
0.512	0.624	0.600	0.604	0.594	0.610	0.603
0.573	0.597	0.562	0.564	0.564	0.566	0.564
0.633	0.549	0.525	0.530	0.534	0.536	0.530
0.693	0.508	0.489	0.506	0.502	0.518	0.501
0.753	0.467	0.466	0.475	0.474	0.488	0.478
0.814	0.440	0.442	0.452	0.450	0.458	0.449
0.874	0.424	0.413	0.425	0.422	0 434	0.425
0.934	0.403	0.384	0.400	0.399	0.409	0.402
0.994	0.376	0.361	0.376	0.375	0.385	0.379
1.115	0.328	0.318	0.332	0.335	0.335	0.337
1.236	0.296	0.284	0 289	0.295	0.295	0.291
1.356	0.248	0.243	0.252	0.254	0.258	0.257
1.477	0.221	0.213	0.221	0.225	0.222	0.222
1.597	0.200	0.188	0.194	0.193	0.198	0.198
1.718	0.167	0.168	0.177	0.173	0.177	0.178
1.838	0.149	0 153	0.156	0 157	0.161	0.158
1.959	0.138	0.137	0.139	0.144	0.144	0.143
(q/Q)	4.9	8.2	15.2	20.8	27.0	34.1

A.1.3a TURBINE BATCH MIXING TIME EXPERIMENTS

Experimental Batch Mixing Times A.1.3a.1

$2\frac{1}{2}$" dia Turbine Impeller Position 0.33Z

10"/10" Cylindrical System

Rpm	q	Batch mixing time (seconds) 1	2	3	4	5	AVE(mins)
20	4.8	186	180	172	184	190	3.05
55	13.2	78	79	82	80	76	1.3
80	19.2	61	57	59	62	60	1.0
100	24.1	50	50	47	51	52	0.85
136	32.6	41	40	39	38	36	0.65
140	33.7	37	36	36	38	36	0.62
172	41.4	27	26	27	26	25	0.45
200	48.1	23	22	20	22	22	0.33
210	50.5	21	21	21	20	21	0.30
240	57.7	16	17	15	14	15	0.25
260	62.6	15	16	16	16	16	0.25

Experiments Batch Mixing Times A.1.3a.2

$2\frac{1}{2}$"dia. Turbine Impeller Position 0.5Z

10"/10" Cylindrical System

rpm	q	Batch mixing times (seconds) 1	2	3	4	5	AVE(mins)
20	4.81	185	190	175	190	180	3.1
30	7.22	155	150	147	153	145	2.5
60	13.4	80	81	77	76	75	1.3
80	19.2	58	62	63	59	58	1.0
110	26.5	47	46	49	46	49	0.8
140	33.7	40	40	41	42	43	0.7
205	49.3	31	32	30	30	32	0.52
280	67.65	20	21	21	20	22	0.34

Experimental Batch Mixing Times A1.3a.3

$2\frac{1}{2}$"dia. Turbine Impeller Position 0.33Z

13"/12" Cylindrical System

rpm	q	Batch mixing time (seconds) 1	2	3	4	5	AVE(mins)
10	2.4	650	630	670	610	690	10.8
40	9.6	260	225	275	255	257	4.25
70	16.8	169	166	155	161	160	2.70
110	26.5	106	110	112	111	108	1.84
160	38.5	76	72	80	74	74	1.25
230	55.3	48	45	45	46	43	0.75
280	67.4	36	34	33	37	37	0.60

Experimental Batch Mixing Times A.I.3a.4

$2\frac{1}{2}$" dia. Turbine Impeller Position 0.5Z

13"/12" Cylindrical System

rpm	q	Batch mixing time (seconds) 1	2	3	4	5	AVE(mins)
14	3.4	450	440	470	400	410	7.8
30	7.3	216	221	208	220	204	3.5
90	21.6	135	130	I13	138	136	2.2
120	28.8	91	87	86	94	92	1.5
160	38.5	61	62	61	61	57	1.0
200	48.1	46	44	43	47	45	0.75
250	60.1	33	36	33	33	33	0.56

Experimental Batch Mixing Times A.1.3a.5

3"dia. Turbine Impeller Position 0.33Z

10"/10" Cylindrical System

rpm	q	Batch mixing time (seconds) 1	2	3	4	5	AVE(mins)
10	4.16	180	175	186	183	181	3.0
48	19.9	64	63	62	65	62	1.05
100	41.6	40	38	38	37	37	0.65
140	58.2	27	26	23	24	23	0.4
190	79.0	22	22	21	21	21	0.3
260	108.0	13	12	13	12	12	0.2

Experimental Batch Mixing Times A.1.3a.6

3" dia. Turbine Impeller Position 0.5Z

10/10"Cylindrical System

rpm	q	Batch mixing time (seconds) 1	2	3	4	5	AVE(mins)
10	4.16	171	161	165	167	172	2.84
35	14.6	74	76	78	71	74	1.25
75	31.2	48	49	46	44	44	0.75
120	49.9	30	27	26	28	27	0.45
170	70.7	16	16	16	16	14	0.24
230	95.6	10	10	10	10	10	0.15

Experimental Batch Mixing Times A1.3a.7

3"dia. Turbine Impeller Position 0.33Z

13"/12" Cylindrical System

rpm	q	Batch mixing time (seconds) 1	2	3	4	5	AVE (mins)
10	4.16	433	417	431	426	404	7.2
35	14.56	132	124	121	132	124	2.1
90	36.9	61	63	60	57	57	0.97
140	58.23	42	42	46	46	49	0.75
200	83.18	32	34	33	33	33	0.55
240	99.8	25	23	23	24	25	0.40

Experimental Batch Mixing Times A.13a.8

3" dia. Turbine Impeller Position 0.5Z

13"/12" Cylindrical System

rpm	q	Batch mixing time (seconds) 1	2	3	4	5	AVE(mins)
18	7.44	248	250	235	235	242	4.0
60	24.9	66	64	63	64	60	1.05
116	48.13	40	44	42	42	42	0.70
160	66.5	35	37	36	36	35	0.60
200	83.2	26	26	28	26	29	0.45
240	99.8	20	20	18	18	18	0.31

Experimental Batch Mixing Times A.1.3a.9

4"dia. Turbine Impeller Position 0.33Z

19"/19" Cylindrical System

rpm	q	Batch mixing time (seconds) 1	2	3	4	5	AVE(mins)
24	23.9	340	321	331	370	310	5.36
45	44.9	216	208	210	230	210	3.65
60	59.8	133	139	139	143	137	2.30
90	89.8	81	84	86	82	81	1.36
140	139.0	54	52	54	56	50	0.90
180	178.5	42	42	43	47	46	0.75
220	218.0	36	33	33	33	35	0.60

A.1.3b PROPELLER BATCH MIXING TIME EXPERIMENTS

Experimental Batch Mixing Times A.1.3b.1

3" dia. Propeller Impeller Position 0.33Z

10"/10" Cylindrical System

rpm	q	Batch mixing time (seconds) 1	2	3	4	5	AVE(mins)
15	6.24	306	310	295	316	295	5.15
36	14.7	120	125	119	118	115	2.00
85	35.3	65	60	66	60	63	1.05
150	62.3	40	41	40	38	38	0.675
210	87.34	25	22	22	22	22	0.37
240	99.16	15	16	17	15	16	0.25

Experimental Batch Mixing Times A.13b.2 -

2½" dia. Propeller Impeller Position 0.33Z

10/10" Cylindrical System

rpm	q	Batch mixing time (seconds) 1	2	3	4	5	AVE(mins)
30	7.22	306	316	310	312	306	5.2
70	16.85	140	140	145	148	141	2.4
120	28.8	66	61	59	62	65	1.05
160	38.5	45	48	46	42	40	0.75
200	48.14	30	31	29	28	30	0.49
240	57.7	20	21	22	23	19	0.33

Experimental Batch Mixing Times A.1.3b.3

$2\frac{1}{2}$" dia. Propeller Impeller Position 0.33Z

13"/12" Cylindrical System

rpm	q	Batch mixing time (seconds) 1	2	3	4	5	AVE(mins)
20	4.8	640	621	610	630	640	10.5
52	12.5	270	260	260	266	254	4.45
100	24.07	130	132	141	130	132	2.26
160	38.5	84	82	70	82	84	1.35
195	46.9	60	64	56	50	56	0.95
270	64.9	39	36	37	38	40	0.65

ExperimentalBatch Mixing Times A.1.3b.4

$2\frac{1}{2}$" dia. Propeller Impeller Position 0.5Z

13"/12" Cylindrical System

rpm	q	Batch mixing time (Seconds) 1	2	3	4	5	AVE(mins)
20	4.8	680	670	660	640	650	11.0
60	14.44	268	266	258	265	261	4.65
100	24,07	150	149	154	160	160	2.6
125	30.3	125	118	119	119	118	2.0
160	38.5	76	70	76	74	75	1.23
200	48.14	56	56	57	58	59	0.9
260	62.6	40	37	38	40	43	0.65

Experimental Batch Mixing Times A.1.3b.5

3" dia. Propeller Impeller Position 0.33Z

13"/12" Cylindrical System

rpm	q	Batch mixing time (seconds) 1	2	3	4	5	AVE (mins)
32	13.2	400	405	391	389	385	6.6
60	24.9	165	160	163	159	164	2.7
100	41.0	115	120	116	118	120	1.95
140	58.7	76	73	76	74	76	1.25
180	74.3	45	45	46	49	50	0.77
240	99.7	26	27	30	28	27	0.475

Experimental Batch Mixing Times A.1.3b.6

3" dia. Propeller Impeller Position

13"/12" Cylindrical System

rpm	q	Batch mixing time (seconds) 1	2	3	4	5	AVE(mins)
32	13.2	316	320	306	309	295	6.2
60	24.9	165	170	160	159	170	2.75
100	41.0	90	92	93	96	93	1.66
140	58.7	71	60	65	63	63	1.1
180	74.32	50	50	55	57	55	0.90
240	99.7	40	36	38	36	37	0.65

A.2 NORMALISATION PROGRAMME

A.2. Normalisation Programme

The programme is fed into the computer followed by a calibration curve tape, a run-details tape and then the logged experimental voltages tape. The program calculates from the run-details tape how many items of the experimental data are to be read from the logged voltage tape i.e. ($V/Q.Tr.$). The first (D/Q) items of data are then discarded and all voltages changed to concentrations and stored. The area between successive pairs of concentration points is computed by the trapezoidal rule and summed over the time of the response (Tr) The total area is then calculated by assuming that the section of the curve after the truncation point behaves as an exponential decay. The output of normalised concentrations and reduced time are then calculated by dividing the stored actual concentrations by the area under the response curve and the time scale by the system meantime.

Input Data:-

Calibration tape

As the calibration of the photocell detector was not linear, pairs of concentration - voltage points were required so that the logged voltages of each experimental run could be correctly analysed. The voltages were changed to concentrations by linear interpolation. An example of a typical calibration tape is as follows:-

C		V	
0.00	0.04	00010	00050
0.04	0.08	00050	00085
0.08	0.12	00085	00110
0.11	0.16	00110	00129
0.16	0.20	00129	00140
0.20	0.24	00140	00149

Run-Details Tape:-

Run Number		1
Flow Rate	Q	1.1
Vessel Volume	V	9.37
RPM		120
Trunc. Point	Tr	2.0
Dead Volume	D	0.200

Truncation point is the point at which the response is to be curtailed; a value of 2 results in the response being stopped at twice the meantime.

Experimental Tape:-

The logged voltages were logged at one per second. An example of such a tape is:-

+00010+00010+00012+00022+00036+00060 etc.

As the conductivity cell calibration of the voltage versus concentration was linear over the whole range of voltages recorded, a modified version of the programme was developed which omitted the calibration routine, the remainder of the programme and data input was as described previously.

APPENDIX 3. MARKOV PROGRAMME

Markov Programme

The solution of sets of linear differential operations derived from flow models consisting of networks of stirred tanks, by the Markov procedure was initiated by Gibilaro (26),(27). The analogy between the network and the Markov process being based on the probabilistic treatment of the ideal vessel. The equations which describe this procedure being

$$Sj(n+1) = \sum_{i=1}^{N} Si(n)\,Pij \quad , \quad n = 0, 1, 2 \ldots$$

$$S(n+1) = Sn(\underline{P})$$

$$\text{ie} \quad S(n) = So(P^N) \qquad (1)$$

where

p_{ij} is the probability of transition from state i to state j

P is the transition matrix containing the elements p_{ij}. The rows P consist of all possible transitions from a given state and so sum to 1.

This matrix completely describes the Markov Process.

So that:

$$P = \begin{bmatrix} p_{11} & p_{12} & p_{13} \cdots\cdots\cdots\cdots p_{1N} \\ p_{21} & p_{22} & p_{23} \cdots\cdots\cdots\cdots p_{2N} \\ --- & --- & --- \cdots\cdots\cdots\cdots --- \\ --- & --- & --- \cdots\cdots\cdots\cdots --- \\ p_{N1} & p_{N2} & p_{N3} \cdots\cdots\cdots\cdots p_{NN} \end{bmatrix}$$

$s_i(n)$ is the state probability. Defined as the probability that the system will be in state i after n transitions from a given starting point.

S(n) is the state probability vector: a line vector composed of elements $S_i(n)$

$$S(n) = (s_1(n), s_2(n), s_3(n) \quad . \quad . \quad . \quad . \quad . \quad s_N(n))$$

The computer programme which applies equation (1) for the solution of flow models is well documented (26), (27).

A sample data input for the double loop model of Figure A.3.1 is shown below:-

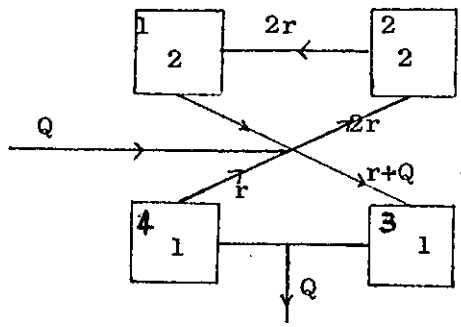

Fig. A.3.1.

Throughput flow	Q	1.0
Total volume	V	9.37
Print out increment		0.05
Truncation pt of response	Tr	2.0
Total number of states	N	6
Required Response	Nr	3

Flow Matrix $P_{ij} = q_{ij}$

$$\begin{bmatrix} 0 & 2r & 0 & 0 & 0 & 0 \\ 0 & 0 & 0 & 0 & 2r & 0 \\ 0 & 0 & 0 & r & 0 & Q \\ 0 & 0 & 0 & 0 & r & 0 \\ 2r & 0 & (r+Q) & 0 & 0 & 0 \\ \end{bmatrix}$$

Volume Vector $\begin{bmatrix} 2 & 2 & 1 & 1 & 0 & 6 \end{bmatrix}$

Initial State Vector $\begin{bmatrix} 0 & 0 & 0 & 0 & 1 & 0 \end{bmatrix}$

The units are mutually consistent.

Certain modifications have been implemented to the output routine of the main program to accommodate various needs.

For batch mixing time computation the program was adjusted to give the unnormalised real time response of each vessel in the input network.

The least squares optimisation, for the comparison of the flow and gamma function models, was achieved by computing the normalised response of the flow network using the Markov routine, storing these values, and then comparing each in turn with computed values obtained from a subroutine which calculated the corresponding gamma function values. A simple logic routine enabled the sum of the squares for a particular gamma function parameter to be stored and used for comparison until the smallest sum of least squares was found.

The variance analysis was conducted in a similar way, values of the normalised response were calculated using the normal program and stored. The variance was calculated by squaring these values and applying the trapezoidal rule between successive pairs of points throughout the response to find the area under the "squared" curve. As the upper limit of the time axis for the analytical variance is infinity a value of 10 times the mean time was used to accommodate this.

The Markov routine was used as the base in the intensity function calculation. The normalised impulse response was computed along with step response - the step response being found by integrating the impulse response using the dummy trapping state technique. A simple routine was then called and the intensity function computed for a particular time interval.

4. OPTIMISATION PROCEDURES

Criteria for fitting

The following techniques, for least squares fit, were adopted for the optimisation of the gamma function model parameter (n) against experimentally derived and the theoretical model values.

i) Absolute

The conventional criterion for sum of the errors is:-

$$\sum e^2 = \sum_{i=1}^{i=N} \left(Zi - Yi \right)^2$$

Whilst it is simple to apply, it has two disadvantages: firstly, unlike most other quantitative criteria it is dimensional and the numerical value of the minimum is dependent upon the units of Y and secondly, its use implies that a given absolute error has the same importance over the whole range of the dependent variable Y.

ii) Fractional

As a first alternative the sum of the squares of the fractional errors was considered:-

$$\sum e^2 = \sum_{i=1}^{i=N} \left(\frac{Zi - Yi}{Yi} \right)^2$$

iii) Logarithmic

For many engineering problems, the most satisfactory criterion is probably that of the sum of the squares of the logarithms of the ratio.

$$\sum e^2 = \sum_{i=1}^{i=N} \left(\log \frac{Zi}{Yi} \right)^2$$

Its use is restricted to cases where the values of Y are positive and absolute, but these are common.

A.5 A PAPER TO BE PUBLISHED IN THE TRANSACTIONS OF THE INSTITUTION OF CHEMICAL ENGINEERS.

Continuous Blending of Low Viscosity Fluids:-

An Assessment of Scale-up Criteria.

by

H.I.Berresford, B. Tech.

L.G.Gibilaro, B.Sc., Ph.D.

D.J.Spikins, B.Sc., Ph.D., C.Eng., A.M.I.Chem.E., A.M.Inst.F.

H.W.Kropholler, B.Sc., C.Eng., A.M.I.Chem.E.

SYNOPSIS

Impulse response experiments were performed for geometrically similar, turbine stirred vessels and the results fitted to a mathematical model. A comparison is drawn, using this model, between the residence time distributions of the scaled system, after having scaled the stirrer variable by one of the general rules for scale-up of batch blenders.

The ratio of impeller pumping capacity to vessel throughput is proposed as a criterion for scale-up. This criterion is easy to predict and has a wide application. It is the first "continuous" scale-up rule.

INTRODUCTION

Continuous blending is distinguished from batch mixing in that constant composition of product over a period of time rather than uniformity of the mixer contents is the objective. A continuous blender mixes material that enters over a period of time so that the extent of product composition variation may be assessed from the residence time distribution. One way in which process characteristics may be matched is to preserve the RTD in the scale up procedure. It will be seen that this apparently restrictive criteria leads to a useful design method in terms of a parameter based on the flows in the system.

Batch scale-up rules take no account of flow through a system, their application to the continuous case therefore has been without foundation. Hence there is a definite need for a dynamic parameter which can be adjusted for batch and continuous systems.

It is the purpose of this paper to demonstrate the use of the ratio of impeller pumping capacity to throughput flow as a means of scaling continous blenders and to propose an extension of this for use in the batch case.

SCALE-UP OF BATCH BLENDERS

A review of the derivation of methods used in batch scale-up is necessary as these techniques are adopted for use in the continuous case.

There are certain general concepts for the scale-up of batch liquid systems, which have their roots in the principle of similarity. These criteria have been developed in an attempt to bring about the same process result

in the laboratory (unscaled) and scaled cases.

The types of similarity associated with fluid motion are as follows:-

(a) Geometric Similarity

Geometric similarity exists when the linear dimensions of the unscaled and scaled up vessels bear a constant ratio to each other.

(b) Kinematic Similarity

If two systems are geometrically similar, then kinematic similarity exists when the ratios of velocities between corresponding points in each system are equal.

(c) Dynamic Similarity

After having obtained geometric and kinematic similarity between two systems, dynamic similarity exists if the ratios of forces between corresponding points in each system are the same.

Further criteria of similarity exist such as thermal and chemical similarity, but as these similarities are difficult to maintain practically in the scale-up of stirred vessels, their use is limited. It is rarely possible to maintain all or the majority of the various similarity criteria when scaling-up batch blenders. Usually one criterion is possible and the others are approximated.

The principle of similarity can be expressed as:

$$A = f(B, C, D \ldots\ldots) \qquad (1)$$

where A is a dimensionless group which is a function of other dimensionless groups B, C, D, (1).

The groups A, B, C, D can be derived for any particular system either from the basic equations, in this

case of fluid mixing the Navier Stokes equation, or by dimensional analysis. Each method gives an expression for the behaviour of the system using the minimum number of independent variables. From the above expression, the interconnection between the principle of similarity and dimensionless groups becomes apparent. As nearly all the data for batch liquid mixing systems have been correlated using the method of dimensionless groups, this correspondence is essential.

Any dimensionless group in an expression similar to equation (1) can be used as a scale-up criterion. If, however, there is interaction between the dimensionless groups reliable scale-up cannot be achieved. One of the groups must dominate the remainder in the expression. This is the regime concept. If a pure regime exists, one dimensionless group being dominant, scale-up is comparatively easy. In the case of a mixed regime, no group dominating the others, scale-up design is virtually impossible. It is usual, in this case to conduct experiments in which one of the effects is eliminated and then derive a new expression with only one group dominant.

To illustrate the regime concept, consider the expression derived from dimensional analysis for stirred liquid systems (10). The Weber group is ignored as it only applies when separate physical phases are present in the system.

$$\frac{Pg_c}{\rho N^3 D^5} = K \cdot \frac{\rho ND^2}{\mu} \cdot \frac{N^2D^2}{g_c} \cdot \frac{T}{D} \cdot \frac{Z}{D} \cdot \frac{C}{D} \cdot \frac{P}{D} \cdot \frac{W}{D} \cdot \frac{L}{D} \cdot \frac{N_2^1}{N_1^1} \qquad (2)$$

The last seven terms of the above relationship describe the system geometry; $\frac{N_1^1}{N_2^1}$ accounts for any change in the number of blades. If complete geometric similarity is assumed, the expression reduces to:-

$$\frac{Pg_c}{\rho N^3 D^5} = K \cdot \frac{\rho ND^2}{\mu} \cdot \frac{N^2D^2}{g_c} \qquad (3)$$

As Reynolds number is proportional to ND^2, and Froude number proportional to N^2D^2, it can be seen that if either the Reynolds number group or the Froude number group is used as a basis for scale-up the value of the other group is changed - if the physical properties of the fluid remain the same; this is a mixed regime. If the fluid properties in the original and scaled up case are different then scale-up with both Reynolds number and Froude number constant is possible. A relatively pure regime, with the Reynolds number dominant, can be obtained by suppressing the vortex effect. This is achieved experimentally by the introduction of baffles to reduce the swirling motion of the fluid, hence a correlation can be found relating the unknown with Reynolds number.

Experiments were conducted by Rushton, Costich and Everitt (10) for various impellers in a series of tanks of different diameter. From their curves, it is possible to predict power requirements in the scaled up vessel for a whole range of impellers and Reynolds numbers.

Equation (3) leads to two general rules of scale-up. They are scale-up by:

(a) Constant Reynolds number

(b) Constant Froude number

Scale-up using the latter criterion is rarely met, but when employed it attempts to ensure similarity between the gravitational effects in the two vessels, Scale-up at constant Reynolds number is used as an attempt to obtain hydrodynamic similarity between the two vessels; it is also used because of the ease of its measurement. Rushton found that this scale-up criterion gave the same overall flow pattern, but not equality of instantaneous velocities. These may differ considerably in the original and scaled up vessel at equal Reynolds number. This fact has caused other relationships to be used, which permit the scale-up of model conditions over a wider range of flow velocities. Scale-up using constant impeller tip speed is such a relationship which has found general acceptance; this criterion ensures that the velocities leaving the impellers in each case are the same.

The use of a constant dimensionless group as a rule of scale-up leaves much to be desired, as it gives no indication as to the final process result of the scaled up system. In an attempt to bring about a closer relationship between the final products obtained in laboratory and scaled mixing vessel, the rule of scale-up using constant power per unit volume was introduced. Although this rule has been much maligned due to its excessive power requirements in the scaled up vessel, it has been found to give good results over a wide range of applications where a reasonable rate of flow and shear are required, (11, 19).

In recent years, with the greater understanding of impeller characteristics, new parameters have come to light in fluid mixing. Some of these parameters have been

suggested as possible criteria for scale-up, but as yet no published data is available to indicate their usefulness. Such suggested scale-up parameters are constant pumping capacity, constant circulation time and constant mixing time. (12, 13).

The pumping capacity of an impeller is the volume of liquid discharging from it in unit time. The circulation time is defined as the ratio of liquid volume pumping capacity. The mixing time definition varies, but in general it is the time required to achieve a uniformity of composition in a specified sample size, which is not further changed by additional mixing. (6).

The introduction of these three criteria, especially the latter two, should lead to greater compatibility between the mixing in the original and scaled vessels, because each is fundamentally concerned with the actual fluid flow within the vessel.

Mixing time has appeared in dimensionless groups which have been developed by van de Vusse, Fox and Gex, Metzner and Norwood, Kramers et al and Oldshue, (6, 7, 8, 9, 14). They derived, by dimensional analysis, relationships for the mixing time group with respect to other dimensionless groups. They then proceeded by experiment to study the effect of each of these groups in turn on the mixing time group. The following are the mixing time relationships derived by some of the above authors.

i) van de Vusse (7). In an unbaffled vessel.

$$\frac{\theta q}{V} = f_1 \cdot \frac{N D^2 \rho}{\mu} \cdot f_2 \frac{\rho N^2 D^2}{\Delta \rho g Z} \cdot f_3 \cdot \frac{D^3}{T^{2.5} Z^{0.5}} \qquad (4)$$

which reduces, for geometrically similar systems, to

$$\frac{\theta q}{V} \propto \left(\frac{N^2 D^2}{\Delta e g Z}\right)^{-a}, \quad N_{Re} > 10^5 \tag{5}$$

a = 0.25 for propellers

a = 0.30 for flat paddle impellers

a = 0.35 for pitch blade paddle impellers

ii) Fox and Gex (6). Correlation for propellers; a similar correlation exists for jet mixing.

$$N\theta \cdot \left(\frac{D}{T}\right)^{3/2} \cdot \frac{g^{1/6}}{(N^2 D)^{1/6}} \cdot \left(\frac{T}{Z}\right)^{1/2} = f(N_{Re}) \tag{6}$$

iii) Metzner and Norwood (9). Correlation for turbine impellers

$$N\theta \cdot \left(\frac{D}{T}\right)^{2} \cdot \frac{g^{1/6}}{(N^2 D)^{1/6}} \cdot \left(\frac{T}{Z}\right)^{1/2} = f(N_{Re}) \tag{7}$$

for $N_{Re} > 10^5$

$$\theta = K_2 \frac{T^2 \cdot (N^2 D)^{1/6} \cdot Z^{1/2}}{ND^2 \cdot g^{1/6} \cdot T^{1/2}} \quad \text{where } K_2 = 5 \tag{8}$$

The correlation of Kramers et al and Oldshue (14, 15) incorporate a power term in their expression for mixing time, which when used for, scale-up of constant mixing time, give the same expression as that derived by Corrsin (23) for isotropic turbulence. Geometric similarity is assumed between the two systems. The expression is $p^1 = K^5 p$

Direct use of the dimensionless groups of van de Vusse, Fox and Gex, etc., for scale-up of constant mixing time, is fairly straightforward if the mixing takes place in the range of Reynolds number for which the value of the mixing time group remains unchanged, i.e. $N_{Re} > 10^5$. The use of these dimensionless groups for scale-up is thus fairly limited. The correlations of mixing time group versus Reynolds number, are however, of great use in the prediction of mixing times for a scaled vessel after having used a more elementary scale-up rule.

Various attempts have been made to relate mixing time to circulation time in a stirred vessel. van de Vusse (7, 8) states that mixing time is approximately proportional to the circulation time. Holmes et al (12) found the mixing time to be approximately equal to 5 times the circulation time. Other values have been quoted. Thus if mixing time is directly proportional to the circulation time as appears to be the case, then scale-up using constant mixing time will produce the same result as scale-up at constant circulation time.

Continuous blending is much less flexible than batch operations: it is usually necessary to design a continuous blender for a specific purpose. Situations where continuous blending is employed include diluting concentrated solutions with solvent; washing of liquids with solvents; chemical treatment of liquids and manufacture of emulsions.

RESIDENCE TIME DISTRIBUTION MODELS

The manner in which mixing takes place in a mechanically - agitated vessel depends upon the impeller characteristic and the flow pattern induced within the fluid. The residence time distribution depends on the nature of the mixing and of the process. This concept has found great application in model building. (26).

In a perfect mixer, one in which all elements have an equal chance of leaving, the residence time distribution is an exponential decay. This can only be approximated to in reality.

Early attempts to obtain a theoretical model to describe the real behaviour of a stirred tank produced a series of models which were not based on the physical flow pattern within the vessel. Cholette and Cloutier (22) offered the following possible reasons for the deviation of measured residence time distributions from the experimental decays: stagnant regions in the vessel; by-passing of a fraction of the feed directly to the outlet; and regions of the vessel through which material flows but in which no mixing takes place.

A model based on flow patterns is useful because it explains why the residence times are so distributed. It also enables the model to be used for predictive purposes, so that the effect of changing operating conditions - through-put, impeller speed and inlet/outlet positioning, etc., - can be assessed.

Since the impeller characteristics govern the flow pattern within the fluid, it is not surprising that the first flow models for stirred vessels incorporated the pumping

capacity of the impeller as their key parameter. A rotating impeller may be looked upon as a caseless pump discharging into the body of the fluid.

SINGLE LOOP MODELS

The simplest model that can be derived using pumping capacity contains a single circulation loop: fluid pumped by the impeller flows through the whole vessel before returning to the impeller region. Variety may be introduced by the way in which the mixing in the recirculation loop and the impeller region is characterised. Single loop models do not always present the flow in stirred vessels; the turbine stirred vessel having a double-loop flow pattern.

A generalised form of the transfer function for a single recirculation loop model is derived from Fig. 1.

Mass Balance at X and Y

$$Q.Ci + qCo.F_2(s) = (q+Q).Cx$$

$$(q+Q).Co = (q+Q).Cx.F_1(s)$$

hence the Laplace transform:-

$$G(s) = \frac{Q}{(q+Q)/F_1(s) - q.F_2(s)} \qquad (9)$$

MULTILOOP MODELS

Nagata et al described the flow patterns in turbine-stirred tanks in the following way: (see Fig. 2)

a) horizontal discharge from the turbine-stirred tanks;

b) separation of the flow into a two vertical components at the wall;

c) horizontal flow returning the fluid to the centrally placed stirrer shaft;

d) vertical flow back to the impeller region.

Subsequently, van de Vusse proposed the first multi-loop model, which consisted of three circulation loops. He derived the transfer function, inverted it for certain values of the parameters and compared experimental and calculated curves.

From Fig. 2 it is reasonable to assume that a realistic flow model for a turbine stirred vessel should incorporate four loops as shown in Fig. 3. The volume allotted to each stage is determined by the position of the impeller: for example, with an impeller situated at one third of the liquid depth from the base of the vessel, the stages in the upper loop would have twice the volume of those in the lower one.

The number of stages per loop is adjusted to fit the responses. Fig. 3 shows the model for a turbine positioned ($z/_3$) from the bottom of the tank with the pumping capacity distributed to give equal circulation times in the upper and lower loops. By symmetry, the model can be further simplified to the double loop model in Fig. 4.

It is a feature of models consisting of sets of linear differential equations (obtained from dynamic mass balances on the stages) that the system transfer function can be derived without too much difficulty. As inversion of the transfer function is difficult, the numerical method of Gibilaro, Kropholler and Spi[illegible]ins (18) was adopted to solve

the original differential equations in this work.

SCALE-UP CRITERION

In all the models based on circulation loops, the key parameter is the ratio of pumping capacity to flow-rate through the vessel. (Eq. 9). This suggests that it would be possible to use q/Q as a basis for scale-up by fitting a model containing this parameter to residence time distributions for geometrically similar vessels. As so many models have q/Q as the key parameter, it follows that scale-up on the basis of constant q/Q should be most useful. Scale-up of impeller speed using this criterion would be accompanied by the assurance that the unscaled and scaled system would have the same residence time distributions.

This work investigated the possibility of using constant q/Q as a scale-up rule. The double loop model shown in Fig. 4 was found to be a suitable representation of the experimental response for two vessels of 9" and 19" diameter respectively. The model was then used to compare the residence time distributions obtained on the laboratory scale with those computed for the larger vessel, after having scaled up the impeller speed by one of the batch criteria previously mentioned.

EXPERIMENTAL WORK

Apparatus

The experiments were conducted in cylindrical, flat-bottomed, baffled and unbaffled tanks of 9" and 19" dia. The fluid was agitated by centrally positioned turbines having 6 flat blades ($W/_D = 1/_8$) of diameter 2.1/2" and 4". The turbines were geometrically similar. The impellers were placed at one third of the liquid (water) depth from the base of the vessel.

Liquid depth was equal to vessel diameter. The impeller shaft was driven by a Chemineer variable speed motor. Dynamic tests were performed using nigrosine dye as tracer and a photocell detector.

Method

Impulse response curves were obtained for a 9" diameter unbaffled vessel with a 2.1/2" diameter turbine, using a dye injection technique. As the injection time was less than 1/250 if the mean residence time, the injection can be regarded as a true impulse. Runs were conducted at various impeller speeds, with the inlet either directed into the impeller or into the upper region of the vessel. No vortex formed in any of the runs. The output from a photocell detector situated immediately beneath the vessel was logged automatically at pre-set time intervals. The normalised response was computed and compared with the theoretical model response. Similar response curves were obtained for the 19" diameter, 4" turbine system using a value of twice the mean residence time of the smaller vessel. These were again compared with the model response. The pumping capacity of the 2.1/2" diameter turbine was determined by the flow-follower technique suggested by Marr and Johnson (24) and it was found to be characterised by the equation $q = 0.94\ ND^3$ (5). As the two impellers were geometrically similar ($W/_D$ - constant) this expression holds for both impellers (2).

Results

Figs. 5 and 6 show that the experimental and theoretical responses compare very well for both inlet positions, and for both systems. The range of q/Q studied

was 6.8 to 35.9, and only at the lower value, i.e. at q/Q = 6.8, was there any marked deviation of the experimental response from the theoretical. This was probably due to the by-passing which had occurred because the flow pattern had not been established in the larger vessel. The range of the Reynolds number in the experiments with the 9" dia. vessel was $1.8 \times 10^3 - 1.2 \times 10^4$, in the (4" - 19") system $3.5 \times 10^3 - 4.5 \times 10^4$.

ASSESSMENT OF BATCH SCALE-UP CRITERIA FOR CONTINUOUS SYSTEMS

Having found that the two-circulation-loop model fitted the experimental residence time distributions of both vessels, it is now possible to compare the residence time distribution curves which would be obtained after establishing the impeller size and speed by one of the batch scale-up criteria listed below.

Relationships which could be used in Scale-up Calculations

	Small Vessel		Large Vessel	
Reynolds Number	$N_1 D_1^2$	=	$N_2 D_2^2$	(10)
Tip Speed	$N_1 D_1$	=	$N_2 D_2$	(11)
Pumping Capacity	$N_1 D_1^3$	=	$N_2 D_2^3$	(12)
Circulation Time	$\frac{V_1}{N_1 D_1^3}$	=	$\frac{V_2}{N_2 D_2^3}$	(13)
Mixing Time	$\frac{T_1^2 (N_1^2 D_1)\ Z_1^{\frac{1}{2}}}{N_1 D_1^2 T_1^{\frac{1}{2}}}$	=	$\frac{T_2^2 (N_2^2 D_2)\ Z_2^{\frac{1}{2}}}{N_2 D_2^2 T_2^{\frac{1}{2}}}$	(14)

The dimensionless plots of mixing time group and power number against Reynolds number do not allow reliable scale-up in the range of Reynolds number used in the

experimental work; the dimensionless groups are not constant in this range. Thus scale-up using the mixing time groups of Fox and Gex and van de Vusse was not attempted; scale-up using constant power per unit volume was similarly thwarted. As Norwood and Metzner derived their mixing time group for turbines, the assumption of zero slope over this range of Reynolds number was used (i.e. the value of the mixing time group remains constant). For laboratory scale experiments with Reynolds numbers greater than 10^5, it was calculated that scale-up using either the mixing time group of Fox and Gex or van de Vusse resulted in a value of q/Q which was similar to that obtained by scale-up using the Metzner and Norwood mixing time group.

Scale-up in the range of $N_{Re} > 10^5$, using constant power per unit volume, resulted in values of q/Q which were slightly higher than scale-up at constant q/Q. Thus scale-up using this criterion will give good correspondence of residence time distribution between the laboratory and the scaled vessel.

For each of the batch scale-up criteria listed, the value of the stirrer variable (impeller speed N_2) was calculated so that the conditions in the 19" diameter vessel with the 4" diameter impeller corresponded with those in the 9" diameter vessel with the 2.1/2" diameter (impeller speed N_1). Having calculated the 4" diameter impeller speed to satisfy each scale-up rule, the pumping capacity was then found and hence the ratio of impeller pumping capacity to flow rate. Data was then prepared and the theoretical response curve for this condition computed. This procedure was repeated for each criterion over the range of

2.1/2" diameter impeller speeds. Hence, it was possible to compare the variation in residence time distribution, for every scale-up rule, for each experimental run of the 2.1/2 - 9 diameter system.

Table 1 shows the calculated values of the parameter q/Q for each particular scale-up criterion. Column 1 illustrates the values of q/Q used in both experimental cases i.e. for the 9" and 19" diameter vessels. Column 2 shows the values of q/Q calculated when scale-up at constant Reynolds number is observed. An example of this calculation is shown below.

Example

For experimental run No. 1 (2.1/2" - 9") dia. system, the impeller speed was 28 r.p.m.

Now $N_{Re} \propto ND^2$

$\therefore$ experimental $N_{Re} = K \cdot 28 \cdot (2{\cdot}5)^2$

For constant N_{Re}, $N_1D_1^2 = N_2D_2^2$

For constant N_{Re} in the (4" - -9") diameter system, the impeller speed N_2 is

$$N_2 = \frac{28 \times (2.5)^2}{(4)^2} = 11.9 \text{ r.p.m.}$$

from $q = 0.94\ ND^3$, the pumping capacity, q = 11.6 litre/min. The experimental flow rate for the (4" - 19") diameter system was 5.25 litre/min. Hence for this criterion,

$$\left(\frac{q}{Q}\right)_s = \frac{11.6}{5.25} = 2.2$$

Column 3 shows the impeller speed and values of q/Q calculated for scale-up using constant tip speed.

The calculation is similar to that just shown.

Similarly columns 4 and 5 illustrate scale-up using constant pumping capacity and circulation time respectively.

In the last column of Table 1, the value of impeller speed for the scaled up case is calculated by using constant mixing time as found in the mixing time group of Norwood and Metzner, as shown in the example below:-

Example

Mixing time in the unscaled and scaled up vessels is represented by:-

$$\theta_E = K_1 \frac{T_1^2 \cdot (N_1^2 D_1)^{1/6} \cdot Z_1^{1/2}}{N_1 D_1^2 \cdot g^{1/6} \cdot T_1^{1/2}} \qquad \text{(i)}$$

$$\theta_S = K_2 \frac{T_2^2 \cdot (N_2^2 D_2)^{1/6} \cdot Z_2^{1/2}}{N_2 D_2 \cdot g^{1/6} \cdot T_2^{1/2}} \qquad \text{(ii)}$$

assuming the mixing time group to be constant over the range of Reynolds number considered we have

$$K_1 = K_2$$

For constant mixing time $\theta_E = \theta_S$

Substitute in (i) the respective values for the (2.1/2" - 9") diameter system, and in (ii) the respective values for the (4" - 19") diameter system. Combining (i) and (ii) we find

$$N_1^{2/3} \qquad 1.98 \qquad = \qquad N_2^{2/3}$$

$$N_2 = 2.8 \times N_1$$

The experimental value of impeller speed is:-

$N_1 = 28$ r.p.m.

$$N_2 = 2.8 \times 28$$

$$= 73.6 \text{ r.p.m.}$$

From $q = 0.94\ ND^3$, the pumping capacity is 72 litre/min.

The conditions in the scaled vessel using this criterion were taken to be the same as those used in the experimental runs for the (4" - 19") diameter system, i.e. flow rate = 5.25 litre/min.

$$\text{Hence } \left(\frac{q}{Q}\right)_s = \frac{72.0}{5.25} = 13.7$$

An indication of the difference between that of the scaled residence time distribution and the corresponding unscaled experimental residence time distribution is the difference between the calculated value $(q/Q)_s$ for the scaled-up rule and that of the corresponding experimental value $(q/Q)_E$. The following relationships were derived for geometrically similar systems, having the same mean time and with a length scale up ratio of L., i.e. $(LD_1 = D_2)$. They illustrate mathematically the deviation of the unscaled and scaled values of q/Q inherent in each batch scale-up rule.

$\frac{q}{Q}$ Relationships for various batch Scale-up Criteria

Constant Reynolds Number

$$\left(\frac{q}{Q}\right)_s = \left(\frac{q}{Q}\right)_E \cdot \left(\frac{1}{L^2}\right) \tag{15}$$

Constant Tip Speed

$$\left(\frac{q}{Q}\right)_s = \left(\frac{q}{Q}\right)_E \cdot \left(\frac{1}{L}\right) \tag{16}$$

Constant Pumping Capacity

$$\left(\frac{q}{Q}\right)_S = \left(\frac{q}{Q}\right)_E \cdot \left(\frac{1}{L^3}\right) \tag{17}$$

Constant Circulation Time

$$\left(\frac{q}{Q}\right)_S = \left(\frac{q}{Q}\right)_E \cdot \left(\frac{1}{1}\right) \tag{18}$$

Constant Mixing Time

$$\left(\frac{q}{Q}\right)_S = \left(\frac{q}{Q}\right)_E \cdot \left(\frac{L^{1/6}}{1}\right) \tag{19}$$

Constant Power/Unit Volume

$N_{Re} > 10^5$,

$$\left(\frac{q}{Q}\right)_S = \left(\frac{q}{Q}\right)_E \cdot \left(\frac{1}{L^{2/3}}\right) \tag{20}$$

With the exception of scale up using constant circulation time, it can be seen that scale-up using the batch criteria will produce a marked difference between the experimental and the resulting scaled-up residence time distributions.

DISCUSSION

For geometrically similar systems of constant meantime the previous relationships show that scale-up using Reynolds number, tip speed, pumping capacity and power per unit volume will always give a value of scaled q/Q which is less than the predicted value to ensure identical residence time distributions. Scale-up using constant mixing time will give higher values of q/Q than required to obtain the same residence time distribution in two systems. Constant circulation time scale-up will result in the same q/Q and consequently the same residence distribution.

Figs. 7 and 8 are typical of the family of curves obtained when the various batch scale-up rules are compared over the range of impeller speeds.

If the value of $(q/Q)_s$ calculated from the batch scale-up rules is less than the experimental value, for the case of feed to the impeller, a greater degree of by-passing will result as shown by the initial section of the residence time distribution. For feed directed towards the loop region, the bulk of the fluid will reside longer in the vessel. These factors are due to the decrease of circulatory flow, the predicted pumping capacity being lower for these batch scale-up rules.

If $(q/Q)_s$ is greater than the experimental value i.e. scale-up using constant mixing time, the predicted pumping capacity is greater than the experimental and hence better circulation is available in the vessel. This reduces the by-passing effect for feed to the impeller and distributes the elements of fluid more evenly for feed to the loop.

The mean time of the scaled system used in this analaysis was twice that of the smaller vessel, thus the deviation between responses shown in Fig. 7 and 8 is correspondingly less marked than for the case of using constant mean time. Again complete geometrical similarity was not observed, (length ratio 2.1, impeller diameter ratio 1.6) the effect of this is to further mark the differences predicted by the scale-up relationships.

CONCLUSION

As Reynolds number and tip speed have only an indirect relationship with the mixing action of the fluid inside a vessel, it is not surprising that scale-up using these two as criteria should fall down in the continuous case. Likewise this discrepancy between the process result of the laboratory and scaled vessels would also be apparent for scale-

up of the batch case.

Scale-up using either constant mixing time or constant circulation time, takes into consideration the fluid flow paths within the vessel. It would therefore be expected that scale-up using these criteria should give a closer comparison between laboratory and scaled up vessels' residence time distribution, than the previous two.

Constant pumping capacity scale-up should be abandoned. Only if the throughput of the larger system is much smaller than the laboratory system should this criterion be used. As this hardly ever occurs practically, (the mean time of the larger system would be much greater than the smaller system), this scale-up rule has very little application.

The most striking conclusion to be drawn from this investigation is that if scale up should take place using the scale-up rule of constant q/Q, it would ensure that the same residence time distribution would appear in the laboratory and the scaled up vessel. This new scale up rule is flexible in application, it follows for any throughput flow rate required and consequently takes into account any variation in mean time between the two systems. It is also easier to manipulate than scale-up using either the mixing time or the circulation time approach.

Scale-up by constant q/Q not only takes into account impeller characteristics and hence circulatory flow patterns but also the volumetric throughput of the system. Both considerations are tremendously important when considering scale up of continuous systems.

Furthermore, as the theoretical models which have been derived and fitted to experimental responses for a

number of systems, over recent years all use q/Q as the key parameter, it would appear that this particular scale-up rule has wide application throughout a whole range of stirred vessels.

The double loop circulation concept can be adapted to a batch system, the the model parameter reducing to the pumping capacity; it follows from the above discussion that scale-up using constant circulation time would be the most useful for this case.

Notation

N_1	=	unscaled impeller speed
N_2	=	scaled impeller speed
p	=	power requirement
D	=	impeller diameter
μ	=	viscosity of fluid
ρ	=	density of fluid
T	=	tank diameter
z	=	liquid depth
P	=	pitch of blade
W	=	width of blade
L	=	length of blade
N_1^1, N_2^1	=	number of blades
θ	=	mixing time
q	=	pumping capacity of impeller
Q	=	throughput (volumetric)
V	=	volume of vessel
b,a	=	indices
p^1	=	scaled up power requirement
Ci	=	inlet concentration
Co	=	outlet concentration
$F_1(S), F_2(S)$	=	system Laplace transforms
$(q/Q)_S$	=	scaled up value of parameter
$(q/Q)_E$	=	unscaled value

Bibliography

1. Johnstone, R.E., and Thring, M.W., Pilot Plants, models and Scale-up Methods, 1957. McGraw Hill

2. Uhl, V., and Gray, J., Mixing Theory and Practice, 1960. Academic Press.

3. Sterbacek, H., and Tausk, C., Mixing in the Chemical Industry, 1965. Pergamon.

4. Hyman, O., Advances in Chemical Engineering, Vol. 4.

5. Gibilaro, L., Ph.D. Thesis, Mixing in Stirred Tanks, 1967, Loughborough University.

6. Fox, E., and Gex, V., A.I.Ch.E. Journal 2, 1956.

7. van de Vusse, J.G., Chem.Eng.Sci., 1955, 4, 178, 209.

8. van de Vusse, J.G., Chem.Eng.Sci., 1964, 10, 507.

9. Norwood, K., and Metzner, A., A.I.Ch.E. Journal, 1960 September.

10. Rushton, J.H., Costich, E.W., and Everitt, M.J., Chem.Eng. Prog. 1950., 46, 396, 467.

11. Holland, F., Chem.Eng. Nov., 1962.

12. Holmes, D., Voncken, R., and Dekker, J.A., Chem. Eng.Sci., 1964, 19, 201.

13. Copper, C., and Wolf, R., Canadian J. Chem. Eng., 1966.

14. Kramers, H., Baars, G., and Knoll, W., Chem.Eng. Sci., 1953, 2, 35.

15. Oldshue, J.V., Hirchland, H.E., and Gretton, A.J., Chem.Eng.Prog., 1956, 52, 481.

16. Bates, R.L., Fondy, P.L. and Corpstein, R., Ind. Eng.Chem. Process Design, 1963, 2, 310.

17. Bates, R.L., Ind.Eng.Chem., 1959, 51.

18. Gibilaro, L., Kropholler,H.W., Spikins, D.J., Chem.Eng.Sci., 1967.

19. Holland, F., Chemical and Process Engineering, March, 1964.

20. Briggs, R., A.I.Ch.E. Journal, 1963.

21. van de Vusse, L.G., Joint Symposium. The Scaling Up of Chemical Plant and Processes, London, 1957.

22. Chollet, A., and Cloutier, L., Cn.J.Chem.Eng., 1959, June.

23. Corrsin, S., A.I.Ch.E.J., 1957.

24. Marr, G., and Johnson, E., A.I.Ch.E.J., 1963, 9.

25. Nagata, S., Yamamoto, K., Hasimoto, K., and Naruse, T., Chem.Eng. (Tokyo) 1957, 21, 278.

26. Levenspiel, O. Chemical Reaction Engineering, Wiley 1962.

TABLE 1

EXPERIMENTAL FEED DIRECTED TO LOOP AND IMPELLER		CONSTANT REYNOLDS NUMBER SCALE-UP	CONSTANT TIP SPEED SCALE-UP	CONSTANT PUMPING CAPACITY SCALE-UP	CONSTANT CIRCULATION TIME SCALE-UP	CONSTANT MIXING TIME SCALE-UP
$2\frac{1}{2}$-9" q/Q	4"-19" q/Q	q/Q	q/Q	q/Q	q/Q	q/Q
6.8	6.8	2.2	3.12	1.44	12.6	13.7
9.5	9.5	3.1	5.0	2.02	17.5	22.4
12.7	12.7	5	6.65	2.7	23.6	29.6
16.8	16.8	5.8	9.05	3.52	31.2	40.6
20.0	20.0	7.0	11.4	4.2	37.0	50.8
25.4	25.4	9.5	15.2	5.4	47.0	67.0
29.4	29.4	10.8	17.3	6.23	54.5	78.0
35.9	35.9	12.65	20.2	7.6	66.7	91.5

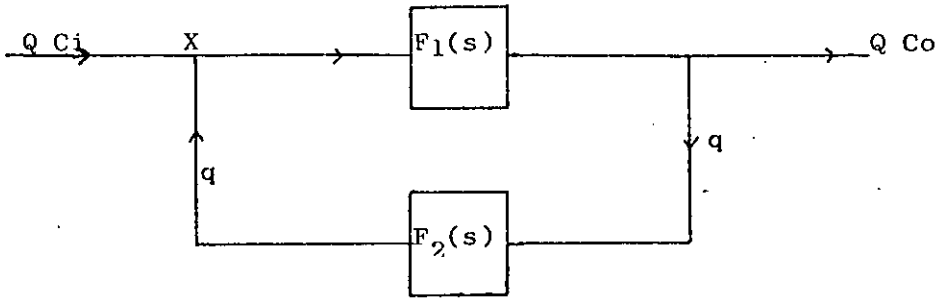

Fig. 1 A generalised form of the single recirculation loop models

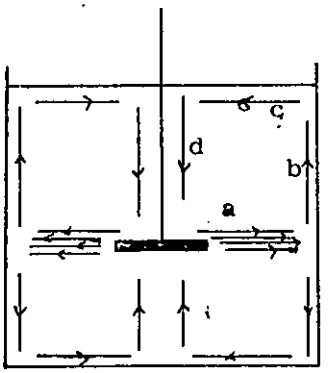

Fig 2 A diagrammatic representation of the streamline flow pattern in a turbine stirred vessel

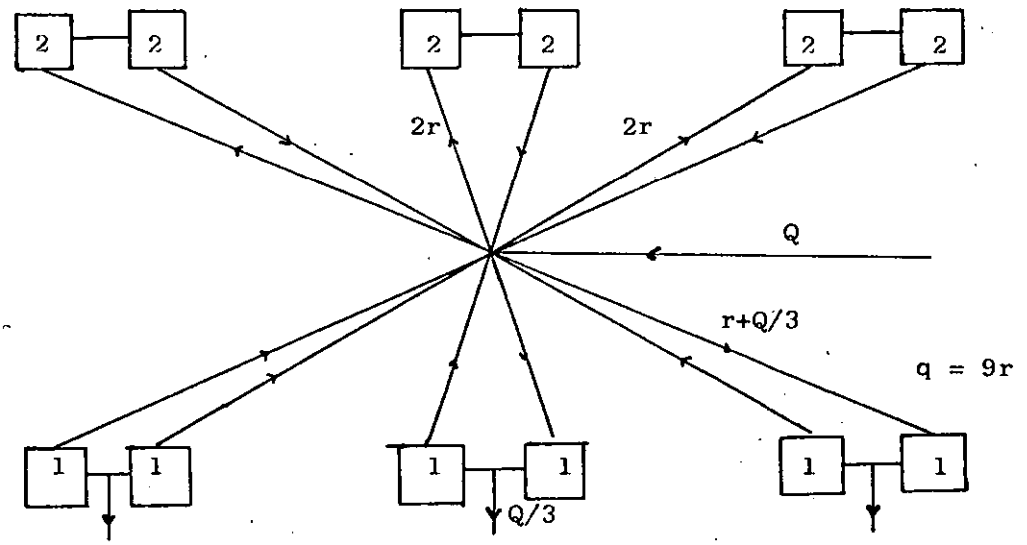

Fig 3 A multi-loop model derived from Fig 2

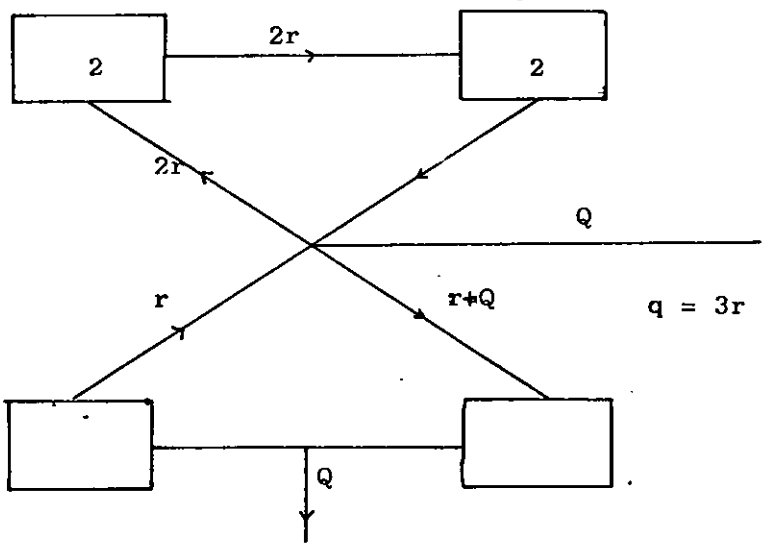

Fig 4 Double loop model derived by symmetry from Fig 3

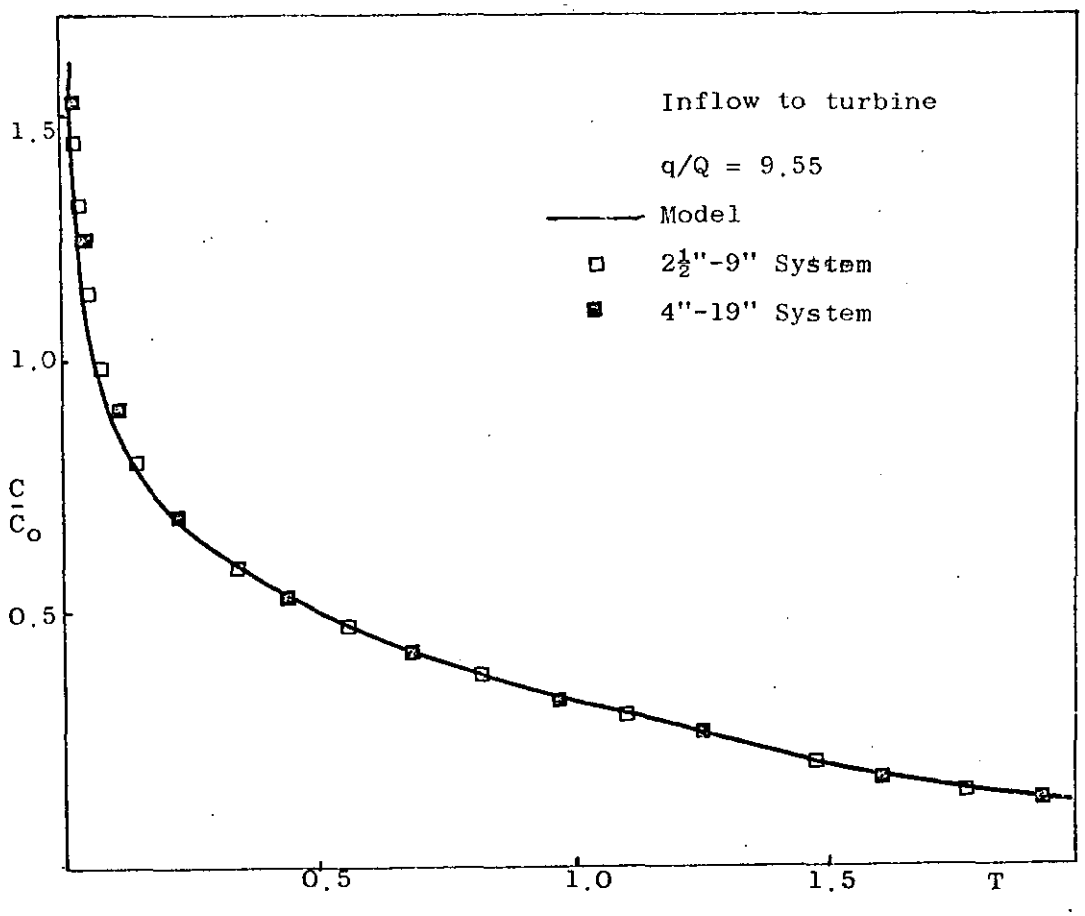

Fig.5 Comparison of experimental results and model predictions

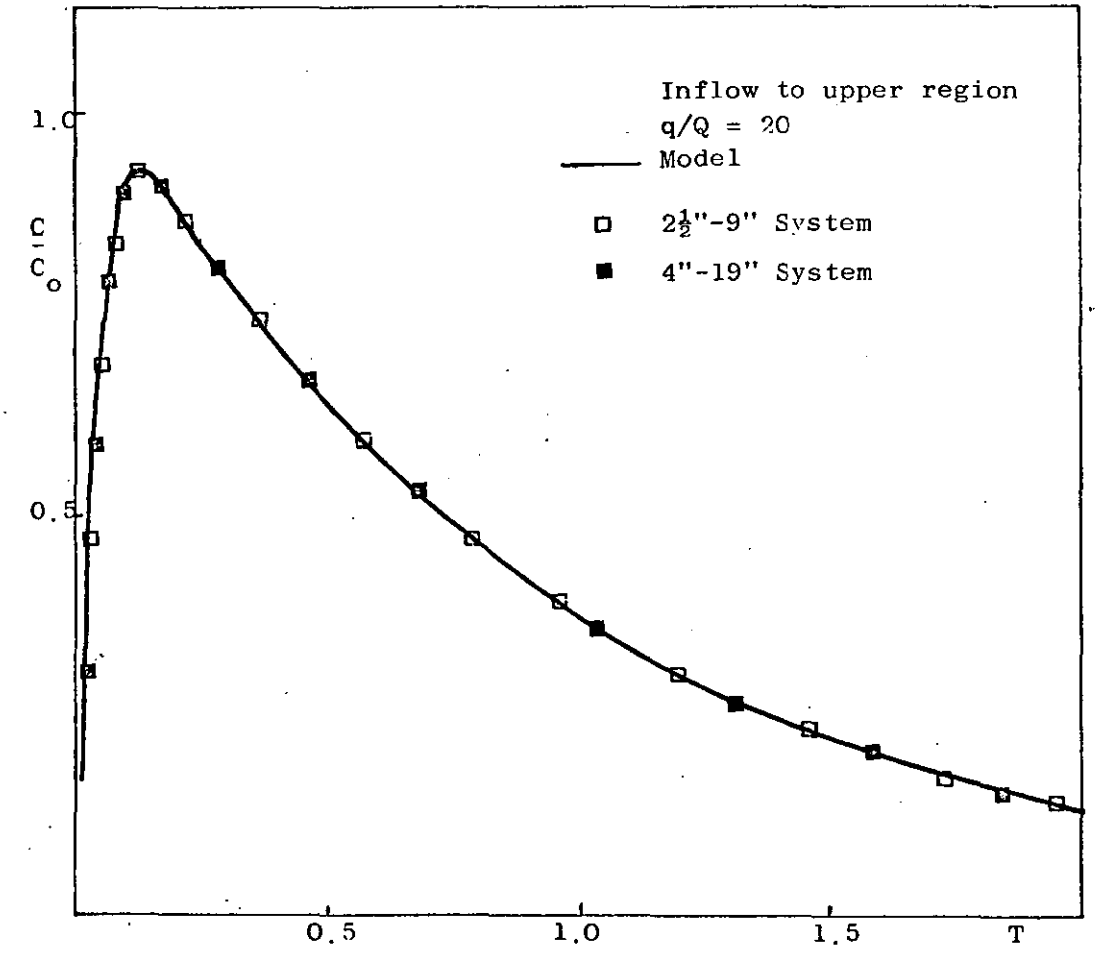

Fig.6 Comparison of experimental results and model predictions

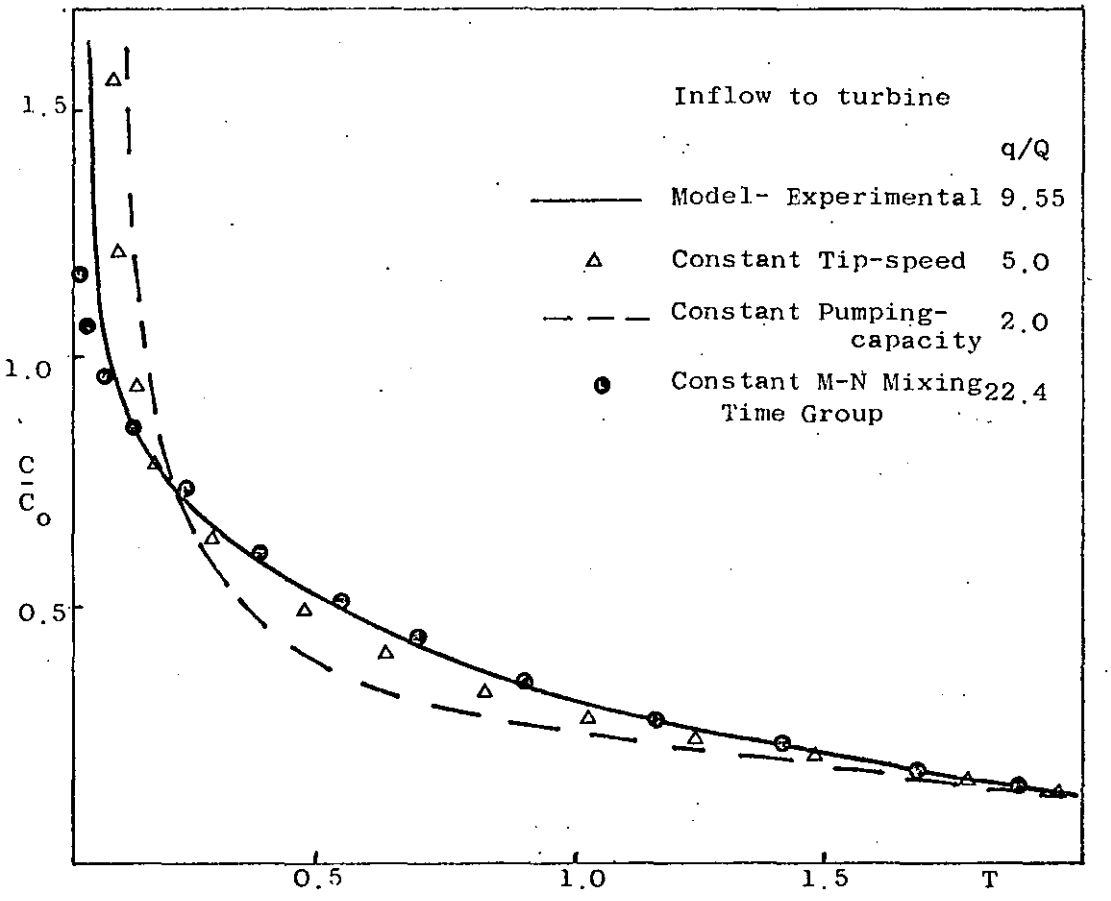

Fig.7 Comparison of residence time distributions for various batch scale-up criteria

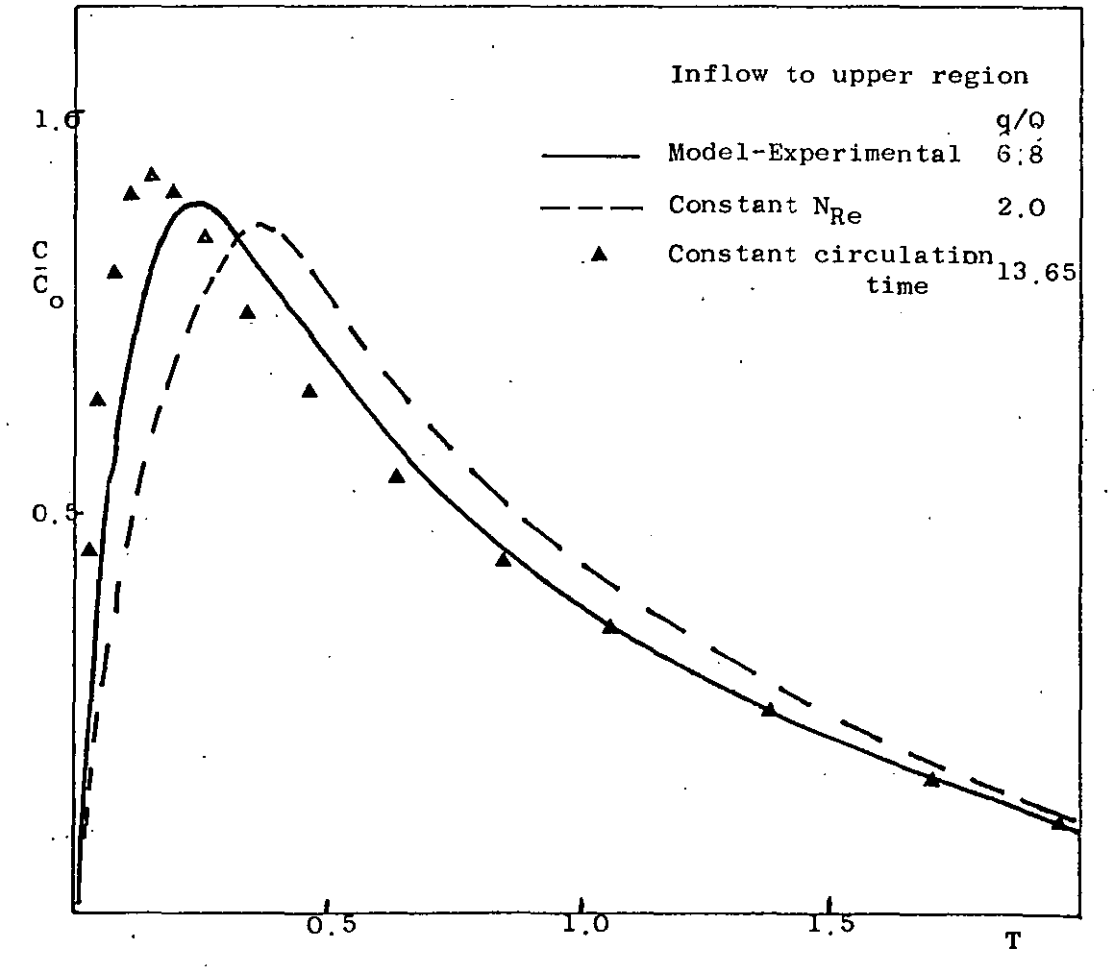

Fig.8 Comparison of residence time distributions for various batch scale-up criteria